Characterisation of Endometrial B Cells and Lymphocytes in the Peri-implantation Window



Mengni Shen

Linacre College

Supervised by:

Dr. Ingrid Granne

Dr. Jen Southcombe

Nuffield Department of Women's and Reproductive Health

University of Oxford

A thesis presented for the degree of Doctor of Philosophy

Trinity Term 2021

Acknowledgement

I could not have gotten the opportunity of studying for a DPhil degree without the support from my supervisors, Dr. Ingrid Granne and Dr. Jen Southcombe, the savviest and menschiest supervisors that any PhD student could hope to work with. Like many DPhil journeys, this DPhil is filled with ups and downs, and pivots along its way; while unlike many DPhil journeys, this DPhil is challenged by a global pandemic with its first outbreak in my beloved hometown, Wuhan. Thank you for always believing in me and helped me navigate through these uncertain times in research, and in life. Thanks also to all the amazing scientists at the Women's centre, John Radcliffe Hospital, especially Dr. Jen Southcombe, Dr. Helena Rodriguez Caro, Dr. Elizabeth O'Donnell, Dr. Wei Zhang, Ms. Janet Carver and Dr. Ana Kisovar for helping me troubleshoot all the unexpected result, and lending me reagents that I possibly have forgotten to return. I would also like to express my gratitude to Dr. Helen Ferry, Dr. Neil Ashley and Mr. Liam Hardy for helping me with RNA-seq library preparation and cell sorting, I would not have been able to explore the role of now my favourite cell type, B cells, without your dedication.

Special thanks to all the patients from Wolfson Fertility Centre, Oxford Fertility and John Radcliffe Hospital Recurrent Miscarriage Clinic who attended these studies, and to Dr. Ginny Mounce and all the doctors, nurses and research midwives who are fantastic at recruiting patients and collecting samples.

I am especially grateful for the generosity of Finox Funds, Funds for Women Graduates and Sir Richard Stapley Educational Trust for funding my study.

I owe a special debt to the people I lived with, all of whom have become close friends, Yaqiong Liu, Zhichao Ai, Bin Liu. Thanks for fixing me dinners and lunches while I am stuck in my experiments or thesis writing, and thanks for always be kind and patient to me, I know this can be challenging sometimes. I also relied on the support and help of countless friends, family members and colleagues, including Xinyan Li, Siyu Bian and Ramsha Nawaz, who remain close enough even though we barely had chance to meet,

during the years of my study.

Most of all I thank my family, my mum Xuejuan Yin and my dad Shunan Shen, who made the world a warmer place. Thanks for always supporting my decisions even though it meant studying abroad for 4 years (instead of 1 year as we initially agreed on) and relying on family financial support as a 26-year-old.

And to my beloved Steven (a.k.a. Shang-kuan Lin), who might just be the most wonderful person I met. During the years of my DPhil, he fixed my coding bugs, edited my drafts, sharpened my ideas, made me food, made me laugh, and filled my heart with love.

Characterisation of Endometrial B Cells and Lymphocytes in the Peri-implantation Window

Abstract

Mengni Shen

Trinity Term 2021, Linacre College

A thesis submitted in partial fulfilment of the requirements for the degree of Doctor of Philosophy at the University of Oxford.

Immunological regulation at the implantation site is a complex process, dysfunction may contribute to infertility, recurrent implantation failure (RIF) or recurrent pregnancy loss (RPL). Apart from endometrial NK and T cells, whose phenotypic profile and functional involvement have been recognised, evidence suggests that endometrial B cells may also have a potential role in reproductive pathologies. This thesis aimed to investigate endometrial immune profiles during human implantation, with a specific focus on the role of endometrial B cells.

Both healthy women and infertility, RIF or RPL patients were recruited for endometrial immune profiling, focusing on cell proportions (NK, T and B cells) and activation status. Additionally, peripheral blood samples were collected and analysed in parallel. Significant differences were observed between peripheral and endometrial immune profiles, in minor cell populations like $CD56^{bright}$ $CD16^{dim}$ NK cells and CD4 CD8 double positive T cells, such differences were not previously reported. A standard operating protocol (SOP) was established so that comparison between controls and infertility, RIF or RPL patients could be made with more patients being enrolled in the near future.

The role of B cells in the human endometrium was investigated. A systematic review was performed to understand the B cell involvement in reproductive pathologies. A number of immunohistochemistry studies were retrieved that identified endometrial B cells in association with T cells in 'lymphoid aggregates (LAs)', however, neither have been extensively characterised. RNA-sequencing and flow cytometric analysis were performed on $CD19^{+}$ endometrial B cells. B cells comprised 1-5% of endometrial immune cells, the majority were naïve or memory B cells, with few plasma cells. Compared with circulating B cells, endometrial B cells had an activated phenotype, with increased expression of CD69, HLA-DR, CD74 and CD83, and IL-10 production capacities. $PD1^{+}CXCR5^{+}ICOS^{+}$ T follicular helper-like cells and $FAS^{+}IgD^{-}$ germinal centre-like B cells were present in the endometrium. Together with previously reported LAs, endometrial B cells may be an active player in shaping the endometrial immune environment.

Contents

List of Figures **10**

List of Tables **13**

List of Abbreviations **15**

1 Introduction **18**
1.1 The Human Menstrual Cycle 19
1.2 Human Embryo Implantation 21
1.3 The Role of the Maternal Immune System in Pregnancy 22
1.3.1 Maternal Immune Cells in Embryo Implantation 24
1.3.1.1 Endometrial NK cells 25
1.3.1.2 Endometrial T cells 26
1.3.1.3 Endometrial B cells 28
1.3.1.4 Other immune cells 28
1.4 Aims of this Thesis 30

2 The Peri-implantation Immune Profiling (PIP) Study **31**
2.1 Introduction 31
2.1.1 Current evidence for diagnosis and treatment of immune dysfunction associated infertility, RIF and RPL 31
2.1.2 Endometrial immune cells and their association with infertility, RIF or RPL 33
2.1.2.1 Endometrial NK cells 33
2.1.2.2 Endometrial T cells 33
2.1.2.3 Endometrial B cells 34
2.1.3 Differences between peripheral and endometrial immune cells . . 35
2.1.4 CD69 as a marker of tissue residency and cell activation 37
2.2 Chapter Aims 39
2.3 Materials and Methods 40

2.3.1 Subject recruitment . . . 40
2.3.2 PBMCs isolation . . . 42
2.3.3 Endometrial biopsy processing . . . 42
2.3.4 Flow cytometry analysis . . . 43
2.3.4.1 t-SNE plot . . . 43
2.3.4.2 FlowSOM . . . 44
2.3.5 Statistical analysis . . . 44
2.4 Results . . . 45
2.4.1 Establishing a SOP for the PIP study . . . 45
2.4.1.1 Standardization of sample size . . . 45
2.4.1.2 Standardization of ES digestion method . . . 46
2.4.1.3 Standardization of flow cytometric staining protocol . . . 47
2.4.1.4 Standardization of flow cytometric gating strategies . . . 50
2.4.1.5 Determining time limits for sample processing . . . 56
2.4.2 Peripheral versus endometrial immune profiles . . . 58
2.4.2.1 Flow cytometry gating and statistical analysis . . . 58
2.4.2.2 t-SNE analysis . . . 70
2.4.2.3 FlowSOM analysis . . . 72
2.4.3 Control versus infertility, RIF or RPL patients' immune profiles . . . 74
2.5 Discussion . . . 75
2.5.1 Establishment of the SOP . . . 75
2.5.2 Peripheral versus endometrial immune profiles . . . 75
2.5.3 Future plans . . . 77

3 The Role of Endometrial B Cells in Normal Endometrium and in Benign Female Reproductive Pathologies: a Systematic Review 79
3.1 Introduction . . . 79
3.1.1 B cells in mucosa-associated lymphoid tissues (MALTs) . . . 79
3.1.2 B cells in female reproductive tract (FRT) . . . 80
3.2 Chapter Aims . . . 82
3.3 Methods . . . 83
3.3.1 Search strategy . . . 83
3.3.2 Inclusion criteria and study selection . . . 84
3.3.3 Data extraction . . . 85
3.3.4 Quality assessment . . . 85
3.4 Results . . . 86
3.4.1 Study selection . . . 86
3.4.2 B cells in the normal endometrium . . . 88

3.4.3 Endometriosis . . . 92
3.4.4 Infertility, RIF and RPL . . . 95
3.4.5 Endometritis . . . 100
3.4.6 Other pathologies . . . 106
3.5 Discussion . . . 109
3.5.1 Summary of findings . . . 109
3.5.2 Possible tertiary lymphoid structures in endometrium . . . 111
3.5.3 Future directions . . . 114

4 RNA-seq Analysis of Human Endometrial B Cells During the Mid-luteal Phase 116
4.1 Introduction . . . 116
4.1.1 RNA and the transcriptome . . . 116
4.1.2 RNA-seq workflow . . . 117
4.1.2.1 RNA preparation . . . 117
4.1.2.2 Sequencing platforms . . . 118
4.1.2.3 Computational analysis . . . 121
4.1.3 Transcriptomic characterization of human endometrium . . . 124
4.1.3.1 Endometrial characteristics during the menstrual cycle . 124
4.1.3.2 Endometrial characteristics in RPL patients . . . 125
4.2 Chapter Aims . . . 127
4.3 Materials and Methods . . . 128
4.3.1 Subject recruitment . . . 128
4.3.2 RNA isolation and quantification . . . 130
4.3.2.1 Sample processing . . . 130
4.3.2.2 Cell sorting . . . 130
4.3.2.3 RNA extraction . . . 131
4.3.2.4 RNA quantification . . . 131
4.3.3 Library preparation and RNA sequencing . . . 131
4.3.4 Early analyses (undertaken by Novogene Co., Ltd) . . . 132
4.3.4.1 Quality control procedures . . . 132
4.3.4.2 Read alignment and quantification . . . 132
4.3.5 Sample variance visualization (undertaken by Mengni Shen) . . . 132
4.3.6 Differentially gene expression analysis (undertaken by Mengni Shen) 133
4.3.7 Pathway enrichment analysis (undertaken by Mengni Shen) . . . 133
4.3.7.1 GO term and KEGG analysis . . . 133
4.3.7.2 GSEA analysis . . . 134
4.4 Results . . . 135

4.4.1 Cell sorting and RNA quantification . . . 135
4.4.2 Quality control (QC) . . . 140
4.4.3 Sample variance visualization . . . 142
4.4.3.1 Correlation coefficient . . . 142
4.4.3.2 Dendrogram clustering . . . 144
4.4.3.3 Principal component analysis (PCA) . . . 144
4.4.3.4 Cook's distance . . . 147
4.4.4 Endometrial B cells gene expression analysis . . . 148
4.4.4.1 Top expression genes in endometrial B cells . . . 148
4.4.4.2 B cell specific genes in endometrial B cells . . . 149
4.4.4.3 Pathway enrichment analysis of B cell specific genes . . . 152
4.4.5 Differential gene expression analysis between controls and RPL groups . . . 166
4.4.5.1 Control versus RPL . . . 166
4.4.5.2 Intersect of the expressed genes in study groups . . . 168
4.4.5.3 Nulliparous controls versus PRPL . . . 169
4.4.5.4 PRPL versus SRPL . . . 171
4.4.5.5 Intersect of differentially expressed genes in comparison groups . . . 173
4.5 Discussion . . . 176
4.5.1 Endometrial B cells have an activated gene expression profile . . . 176
4.5.2 Limited differences in gene expression profiles between study groups 177
4.5.3 Future directions . . . 178
4.5.3.1 Endometrial B cell subtyping . . . 178
4.5.3.2 Experimental validation of RNA-seq data . . . 179
4.5.3.3 Future transcriptomic studies on endometrial B cells . . . 179

5 Analysis of Endometrial B Cell Subsets, Phenotypes and Cytokine Production 181
5.1 Introduction . . . 181
5.1.1 B cell development . . . 181
5.1.2 B cell subsets . . . 184
5.1.2.1 Transitional B cells . . . 184
5.1.2.2 Regulatory B cells . . . 185
5.1.2.3 Naïve B cells . . . 186
5.1.2.4 GC B cells . . . 187
5.1.2.5 Memory B cells . . . 190
5.1.2.6 Plasmablasts and plasma cells . . . 190

5.1.3 Endometrial B cells . . . 191
5.2 Chapter Aims . . . 192
5.3 Materials and Methods . . . 193
5.3.0.1 Subject recruitment . . . 193
5.3.0.2 Sample processing . . . 194
5.3.0.3 Heatmap analysis of endometrial B cell RNA-seq data . 195
5.3.0.4 Cell sorting . . . 195
5.3.0.5 B cell stimulation assay . . . 195
5.3.0.6 Flow cytometry analysis . . . 196
5.3.0.7 Statistical analysis . . . 198
5.4 Results . . . 199
5.4.1 endometrial B cell subset analysis . . . 199
5.4.2 Endometrial B cell residency, assessed by CD69 and CD62L expression levels . . . 202
5.4.3 The activation status of endometrial B cells, assessed by CD74, CD83 and HLA-DR expression levels . . . 204
5.4.4 Identification of endometrial Tfh cells and GC B cells . . . 206
5.4.4.1 Identification of GC B cells . . . 206
5.4.4.2 Identification of Tfh cells . . . 208
5.4.5 IL-10 and TGF-β production capabilities of peripheral and endometrial B cells . . . 210
5.4.5.1 Cell sorting . . . 210
5.4.5.2 IL-10 and TGF-β production capabilities of peripheral and endometrial B cells . . . 211
5.4.5.3 IL-10 production capacity of peripheral and endometrial $CD27^{+}CD24^{hi}$ and $CD38^{hi}CD24^{hi}$ B regulatory cells 213
5.5 Discussion . . . 215
5.5.1 A distinct phenotype of endometrial B cells compared with peripheral blood B cells . . . 215
5.5.2 Potential GC reactions in the human endometrium . . . 216
5.5.3 Peripheral and endometrial B cells are capable of IL-10 production 218

6 Summary and Future Perspectives **219**

Appendices **222**
A PIP study patient data collection template . . . 222

B Isolation and Flow Cytometry Analysis of Various Immune Cells from Human Peripheral Blood and Endometrium: an SOP that Describes the Procedures for Assessing the Feasibility of the PIP Study. 228
C Endometrial T cell RNA isolation, quantification and QC 248
D Negative controls for endometrial B cell flow cytometric analysis 257

References **261**

List of Figures

1.1 The human menstrual cycle. 20
1.2 Human embryo implantation and invasion process. 22

2.1 Peripheral and endometrial immune profiles. 37
2.2 The effect of four endometrium digestion methods on various immune cell surface markers. 47
2.3 PIP flow panel titration results. 49
2.4 Representative example of Foxp3 gating strategy. 51
2.5 Foxp3 is highly expressed in $CD3^+$ $CD4^+$ $CD25^{bright}$ $CD127^{dim}$ cells compared with other $CD3^+$ $CD4^+$ cells. 52
2.6 CD69 expression in peripheral and endometrial NK and T cell subsets. . 54
2.7 Different CD69 gating strategies in peripheral NK and T cell subsets. . . 55
2.8 The effect of blood storage on cellular activation markers' expression. . . 57
2.9 Comparison of $CD45^+$ lymphocyte subsets between peripheral blood and endometrial samples, analysed by CD56 and CD3. 59
2.10 Comparison of $CD56^+$ NK cell subsets between peripheral blood and endometrial samples, assessed by CD56 and CD16 expression. 61
2.11 Comparison of $CD3^+$ T cell subsets between peripheral blood and endometrial samples, assessed by CD4 and CD8. 63
2.12 Comparison of $CD25^{bright}$ $CD127^{dim/-}$ T regulatory cells' proportions between peripheral blood and endometrial samples. 64
2.13 Comparison of $CD69^+$ expression levels on 5 lymphocyte subsets in peripheral blood and endometrial samples. 66
2.14 t-SNE analysis of peripheral blood and endometrial immune profiles. . . . 71
2.15 FlowSOM analysis of peripheral blood and endometrial immune profiles. . 73

3.1 PRISMA flow diagram of study selection. 87
3.2 Illustration of lymphoid aggregates in human endometrium. 89

4.1 Outline of the Smart-seq2 protocol. 120
4.2 A typical computational workflow of RNA-seq data analysis. 123

4.3 Gating strategy for endometrial B cell sorting and cell proportions of endometrial B cells acquired by sorting. 136
4.4 CD127 and CD25 expression on endometrial B cells. 138
4.5 Endometrial B cell RNA quality assessment. 139
4.6 Representative figure of endometrial B cell RNA sequencing QC results (n=16). 141
4.7 Correlation coefficient analysis between 16 endometrial B cell samples. . 143
4.8 Heatmap with clustering dendrogram of euclidean distances between 16 endometrial B cell samples. 144
4.9 Visualization of principal component analysis (PCA) and auto clustering of T and B cells RNA-seq data. 146
4.10 Cook's distance of 16 endometrial B cell RNA sequencing data. 147
4.11 Heatmap of the top 20 expressed genes in endometrial B cells. 148
4.12 Heatmap of endometrial B cell-specific most highly expressed genes. . . . 150
4.13 GO term enrichment analysis of endometrial B cell-specific genes. 151
4.14 KEGG term enrichment analysis of endometrial B cell-specific genes. . . 152
4.15 A snapshot of top 9 gene set enrichment plots generated by GSEA using GO term gene sets. 155
4.16 Visualization and auto annotation of upregulated GO terms in endometrial B cells implemented by GSEA and Cytoscape. 156
4.17 Visualization of the largest GO term annotation cluster upregulated in endometrial B cells implemented by GSEA and Cytoscape. 157
4.18 A snapshot of top 9 gene set enrichment plots generated by GSEA using curated gene sets. 159
4.19 Visualization and auto annotation of upregulated curated gene sets in endometrial B cells implemented by GSEA and Cytoscape. 160
4.20 Visualization of the top 2 largest curated gene sets annotation cluster upregulated in endometrial B cells implemented by GSEA and Cytoscape. 161
4.21 A snapshot of top 9 gene set enrichment plots generated by GSEA using immunologic gene sets. 162
4.22 Visualization and auto annotation of upregulated immunologic gene sets in endometrial B cells implemented by GSEA and Cytoscape. 163
4.23 A snapshot of top 9 gene set enrichment plots generated by GSEA using hallmark gene sets. 165
4.24 Heatmap depicting differentially expressed genes between control and RPL patients. 167

4.25 Volcano plot of differentially expressed genes between control and RPL patients. . . . 168
4.26 Venn diagram representing the intersect of the expressed genes in nulliparous controls and RPL groups. . . . 169
4.27 Heatmap depicting differentially expressed genes between NULLPC and PRPL patients. . . . 170
4.28 Volcano plot of differentially expressed genes between NULLPC and PRPL patients. . . . 171
4.29 Heatmap depicting differentially expressed genes between PRPL and SRPL patients. . . . 172
4.30 Volcano plot of differentially expressed genes between PRPL and SRPL patients. . . . 173
4.31 Venn diagram representing the intersect of differentially expressed genes between NULLPC versus PRPL and PRLP versus SRPL comparison groups. 174
4.32 Gene expression level of 12 differentially expressed genes shared between NULLPC versus PRPL and PRLP versus SRPL comparison groups. . . . 175

5.1 B cell development and differentiation pathways. . . . 183
5.2 Overview of GC reactions and the phenotypic features of GC B cells and Tfh cells. . . . 189
5.3 Heatmaps of endometrial B cell markers genes expression levels. . . . 200
5.4 Flow cytometry analysis of endometrial B cell phenotype. . . . 201
5.5 Flow cytometric analysis of endometrial B cell residency, assessed by CD69 and CD62L expression levels. . . . 203
5.6 Flow cytometric analysis of the activation profile of endometrial B cells, assessed by CD74, CD83 and HLA-DR expression levels. . . . 205
5.7 Flow cytometric identification of endometrial GC B cells. . . . 207
5.8 Flow cytometric identification of endometrial Tfh cells. . . . 209
5.9 Representative figure of the gating strategy for peripheral and endometrial B cell sorting. . . . 210
5.10 Flow cytometric analysis of IL-10 and TGF-β expression levels in peripheral and endometrial B cells after stimulation. . . . 212
5.11 Flow cytometric analysis of IL-10 expression levels in stimulated peripheral and endometrial B regulatory cells. . . . 214

List of Tables

1.1 Possible endometrial immunological factors contributing to pregnancy related pathologies in humans. 24

2.1 PIP study participant information. 41
2.2 Optimal titres for reagents involved in the PIP flow panel for both PBMCs and ES single-cell digests. 43
2.3 Comparison of major immune cell population percentages in PBMCs and endometrial cells. 46
2.4 PIP study data summary. 67

3.1 Example of searching strategy in the MEDLINE database. 84
3.2 Study characteristics of papers examining B cells in the normal endometrium. 90
3.3 Study characteristics of papers examining endometrial B cells in controls and endometriosis patients. 93
3.4 Study characteristics of papers examining endometrial B cells in infertility, RIF or RPL patients. 97
3.5 Study characteristics of papers examining endometrial B cells in endometritis patients. 102
3.6 Study characteristics of papers examining endometrial B cells in controls and abnormal uterine bleeding, endometrial polyps and uterine fibroids patients. 107
3.7 Comparison of the bona fide definition of tertiary lymphoid structures with evidence from endometrial lymphoid aggregates. 113

4.1 Patient characteristics for RNA-seq samples. 129
4.2 Endometrial B cell numbers and proportions after cell sorting. 137
4.3 Summary of RNA sequencing QC results for 16 endometrial B cell samples. 142
4.4 GSEA generated top 10 marker genes for endometrial B cells. 153

5.1 Clinical characteristics of patients recruited for endometrial B cell subsets analysis. 193
5.2 Clinical characteristics of patients recruited for endometrial B cell residency and activation profile analysis. 194
5.3 Clinical characteristics of patients recruited for endometrial B cells and Tfh cells identification. 194
5.4 Clinical characteristics of patients recruited for endometrial B cells IL-10 and TGF-β production analysis. 194
5.5 10-colour flow cytometry panel for endometrial B cell subset analysis. . . 197
5.6 8-colour flow cytometry panel for endometrial B cell residency and activation analysis. 197
5.7 12-colour flow cytometry panel for Tfh and GC B cells identification. . . 198
5.8 8-colour flow cytometry panel assessing B cell phenotype and their IL-10 and TGF-β production capacity. 198

List of Abbreviations

A

APS Antiphospholipid Syndrome

B

BALT Bronchus-Associated Lymphoid Tissues

BCR B Cell Receptor

C

CSR Class Switch Recombination

D

DN Double Negative

dNK decidual Natural Killer

DP Double Positive

E

ERA Endometrial Receptivity Analysis

EVTs Extravillous Trophoblasts

F

FDR False Discovery Rate

FGF Fibroblast Growth Factor

FMO Fluorescence Minus One

FRT Female Reproductive Tract

FSH Follicle Stimulating Hormone

G

GALT Gut-Associated Lymphoid Tissue

GC Germinal Centre

GO Gene Ontology

GSEA Gene Set Enrichment Analysis

H

HLA Human Leukocyte Antigen

I

IHC Immunohistochemistry

IVF *In Vitro* Fertilization

K

KEGG Kyoto Encyclopedia of Genes and Genomes

KIRs Killer Immunoglobulin-like Receptors

L

LA Lymphoid Aggregate

LH Luteinizing Hormone

M

MALT Mucosal-Associated Lymphoid Tissue

MFI Mean Fluorescence Intensity

MHC Major Histocompatibility Complex

mRNA messenger RNA

N

NALT Nasopharyngeal-Associated Lymphoid Tissue

NGS Next Generation Sequencing

NK Natural Killer

NULLPC Nulliparous Control

P

PC Parous Control

PCA Principal Component Analysis

PGS Genetic Aneuploidy Screening

PIP Peri-implantation Immune Profiling

PRPL Primary Recurrent Pregnancy Loss

R

RIF Recurrent Implantation Failure

RINe RNA Integrity Number equivalent

rlog regularized logarithm

RPL Recurrent Pregnancy Loss

S

SAGE Serial Analysis of Gene Expression

SHM Somatic Hypermutation

SOP Standard Operating Protocol

SRPL Secondary Recurrent Pregnancy Loss

T

Tfh T follicular helper

TLS Tertiary Lymphoid Structure

Treg T regulatory cells

tRNA transfer RNA

V

VEGF Vascular Endothelial Growth Factor

vst variance stabilizing transformations

W

WHO World Health Organisation

Chapter 1

Introduction

In humans, the inability to conceive or to carry a pregnancy to term is a surprisingly frequent event, and has been recognised as a public health issue by the World Health Organisation (WHO) (WHO 2020). It affected an estimated 48 million to 186 million individuals in 2020, which is the equivalent of one in every four couples in developing countries, or 15% of reproductive-aged couples worldwide (WHO 2020). Many of these couples are affected by infertility, defined as not being able to conceive after 12 months or longer of unprotected sexual intercourse (Vander Borght and Wyns 2018, Gnoth et al. 2005). It has been widely recognised that infertility negatively impacts women's physical and mental health, causing psychological disorders such as depression and anxiety (WHO 2009, Bakhtiyar et al. 2019).

The most common intervention for infertility is *in vitro* fertilisation (IVF). In the UK in 2018, approximately 54,000 patients had in total 68,724 fresh and frozen IVF cycles (HFEA 2020). Although many couples had a successful pregnancy, the average birth rate per embryo transferred for all IVF patients remains at approximately 23% (HFEA 2020). A common complication for IVF failure is recurrent implantation failure (RIF), which has a prevalence of 5-25% in women undergoing IVF cycles (Somigliana et al. 2018). Although there is no universally agreed definition for RIF, authors have suggested definitions such as more than 3 failed embryo transfers with high-quality embryos, or the

failed transfer of 10, or more than 10, embryos in multiple transfers (Cimadomo et al. 2021, Thornhill et al. 2005). RPL is defined as the loss of two or more pregnancies before 24 weeks of gestation, and can be categorized into primary or secondary RPL (ESHRE 2018, Pillarisetty and Gupta 2020). Primary RPL (PRPL) refers to women who have experienced two or more miscarriages and have never had a live birth. In contrast, secondary RPL (SRPL) occurs in women who have had a previous live birth (ESHRE 2018, Pillarisetty and Gupta 2020).

A large proportion of infertility, RIF, and RPL cases may have a shared aetiology of embryo and fetal aneuploidy (Kort et al. 2018, Hyde and Schust 2015). However, a euploid embryo may also lead to an unsuccessful pregnancy. Randomised control trials (RCTs) have demonstrated a pregnancy rate of 70% with pre-implantation genetic screening (PGS) for aneuploidy (Donoso et al. 2007, L'Heveder et al. 2020), suggesting factors other than embryo euploidy are important in successful implantation and maintenance of early pregnancy. The causes of subfertility, RIF, and RPL (not associated with aneuploidy) are yet to be fully elucidated and maternal factors including uterine anatomic abnormalities, thrombophilias, non-receptive endometrium, and immunological factors such as dysregulation of various immune cells at the implantation site may be implicated (Stephenson and Kutteh 2007).

1.1 The Human Menstrual Cycle

The menstrual cycle is a complex, orchestrated sequence of events involving central hormone production, cyclic ovarian function, and endometrial alterations. The follicle stimulating hormone (FSH) and luteinizing hormone (LH) secreted from the anterior pituitary stimulate the ovary to produce ovarian steroid hormones, such as progesterone or estrogen/estradiol, which in turn stimulate endometrial proliferation and induce other downstream effects in the ovary (Figure 1.1). The menstrual cycle is divided into the follicular phase, ovulation, and luteal phase. The follicular phase begins from the first

day of menses until ovulation. During this phase, the ovaries typically produce one fully mature graafian follicle that has completed all the steps of folliculogenesis. Towards the end of the follicular phase, there is a sharp increase in LH. This LH surge lasts for 24-48 hours and triggers ovulation by causing the rupture of the ovarian follicle, and oocyte release from the ovary. After ovulation, the ovarian follicles continue to develop through the luteal phase and form the corpus luteum. The corpus luteum produces hormones, particularly progesterone that contributes to the morphological and functional changes in the endometrium in a process known as decidualisation. Decidualisation involves changes in endometrial stromal cells, decidual leukocytes, and vascular remodelling to maternal arteries in preparation for pregnancy (Gellersen et al. 2007, Dunn et al. 2003), which will be discussed in more detail in the next section. In the absence of pregnancy, the corpus luteum undergoes structural and functional degradation (known as luteolysis) with a reduced level of progesterone secretion towards the end of the luteal phase, and the decidualised endometrial lining is then shed during menstruation.

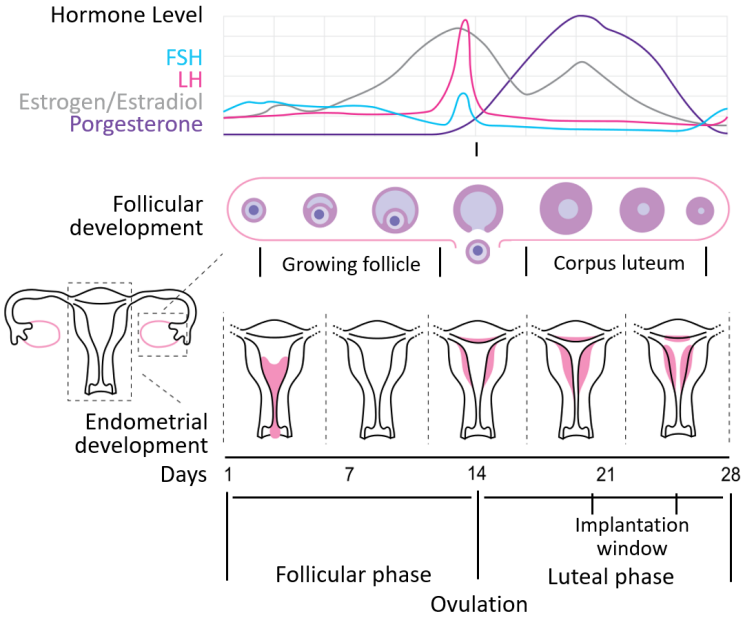

Figure 1.1: The human menstrual cycle. Diagram detailing the hormone level, follicular and endometrial development throughout the menstrual cycle. Human menstrual cycle is divided into the follicular phase, ovulation, and the luteal phase. Implantation can only happen at a certain point of the menstrual cycle, during the implantation window of the luteal phase. Figure is adapted from Isometrik, 2009.

1.2 Human Embryo Implantation

When released from the ovary, oocytes travel through the fallopian tube where they may be in direct contact with the sperm. Their fusion triggers the fertilisation process which leads to the production of the zygote. In human embryonic development, zygotes undergo rapid cell division and at around day 5-9 after fertilisation, the zygote develops into a blastocyst that reaches the uterus, ready for implantation. The Blastocyst represents a distinct embryonic structure, where an outer layer of cells, collectively called the trophectoderm, surrounds the inner cell mass and blastocoel (Figure 1.2a). Trophectoderm later forms the placenta, which supports fetal growth during pregnancy (Silverthorn 2015).

Embryo implantation consists of a series of sequential steps.

1) Apposition. The embryo positions near the implantation site with the inner mass towards the side of contact (Figure 1.2a).

2) Adhesion. The embryo attaches to the luminal endometrial epithelium. During this stage, the trophectoderm layer exhibits highly differentiated cellular functions, forming syncytiotrophoblast at the site of embryo-maternal contact (Figure 1.2b).

3) Invasion. The embryo breaches and penetrates into the maternal endometrium, which eventually surrounds the conceptus (Figure 1.2c-d). At this stage, syncytiotrophoblast, now the epithelial covering of the highly vascular embryonic placental villi, would first come into contact with maternal blood. Another subset of trophoblast, extravillous trophoblasts (EVTs), invade decidua and travel deep to the myometrium and associate with spiral arteries (Chazara et al. 2011, Moffett and Loke 2006, Jansen et al. 2020).

During the window of implantation, the endometrium transforms into a receptive status in a process known as decidualisation (Gellersen and Brosens 2014). This process is crucial in facilitating successful implantation. Under the influence of hormones (predominantly progesterone), endometrial stromal cells differentiate from fibroblast-like cells into enlarged round secretory cells. Additionally, endometrium undergoes vascular

remodelling to support the maternal blood supply to the growing conceptus, and a diverse influx of immune cells are observed in the maternal endometrium. As the main maternal-fetus interface, decidua plays an integral role in establishing immunological tolerance toward the allogeneic fetus during implantation, where a number of immune cells are in direct contact with invading trophoblasts (Figure 1.2). In the next section, the composition, phenotypes and functional of endometrial/ decidual immune cells will be discussed in detail.

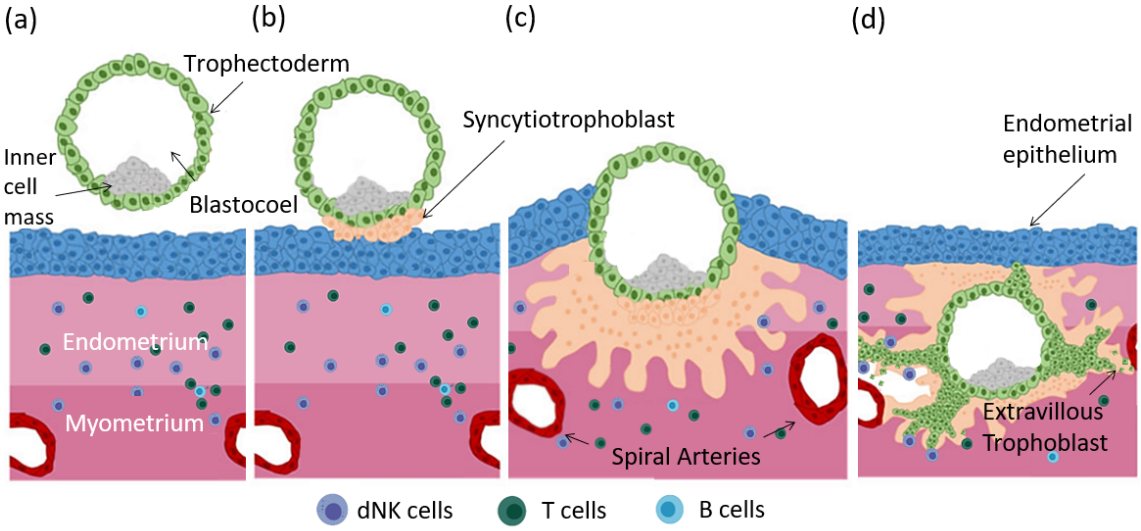

Figure 1.2: Human embryo implantation and invasion process. (a) The embryo inner mass positions towards the site of implantation. (b) The syncytiotrophoblast invades the epithelial wall of the uterus. (c) The embryo invades through the uterine wall. (d) The embryo is completed embedded into the endometrium. Extravillous trophoblasts (EVTs), that are in direct contact with uNK cells, remodel spiral arteries for successful placentation. Endometrial/ decidual NK, T and B cells are illustrated. Figure is adapted from Jansen et al., 2020.

1.3 The Role of the Maternal Immune System in Pregnancy

A fundamental function of the immune system is to protect the host against foreign substances. However, in the case of successful pregnancies, the semi-allogenic fetus

does not provoke a maternal immune response leading to fetal rejection, and it is not the result of the universal suppression of maternal immune cells. Instead, the maternal immune environment remains functional and active to support the embryo growth, with immune regulations initiated even before the implantation occurs. Understanding the maternal immune cell populations, and how they are regulated to achieve maternal immune tolerance towards the semi-allogenic fetus, has been the key research focus for reproductive immunologists.

The maternal immune system undergoes dynamic alternations to accommodate different embryonic developmental stages throughout pregnancy. Implantation and placentation involve an initial pro-inflammatory response, shortly after, anti-inflammatory decidual cells emerge to support the rapid fetal growth. At a later gestational age, a pro-inflammatory immune environment is established to induce labour (Mor et al. 2017). At each stage, immune system dysfunction may contribute to adverse pregnancy outcomes, although the exact mechanism has yet to be elucidated, key findings are detailed in Table 1.1. Interestingly, immune cell defects during implantation have been implicated in pregnancy pathologies that occur during later stages of pregnancy (i.e. pre-eclampsia) (Laresgoiti-Servitje et al. 2010), highlighting the importance of understanding maternal endometrial immune environment at the implantation site.

Trimester	Subfertility/ Pathology	Possible Endometrial/ Decidual Immunological Factor
1st	RIF	Autoimmune disease (e.g. antiphospholipid syndrome (Santos et al., 2017)); dNK number ↑; altered dNK subset composition and function (Guo et al., 2021); insufficient interaction between dNK receptor with HLA-C (Colucci, 2017); altered CD8 T cell phenotype and function (Southcombe et al., 2017); endometrial Treg number ↓ (Jiang et al., 2014); altered endometrial cytokines (Saini et al., 2011)
	Early RPL	
2nd	Late RPL	
3rd	Pre-eclampsia	Autoimmune disease; abnormal interaction between dNK receptor with HLA-C (Taylor and Sasser, 2017), endometrial Treg number ↓ (Rahimzadeh et al., 2016)
	IUGR	Autoimmune disease; dNK dysfunction (Fu et al., 2017)
	Prematurity	
	Neonatal disorders	Autoimmune disease (Chang, 2012)

Table 1.1: Possible endometrial immunological factors contributing to pregnancy related pathologies in humans. RIF, recurrent implantation failure; RPL, recurrent pregnancy loss; IUGR, Intrauterine growth restriction; dNK, decidual natural killer cells.

1.3.1 Maternal Immune Cells in Embryo Implantation

At the embryo implantation site, several immune cell populations are present, including natural killer (NK) cells, T and B lymphocytes, neutrophils, eosinophils, macrophages and mast cells, with NK and T cells being the most abundant endometrial immune cell subsets (Salamonsen and Lathbury 2000). Throughout the menstrual cycle, the endometrial immune cell composition fluctuates and cellular phenotypes change in response to hormonal signals (Wira et al. 2015). Compared with the follicular phase, an increased proportion of NK cells and a decreased proportion of T cells are seen in the mid-luteal phase, participating in the development of a receptive endometrium during the window of implantation (Flynn et al. 2000, Wira et al. 2015). A recent large-scale single cell sequencing study performed on human endometrium collected across menstrual cycles illustrated that mid-luteal endometrial NK cells possess a more diverse repertoire of both

activating and inhibitory NK receptors, that are responsible for major histocompatibility complex (MHC) recognition (Wang et al. 2020). This study highlighted the functional involvement of NK cells in embryo implantation. For endometrial B cells, their frequency does not seem to fluctuate throughout the menstrual cycle, typically accounting for $<5\%$ of all $CD45^{+}$ immune cells (Klentzeris et al. 1992, Chen et al. 1995, Antsiferova et al. 2005). Recent evidence from a single cell sequencing study illustrated the presence of naive B cells in the mid-luteal phase endometrium, along with three NK cell subsets, monocytes and macrophage/ dendritic cells (Lucas et al. 2020). However, the amount of data pertaining to immune cells obtained from these broader tissue atlas single cell studies has been limited in expanding our understanding of the endometrial immune environment, as the majority of endometrial cells are stromal and epithelial cells, and no single cell sequencing study has yet been undertaken specifically on isolated endometrial immune cells. Our current knowledge on endometrial NK, T and B cells are discussed in the following sections.

1.3.1.1 Endometrial NK cells

Endometrial NK cells are the most predominant immune cells in peri-implantation endometrium. Identified by $CD56^{+}$ ($CD56^{dim}$ or $CD56^{bright}$), endometrial NK cells typically account for $>60\%$ of total immune cells (Wira et al. 2015, Lee et al. 2011). Different NK cell subsets have different phenotypes and functions, especially in terms of their cytotoxicity and secretory cytokine profiles. $CD56^{dim}CD16^{bright}$ NK cells have significantly higher cytotoxicity than $CD56^{bright}CD16^{-}$ NK cells, and contain more cytolytic granules (Poli et al. 2009, Nagler et al. 1989, Cooper et al. 2001). High levels of CD16 expression enabled $CD56^{dim}CD16^{bright}$ NK cells to be efficient mediators of antibody-dependent cellular cytotoxicity, which is only partially enabled in $CD56^{bright}CD16^{dim}$ NK cells, and disabled in $CD56^{bright}CD16^{-}$ NK cells (Poli et al. 2009, Nagler et al. 1989, Cooper et al. 2001). With lower cytotoxicity, $CD56^{bright}CD16^{-}$ NK cells produce significantly more cytokines (Cooper et al. 2001); up to 30 times more IFN-γ upon stimulation

compared with $CD56^{dim}CD16^{bright}$ NK cells (Fehniger et al. 1999). IFN-γ play critical roles in early pregnancy by initiating endometrial vasculature remodeling and angiogenesis at the implantation site (Murphy et al. 2009). Apart from IFN-γ, $CD56^{bright}CD16^{-}$ NK cells also produce IL-10, IL-13, TNF-α, *etc.* (Fehniger et al. 1999). In human endometrium, most NK cells are $CD56^{bright}CD16^{-}$ NK cells (Lee et al. 2011, Manaster and Mandelboim 2008). When implantation occurs, they differentiate into decidual NK (dNK) cells, which play pivotal roles in trophoblast invasion and the maintenance of successful pregnancy (Bulmer and Lash 2019, Lee et al. 2011).

dNK cells express killer immunoglobulin-like receptors (KIRs) on their membrane which bind to human leukocyte antigen (HLA)-C present on the EVTs of the placenta. The invasion process puts EVTs in direct contact with dNK cells in early gestation (Figure 1.2d), forming HLA-C KIR receptor-ligand complex which has been widely characterised by genetic analysis (Vento-Tormo et al. 2018, Hiby et al. 2010, Díaz-Hernández et al. 2021), with certain combinations associated with disorders such as RPL, pre-eclampsia and fetal growth restriction at a later stage of pregnancy (Hiby et al. 2010, Wallace et al. 2012). Apart from their interaction with trophoblasts, dNKs also produce various angiogenic factors and cytokines that favour implantation and placentation. For example, dNK cells have been implicated in spiral artery remodeling independent of EVTs, contributing to the maternal-fetal interface establishment prior to EVTs invasion (Craven et al. 1998, Smith et al. 2009).

1.3.1.2 Endometrial T cells

The second most predominant endometrial immune cell population is the T cell. Identified by $CD3^{+}$, T cells typically account for 30-50% of $CD45^{+}$ lymphocytes (Wira et al. 2015, Lee et al. 2011). Within the T cell populations, 45-75% are $CD8^{+}$ T cells and 30-45% are $CD4^{+}$ T cells, minor cell populations of CD4 CD8 $^{\text{double positive}}$ T cells (DP T cells), CD4 CD8 $^{\text{double negative}}$ T cells (DN T cells) and $CD3^{+}CD56^{+}$ NKT cells are also present in the human endometrium(Nancy and Erlebacher 2014, Tilburgs et al. 2010).

$CD8^+$ T cells, known as cytotoxic T cells, are functionally important in protecting the host against infected or malignant cells. While at the implantation site, their cytotoxicity is believed to be suppressed, possibly by estradiol and TGF-β (the latter is abundantly expressed in mid-luteal endometrium under hormonal control) (Lee et al. 2011, Shen et al. 2021). For $CD4^+$ T cells, there are three main cell subsets, Th1, Th2 and Th17, each regulated by different transcription factors they express (T-bet and STAT-1; GATA-3 and STAT-6; RORγT and STAT-3 respectively), and conferring different functionalities. Th1 cells are the primary $CD4^+$ T cells that drive inflammation and allograft rejection, therefore long considered as a major threat to embryo implantation and the maintenance of pregnancy. Th2 cells, on the other hand, appear to be anti-inflammation, and are able to provide a much less embryotoxic differentiation state for $CD4^+$ T cells. They have also been shown to repress Th1 cells differentiation and function. Th17 cells produce cytokines such as IL-17, and play important roles in inflammation induction (Nancy and Erlebacher 2014). Due to their different roles in the immune system, Th2-skewing of the T cell response was proposed for successful pregnancies. However, this idea has been proven to be over simplistic as Th1, Th2, Th17 cells are highly interactive and a fine balance of Th1/Th2/Th17 is required in successful implantation (Nancy and Erlebacher 2014, Saito et al. 2010).

Apart from Th1, Th2 and Th17 cells, an additional subset of $CD4^+$ T cells are regulatory T cells (Treg), Treg cells are regulated by its signature transcription factor Foxp3, and can be identified by surface expression of $CD25^{bright}$ $CD127^{dim/-}$ (Fontenot et al. 2003, Liu et al. 2006). They are crucial mediators in immune tolerance and need to be presented in sufficient numbers in the endometrium to ensure implantation success (Sharma 2014, Robertson and Moldenhauer 2014). Mice studies demonstrated that in allogeneic mating, the absence of maternal Tregs leads to gestation failure due to immunological rejection of the fetus (Aluvihare et al. 2004), and pregnancies were the most vulnerable when Tregs were depleted in the pre- and peri-implantation phase, while in late pregnancy, Treg depletion had no effect (Zenclussen et al. 2005, Shima

et al. 2010). Treg dynamics are essential in facilitating successful implantation and the maintenance of early pregnancy in mice, which may mirror those in human pregnancy.

1.3.1.3 Endometrial B cells

Studies investigating B cell number, phenotype and function in the human endometrium are scarce. To date, there are no data on endometrial B cell phenotypic subsets or function, and data is conflicting as to whether altered B cell numbers are associated with infertility, RIF and RPL (Lachapelle et al. 1996, Quenby et al. 1999). However, in human decidua collected from the third trimester, functionally altered B cells are implicated in pregnancy complications associated with preterm labour (Huang et al. 2017). Considering the vital roles of B cells in other mucosal immune environments (Vajdy 2006, McGhee and Fujihashi 2012, Ruddle and Akirav 2009), and that reproductive complications such as infertility and endometriosis have been associated with a range of autoimmune diseases (which typically result from an expanded population of autoreactive B cells) (Shigesi et al. 2019, Rawlings et al. 2017, Hershberg and Luning Prak 2015, Khizroeva et al. 2019), endometrial B cells could be an active player at the implantation site.

1.3.1.4 Other immune cells

Apart from NK, T and B cells, other immune cells are also present at the implantation site, help to facilitate successful pregnancy. For example, macrophage depletion in mice causes implantation failure due to the substantial disruption of the luteal microvascular network and decreased progesterone production in the corpus luteum (Care et al. 2013). In human embryo implantation and early pregnancy, decidual macrophages are involved in a number of physiological and biological processes, such as angiogenesis, spiral artery remodeling, EVTs invasion, and immunomodulation via the production of various factors (vascular endothelial growth factor (VEGF), fibroblast growth factor (FGF), IL-10, etc.) (Ning et al. 2016, Yao et al. 2019). Additionally, dendritic cells

are implicated in maternal-fetal immune tolerance establishment and pregnancy maintenance (Tagliani and Erlebacher 2011, Collins et al. 2009). Dendritic cells are professional antigen-presenting cells and in early pregnancy dendritic cells gradually present low levels of antigens to T cells, resulting in the activation and expansion of Tregs; whereas in organ transplantation, high levels of antigens are presented, resulting in effector T cell expansion that contributes to the subsequent immune rejection (Mor et al. 2017).

In the following chapters of this DPhil thesis, the frequencies and phenotypes of endometrial immune cells (NK, T and B cells), and their association with reproductive pathologies will be discussed in detail, and endometrial B cells are characterised for the first time, as detailed in the following thesis aims section.

1.4 Aims of this Thesis

In recent years, several attempts have been made to understand immune cell involvement in normal endometrial as well as how immune cells are implicated in infertility, RIF and RPL (Diao et al. 2020, Lédée et al. 2020, Kuon et al. 2015). However, there are wide discrepancies in study designs, and no research has been performed on endometrial B cells, despite its key role in the adaptive and mucosal immune system (Vajdy 2006, McGhee and Fujihashi 2012, Ruddle and Akirav 2009). To date, B cell frequency, phenotype, and function has not yet been properly characterised in the human endometrium.

To address the gaps in knowledge in the field, this thesis presents the four following chapters:

Chapter 2 proposes a well-designed immune profiling protocol assessing the peripheral and endometrial immune cell (NK, T and B cells) frequencies, phenotype and activation status (measured by CD69) in patients with a history of infertility, RIF or RPL during the mid-luteal phase, and investigates immune differences between infertility, RIF or RPL patients' peripheral and endometrial samples compared with controls.

Chapter 3 presents a systematic review summarising the existing knowledge of endometrial B cells in reproductive pathologies.

Chapter 4 investigates the endometrial B cell transcriptome by performing a RNA-seqencing analysis of B cells isolated from the mid-luteal phase endometrium of RPL patients and healthy controls.

Chapter 5 investigates which B cell subsets are present in the mid-luteal endometrium using flow cytometry. Additionally, endometrial B cell phenotype (assessed by tissue residency and MHC activation related markers) and cytokine production capacity (IL-10 and TGF-β) are compared with that of matched circulating B cells.

Chapter 2

The Peri-implantation Immune Profiling (PIP) Study

2.1 Introduction

2.1.1 Current evidence for diagnosis and treatment of immune dysfunction associated infertility, RIF and RPL

Advances in reproductive science have identified a number of maternal risk factors for RIF, including lifestyle factors (smoking and obesity), uterine factors (septate uterus, endometrial polyps, submucosal fibroids, intramural fibroids, intrauterine adhesions, adenomyosis, endometriosis and hydrosalpinx), thrombophilias, and immunological factors (Vomstein et al. 2020, Somigliana et al. 2018). Many of these factors are also associated with infertility and RPL (Ford and Schust 2009, Olooto et al. 2012). The majority of these etiologies can be diagnosed by hysteroscopy, laparoscopy or blood test. While for immunological factors, although there are proven instances of autoimmune causing RIF, notably the anti-phospholipid syndrome (APS) (Rai et al. 1995, Kwak-Kim et al. 2013), many other infertility, RIF and RPL patients do not have observable autoimmune diseases, but harbour an altered immune profile at the implantation site (Fukui et al.

2017, Ticconi et al. 2019, Lachapelle et al. 1996). Most of the previous studies that identified such alternations in the immune cell subset's frequency, phenotype and function in patients with a history of infertility, RIF or RPL (Fukui et al. 2017, Ticconi et al. 2019, Lachapelle et al. 1996) have only focused on a single cell type (most frequently NK cells or Treg cells), and have failed to provide a comprehensive assessment of the immune cell subsets at the implantation site in well-defined cohorts. How to perform such assessment, and whether immune alterations can be utilized in the diagnosis and importantly the treatment of immune-mediated infertility, RIF and RPL are still debated (Lédée et al. 2020, Diao et al. 2020, Moffett and Shreeve 2015).

While in practice, many fertility clinics offer testing for endometrial NK cells, and offer treatments including corticosteroids, immunoglobulin, intralipids, biologic agents (e.g.: anti-TNFα therapy) to treat 'abnormal' results (Moffett and Shreeve 2015, Sacks 2015). Using only one or two parameters to assess the endometrial immune profile, these tests have oversimplified the immune interactions at the implantation site, which is highly dynamic and complex, and involves many different types of immune cells (Lee et al. 2011). To deliver a more personalized IVF treatment approach and increase associated IVF success rates, recent attempts have been made at assessing 5 or more immune parameters in the mid-luteal phase endometrium (Diao et al. 2020, Lédée et al. 2020). However, without a standard operating procedure (SOP), variations in patient recruitment, sample handling (collection, transport and storage), and data analysis could lead to unreliable results and makes it impractical to implement in practice.

Aside from endometrial immune profiling, altered peripheral immune cell parameters have also been associated with RIF, RPL and infertility (Beer et al. 1996, Alhalabi et al. 2011, Chernyshov et al. 2010). Many fertility clinics offer testing for a variety of peripheral blood immune cell parameters (NK cell numbers, cytotoxicity assays, Tregs, cytokine assays, *etc.*). and treatment options for patients with altered peripheral immune profiles (Moffett and Shreeve 2015, Sacks 2015). However, considering the immune cell populations in the endometrium are phenotypically and functionally different to those in

the periphery (detailed in Chaper 2.1.3), blood testing may be of limited value for the diagnosis of immune-mediated RIF, RPL and infertility.

2.1.2 Endometrial immune cells and their association with infertility, RIF or RPL

2.1.2.1 Endometrial NK cells

In infertility, RIF or RPL patients, a number of studies have demonstrated a significantly higher percentage/ density of endometrial NK cells compared with controls (Marron et al. 2019, El-Azzamy et al. 2018, Harrity et al. 2019). However, IHC and flow cytometric studies are also present where researchers did not observe an altered endometrial NK cell count, or a reduced NK cell abundance in infertility, RIF or RPL patients compared with controls (Donoghue et al. 2019, Matteo et al. 2007, Lucas et al. 2020). A systematic review and meta-analyses of two studies that evaluated endometrial NK cells frequencies in infertile women versus fertile controls, and six studies that evaluated endometrial NK cells frequencies in RPL versus controls also failed to find significant difference between comparison groups (Seshadri and Sunkara 2014). To date, there is no consensus as to whether an altered endometrial NK cell frequency is associated with infertility, RIF or RPL. Furthermore, well-designed studies are scarce in evaluating the proportion of different endometrial NK cell subsets in both infertility, RIF or RPL patients and controls, as most studies only used immunohistochemistry (IHC), often analysing just one or two markers to identify cell types when endometrial immune profiling.

2.1.2.2 Endometrial T cells

Differences in T cell subset frequencies and phenotypes have also been associated with infertility, RIF and RPL. In RPL, an altered peri-implantation $CD8^+$ tissue resident memory T cell phenotype has been described in the endometrium, more specifically on the tissue resident memory $CD8^+$ T cell subset (Southcombe et al. 2017). However,

data is conflicting as to whether there is an altered frequency of $CD8^+$ T cells at the implantation site (Southcombe et al. 2017, Marron and Harrity 2019, Klentzeris et al. 1994).

For $CD4^+$ T cells, data is also conflicting as to whether there is an altered abundance level of $CD4^+$ T cells at the implantation sites in infertility, RIF or RPL patients versus controls (Southcombe et al. 2017, Marron and Harrity 2019, Klentzeris et al. 1994). Specifically on Treg cells, a recent systematic review showed there is a significantly decreased level of Treg cells in the decidua of pregnant women with RPL compared to controls (Keller et al. 2020). However, data is conflicting as to whether there is a decreased level of Treg cells at the implantation sites in infertility, RIF or RPL patients versus controls (Abdolmohammadi et al. 2019, Southcombe et al. 2017, Marron and Harrity 2019).

Other $CD3^+$ T cell subsets are DP T cells, DN T cells and $CD3^+CD56^+$ NKT cells. Their presence have been identified in the decidua (Tilburgs et al. 2010), and for certain subpopulations such as $\gamma\delta$ DN T cells and invariant $CD3^+CD56^+$ NKT cells, their involvement in human pregnancy has been studied (Chapman et al. 2015, Boyson et al. 2002). However, the frequencies of DP T cells, DN T cells and $CD3^+CD56^+$ NKT cells at the implantation site have not been properly investigated, either in infertility, RIF or RPL patients or controls.

2.1.2.3 Endometrial B cells

Despite the commonly reported claim that B cells are rare or absent in the endometrium (Lee et al. 2011, Schumacher et al. 2018, Guzman-Genuino and Diener 2017), several IHC and flow cytometric immune profiling studies have identified B cells (by the B cell markers $CD19^+$, $CD20^+$ or $CD22^+$) throughout the menstrual cycle, typically accounting for $<5\%$ of all $CD45^+$ immune cells. (Klentzeris et al. 1992, Chen et al. 1995, Antsiferova et al. 2005). Current data is conflicting as to whether an altered B cell frequency is present in infertility, RIF or RPL patients compared with controls, and could benefit

from well-designed studies (Michimata et al. 2002, Lachapelle et al. 1996, Quenby et al. 1999). A systematic review of B cell frequencies in reproductive pathologies including infertility, RIF and RPL is presented in Chapter 3.4.4.

2.1.3 Differences between peripheral and endometrial immune cells

Aside from endometrial immune cell profiling, many fertility clinics offer testing for a variety of peripheral blood immune cell parameters (NK cell numbers, NK cell cytotoxicity assays, Tregs numbers, cytokine assays, *etc.*). and treatment options for 'abnormal' results (Moffett and Shreeve 2015, Sacks 2015). However, this blood testing may be of no value for the diagnosis and treatment of RIF, RPL and infertility considering there are significant differences between the immune cell populations found in the peri-implantation endometrium and those circulating in the peripheral blood. As illustrated in Figure 2.1, throughout the menstrual cycle, endometrial immune cell populations typically have higher levels of $CD56^{+}$ NK cells and lower levels of $CD3^{+}$ T cells compared with their circulating counterparts. B cells are also present in both the peripheral blood and the endometrium, however, their frequencies have not been properly compared between these the peripheral blood and the endometrium. For NK and T cell subsets, $CD56^{bright}CD16^{-}$ NK cells are more abundant in the endometrium, while $CD56^{dim}CD16^{bright}$ NK cells are more abundant in the peripheral blood, $CD4^{+}$ T cells are more abundant in the peripheral blood compared with the endometrium (Lee et al. 2011). Apart from the proportional differences, these immune cell subsets also exhibit different functionalities in the endometrial immune environment. For example, endometrial NK cells have distinct KIR expression pattern compared with peripheral NK cells, which is crucial in mediating trophoblast invasion in the early pregnancy (Jacobs et al. 2001, Moffett et al. 2016).

The origin of endometrial immune cells is not known, it has been suggested that these immune cells themselves, or their precursors, are recruited to the endometrium from the

circulation during the luteal phase of the menstrual cycle(Chantakru et al. 2002, Carlino et al. 2008, Male et al. 2010). However, this theory has been questioned. For example, endometrial NK cells do not express the necessary chemokine receptors in neither the follicular nor the luteal phase, making migration from the periphery unlikely (Manaster et al. 2008). Additionally, a number of studies have suggested that endometrial $CD34^{+}$ hematopoietic stem cells can differentiate into endometrial NK cells upon the interaction with stromal cells (Vacca et al. 2011, Thiruchelvam et al. 2016).

To date, evidence of the direct involvement of peripheral immune cells in early pregnancy is scarce (apart from in systemic diseases, such as certain autoimmune disorders) (Rai et al. 1995). And due to the above mentioned difference between peripheral and endometrial immune cells, whether peripheral immune profile could represent the immune status at the implantation site is questionable. Current studies rarely assess the relationship between endometrial and peripheral immune profile from the same individual, and data is conflicting as to whether there is an association between an altered peripheral immune profile with infertility, RIF or RPL (Winger and Reed 2011, Coulam and Roussev 2003, Sharma 2014). Additionally, many of the existing publications fail to provide absolute cell counts (cells/ml) for the peripheral immune cell subsets being assessed, therefore could not serve as a reference range for clinical practice.

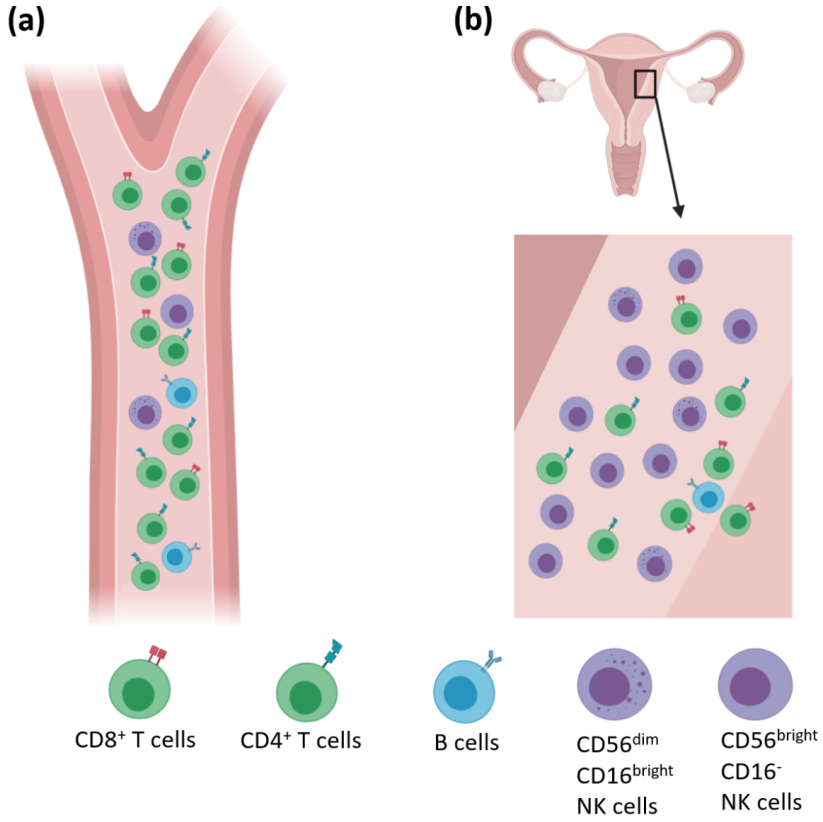

Figure 2.1: Peripheral and endometrial immune profiles. (a), Peripheral immune profile. (b), Endometrial immune profile. The proportions of 5 immune cell subsets, $CD8^+$ T cells, $CD4^+$ T cells, $CD19^+$ B cells, $CD56^{dim}CD16^{bright}$ NK cells and $CD56^{bright}CD16^-$ NK cells, are shown.

2.1.4 CD69 as a marker of tissue residency and cell activation

Aside from altered endometrial and/or peripheral blood immune cells frequencies and phenotypic profiles, the activation status of immune cells, typically assessed by the expression level of surface CD69, are suggested to be linked with infertility, RIF or RPL. CD69 is a human transmembrane C-Type lectin. As the earliest inducible cell surface glycoprotein after cell activation, it is recognized as a classical early marker of lymphocyte activation (Ziegler et al. 1993, Cibrián and Sánchez-Madrid 2017). Increased CD69 expression by peripheral NK and T cells has been suggested by a number of studies to be associated with infertility, RIF or RPL (Thum et al. 2008, Marron et al. 2019, Ghafourian et al. 2014). Additionally, CD69 has been suggested to exhibit a regulatory role during the inflammatory response, and regulates Th1/Th17/Treg balance by controlling Th cells differentiation (Sancho et al. 2005, Cibrián and Sánchez-Madrid 2017,

Ziegler et al. 1993).

Apart from its role as a cell activation marker, CD69 can also been used as a tissue resident marker (Sancho et al. 2005). Highly expressed in a number of tissue resident immune cells, CD69 expression promotes the retention and the survival of tissue resident immune cells (Mackay and Kallies 2017, Sathaliyawala et al. 2013, Allie et al. 2019).

Although existing research has shown that the presence of endometrial immune cells at the implantation site is vital in facilitating successful implantation and the maintenance of pregnancy, whether changes in their frequency, phenotype and function could be linked to infertility, RIF or RPL is still debatable. To help answer this question, here we present the PIP study, which is a well-designed clinical study hoping to provide a SOP for comprehensive peripheral and endometrial immune profiling by flow cytometry. By recruiting fertile controls, infertility patients, RIF patients and RPL patients, we aim to firstly define the normality of peripheral and endometrial immune parameters, secondly, to compare the immune parameters of controls versus infertility, RIF or RPL patients. To achieve this, we recruited all women under the age of 40 (at time of egg collection) from the Wolfson Fertility Centre, Oxford Fertility or John Radcliffe Hospital Recurrent Miscarriage Clinic who are eligible and wish to recruit to the study. Women who are undergoing a first cycle or second cycle of IVF for male factor subfertility requiring Intracytoplasmic Sperm injection (ICSI) will be recruited. Those women who go on to have a live birth will be considered to be fertile controls (as their reason for IVF was a male factor and pregnancy was achieved at the first attempt). Women with a history of RIF (RIF group) or a history of RPL (RPL group), and any women who is unable to establish a clinical pregnancy for at least 1 year (infertility group) will also be recruited. We wish to recruit broadly to the study 250 women overall to evaluate whether infertility, RIF or RPL patients possess an altered immune profile compared with controls. Further studies will focus on different patient groups, and power calculation will be utilised to determine the sample size once sufficient pilot data is obtained.

2.2 Chapter Aims

This chapter investigates the association between infertility, RIF or RPL and the variations in numbers or phenotypes of NK, T, B cells in human endometrium during the implantation window. I hypothesise that altered immune profiles in endometrium, but not blood, are associated with infertility, RIF or RPL.

Objectives:

1) Establish a SOP for profiling immune parameters in endometrial and blood samples.

2) Describe the normal variation in blood and endometrial immune cell populations in the mid-luteal phase of the menstrual cycle of nulliparous fertile women (control group) prior to IVF.

3) Identify differences in immune cell frequencies, phenotype and activation status between controls and infertility, RIF or RPL patients.

4) Identify if there is a relationship between endometrial and peripheral blood immune cell parameters.

2.3 Materials and Methods

Materials and methods for the PIP study SOP work-up are not shown. The work-up includes the standardization of sample size, ES digestion method, flow cytometric staining protocol and gating strategies and determining the time limits for sample processing.

Materials and methods for the PIP study are detailed below.

2.3.1 Subject recruitment

The study was approved by the Oxford Research Ethics Committee C (ref: 18/SC/0216) and registered on ClinicalTrials. gov (ClinicalTrials.gov Identifier: NCT03660735). All participants gave written informed consent.

All recruits are patients attending Wolfson Fertility Centre, Oxford Fertility or John Radcliffe Hospital Recurrent Miscarriage Clinic between 2018 to 2020. Both blood and endometrial samples were collected between 7–11 days post LH pre-ovulatory surge in the menstrual cycle before IVF commenced. All women with RPL had thyroid function screening, antiphospholipid screen (cardiolipin Ab, anti-beta-2 glycoprotein and DRVVT), thrombophilia screening (including Factor V Leiden, prothrombin gene mutation, Antithrombin III, protein C, protein S) and uterine structural screening (identified by ultrasound scan or hysteroscopy). All screening results along with other patient information including female demographics, male demographics, semen analysis on the day of insemination, current treatment details and outcome data were collected using PIP study patient data collection survey (Appendix A). Key participant information is presented in Table 2.1.

ID	Age (yrs)	BMI	Cycle length (days)	Reason for IVF	Number of previous miscarriage	Number of previous live birth	Cycle No.	Pregnancy outcome (in the subsequent IVF cycle)	Diagnosed with abnormal thyroid function or APS?	Any uterine structure abnormality (Endometriosis, adenomyosis, *etc.*)?
RIF patients										
A	37	21.9	26-30	Tubal factor	0	0	3	Live birth	No	Endometriosis
B	36	28.3	30-31	Unexplained	0	0	3	Ectopic pregnancy	Hypothyroidism	No
C	34	22.5	28-32	Male factor	1	0	3	Not pregnant	No	No
D	38	21.1	30-34	Unexplained infertility	0	0	4	Ongoing pregnancy	No	No
Infertility patients										
E	32	18.4	28-30	Unexplained infertility	1	0	1	No live birth, uterine test positive	No	No
F	37	26.4	29-31	Unexplained infertility	0	0	2	Live birth	No	No
RPL patients										
G	33	20.9	28	RPL	3	0	-	-	-	No
H	33	28.2	36	RPL	3	0	-	Ongoing pregnancy	APS	No
Others										
I	31	27.6	30-33	Male factor	0	0	2	Not pregnant	No	No
J	35	21.5	21	Male factor	0	0	2	Not pregnant	No	No
K	38	26.6	-	Male factor	1	0	1	No live birth, uterine test positive	No	No
L	40	25.4	25-31	Tubal factor	0	0	2	Not pregnant	No	Endometriosis
M	34	-	25-28	Uterine fibroids	0	0	-	Not pregnant	No	Uterine fibroids
N	34	22.3	28-35	Tubal factor	0	0	2	Not pregnant	No	Endometriosis
O	37	23.3	28-35	Male factor & tubal factor	1	0	2	Pregnancy loss	Hypothyroidism	No

Table 2.1: PIP study participant information. BMI, body mass index; RPL, recurrent pregnancy loss.

2.3.2 PBMCs isolation

For each woman enrolled in the study, 3 x 4.5 ml venous blood samples were obtained during the mid-luteal phase of the menstrual cycle prior to IVF. All samples were couriered to Nuffield Department of Women's and Reproductive Health, University of Oxford within 6 hours. PBMCs will be prepared by density gradient centrifugation using Lymphoprep^{TM} (Alere Technologies, USA) from 2 x 4.5 ml Lithium/Sodium Heparin vacutainer collected blood samples according to manufacturer's instruction. To enable cell analysis without variation caused by patient hydration levels, an absolute cell count (immune cells per millilitre whole blood) was obtained using Precision Count Beads^{TM} (Biolegend, USA) according to manufacturer's instruction. Additionally, 1 x 4.5 ml EDTA vacutainer collected blood samples were centrifuged at 2000 x g, 10 minutes at room temperature for plasma isolation.

2.3.3 Endometrial biopsy processing

For each woman enrolled in the study, ES with a minimal size of 5mm^3 was also collected during the mid-luteal phase prior to IVF, and couriered to Nuffield Department of Women's and Reproductive Health, University of Oxford within 6 hours. Upon receipt, mucus was removed and ES tissues were cut into 1mm^3 fragments using a scalpel. ES tissue fragments were digested using 100 μg/ml DNase I and 2mg/ml Collagenase D in Digestion Medium (Dulbecco's Modified Eagle's Medium + 10% Fetal bovine serum) for 30 minutes at 37°C in a shaking incubator. Next, tissue digests were passed through sequential 70 μm and 40 μm cell strainers, run-though was collected and centrifuged for 10 minutes at 300 x g. Supernatant was aspirated and the cell pellet was re-suspended in 1 ml PBS. Cell counting was performed using a hemocytometer.

2.3.4 Flow cytometry analysis

After obtaining single-cell suspensions from PBMCs and ES tissue samples, 2 million cells were stained for flow cytometry analysis. An 11-colour panel shown in Table 2.2 was used in the PIP study. This flow panel will be referred to as the "PIP flow panel" in the following sections. After staining and flow acquisition, all flow data was analysed according to the established SOP using FlowJo v10 (Appendix B).

Reagents	Clone	Fluorophore	Concentration (µg/ml)	
			PBMCs	HECs
anti-CD45	HI30	BV650™	0.5	
anti-CD3	UCHT1	APC/Fire™ 750	12	
anti-CD56	HCD56	BV421™	3.6	1.8
anti-CD4	OKT4	FITC	16	
anti-CD8a	RPA-T8	BV711™	1.5	
anti-CD16	3G8	BV785™	7.2	
anti-CD25	BC96	PE	3	1
anti-CD127	A019D5	APC	3	
anti-CD19	HIB19	PE/Cy7	4	
anti-CD69	FN50	PE/DAZZLE™ 594	4	
Zombie Aqua™	-	BV510™	0.1µl/ 2 x 10^6 cells	

Table 2.2: Optimal titres for reagents involved in the PIP flow panel for both PBMCs and ES single-cell digests. All reagents are from Biolegend, USA.

2.3.4.1 t-SNE plot

Apart from applying standard gating strategies, t-SNE plot and FlowSOM analysis were performed on PIP flow dataset using FlowJo v10. t-SNE analysis was performed on $CD45^+$ live singlet population (PBMCs $CD45^+$ live singlet population was downsampled to 30,000 events to reduce the computational cost). Compensated parameters CD3, CD4, CD8, CD25, CD127, CD56, CD16, CD19 and CD69 were selected. Default settings on interactions, perplexity, learning rate, and theta were applied. After the t-SNE plot was generated, all major immune cell subsets ($CD3^+$ T cells, $CD3^+CD4^+$

T cells, $CD3^+CD8^+$ T cells, $CD3^+CD4^+CD25^{high}CD127^{low}$ T cells, $CD56^+$ NK cells, $CD56^{bright}CD16^{dim}$ NK cells, $CD56^{bright}CD16^{dim}$ NK cells, $CD56^{dim}CD16^{bright}$ NK cells, $CD56^+CD3^+$ NKT cells, $CD19^+$ B cells were overlayed in the t-SNE space. t-SNE and downsampling were performed using FlowJo plugins t-SNE (within FlowJo v10.5) and Downsample (v3.3).

2.3.4.2 FlowSOM

FlowSOM was performed on $CD45^+$ live singlet population (PBMCs $CD45^+$ live singlet population was downsampled to 30,000 events to reduce the computational cost). Compensated parameters CD3, CD4, CD8, CD25, CD127, CD56, CD16, CD19 and CD69 were selected. FlowSOM minimal spanning tree plot and FlowSOM heatmaps (with 8 meta-clusters and 10 x 10 SOM grid) were generated. Seed was set randomly. Additionally, FlowSOM heatmap for 8 meta-clusters and the size of each cluster were integrated in the heatmap by in-house R code developed by the author. FlowSOM was performed using FlowSOM v2.6 (Van Gassen et al. 2015).

2.3.5 Statistical analysis

Statistical analysis was performed using GraphPad Prism 7.03. If n number is sufficient, normality of the data was confirmed using Shapiro-Wilk tests. Parametric data was then analysed using paired Student's t-test. For statistical analysis involving three or more variables, One-way ANOVA with multiple comparisons were performed among comparison groups. Data were represented as mean $\pm$ SD. Differences were considered significant if $p < 0.05$.

2.4 Results

2.4.1 Establishing a SOP for the PIP study

Although a number of studies have investigated the endometrial and/or peripheral immune profiles during the mid-luteal phase in controls and infertility, RIF or RPL patients, many studies lack a SOP, which might cause variations during the data generation and interpretation processes, therefore making it difficult to assure reproducibility. In sample collection, it is unclear what is the appropriate size of the endometrial biopsy to ensure there are enough data points for each immune cells subset being examined. In sample processing, it is unclear what endometrium digestion method has the best yield in terms of cell counts, at the same time preserve the immune cell surface markers' expression. It is unclear what is the optimal antibody concentration for flow cytometric analysis. It is unclear how long can samples be stored in room temperature before being processed without influencing the immune cell activation markers' expression levels. In data analysis, there is no guideline as to how to analyse different immune cell subsets' frequencies and activation status in flow cytometry.

Here, I present the SOP work-up for the PIP study that addressed the above issues.

2.4.1.1 Standardization of sample size

All samples for the PIP study were aimed to be processed and fixed on the day of collection, following an overnight storage before flow acquisition (due to access to the flow cytometer). Therefore, the experimental process was optimised to obtain a peripheral blood $CD3^{+}CD4^{+}$ absolute cell count (data now shown). In short, anti-CD3 APC/Fire^{TM} 750 and anti-CD4 FITC antibodies' staining and FACS^{TM} lysing red blood cell lysis (BD, USA) were performed on the day of sample collection, Precision Count Beads^{TM} were added the day after prior to flow acquisition, 2000 beads were recorded during the acquisition.

For ES samples obtained through biopsy, preliminary work demonstrated at least 50,000 $CD45^+$ events needed to be recorded to ensure immune profiling of all cell subsets ($>$ 20,000 $CD56^{+/bright}$ events, NK cells; $>$ 20,000 $CD3^+$ events, T cells; $>$ 200 $CD19^+$ events, B cell; $>$ 8,000 $CD3^+CD4^+$ events, $CD4^+$ T cell; $>$ 9,000 $CD3^+CD8^+$ events, $CD8^+$ T cell; $>$ 1,000 $CD4^+CD25^{bright}CD127^{low}$ events, T regulatory cells. Cell proportions are detailed in Table 2.3), therefore $5mm^3$ was the minimum size required.

Cell Type	PBMCs (%)	Endometrial cells (%)
$CD45^+$ Zombie $Aqua^{TM-}$ (of total events)	60.4 (±8)	2.7 (±1)
$CD16^{-/dim}$ $CD56^{bright}$	1.96 (±2)	-
$CD16^+$ $CD56^+$	10.6 (±5)	41.7 (+25; -9)
$CD3^+$	75 (±7)	44.8 (+9; -19)
$CD4^+$ $CD8^-$	57.85 (±14)	17.2 (±8)
$CD4^-$ $CD8^+$	13.7 (±8)	18.8 (±12)
$CD19^+$	5.57 (±5)	1.0 (+2; -1)
$CD25^{bright}$ $CD127^{dim}$	3.35 (±2)	2.2 (±1)

Table 2.3: Comparison of major immune cell population percentages (of $CD45^+$ Zombie $Aqua^{TM-}$, unless stated otherwise) in PBMCs and endometrial cells. Data displayed as mean value ($\pm$ range), n $\geq$ 5.

2.4.1.2 Standardization of ES digestion method

To determine the optimal ES sample dispersion method, three commonly used digestion enzymes (Liberase^{TM} (Roche, Switzerland), Collagenase IV (Sigma, USA) and Collagenase D (Roche, Switzerland)), and mechanical dissection were compared. All enzymes were titrated before use (data not shown). PIP flow panel staining was performed after tissue digestion, $CD56^+$ and $CD3^+$ cell subsets' percentages and the majority of cellular markers had consistent mean fluorescence intensity (MFI) despite the digestion methods used (data not shown). However, BV421^{TM} CD56, FITC CD4, and BV711^{TM} CD8 MFI were altered (Figure 1). The Liberase^{TM} treated group displayed a significantly lower MFI on FITC CD4 and BV711^{TM} CD8 compared with other groups. For BV421^{TM}

CD56, Liberase^{TM} treated group showed a five-fold decrease (mean value) in MFI compared with other groups. An additional paired t-test was performed on BV421^{TM} CD56, FITC CD4 and BV711^{TM} CD8 MFI in Collagenase IV and Collagenase D treated groups, BV711^{TM} CD8 was significantly higher in Collagenase D treated group ($p = 0.03$, Figure 2.2).

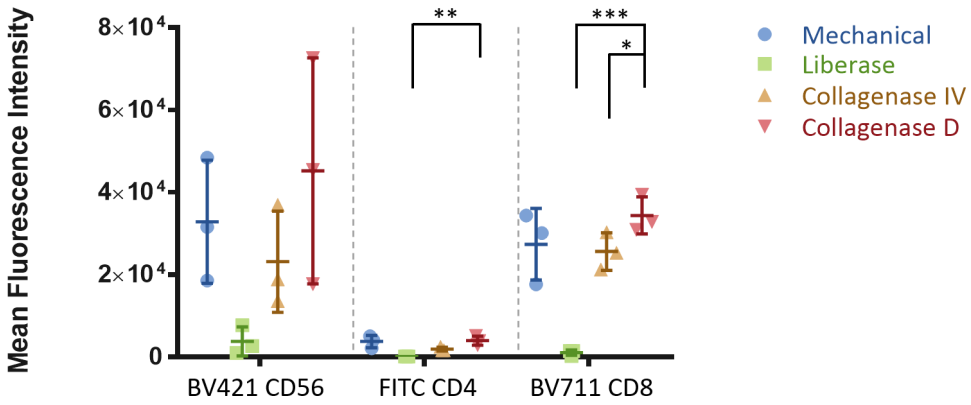

Figure 2.2: The effect of four endometrium digestion methods on various immune cell surface markers. Endometrium was spilt into four equal sizes and single cell suspensions were obtained by four different methods (enzymatic digestion methods (Liberase^{TM} (Roche, Switzerland), Collagenase IV (Sigma, USA) and Collagenase D (Roche, Switzerland)), or mechanical dissection). Cells were stained using the PIP flow panel. Mean fluorescence intensity (MFI) of CD56 was measured in live CD45^{+} single lymphocytes. MFI of CD4 and CD8 were measured in live CD45^{+}CD3^{+} single lymphocytes. Scatter plot shows the MFI of CD56, CD4, and CD8 under different conditions. Statistical analysis: MFI of CD56, CD4 and CD8 were considered to be normally distributed, as in larger sample set (Figure 2.9 and 2.11), they passed the Shapiro-Wilk tests. One-way ANOVA with multiple comparisons among all groups were performed. $\star\star$ $p \leq 0.01$, $\star\star\star$ $p \leq 0.001$. Paired t-test was also performed on Collagenase IV and Collagenase D digested samples, CD8 is significantly higher in Collagenase D treated samples ($p = 0.03$). Error bar shows mean $\pm$ SD. $n = 3$.

2.4.1.3 Standardization of flow cytometric staining protocol

Titrations of all reagents included in the PIP flow panel were performed using PBMCs and single cell suspensions of endometrial cells. Optimal concentrations were determined

by stain index with adjustments to best serve the gating process (Table 2.2, Figure 2.3), e.g.: CD45 and CD56 had high fluorescence levels that were beyond the linear detection of the flow cytometer if too much was used (Figure 2.3b), therefore their optimal concentrations were chosen at a lower level despite the stain indexes indicating a higher value. For PE/DAZZLE^{TM} CD69, the optimal titre was defined by stain index of endometrial CD56^{+} and CD3^{+} cells (n $=$ 3, data not shown), the same concentration was used in PBMCs. The CD69 gating strategy is discussed in the next section.

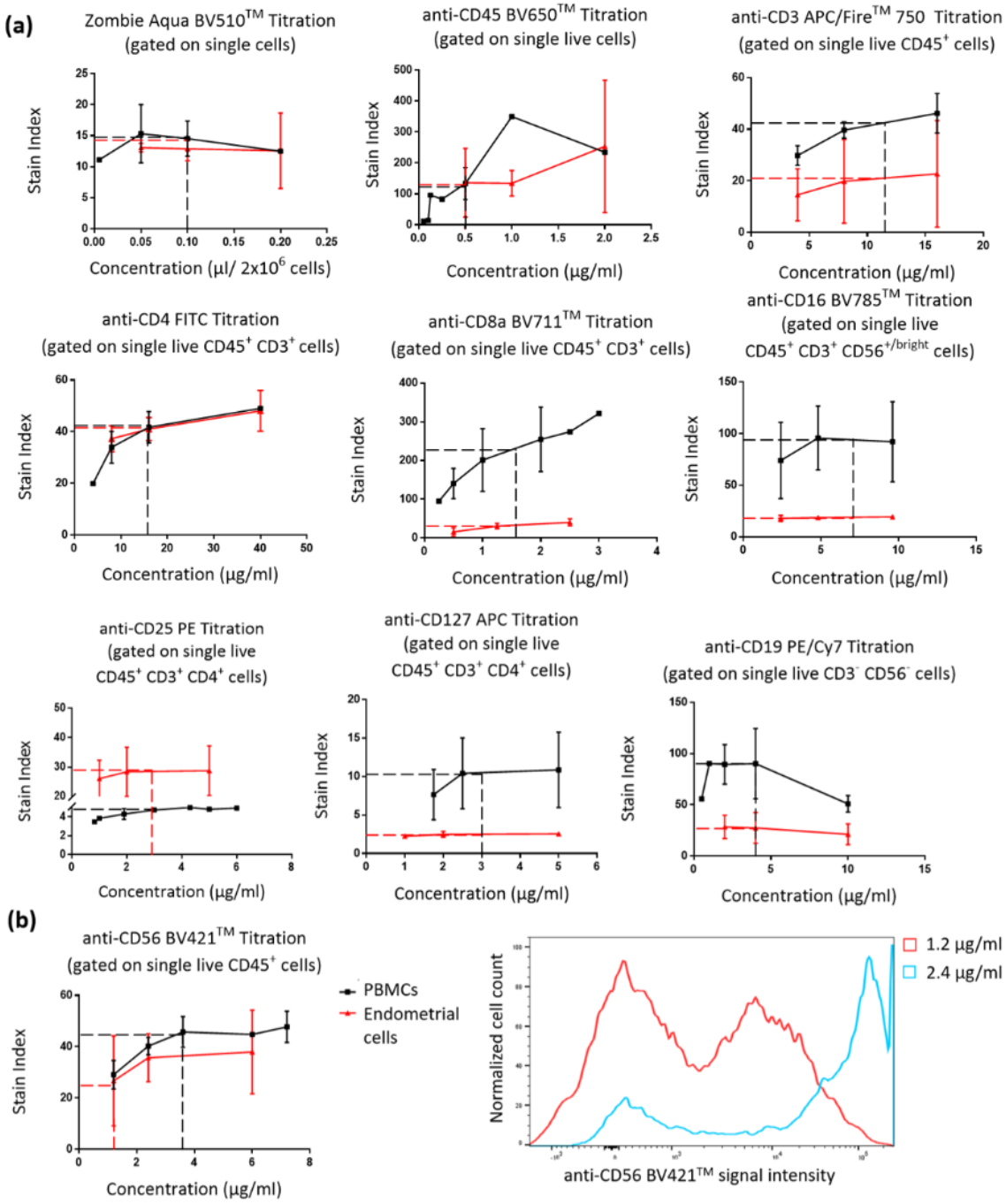

Figure 2.3: PIP flow panel titration results. PBMCs were isolated from whole blood by density gradient centrifugation using Lymphoprep™. Endometrial cells were isolated by Collagenase D treatment. Titrations of the PIP flow panel were undertaken in PBMCs and endometrial cells by flow cytometry. (a) and (b, left), Titration results are presented as stain index (SI) with gating strategies specified under individual figures' titles. SI of PBMCs are illustrated in black dots, SI of endometrial cells are presented in red. Determined optimal titres are marked by dash lines, PBMCs in black, endometrial cells by red. Error bars represent mean ± SD. n = 3 for PBMCs. n = 3 for endometrial cells. (b, right), anti-CD56 BV421™ signal is off scale when concentration is 2.4μg/ml, as shown in the histogram.

2.4.1.4 Standardization of flow cytometric gating strategies

In the PIP flow panel, most markers had a distinct separation between negative and positive on target populations. Two exceptions were T regulatory cells and $CD69^{+}$ cells in PBMCs.

T regulatory cells can be identified by low expression of CD127 (which has inverse correlation with Foxp3 expression), combined with CD4 and high CD25 expression (Liu et al. 2006). I confirmed that the staining protocol correctly identified T regulatory cells by using a modified PIP flow panel replacing PE/Cy7 CD19 with PE/Cy7 Foxp3 (clone 236A/E7, eBioscience^{TM}) (Figure 2.5 and 2.4). Foxp3 was highly expressed on $CD4^{+}$ $CD25^{bright}$ $CD127^{dim}$ (population i, 98.0%) cells compared with $CD4^{+}$ $CD25^{dim}$ $CD127^{dim}$ (population ii, 68.9% positive) and $CD4^{+}$ $CD25^{-}$ $CD127^{+/-}$ T cells (population iii, 2.99%). Similar results were observed in PBMCs using the same gating strategies.

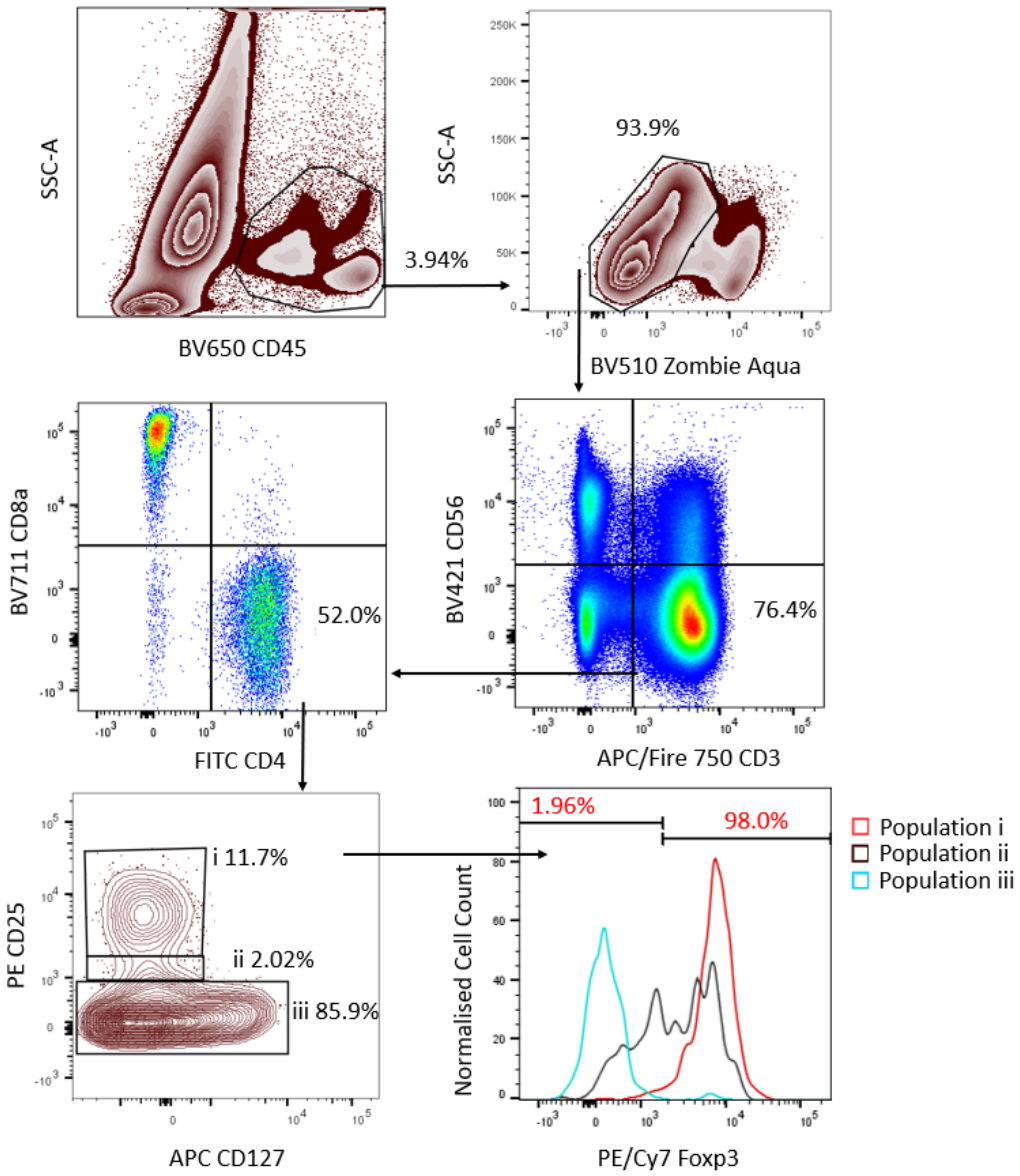

Figure 2.4: Representative example of Foxp3 gating strategy. Endometrial cells were isolated by Collagenase D treatment. Modified PIP flow panel with intranuclear Foxp3 staining (True-nuclear kit, Biolegend) was performed afterwards. (a), $CD45^{+}$ lymphocytes were gated on $BV650^{TM}$ (CD45) versus SSC-A; (b), and single cells were selected (not shown), live cells were gated based on $BV610^{TM}$ Zombie $Aqua^{TM}$ signal; (c), $CD3^{+}$ $CD56^{-}$ cells were selected; (d) $CD4^{+}$ $CD8^{-}$ cells were selected; (e), three populations (i, ii, iii) were gated based on their CD25 and CD127 expression; (f), Foxp3 expressions of three previously selected populations are illustrated. Gate was applied to separate $Foxp3^{-}$ from $Foxp3^{+}$, with percentages of populations labelled at the upper corners. n = 3 for PBMCs. n = 3 for endometrial cells.

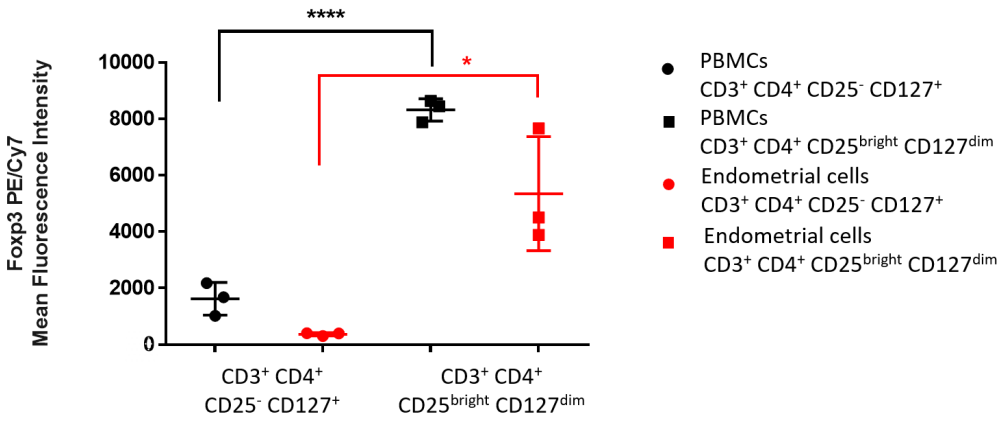

Figure 2.5: Foxp3 is highly expressed in $CD3^+$ $CD4^+$ $CD25^{bright}$ $CD127^{dim}$ cells compared with other $CD3^+$ $CD4^+$ cells. PBMCs were isolated from whole blood by density gradient centrifugation using Lymphoprep^{TM}. Endometrial cells were isolated by Collagenase D treatment. Modified PIP flow panel with intracellular (True-nuclear kit, Biolegend) Foxp3 staining was performed afterwards. Only live $CD45^+$ single lymphocytes were selected. Foxp3 expression was measured by mean fluorescence intensity. Statistical test: MFI of Foxp3 was considered to be normally distributed, as in larger sample set (Chapter 2.4.2), MFI of various surface marker expressions all passed the Shapiro-Wilk tests. Paired t-test was performed. $\star$ $p \leq 0.05$, $\star\star\star\star$ $p \leq 0.001$. Error bars represent mean $\pm$ SD. n $= 3$ for PBMCs. n=3 for endometrial cells.

In endometrial $CD45^+$ cells, CD69 was found to be highly expressed as a tissue residency marker (Montaldo et al. 2016, Southcombe et al. 2017), with a clear separation between CD69 negative and CD69 positive populations (Figure 2.6a and 2.6c). In PBMCs, CD69 is as an early activation marker and presents a challenge for flow cytometry analysis (Figure 2.6b and 2.6d). Appropriate controls are to include fluorescence minus one (FMO) or isotype control to set gates, however when PBMCs and endometrial cells were immune profiled with an FMO control (PIP flow panel without PE/DAZZLE^{TM} 594 CD69) or isotype control (PIP flow panel replacing PE/DAZZLE^{TM} CD69 with PE/DAZZLE^{TM} 594 Mouse IgG1, k Isotype (clone MOPC-21, Biolegend)), gates bisected through the main populations (Figure 2.7a and 2.7b). Similar results were also observed when using anti-CD69 antibodies from different providers or with altered fluorophore tag (PE-CF594 CD69, BD; Alexa Fluor 700 CD69, Biolegend; FITC CD69, Biolegend. Data not shown).

An alternate gating strategy is to set the PBMCs $CD69^+$ gate based on the clear

distinction in the corresponding endometrial immune cell populations (Zeng et al. 2018). But it was noted that for minor cell populations, such as $CD25^{bright}$ $CD127^{dim/-}$ Treg cells and $CD19^{+}$ B cells, their flow profile might not have enough data points to present distinct positive and negative cell clusters, therefore the $CD69^{+}$ values need to be interpreted with care. Alternatively, the MFI value instead of $CD69^{+}$ percentage can be used to measure cell activation status. Gating based on endometrial $CD69^{+}$ gate showed 11.7% NK cells and 2.71% T cells as $CD69^{+}$, which is lower than FMO and isotype gating (Figure 2.7), and similar to previous studies (Southcombe et al. 2010).

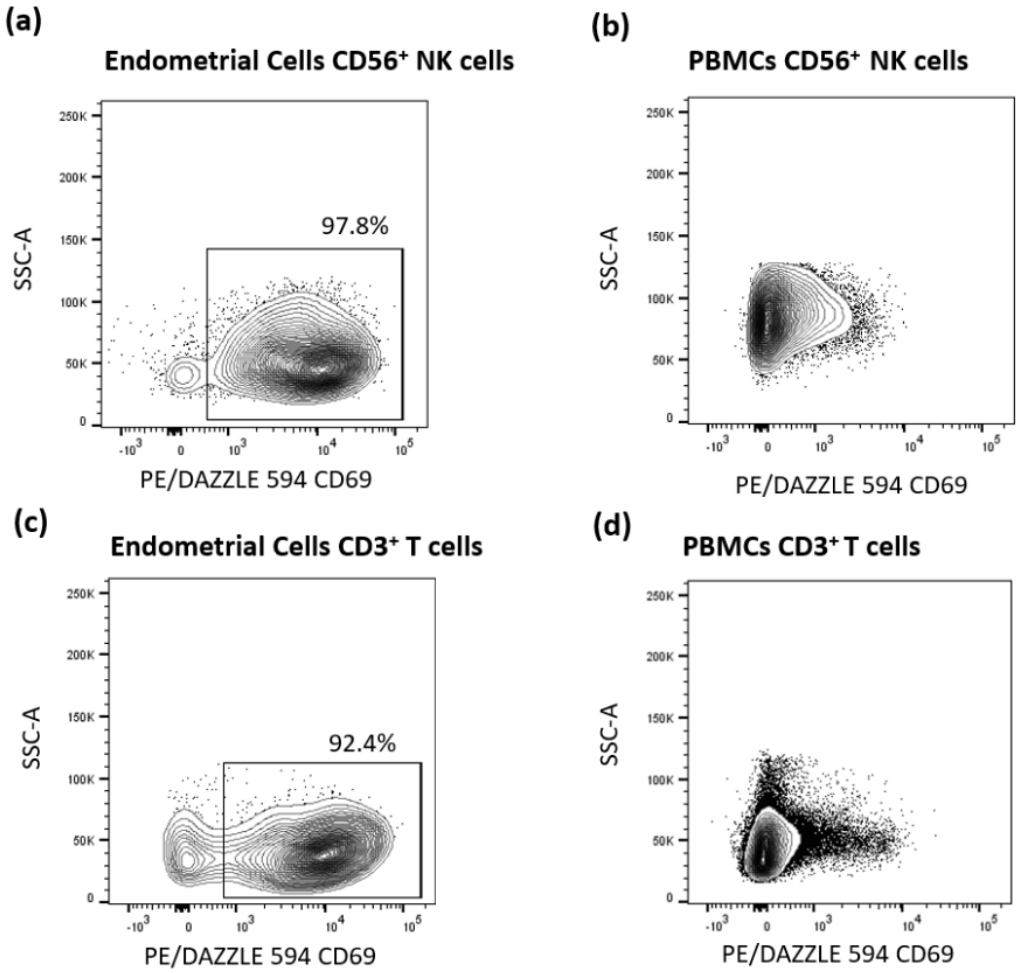

Figure 2.6: CD69 expression in peripheral and endometrial NK and T cell subsets. Endometrial cells were isolated by Collagenase D treatment. PBMCs were isolated from whole blood by density gradient centrifugation using Lymphoprep^{TM}. Flow cytometry based on the PIP flow panel was performed afterwards. Only single live CD45^{+} lymphocytes were selected, representative examples of (a), CD69 expression in endometrial CD56^{+} NK cells, with CD69^{+} cells gated; (b), CD69 expression in PBMCs CD56^{+} NK cells; (c), CD69 expression in endometrial CD3^{+} T cells, with CD69^{+} cells gated; (d) CD69 expression in PBMCs CD3^{+} T cells are shown.

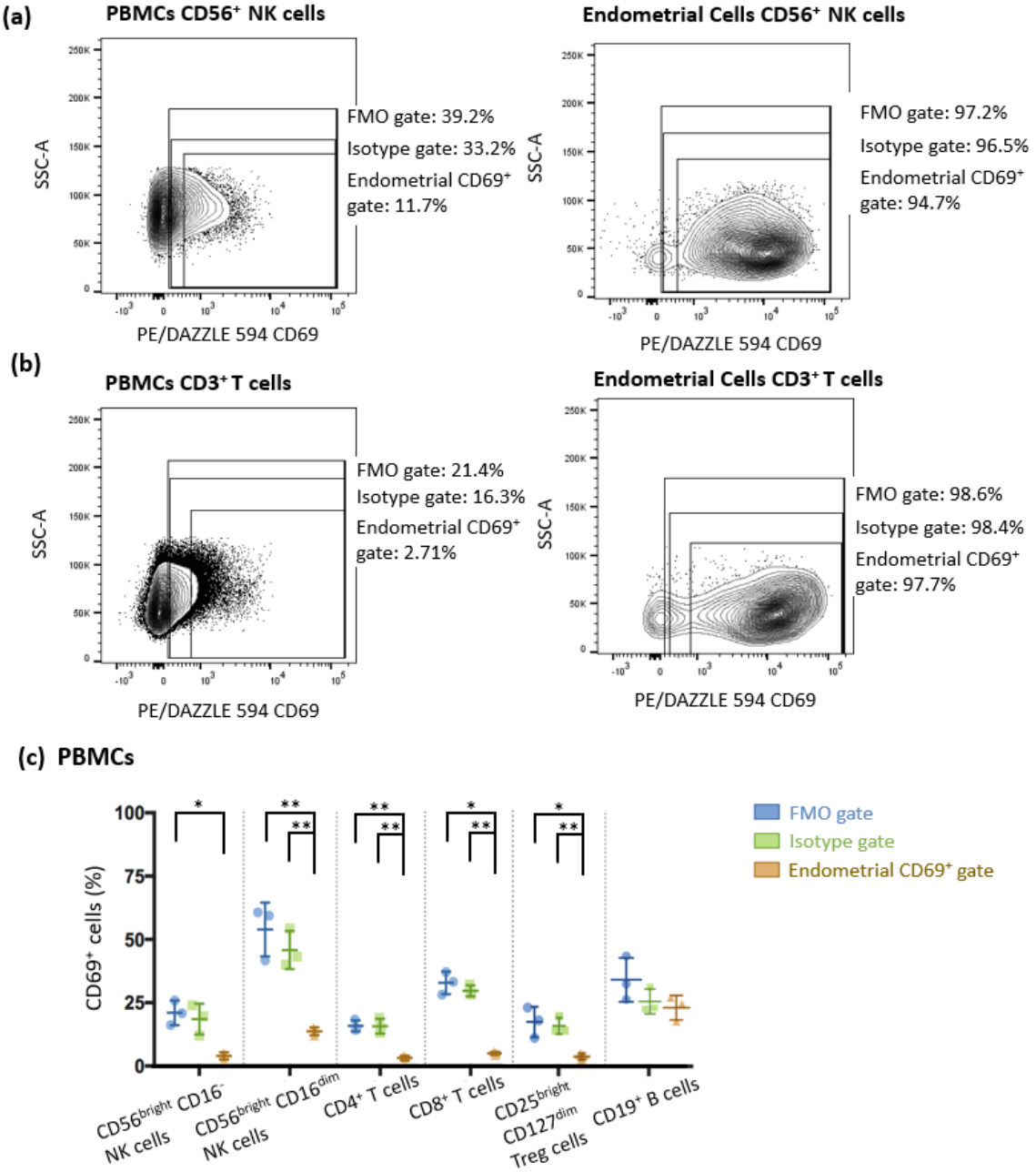

Figure 2.7: Different CD69 gating strategies in peripheral NK and T cell subsets. PBMCs were isolated from whole blood using Lymphoprep^{TM}. Endometrial cells were isolated by Collagenase D treatment. Flow cytometry analysis using PIP flow panel was performed. Only single live CD45^{+} lymphocytes were selected. Representative examples show selected (a), CD56^{+} NK cells and (b), CD3^{+} T cells with three CD69^{+} gates applied. FMO gate is set according to 1% FMO control; isotype gate is set according to 1% isotype control; Endometrial CD69^{+} gate was set identical to the corresponding endometrial immune cell populations. (c), Scatter plot shows PBMCs CD69^{+} cells percentages in six cell subsets based on different gating strategies. Statistical analysis: MFI of CD69 was considered to be normally distributed, as in larger sample set (Figure 2.13), CD69 MFI values passed the Shapiro-Wilk tests. One-way ANOVA with multiple comparisons were performed among all groups. $\star$ $p \leq 0.05$ $\star\star$ $p \leq 0.05$. Error bars represent mean $\pm$ SD. n $= 3$.

2.4.1.5 Determining time limits for sample processing

Some IVF clinics offer immunological testing (including CD69 expression) (Sacks 2015) of blood samples analysed up to 48 hours' after sample collection. Here, I tested the validity of this method. Blood samples were either processed immediately (0 hour) or after storage at room temperature for 6, 24 or 48 hours. Immune cell profiles were measured by the PIP flow panel (Appendix B). Analysis was focused on the expression of activation markers: CD69, CD25, and CD127. Cell subset percentages and all other cellular markers' fluorescent intensities did not change over 48 hours (data not shown).

CD69 MFI significantly increased on NK cells and $CD4^+$ T cells after 48 hours (Figure 2.8a). MFI changes in CD25 and CD127 are shown in Figure 2.8b and 2.8c, a significant increase in CD25 MFI was observed in $CD56^{bright}$ NK cells and $CD4^+$ T cells after 24 hours, for CD127, a significant increase in CD25 MFI was observed in $CD4^+$ and $CD8^+$ T cells after 24-48 hours.

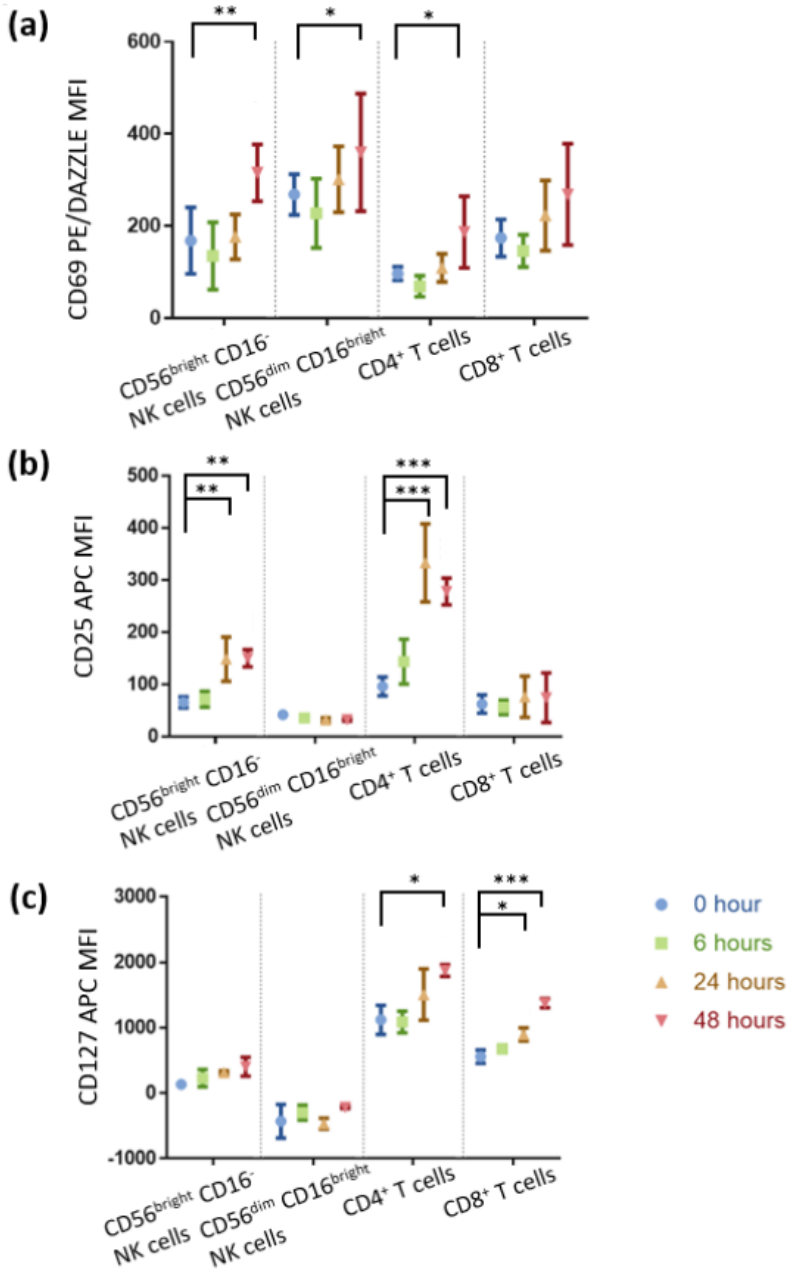

Figure 2.8: The effect of blood storage on cellular activation markers' expression. PBMCs isolation were performed either immediately (0 hour) after blood collection or after storage at room temperature for 6, 24 or 48 hours. Immune cell profiles were measured by the PIP flow panel. (a), Mean fluorescence intensity (MFI) of PE/ DAZZLE^{TM} (CD69) on four cell subsets over 48 hours' period. (b), MFI of PE (CD25) on four cell subsets over 48 hours' period. (c) MFI of APC (CD127) on four cell subsets over 48 hours' period. Statistical analysis: MFI of CD69, CD25 and CD127 were considered to be normally distributed, as in larger sample set (Figure 2.13), they passed the Shapiro-Wilk tests. One-way ANOVA with multiple comparisons among all groups were performed. $\star$ $p \leq 0.05$ $\star\star$ $p \leq 0.01$, $\star\star\star$ $p \leq 0.001$. Error bar shows mean $\pm$ SD. $n = 3$.

2.4.2 Peripheral versus endometrial immune profiles

From 2018 to 2020, 15 PIP samples were collected (participant information shown in Table 2.1) and processed according to the established SOP (Appendix B). The similarities as well as the differences between peripheral blood and endometrial immune profiles were shown by flow cytometry analysis.

2.4.2.1 Flow cytometry gating and statistical analysis

For $CD45^+$ lymphocytes in both peripheral blood and endometrial samples, $CD56^+$ $CD3^-$ NK cells and $CD56^-$ $CD3^+$ T cells were the major cell populations. Together they accounted for approximately 80% of all $CD45^+$ lymphocytes. Other lymphocytes were $CD56^+$ $CD3^+$ NKT cells and $CD56^-$ $CD3^-$ cells, the latter included a $CD19^+$ B cell population (Figure 2.9).

Statistical analysis showed there was no significant difference in NKT cells and B cells proportions between endometrial and peripheral blood samples, most of them accounted for $< 10\%$ of all $CD45^+$ lymphocytes (peripheral NKT cells: $5.8\% \pm 5.7\%$, endometrial NKT cells: $3.0\% \pm 1.6\%$, peripheral B cells: $9.6\% \pm 3.4\%$, endometrial B cells: $6.5\% \pm 10.8\%$, mean $\pm$ SD). Significant differences were observed between peripheral and endometrial samples' T cells and NK cells: T cells accounted for $70.8\% \pm 8.3\%$ (mean $\pm$ SD) of all $CD45^+$ lymphocytes in the peripheral blood, which was significantly higher than that in the endometrium ($38.1\% \pm 15.7\%$, mean $\pm$ SD); NK cells accounted for $10.9\% \pm 5.7\%$ (mean $\pm$ SD) of all $CD45^+$ lymphocytes in the peripheral blood, which was significantly lower than that in the endometrium ($44.9\% \pm 17.2\%$, mean $\pm$ SD). Notably, there was one endometrial sample that had an unexpectedly high level of B cells, that accounted for 45.7% of all $CD45^+$ lymphocytes. This sample was collected from participant C, who had male factor infertility, and was not diagnosed with any observable abnormal thyroid function, APS or unterine structure abnormality (Table 2.1 and Figure 2.9).

For $CD56^+$ NK cells, the major cell population was $CD56^{bright}$ $CD16^-$ NK cells in

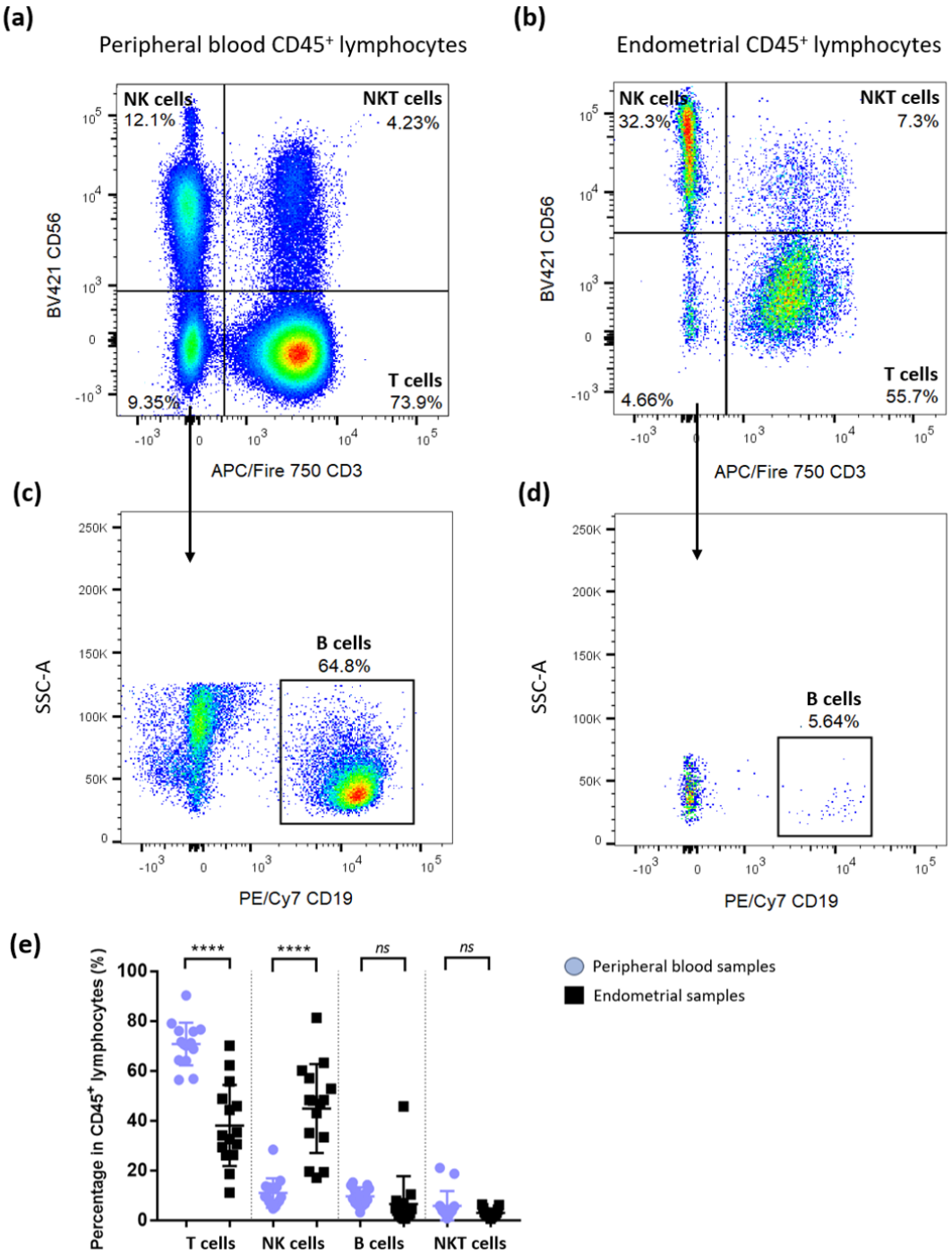

Figure 2.9: Comparison of $CD45^+$ lymphocyte subsets between peripheral blood and endometrial samples, analysed by CD56 and CD3. PBMCs were isolated by Lymphoprep^{TM}, endometrium samples were digested by Collagenase D (Appendix B). (a-b), Representative figure of gating strategy for peripheral blood and endometrial $CD45^+$ lymphocyte subsets. (c-d), Representative figure of gating strategy for peripheral blood and endometrial $CD19^+$ B cells. (e), The proportion of peripheral blood and endometrial $CD45^+$ lymphocyte subsets. Statistical analysis: paired t-test was performed between sample groups. $\star\star\star$ $p \leq 0.001$. $\star\star\star\star$ $p \leq 0.0001$. Error bar shows mean $\pm$ SD. $n = 15$.

the endometrium, and CD56^{dim} CD16^{bright} NK cells in the peripheral blood, accounted for 78.6% ± 17.9% (mean ± SD), and 88.4% ± 5.7% (mean ± SD) of all NK cells respectively. Another NK cell subset was CD56^{bright} CD16^{dim} NK cells, represented 6.7% ± 5.0% (mean ± SD) of all NK cells in the endometrium, and 3.1% ± 1.8% (mean ± SD) of all NK cells in the peripheral blood (Figure 2.10).

Statistical analysis showed significant differences in NK cell subsets' proportions between endometrial and peripheral blood samples. CD56^{bright} CD16^{-} NK cells were 4.4% ± 2.5% (mean ± SD) of all NK cells in the peripheral blood, which was significantly lower than that in the endometrium. CD56^{dim} CD16^{bright} NK cells were 7.8% ± 17.8% (mean ± SD) of all NK cells in the endometrium, which was significantly lower than that in the peripheral blood (Figure 2.10).

Of note, one endometrial sample had only 14.7% of all NK cells being CD56^{bright} CD16^{dim}, which was much lower than other endometrial samples (2.10c). The same sample also had higher level of CD56^{dim} CD16^{bright} NK cells (74.1%) compared with other samples. This sample was collected from participant O, who suffered from anovulatory infertility, and was diagnosed with APS (Table 2.1).

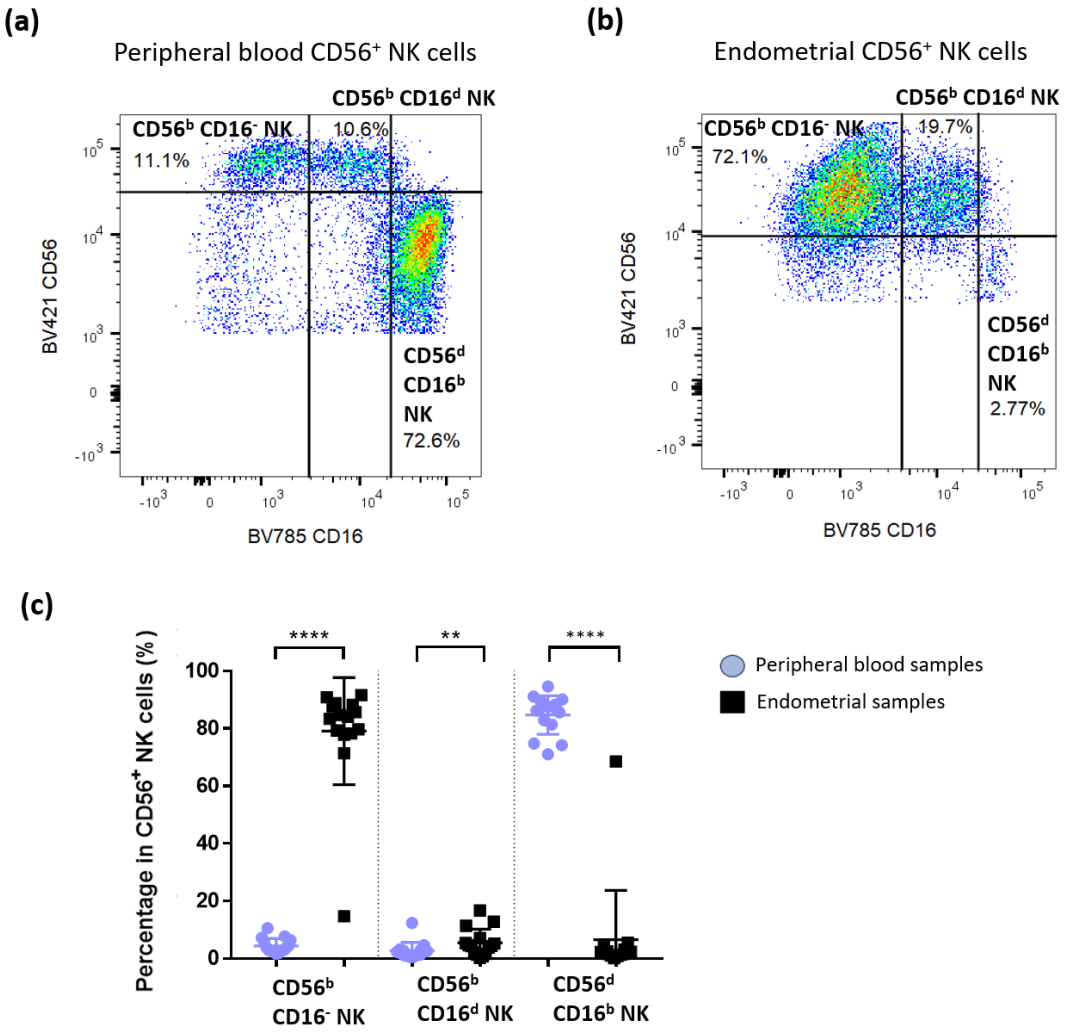

Figure 2.10: Comparison of CD56$^+$ NK cell subsets between peripheral blood and endometrial samples, assessed by CD56 and CD16 expression. PBMCs were isolated by Lymphoprep^{TM}, endometrium samples were digested by Collagenase D (Appendix B). (a-b), Representative figure of gating strategy for peripheral blood and endometrial CD56$^+$ NK cell subsets. (c), The proportion of peripheral blood and endometrial CD56$^+$ NK cell subsets. b, bright; d, dim. Statistical analysis: paired t-test was performed between sample groups. $\star\star$ $p \leq 0.01$. $\star\star\star\star$ $p \leq 0.0001$. Error bar shows mean $\pm$ SD. n $= 15$.

For $CD3^+$ T cells in both peripheral blood and endometrial samples, $CD4^+$ T cells and $CD8^+$ T cells were the major cell populations. Together they accounted for $> 90\%$ of all $CD3^+$ T cells. Other T cells were DP T cells and DN T cells (Figure 2.11).

Statistical analysis showed there was no significant difference in DN T cell proportions between endometrial and peripheral blood samples, most of them were $< 5\%$ of all $CD3^+$ T cells. While for other T cell subsets, significant differences were observed. $CD4^+$ T cells accounted for $68.4\% \pm 9.8\%$ (mean $\pm$ SD) of all $CD3^+$ T cells in the peripheral blood, which was significantly higher than that in the endometrium ($50.0\% \pm 7.7\%$, mean $\pm$ SD). $CD8^+$ T cells accounted for $28.2\% \pm 7.1\%$ (mean $\pm$ SD) of all $CD3^+$ T cells in the peripheral blood, which was significantly lower than that in the endometrium ($44.0\% \pm 8.2\%$, mean $\pm$ SD). DP T cells were $1.1\% \pm 0.8\%$ (mean $\pm$ SD) of all $CD3^+$ T cells in the peripheral blood, which was significantly lower than that in the endometrium ($3.2\% \pm 1.3\%$, mean $\pm$ SD) (Figure 2.11).

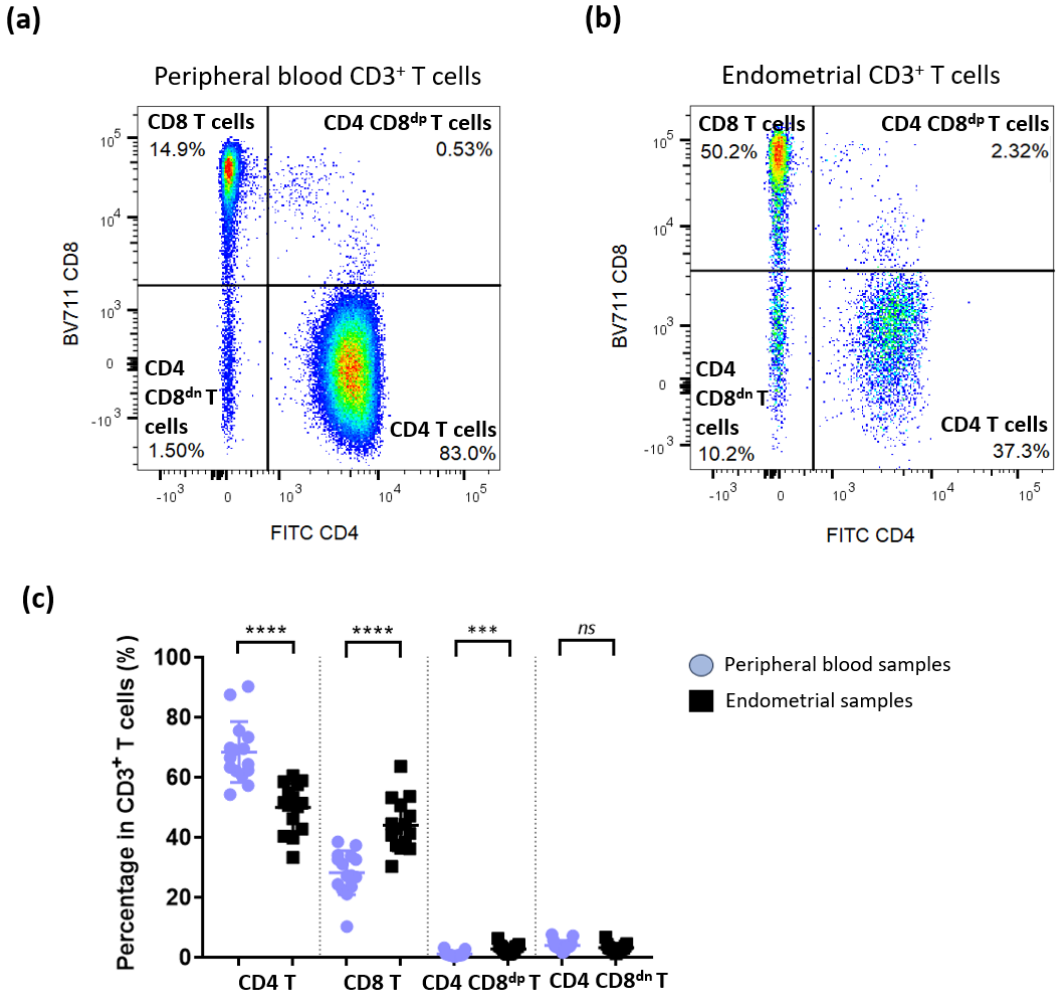

Figure 2.11: Comparison of $CD3^+$ T cell subsets between peripheral blood and endometrial samples, assessed by CD4 and CD8. PBMCs were isolated by Lymphoprep^{TM}, endometrium samples were digested by Collagenase D (Appendix B). (a-b), Representative figure of gating strategy for peripheral blood and endometrial $CD3^+$ T cell subsets. (c), The proportion of peripheral blood and endometrial $CD3^+$ T cell subsets. dp, double positive; dn, double negative. Statistical analysis: paired t-test was performed between sample groups. $\star\star\star$ $p \leq 0.001$. $\star\star\star\star$ $p \leq 0.0001$. Error bar shows mean $\pm$ SD. $n = 15$.

T regulatory cells, a minority cell population in both peripheral blood and endometrial samples, comprised $< 15\%$ of $CD4^+$ T cells in all samples. Statistical analysis showed the proportion of T regulatory cells was significantly higher in endometrium compared with peripheral blood ($7.0\% \pm 3.8\%$, mean $\pm$ SD, of $CD4^+$ T cells versus $4.2\% \pm 2.0\%$, mean $\pm$ SD, of $CD4^+$ T cells) (Figure 2.12).

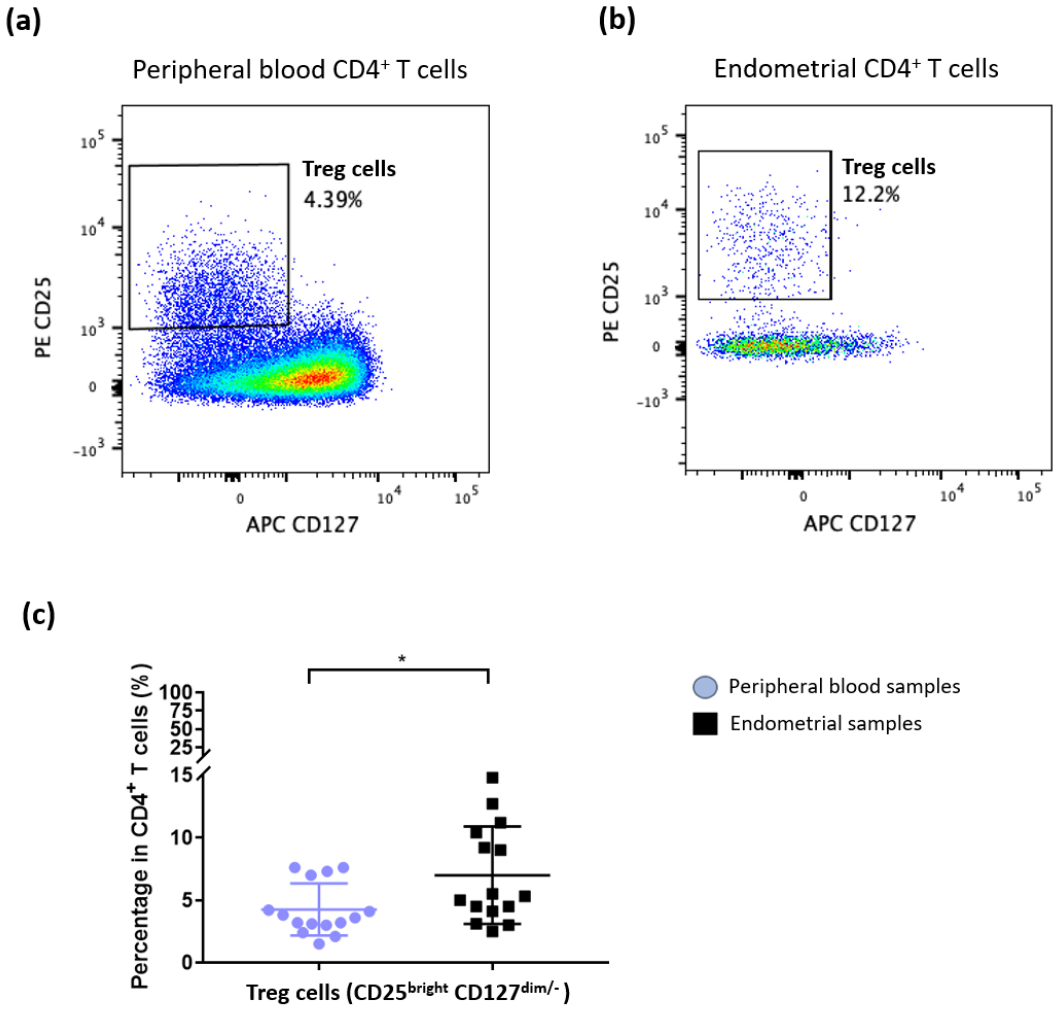

Figure 2.12: Comparison of CD25^{bright} CD127$^{\text{dim}/-}$ T regulatory cells' proportions between peripheral blood and endometrial samples. PBMCs were isolated by Lymphoprep^{TM}, endometrium samples were digested by Collagenase D (Appendix B). (a-b), Representative figure of gating strategy for peripheral blood and endometrial CD25^{bright} CD127$^{\text{dim}/-}$ T regulatory cells. (c), The proportion of peripheral blood and endometrial CD25^{bright} CD127$^{\text{dim}/-}$ T regulatory cells. Statistical analysis: paired t-test was performed between sample groups. $\star$ $p \leq 0.05$. Error bar shows mean $\pm$ SD. n $= 15$.

CD69 expression levels were significantly increased in all 6 endometrial immune cell subsets compared with their peripheral counterparts (measured by MFI and percentages, as illustrated in Figure 2.13).

A summary of the immune profile in all 15 peripheral and endometrial samples were present in Table 2.4. Apart from the immune cell subsets' statistics detailed above, additional data such as the CD69 expression levels in minor cell populations ($CD56^+$ $CD3^+$ NKT cells, DP T cells, DN T cells and $CD56^{bright}$ $CD16^{dim}$ NK cells) and the absolute cell counts for peripheral immune cells are presented.

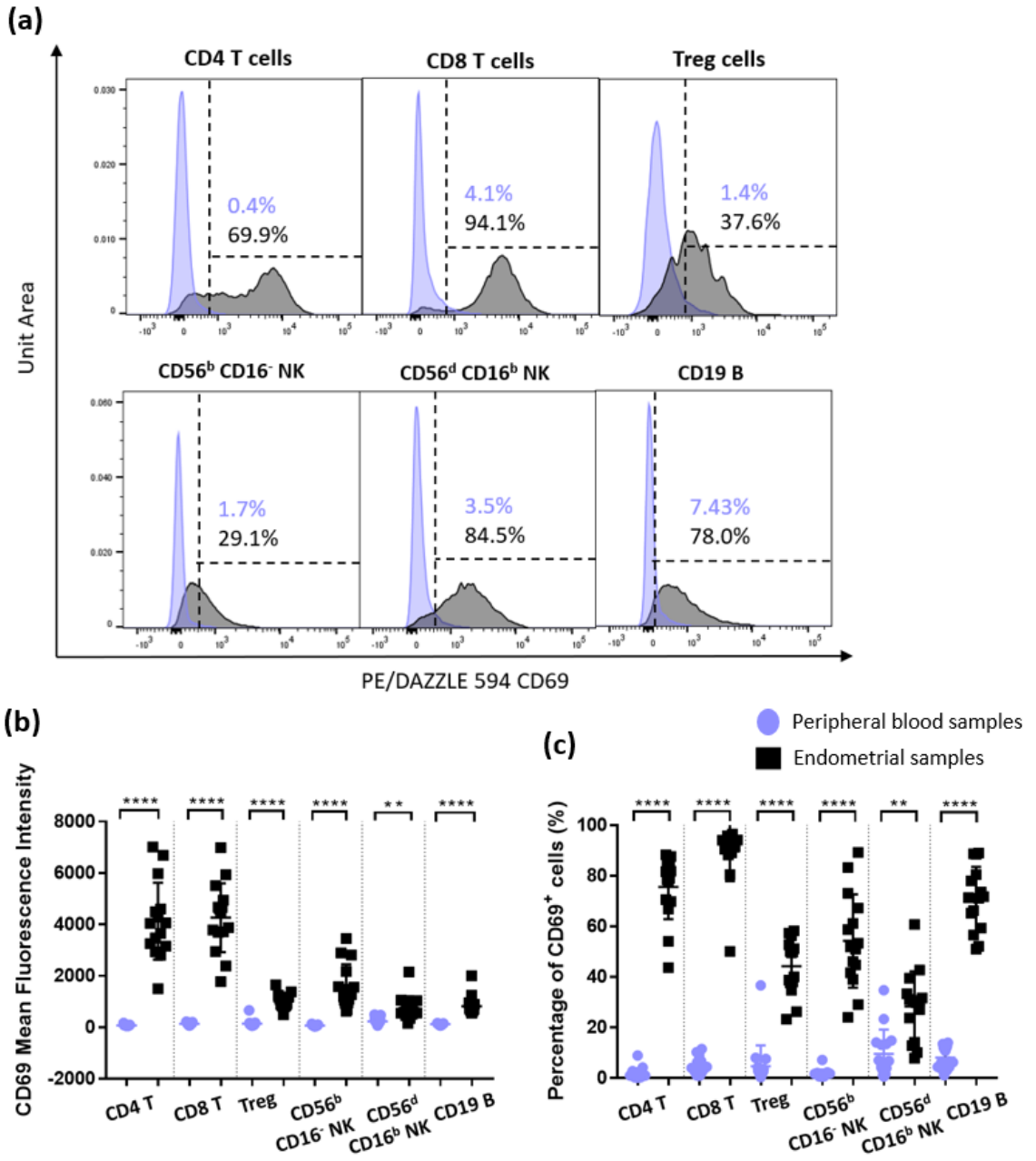

Figure 2.13: Comparison of $CD69^{+}$ expression levels on 5 lymphocyte subsets in peripheral blood and endometrial samples. PBMCs were isolated by Lymphoprep^{TM}, endometrium samples were digested by Collagenase D (Appendix B). (a), Representative histograms of CD69 expression levels in peripheral and endometrial immune cell subsets. (b), MFI of CD69 in lymphocyte subsets in the peripheral blood and endometrium. (c), The proportion of $CD69^{+}$ lymphocyte subsets in the peripheral blood and endometrium. b, bright; d, dim. Statistical analysis: paired t-test was performed between sample groups. $\star$ $p \leq 0.05$. $\star\star$ $p \leq 0.01$. $\star\star\star\star$ $p \leq 0.0001$. Error bar shows mean $\pm$ SD. n $= 15$.

Immune cell populations	PBMCs				Endometrial cells			
	$CD3^+$ T cells	$CD56^+$ NK cells	$CD19^+$ B cells	$CD3^+$ $CD56^+$ NKT cells	$CD3^+$ T cells	$CD56^+$ NK cells	$CD19^+$ B cells	$CD3^+$ $CD56^+$ NKT cells
% of all $CD45^+$ lymphocytes, Mean± SD	70.8 ± 8.3	10.9 ± 5.7	9.6 ± 3.4	5.8 ± 5.7	38.1 ± 15.7	44.9 ± 17.2	6.5 ± 10.8	3.0 ± 1.6
Absolute counts (cells/ml blood $x10^5$), Mean± SD	13.3 ± 5.6	2.3 ± 1.9	1.8 ± 1.0	1.3 ± 2.4	-	-	-	-
CD69 MFI, Mean± SD	98.5 ± 32.0	203.6 ± 88.4	118.6 ± 28.6	338.5 ± 132.5	4211.1 ± 1348.9	1503.3 ± 624.2	823.6 ± 359.4	6001.2 ± 2433.8
% of $CD69^+$ (Gating set according to matched endometrial immune cells), Mean± SD	3.0 ± 3.0	9.3 ± 7.2	8.1 ± 4.2	9.3 ± 6.6	83.4 ± 10.8	60.3 ± 10.9	70.9 ± 12.2	85.7 ± 9.7

Table 2.4: PIP study data summary. Matched peripheral (PBMCs) and endometrial samples were collected during the mid-luteal phase. All samples were processed according to the SOP (Appendix B). Immune profiles for peripheral and endometrial samples, including immune cell subsets frequencies, absolute cell counts (for peripheral immune cells), CD69 MFI and the percentage of $CD69^+$ cells, are shown. n = 15.

Immune cell populations	PBMCs			Endometrial cells		
	$CD56^{bright}$ CD16- NK cells	$CD56^{bright}$ $CD16^{dim}$ NK cells	$CD56^{dim}$ $CD16^{bright}$ NK cells	$CD56^{bright}$ CD16- NK cells	$CD56^{bright}$ $CD16^{dim}$ NK cells	$CD56^{dim}$ $CD16^{bright}$ NK cells
% of all $CD56^{+}$ NK cells, Mean± SD	4.4 ± 2.5	3.1 ± 1.8	88.4 ± 5.7	78.6 ± 17.9	6.7 ± 5.0	7.8 ± 17.8
Absolute counts (cells/ml blood $x10^{4}$), Mean± SD	0.8 ± 0.4	0.6 ± 0.4	20.7 ± 18.4	-	-	-
CD69 MFI, Mean± SD	71.7 ± 25.7	125.6 ± 67.9	233.1 ± 116.5	1587.5 ± 839.8	1877.5 ± 586.5	769.9 ± 423.2
% of $CD69^{+}$ (Gating set according to matched endometrial immune cells), Mean± SD	1.8 ± 1.6	5.1 ± 5.3	9.6 ± 9.3	54.3 ± 17.8	73.3 ± 20.4	28.4 ± 13.3

Table 2.4 *Continued.* : PIP study data summary. Matched peripheral (PBMCs) and endometrial samples were collected during the mid-luteal phase. All samples were processed according to the SOP (Appendix B). Immune profiles for peripheral and endometrial samples, including immune cell subsets frequencies, absolute cell counts (for peripheral immune cells), CD69 MFI and the percentage of $CD69^{+}$ cells, are shown. n = 15.

Immune cell populations	PBMCs					Endometrial cells				
	$CD4^+$ T cells	$CD8^+$ T cells	$CD4^+$ $CD8^+$ T cells	$CD4^-$ $CD8^-$ T cells	$CD25^{bright}$ $CD127^{dim/-}$ Treg cells	$CD4^+$ T cells	$CD8^+$ T cells	$CD4^+$ $CD8^+$ T cells	$CD4^-$ $CD8^-$ T cells	$CD25^{bright}$ $CD127^{dim/-}$ Treg cells
% of all $CD3^+$ T cells, Mean± SD	68.4 ± 9.8	28.2 ± 7.1	1.1 ± 0.8	3.9 ± 1.7	4.2 ± 2.0 (% of all $CD4^+$ T cells)	50.0 ± 7.7	44.0 ± 8.2	2.8 ± 1.4	3.2 ± 1.3	7.0 ± 3.8 (% of all $CD4^+$ T cells)
Absolute counts (cells/ml blood $x10^5$), Mean± SD	8.7 ± 3.3	3.9 ± 2.2	0.1 ± 0.1	0.5 ± 0.5	0.4 ± 0.3	-	-	-	-	-
CD69 MFI, Mean± SD	78.8 ± 27.1	138.3 ± 44.1	219.4 ± 185.1	175.5 ± 81.3	145.3 ± 141.1	4130.1 ± 1441.0	4266.7 ± 1295.4	5743.4 ± 2186.0	4039.5 ± 1582.9	1019.9 ± 274. 9
% of $CD69^+$ (Gating set according to matched endometrial immune cells), Mean± SD	1.7 ± 2.2	4.9 ± 3.2	2.5 ± 1.9	5.3 ± 5.3	5.0 ± 8.7	75.6 ± 12.3	89.7 ± 11.3	89.8 ± 7.3	73.2 ± 14.9	44.3 ± 10.7

Table 2.4 *Continued*. : PIP study data summary. Matched peripheral (PBMCs) and endometrial samples were collected during the mid-luteal phase. All samples were processed according to the SOP (Appendix B). Immune profiles for peripheral and endometrial samples, including immune cell subsets frequencies, absolute cell counts (for peripheral immune cells), CD69 MFI and the percentage of $CD69^+$ cells, are shown. $n = 15$.

2.4.2.2 t-SNE analysis

t-SNE analysis shown in Figure 2.14 illustrated the immune profiles in the peripheral blood and endometrial samples. 7 major immune cell subsets, identified by the gating strategies described above, were mapped to the t-SNE plot using 7 different colours. In both sample sets, these 7 colours were separated in different clusters, meaning the gating strategies successfully identified different cell subsets with different expression patterns as determined by the PIP flow panel.

Additionally, there were clear differences between cell subset proportions between the peripheral blood and endometrial samples, shown as the cluster sizes in Figure 2.14. The differences were similar to the results shown in the last section. However, $CD56^{dim}$ $CD16^{bright}$ NK cells population in the endometrium appeared to have two clusters. After closer inspection, the difference between these two clusters was the expression level of CD8. Around 52% of endometrial $CD56^{dim}$ $CD16^{bright}$ NK cells had a high level of CD8 expression. A similar population were also found in the peripheral blood samples, with around 48% of $CD56^{dim}$ $CD16^{bright}$ NK cells express high level of CD8.

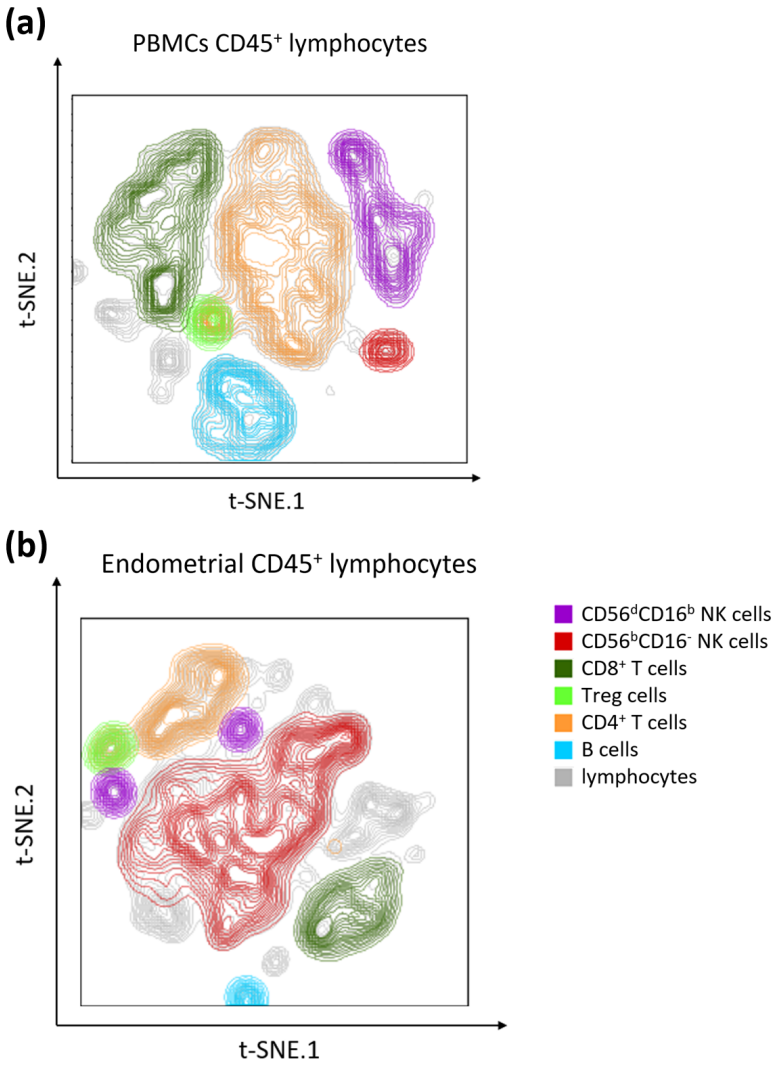

Figure 2.14: t-SNE analysis of peripheral blood and endometrial immune profiles. PBMCs were isolated by Lymphoprep^{TM}, endometrium samples were digested by Collagenase D (Appendix B). CD45^{+} lymphocytes were illustrated, and 6 immune cell subsets were mapped to the t-SNE plots using different colours. (a), Representative t-SNE plot of peripheral blood samples. (b), Representative t-SNE plot of endometrial samples. n=15.

2.4.2.3 FlowSOM analysis

FlowSOM analysis showed the expression pattern, which was determined by the PIP flow panel, of different immune cell populations in the peripheral blood and endometrial samples (Figure 2.15). 8 cell populations were automatically generated according to their expression profiles. FlowSOM analysis enabled us to analyse different marker expression levels in a certain population, which might be overlooked using the conventional gating method.

Similar to gating analysis (Figure 2.13), FlowSOM analysis showed a clear difference in CD69 expression between peripheral and endometrial immune cell subsets (Figure 2.15). In terms of cell proportions, the top 3 cell populations (ranked by proportions in $CD45^+$ lymphocytes) in the peripheral blood appeared to be $CD4^+$ T cells, $CD8^+$ T cells and $CD56^{dim}$ $CD16^{bright}$ NK cells, while in endometrium, they were $CD56^{bright}$ $CD16^-$ NK cells, $CD4^+$ T cells and $CD8^+$ T cells. $CD56^{dim}$ $CD16^{bright}$ NK cells appear to have a moderate level of CD8 expression, which might result from the $CD8^+$ population uncovered in the t-SNE analysis.

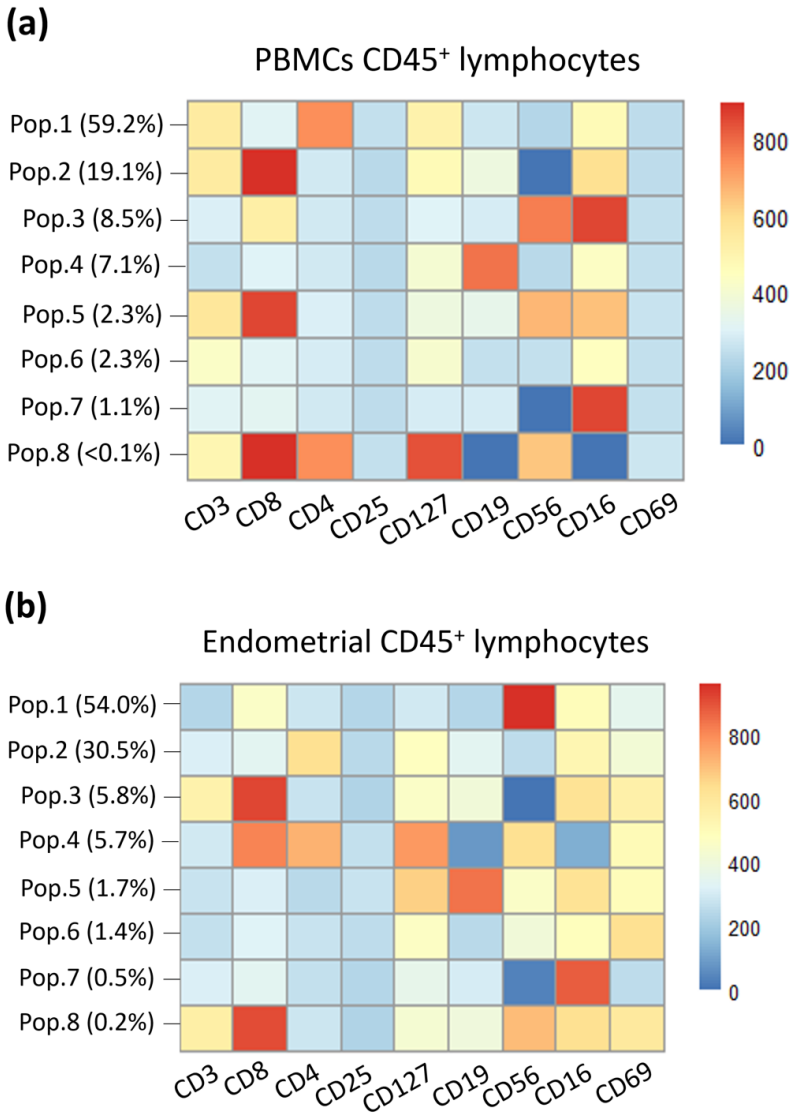

Figure 2.15: FlowSOM analysis of peripheral blood and endometrial immune profiles. PBMCs were isolated by Lymphoprep^{TM}, endometrium samples were digested by Collagenase D (Appendix B). CD45^{+} lymphocytes were autoclustered into 8 populations. Each population's proportion in CD45^{+} lymphocytes were shown in the brackets. 9 markers' expression levels for these 8 populations were illustrated in the heatmap. (a), Representative FlowSOM heatmap of peripheral blood samples. (b), Representative FlowSOM heatmap of endometrial samples. Pop, population. n=15.

2.4.3 Control versus infertility, RIF or RPL patients' immune profiles

Of the total 15 PIP samples collected, 4 are from RIF patients, 2 are from infertility patients, 2 is from RPL patients, 7 are from patients that are neither within RIF, infertility and RPL groups nor controls. No patient was eligible as fertile controls (Table 2.1). This study had planned to recruit a large number of patients (250) who would act as controls (patients having ICSI for make factor subfertility and became pregnant), RIF and RPL. Enrolment number was unfortunately very significantly lower than our initial goal.

Due to the limited sample size, the comparison between controls and infertility, RIF or RPL patients' immune profiles were not performed. We have just resumed patient enrolment to the study but further data cannot be included in the timeframe of this doctorate.

2.5 Discussion

2.5.1 Establishment of the SOP

A cost-effective, efficient and reproducible SOP was established to obtain immune profiles in blood and endometrium (Appendix B). I determined sample processing time limit to minimize variations in absolute cell count and cellular marker expression. Although some IVF clinics offer immunological testing for blood samples up to 48 hours after venepuncture, I found that immune phenotyping must be performed within 6 hours of blood collection. For obtaining single cells from endometrial biopsy for flow cytometry, mechanical dissection impacts cell quantity and viability (White et al. 2000), which is problematic when sample size is limited. Therefore, Collagenase D was chosen for its suitability for the PIP flow panel. The establishment of this SOP enabled a high-quality immune profiling study which could offer valuable insights in understanding the immune environment in the peripheral blood and endometrium, and whether their alterations could be linked with infertility, RIF or RPL.

2.5.2 Peripheral versus endometrial immune profiles

Clear differences were observed between peripheral and endometrial immune profiles. Similar to previous studies, the frequencies of NK cells, T cells, NK cell subsets ($CD56^{bright}$ $CD16^{-}$ NK cells and $CD56^{dim}$ $CD16^{bright}$ NK cells), T cell subsets ($CD4^{+}$ T cells, $CD8^{+}$ T cells, $CD25^{bright}$ $CD127^{dim/-}$ Treg cells) and the CD69 expression levels on immune cell subsets were significantly different between peripheral and endometrial samples (Chen et al. 1995, Marron et al. 2019, Lee et al. 2011).

Apart from these well-studied immune cell subsets, the frequencies of several minor cell populations such as $CD56^{bright}$ $CD16^{dim}$ NK cells and DP T cells were also shown to be significantly different between peripheral and endometrial samples. $CD56^{bright}$ $CD16^{dim}$ NK cells are considered as an intermediate developmental stage from immature $CD56^{bright}$ NK cells to mature $CD56^{dim}$ NK cells, compared with $CD56^{bright}$ $CD16^{-}$

NK cells, they have higher cytotoxicity due to its CD16 expression (Béziat et al. 2010, Cooper et al. 2001, Nagler et al. 1989). However, due to their limited cell numbers, most researchers do not consider nor do they investigate $CD56^{bright}$ $CD16^{dim}$ NK cells, and their function has not yet been studied in human endometrium. In this study, a significantly higher level of $CD56^{bright}$ $CD16^{dim}$ NK cells were found in the endometrium, and akin to other endometrial NK cell subsets, they also have a higher CD69 expression level compared with peripheral NK cells.

The frequencies of DP T cells were also found to be significantly higher in the endometrium compared with peripheral blood, with increased CD69 expression in the endometrium. The involvement of DP T cells during early pregnancy is not well studied, but DP T cells were found to be enriched at the site of inflammation in autoimmune diseases such as rheumatoid arthritis and autoimmune thyroiditis (De Maria et al. 1987, Waschbisch et al. 2014). DP T cells are likely to have an immunoregulatory role in T cell differentiation, favoring the polarization of naïve $CD4^+$ T cells into a Th2 functional profile (Bohner et al. 2019). In depth phenotypic profiling and functional studies are needed to investigate whether DP T cells are an active player at the implantation site.

t-SNE and FlowSOM analysis revealed similar proportional differences between endometrial and peripheral immune profiles. Interestingly, a subset of $CD56^{dim}$ $CD16^{bright}$ NK cells were found to express moderate level of CD8, account for around half of all $CD56^{dim}$ $CD16^{bright}$ NK cells in both the endometrial and peripheral blood. These NK cells are $CD3^-$ and have been previously reported as $CD8^+$ NK cells (Campbell et al. 2008). Compared with other $CD56^{dim}$ $CD16^{bright}$ NK cells, these $CD8^+$ NK cells are characterised by a greater responsiveness to stimulation (in terms of IFN-γ, TNF-α expression levels) and are likely to have a higher cytolytic potential (with higher expression level of granzyme b and perforin) (Ahmad et al. 2014). However, it is unclear whether $CD8^+$ NK cells are involved in early human pregnancy.

In addition to NK and T cells, B cell frequencies and their CD69 expression levels were also assessed in the PIP study. B cells are 6.5% $\pm$ 10.8% of all $CD45^+$ lymphocytes

in the endometrium, and an increased expression of CD69 is observed on endometrial B cells compared with their peripheral counterparts. This study confirmed that the majority of endometrial B cells (70.9% $\pm$ 12.2%) are tissue resident B cells. Interestingly, one of the participants in the study had a more atypical proportion of B cells, 45.7% of $CD45^+$ endometrial lymphocytes were $CD19^+$. But she did not have any observable abnormalities in terms of thyroid function or uterine structure, which have been shown to affect the endometrial immune environment (Kakita-Kobayashi et al. 2020, Riccio et al. 2017). To the best of my knowledge, no study has reported this high level of endometrial B cells, and what could be contributing to the increased level of endometrial B cells at the implantation site. As a key player in the mucosal immune system, understanding B cell involvement in the endometrial immune environment could provide help us unravel the complexity of immune interactions at the implantation site.

2.5.3 Future plans

From November 2018 - March 2020, 15 PIP samples were collected, which is significantly lower than our initial plan of 250. This was for two major reasons, firstly, we had anticipated that IVI Oxford would be the major recruiting site in this multi-centre study but this centre was closed shortly before recruitment commenced. In July 2019 we have added another site in Oxford, but local R&D not granted until January 2020. Secondly, recruitment at all sites was suspended in March 2020 due to the COVID-19 pandemic.

Preliminary data of this feasibility study showed differences between peripheral and endometrial immune cells. With the established SOP, we are positive that we will be able to continue recruitment to achieve a data set that represents normality, and, to compare the immune profiles between controls and infertility, RIF or RPL patients. For the fertile control group, we aimed to get a cohort of 50 women who suffered from male factor infertility and had live birth in the subsequent IVF cycle. This will enable us to obtain the normality distribution on peripheral and endometrial immune parameters, which are highly important data but does not yet exist in this field. For infertility, RIF

and RPL patients, we have not defined a recruitment target so that we can, at the end of the recruitment cycle, identify the proportions of the 250 women who fall into each subgroup (infertility group, RIF group and RPL group). Depending on the findings we may need to target specific groups in future studies.

One of the most interesting findings in the PIP samples I obtained, despite the small sample size, was the variation in endometrial B cells. This led me to question what is currently known about endometrial B cells. In the next chapter, I examined the current evidence on the role of endometrial B cells in normal endometrium and in benign female reproductive pathologies.

Chapter 3

The Role of Endometrial B Cells in Normal Endometrium and in Benign Female Reproductive Pathologies: a Systematic Review

3.1 Introduction

3.1.1 B cells in mucosa-associated lymphoid tissues (MALTs)

B cells, often identified by pan B cell markers CD19, CD20 or CD22, are a part of the adaptive immune system acting as professional antigen presenting cells. After the initial development in the bone marrow, immature B cells migrate to the secondary lymphoid organs (SLOs), such as lymph nodes, tonsils, spleen or mucosal associated lymphoid tissue (MALT), where B cell activation begins. Within the SLOs a specialised microenvironment called the germinal centre (GC) functions as the sites of B cell proliferation and somatic hypermutation, and leads to their differentiation into antibody-producing plasma cells or memory B cells (LeBien and Tedder 2008). In addition to SLOs, GC or GC-like structures have also been described in ectopic or tertiary lymphoid structures

(TLSs), where the GC supports local adaptive immune responses toward locally displayed antigens (Pipi et al. 2018).

B cells and the associated microenvironment GCs are vital in mucosal immunity, playing an important role in protection against the vast array of antigens at the mucosal surface (Vajdy 2006). In the gastrointestinal and respiratory tracts, B cell phenotypes and function have been widely characterised in the associated SLOs, respectively termed the gut-associated lymphoid tissues (GALTs) and bronchus-associated or nasopharyngeal-associated lymphoid tissues (BALTs or NALTs). These secondary lymphoid sites comprise GCs with a distinct B cell compartment that have a high frequency of surface IgA expressing B cells (McGhee and Fujihashi 2012, Ruddle and Akirav 2009), and their dysfunction has been linked with a variety of gastrointestinal and respiratory diseases (Adachi et al. 2015, Koboziev et al. 2010). In non-lymphoid sites in these tissues, such as the lamina propria and epithelial compartments, gut and lung B cells may have unique memory phenotypes and distinct immunoglobulin producing capabilities compared with their peripheral counterparts (Brandtzaeg 2007, Weisel et al. 2020).

3.1.2 B cells in female reproductive tract (FRT)

The FRT is also a mucosal system, however, B cells are comparatively understudied. Despite B cell dysfunction being implicated in benign female reproductive pathologies such as endometriosis, the majority of studies are focused on peripheral B cells instead of endometrial B cells or relevant tissue B cells (Danaii et al. 2020, Gagné et al. 2003, Riccio et al. 2017). As the innermost lining of the uterus, human endometrium is a highly dynamic tissue that cyclically sheds and regenerates under the influence of steroid hormones throughout the menstrual cycle, in preparation for embryo implantation occurring during the mid-luteal phase. Therefore, the endometrium not only provides mucosal immune defence against uterine pathogens, but also exhibits immune tolerance, as a semi-allogeneic embryo must invade through the tissue during placentation for successful pregnancy. At such a dynamic site for immune interactions, B cells were often

considered to be rare or absent from the human endometrium (King et al. 1998, Lee et al. 2011, Schumacher et al. 2018). Recent reviews have not looked into B cell location, number, phenotype or function in the endometrium, instead, their focus were mainly based on data from the decidua or peripheral samples, including emerging evidence that cells with a decidual B regulatory phenotype are important during pregnancy (Esteve-Solé et al. 2018, Guzman-Genuino and Diener 2017, Ticconi et al. 2019).

Nevertheless, some evidence indicates the importance of endometrial B cells in normal endometrium and endometrium obtained from women with female reproductive pathologies: infertility and endometriosis have been associated with a range of autoimmune diseases, which typically result from an expanded population of autoreactive B cells (Hershberg and Luning Prak 2015, Khizroeva et al. 2019, Rawlings et al. 2017, Shigesi et al. 2019); endometrial plasma cell levels are often used as a diagnostic criteria for an endometrial inflammatory disorder known as chronic endometritis (CE) (Cicinelli et al. 2019, Kitaya et al. 2014, Song et al. 2019, Liu et al. 2018). In addition, although GC or GC-like structure have not been properly characterised in the normal FRT, the presence of B cell centred lymphoid aggregates (LAs) have been widely reported, and these have been suggested to be GC-like, with antigen scavenging and antibody production capacities (Kitaya and Yasuo 2010a, Morris et al. 1985, Wira et al. 2014, Zhou et al. 2018).

In this systematic review, we provide a comprehensive summary of current data investigating B cells in normal endometrium and benign female reproductive pathologies. It facilitates further understanding of endometrial B cells in the endometrial mucosal immune environment, and would enhance our understanding of the known link between autoimmune diseases and reproductive pathologies. Here, we discuss the similarities and differences in endometrial B cells in normal endometrium and various reproductive pathologies, which can serve as the foundation for future studies.

3.2 Chapter Aims

This chapter presents a systematic review of endometrial B cells in the endometrium of healthy women and patients with reproductive pathologies. To achieve this, four databases were searched (MEDLINE, EMBASE, Web of Science Core Collection, CINAHL) from database inception until November 2020. Only peer reviewed research papers that studied endometrial B cells in non-pregnant women who were either healthy or had benign female reproductive pathologies were included. Each paper was graded as 'Good', 'Fair', or 'Poor' quality based on NEWCASTLE-OTTAWA quality assessment scale (original or adapted depends on the study type). Only 'Good' quality papers were included for this systematic review. By synthesising eligible publications, I have summarised the frequencies, phenotypes, locations and function of human endometrial B cells in both normal endometrium and benign gynaecological diseases.

Objectives:

1) To provide a comprehensive summary of current data investigating B cells in normal endometrium.

2) To investigate endometrial B cells were studied in which benign female reproductive pathologies.

3) To understand whether women with benign reproductive pathology have altered endometrial B cell profiles compared to healthy controls.

3.3 Methods

This systematic review has been registered in PROSPERO in January 2020 (PROSPERO ID: CRD42020152915) (O'Donnell et al. 2020).

3.3.1 Search strategy

Searches were conducted by two independent reviewers M.S and E.O.D. We performed bibliographic searches according to PRISMA guidelines (Group et al. 2009). The following computerised databases were searched: MEDLINE (via OVID), EMBASE (via OVID), Web of Science Core Collection (Citation Indexes = SCI-EXPANDED, CPCI-S, CPCI-SSH, BKCI-S, ESCI) and CINAHL (via EbscoHost) databases. Each database was searched from the established date until 20 November 2020. The search strategy combined the use of Subject Headings and relevant text words, which included specific terms and free – text terms relating to endometrium (e.g. 'endometri*'), B cells (e.g. 'B cell*', 'B lymphocyte*', 'plasma cell*', 'CD19', 'CD20', 'CD22') and possible B cell derivatives (e.g. 'antibod*', 'immunoglobulin*'). Additionally, non-benign diseases were excluded using free-text terms (e.g. 'cancer*', 'malign*', 'tumour*', 'carcinoma*') and search were limited to English language and human subjects. Additional papers that reviewers were aware of with endometrial B cell data present were also included. All study types were included to maximize the comprehensiveness of the search. A search strategy example for MEDLINE database is detailed in Table 3.1.

1. B-Lymphocytes/
2. (B cell* or b-cell* or b-lymphocyte*).ti,ab,kw.
3. Plasma Cells/
4. plasma cell*.ti,ab,kw.
5. Antibodies/
6. antibod*.ti,ab,kw.
7. Immunoglobulins/
8. immunoglobulin*.ti,ab,kw.
9. Antigens, CD19/
10. CD19.ti,ab,kw.
11. Antigens, CD20/
12. CD20.ti,ab,kw.
13. CD22.ti,ab,kw.
14. CD22.ti,ab,kw.
15. Endometrium/
16. endometri*.ti,ab,kw.
17. (cancer* or malign* or tumour* or tumor* or carcinoma* or adenoma* or adenocarcinoma* or neoplasm* or neoplastic* or sarcoma*).ti,ab,kw.
18. 1 or 2 or 3 or 4 or 5 or 6 or 7 or 8 or 9 or 10 or 11 or 12 or 13 or 14
19. 15 or 16
20. 18 and 19
21. 20 not 17
22. limit 21 to english language
23. limit 22 to human

Table 3.1: Example of searching strategy in the MEDLINE database. Database: Medline (Ovid MEDLINE Epub Ahead of Print, In-Process, Other Non-Indexed Citations, Ovid MEDLINE Daily and Ovid MEDLINE) 1946 to present. Search date: 20 November 2020.

3.3.2 Inclusion criteria and study selection

Peer reviewed research papers that studied endometrial B cells in non-pregnant women who were either healthy or presented with benign female reproductive pathologies were included in this systematic review. Non primary research articles such as reviews, commentaries, correspondence articles, short communications, and letters to the editor were excluded to avoid duplications. Case reports were excluded as their results may not be truly representative of a larger population. Conference abstracts were also excluded as their full publications are not available and have not been peer-reviewed to ensure

scientific rigor.

Two independent reviewers M.S. and E.O.D. carried out the study selection, first by reviewing titles, abstracts, and key words to assess paper relevance for endometrial B cells, then by screening the full text of selected studies identified in the initial phase. Two reviewers then discussed their chosen studies and any discrepancies were resolved through discussion.

3.3.3 Data extraction

Eligible papers were retrieved and read in detail to extract the following data into a standard form: authors, country, study period, publication year, publication journal, number of participants and demography, treatment details (if received), sample obtaining method, sample collection date (menstrual cycle day), sample storage approach, control group selection criteria, diagnostic criteria for gynaecological pathologies (if any), experimental design and reported results.

3.3.4 Quality assessment

An assessment of study quality using either NEWCASTLE-OTTAWA quality assessment scale (Wells et al. 2020) for case-control studies, or adapted NEWCASTLE-OTTAWA quality assessment scale (Modesti et al. 2016) for cross sectional studies. Sample selection, group comparability and study outcome were accessed and graded accordingly. If multiple endometrial immune cell types were studied, quality assessment was based on contents related to B cells. Each paper was graded as 'Good', 'Fair', or 'Poor' quality. Two independent reviewers M.S. and E.O.D performed quality assessment and any disagreement between reviewer judgement was resolved upon discussion with my thesis supervisors.

3.4 Results

3.4.1 Study selection

As shown in Figure 3.1, the database search retrieved 1424 records from MEDLINE, 2108 from Embase, 1658 from Web of Science and 32 from CINAHL. One additional paper that reviewers were aware of was also included in the identification phase. This paper did not mention B cells or B cell derivatives in paper title, abstract or key words, therefore was not retrieved from database search, but has endometrial B cell data present in main text. After de-duplication, in total 3356 papers were exported for first phase screening. After reviewing titles, abstracts, and key words, 2913 papers were excluded for either not using non-pregnant benign endometrium samples or not investigating B cells. The remaining 443 papers were deemed eligible for the next phase of full text screening. 320 papers were excluded for not being primary research articles, comprising 149 reviews, 141 conference abstracts, 8 case reports, 19 commentaries, 1 correspondence articles, 1 short communications, and 1 letter to the editor. Quality assessments were performed on the remaining papers and 'Poor' quality papers (n=78) and 'Fair' quality papers (n=22) papers were excluded from qualitative and quantitative synthesis. Briefly, a paper was excluded if it met one of the following criteria, (i), did not mention whether participants were pre-menopausal or post-menopausal or did not separate pre-menopausal and post-menopausal women in group analysis; (ii), did not mention how B cells were identified or no specific marker was used in B cell identification; (iii), no quantitative data was present, results only described as endometrial B cell presence or absence; (iv), other significant issue in 'Sample selection', 'Group comparability' or 'Study outcome'. Finally, 23 'Good' quality papers were included in the qualitative and quantitative synthesis.

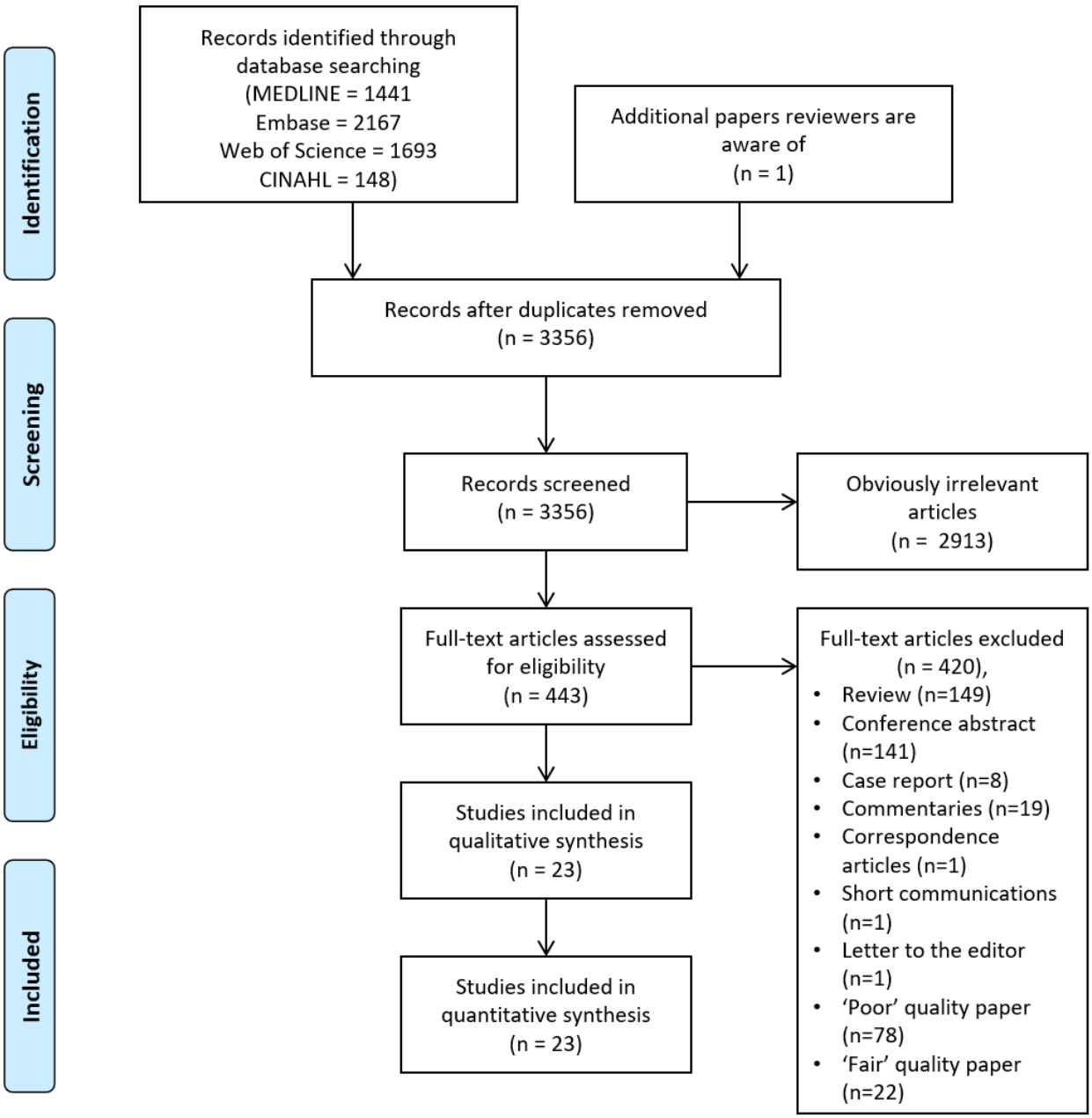

Figure 3.1: PRISMA flow diagram of study selection.

3.4.2 B cells in the normal endometrium

Endometrial B cells and immunoglobulins were studied in normal endometrium in 4 papers (Table 3.2). Dual-colour flow cytometry showed 3% of all endometrial lymphocytes were $CD3^-$ $CD19^+$ B cells in both the follicular and luteal phase, this was significantly lower than corresponding levels in PBMCs (18%) (Chen et al. 1995). Using immunohistochemistry (IHC), similar proportions of B cells were reported (Klentzeris et al. 1992). Single-cell RNA analysis of luteal phase endometrium identified a naïve B cell population in four out of six samples, which were no more than 2% of the total endometrial cell population. Compared with monocytes, macrophage/dendritic cells and NK cells, naïve B cells have a higher expression level of *CD19*, *CD20*, *CD79A*, *LY9*, *CD83*, *BTG1*, *CXCR4* and a moderate level of *CD74* and *HLA-DRA* (Lucas et al. 2020). Mass spectrometry demonstrated the presence of various immunoglobulins (heavy chains of IgG, IgM, IgJ, IgA1, IgA2 and light chain of Igκ) in the human endometrium, although they were less abundant in the endometrium than in the endocervix and ectocervix (Burgener et al. 2013).

Location wise, $CD22^+$ B cells were found both scattered within endometrial stroma as well as in lymphoid aggregates (LAs) (Figure 3.2) (Klentzeris et al. 1992). Evidence for LA associated B cells in normal endometrium were presented in case-control studies' respective control groups (Disep et al. 2004, Fernandez-Shaw et al. 1995, Kitaya and Yasuo 2010a, Klentzeris et al. 1994, 1995, Mettler et al. 1997). Apart from B cells (identified by CD20 or CD22), these aggregates also consist of other $CD45^+$ cells including $CD3^+$ T cells, $CD4^+$ T cells, $CD68^+$ macrophages and $CD57^+$ NK cells, with B cells in the central area, and T cells and macrophages in the margin areas (Disep et al. 2004, Klentzeris et al. 1992, Mettler et al. 1997). LAs were comprised of several hundreds of cells, express endometrial proliferation marker Ki-67 (examined by Ki-S3 antibody) and were mostly $HLA-DR^+$ (Mettler et al. 1997). They were situated in the lower functional layer, or the basal layer, and were observed throughout the menstrual cycle (Fernandez-Shaw et al. 1995, Mettler et al. 1997). Additionally, they appear to have a

cyclical influence, and are more likely to appear in the follicular phase of the menstrual cycle (Mettler et al. 1997). In addition, IgA was mainly located at or adjacent to the columnar endometrium epithelium (Burgener et al. 2013).

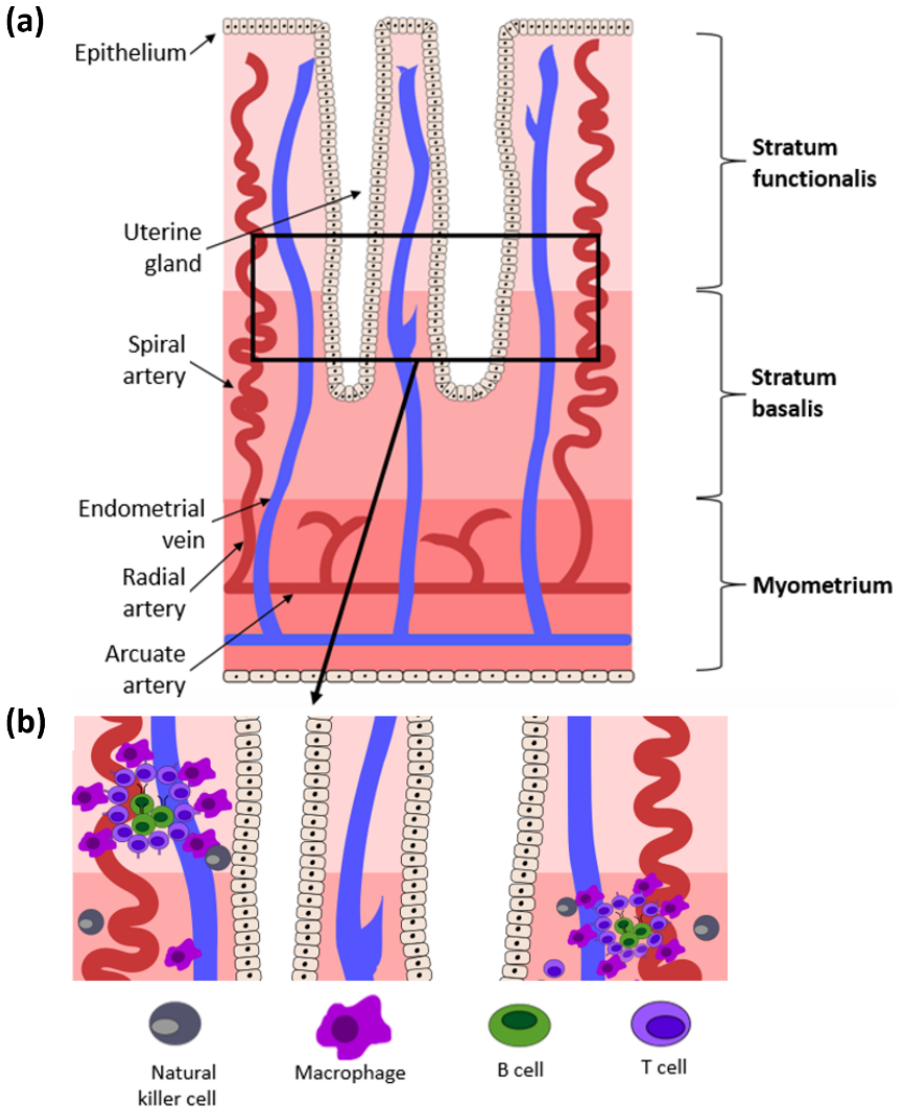

Figure 3.2: Illustration of lymphoid aggregates in human endometrium. (a) The uterine lining, including the stratum functionalis and basalis (the endometrium) and the underlying myometrium. (b) A close-up of the lower functionalis and the basalis layer of the endometrium. The LAs are composed of a B cell core, surrounded by a circle of T cells and a halo of macrophages. Natural killer cells are scattered throughout the stroma.

Citation	Study Type	Participant Information			Menstrual Cycle Phase of the Samples Obtained	Hormone Treatment	Experimental Method	Marker for B cell (subset)	Key Findings
		Age (yrs)	Number	Characteristics					
(Burgener *et al.*, 2013)	Cross-sectional	42-57	7	Without malignant and inflammatory conditions, HIV IgG seronegative and have no clinical symptoms of sexually transmitted infections during the 3 months prior to endometrial sample collection	-	None were on hormonal contraceptives	Mass Spectrometry	heavy chains of IgG, IgM, IgJ, IgHA1, IgHA2 and light chain of Igκ	Various immunoglobulins (heavy chains of IgG, IgM, IgJ, IgA1, IgA2 and light chain of Igκ) were present in human endometrium.
							IHC	IgA	IgA was mainly located at or adjacent to the columnar endometrium epithelium.
(Klentzeris *et al.*, 1992)	Cross-sectional	20-40	24	Had 1 or more successful pregnancies and a regular menstrual pattern, without endometrial pathology, pelvic endometriosis or anatomic abnormalities of the uterus, no coitus for over 48 hours before the sample collection	Luteal phase	No steroid hormone treatment 3 months before biopsy collection	IHC	CD22	B cells represent 2-3% of total CD45+ leucocytes, were detected in stroma as well as lymphoid aggregates.
(Chen *et al.*, 1995)	Cross-sectional	Mean age 42-43	39	Without malignant condition or endometrial pathology, no evidence of infection or inflammation	Follicular phase and luteal phase	-	Flow Cytometry	CD19	Significantly lower B cell percentage in endometrium (3%) compared with PBMCs (18%).

Table 3.2: Study characteristics of papers examining B cells in the normal endometrium.

Citation	Study Type	Participant Information			Menstrual Cycle Phase of the Samples Obtained	Hormone Treatment	Experimental Method	Marker for B cell (subset)	Key Findings
		Age (yrs)	Number	Characteristics					
(Lucas *et al.*, 2020)	Cross-sectional	31-42	6	With regular menstrual cycles, body mass index between 23 and 32 kg/m^2, and absence of uterine pathology on transvaginal ultrasound examination	Mid-luteal phase (LH+8) and late-luteal phase (LH+10)	None	Single cell RNA-seq	-	Naïve B cells, with no more than 2% of total endometrial cell population, were detected in human endometrium.

Table 3.2 *Continued.* : Study characteristics of papers examining B cells in the normal endometrium.

3.4.3 Endometriosis

Endometriosis is defined as the growth of endometrial-like tissue outside of the uterus (Zondervan et al. 2020). Endometrial B cells and immunoglobulins have been studied in endometriosis (Table 3.3). Dual-colour flow cytometry study showed $CD20^+$ B cells were significantly higher in endometriosis samples compared with controls; 10% of the lymphocytes (identified by $CD45^+$ $CD14^-$) were $CD20^+$ endometrial B cells in controls, 12% in eutopic endometrium and 17% in ectopic endometrium from endometriosis patients. Moreover, $CD20^+$ B cells in ectopic endometrium had significantly elevated CD5 and HLA-DR expression levels compared with the eutopic endometrium of endometriosis patients and controls (Antsiferova et al. 2005). Using CD22, three IHC studies reported similar endometrial B cell counts between endometriosis patients and controls (Fernandez-Shaw et al. 1995, Klentzeris et al. 1995, Mettler et al. 1997). Specifically, Klentzeris et al. reported B cells represent 3-4% of total $CD45^+$ cells in all samples. B cells were scattered throughout stroma with a few seen in lymphoid aggregates (Klentzeris et al. 1995). Mettler et al. showed B cells were almost exclusively detected in lymphoid aggregates, and the maximal quantity were present in the early follicular phase (40 $CD22^+$ cells per mm^2), then decreased during the mid-follicular phase and remain relatively constant in the luteal phase (20 $CD22^+$ cells per mm^2) in all samples (Mettler et al. 1997). Fernández-Shaw et al. reported on average 4-5 $CD22^+$ cells per 989 μm^2 (cell count ranging from 0 to 40 per 989 μm^2) in all samples during both the follicular and luteal phases (Fernandez-Shaw et al. 1995).

Citation	Study Type	Control Group		Endometriosis Group		Age (yrs)	Menstrual Cycle Phase of the Samples Obtained
		Control Characteristics	Number of Participants	Endometriosis Diagnosis	Number of Participants		
(Fernández-Shaw *et al.*, 1995)	Case-control	With regular but heavy menstrual cycles and no evidence of pelvic disease	10	Laparoscopically diagnosed, diagnosis and classification of endometriosis was based on the revised criteria of the American Fertility Society (The American Fertility Society, 1985)	8	Premenopausal	Variable
(Antsiferova *et al.*, 2005)	Case-control	Healthy women with previously documented fertility and no relevant gynaecological history	15	Laparoscopically diagnosed	20	21-40	-
(Klentzeris *et al.*, 1995)	Case-control	No endometriosis, 1 or more successful pregnancies in the past, with a regular menstrual cycle	18	Infertile women[1] who had laparoscopically diagnosed endometriosis. Diagnosis and classification of endometriosis was based on the revised criteria of the American Fertility Society (The American Fertility Society, 1985)	18	22-41	Early, mid and late luteal phase
(Mettler *et al.*, 1997)	Case-control	Laparoscopically proven tubal factor infertility resulting from the prior pelvic inflammatory disease. No signs of endometrial inflammation	110	Laparoscopically diagnosed, diagnosis and classification of endometriosis was based on the revised criteria of the American Fertility Society (The American Fertility Society, 1985)	143	Mean age, 30	Variable

Table 3.3: Study characteristics of papers examining endometrial B cells in controls and endometriosis patients. [1]As detailed in Table 3.4, infertility is diagnosed when participants were unable to conceive after at least 12 months of unprotected intercourse (Klentzeris et al. 1995).

Citation	Hormone Treatment	Experimental method	Marker for B cell (subset)	Key Findings
(Fernández-Shaw *et al.*, 1995)	None	IHC	CD22	B cells were detected in stroma as well as lymphoid aggregates. Similar B cell count in control and endometriosis group (on average 4-5 $CD22^+$ cells per 989 μm^2)
(Antsiferova *et al.*, 2005)	None within last 3 months	Flow Cytometry	CD20 (HLA-DR, CD5)	Significantly higher B cell percentage in endometriosis group (12% of all lymphocytes in eutopic endometrium and 17% in ectopic endometrium) compared with controls (10% of all lymphocytes)
(Klentzeris *et al.*, 1995)	None when sample was collected	IHC	CD22	B cells were detected in stroma as well as lymphoid aggregates. Similar B cell count in control and endometriosis group (3-4% of total $CD45^+$ cells)
(Mettler *et al.*, 1997)	-	IHC	CD22	B cells were exclusively detected in lymphoid aggregates. Similar B cell count in control and endometriosis group (20 $CD22^+$ cells per mm^2)

Table 3.3 *Continued.* : Study characteristics of papers examining endometrial B cells in controls and endometriosis patients.

3.4.4 Infertility, RIF and RPL

Endometrial B cells, plasma cells and immunoglobulins were studied in women with a history of infertility, RIF or RPL compared to healthy controls. The diagnostic criteria for RPL, RIF and infertility vary between different papers (Table 3.4). One study used flow cytometry to investigate endometrial B cells (Lachapelle et al. 1996), seven studies used only IHC (Kitaya et al. 2014, Klentzeris et al. 1994, 1995, Liu et al. 2018, Michimata et al. 2002, Quenby et al. 1999, Zargar et al. 2020) and one study combined IHC and an RNase protection assay (a highly sensitive technique detecting and measuring the abundance of specific mRNAs in total cellular RNA) (Bohlmann et al. 2010).

The flow cytometry study reported a significant increase in $CD20^+$ endometrial B cells in RPL when compared with normal controls during the luteal phase ($5 \pm 6\%$ of $CD45^+$ cells in controls versus $16 \pm 8\%$ of $CD45^+$ cells in RPL) (Lachapelle et al. 1996). B cell percentages were similar between primary and secondary RPL and no correlation was observed between B cell percentages and number of pregnancy losses (Lachapelle et al. 1996). Two IHC studies using either CD20 or CD22 as a B cell marker revealed no significant difference in endometrial B cell numbers between control and RPL women (Michimata et al. 2002, Quenby et al. 1999). Specifically, Michimata et al. found similar levels of $CD20^+$ endometrial B cells (2-3% of all endometrial $CD45^+$ cells) in both controls and RPL patients, regardless of their subsequent pregnancy outcome (Michimata et al. 2002). Quenby et al. reported $CD22^+$ B cells comprised 0-4% of total endometrial cells (per 10 high power fields); of note, two out of thirty-one women had an elevated B cell count, and in the pregnancy following endometrium analysis, one patient had a live birth and the other had a miscarriage (Quenby et al. 1999). Using CD19 as the B cell marker, combined with an RNase protection assay for validation, Bohlmann et al. also showed no significant difference in B cell numbers between healthy and RPL women (Bohlmann et al. 2010).

For RIF, immunoglobulin content was also analysed by IHC. There was a significant increase in IgM^+ stromal cell density during the follicular phase in RIF patients (regardless

of endometritis diagnosis) compared with controls (Kitaya et al. 2014).

Investigating women with a history of infertility, no significant differences in endometrial $CD22^+$ B cell numbers between control and infertile patients were found by IHC (Klentzeris et al. 1994, 1995). $CD22^+$ B cells constituted 2-4% of all endometrial $CD45^+$ cells, and were present in the both stroma and lymphoid aggregates (Klentzeris et al. 1994, 1995).

Additionally, two studies included more than 1 patient group. Using IHC $CD138^+$ to identify plasma cells, one cross-sectional study found 36.8% (14 subjects) of patients with RPL and 23.4% (11 subjects) of patients with RIF had over 5 plasma cells per 20 high-power fields in endometrial samples (Zargar et al. 2020). One case-control study reported no significant difference in plasma cell counts when comparing different subgroups, including controls, RPL, RIF and infertile groups, and most samples had $CD138^+$ cell counts < 5 per $0.1mm^2$ (Liu et al., 2018).

Citation	Study Type	Control Group		Reproductive Failure Group			Age (yrs)	Menstrual Cycle Phase of the Samples Obtained
		Control Characteristics	Number of Participants	Participants' Selection		Number of Participants		
(Michimata *et al.*, 2002)	Case-control	Successful pregnancy after IVF treatment for solely male factor infertility	15	A history of two consecutive first-trimester miscarriages, with subsequent IVF treatment outcome	Successful pregnancy	11	Mean age, 30-32	Mid-luteal phase (day 5-8 after LH surge)
					Pregnancy loss (RPL)	6		
(Lachapelle *et al.*, 1996)	Case-control	Healthy fertile women	15	A history of 3 or more unexplained, consecutive, first trimester spontaneous miscarriages with the same partner	Primary RPL	11	22-40	Luteal phase
					Secondary RPL	9		
(Quenby *et al.*, 1999)	Case-control	2 or more normal pregnancies	9	At least three consecutive miscarriages (RPL)		22	20-41	Mid-luteal phase
(Bohlmann *et al.*, 2010)	Case-control	-	10	17 Women had 3 or more idiopathic early miscarriages, and 8 women had 2 early miscarriages. (RPL)		25	21-41	Luteal phase
(Kitaya *et al.*, 2014)	Case-control	Proven fertile women	22	Consecutive negative pregnancy tests following transfer of 3 or more morphologically good embryos and/or blastocysts (RIF)	Non-endometritis patients[1]	23	Mean age, 37	Follicular phase
					Endometritis patients[1]	28		

Table 3.4: Study characteristics of papers examining endometrial B cells in infertility, RIF or RPL patients. [1]As detailed in Table 3.5, endometritis is diagnosed when there is unusual plasmacyte infiltrates within the endometrial stromal compartment (Kitaya et al. 2014).

Citation	Study Type	Control Group		Reproductive Failure Group		Age (yrs)	Menstrual Cycle Phase of the Samples Obtained
		Control Characteristics	Number of Participants	Participants' Selection	Number of Participants		
(Klentzeris *et al.*, 1995)	Case-control	1 or more successful pregnancies in the past	18	Endometriosis patients[2] who are unable to conceive alter at least 12 months of unprotected intercourse (Infertility)	18	22-41	Early, mid and late luteal phase
(Klentzeris *et al.*, 1994)	Case-control	1 or more successful pregnancies	24	A history of involuntary infertility of >2 years (Unexplained infertility)	24	24-43	Luteal phase
(Zargar *et al.*, 2020)	Cross-sectional	-	-	Failure to achieve a clinical pregnancy after 2 good-quality embryo transfers in fresh or frozen cycles (RIF)	47	Mean age, 36	Follicular phase (3 to 5 days after menstruation)
				2 or more consecutive pregnancy losses or 3 or more alternate pregnancy losses (<20 weeks of gestational ages) (RPL)	38		
(Liu *et al.*, 2018)	Case-control	At least 1 live birth within the previous two years	40	Loss of 3 or more consecutive pregnancies before 24 weeks of gestation (RPL)	93	20-40	Mid-luteal phase
				Fail to achieve clinical pregnancy after transfer of at least 4 good-quality embryos in 3 or more transfer cycles (RIF)	39		
				Infertility	48		

Table 3.4 *Continued.* : Study characteristics of papers examining endometrial B cells in infertility, RIF or RPL patients. [2]As detailed in Table 3.3, endometriosis is diagnosed laparoscopically, according to the revised criteria of the American Fertility Society (Andrews et al. 1985, Klentzeris et al. 1995).

Citation	Hormone Treatment	Experimental method	Marker for B cell (subset)	Key Findings
(Michimata *et al.*, 2002)	-	IHC	CD20	Similar B cell count in control and RPL group (2-3% of all endometrial $CD45^+$ cells)
(Lachapelle *et al.*, 1996)	-	Flow Cytometry	CD20	Significant increase in $CD20^+$ endometrial B cells in RPL (16 ± 8% of $CD45^+$ cells) when compared with normal controls (5 ± 6% of $CD45^+$ cells). Similar B cell percentages in primary and secondary RPL.
(Quenby *et al.*, 1999)	-	IHC	CD22	Similar B cell count in control and RPL group (0-4% of total endometrial cells per 10 high power fields)
(Bohlmann *et al.*, 2010)	None within last 3 months	IHC and RNase protection assay	CD19	Similar B cell count in control and RPL group
(Kitaya *et al.*, 2014)	Controlled ovarian stimulation protocol in most RIF patients	IHC	CD138, IgM, IgA1, IgA2, IgG1, IgG2, IgG3, IgG4, IgD, IgE	Significant increase in IgM^+ stromal cell density in RIF group (regardless of endometritis diagnosis) compared with controls
(Klentzeris *et al.*, 1995)	None when sample was collected	IHC	CD22	B cells were detected in stroma as well as lymphoid aggregates. Similar B cell count in control and infertility group (constituted 3-4% of all endometrial $CD45^+$ cells)
(Klentzeris *et al.*, 1994)	-	IHC	CD22	B cells were detected in stroma as well as lymphoid aggregates. Similar B cell count in control and infertility group (constituted 2-3% of all endometrial $CD45^+$ cells)
(Zargar *et al.*, 2020)	-	IHC	CD138[3]	36.8% (14 subjects) of patients with RPL and 23.4% (11 subjects) of patients with RIF had over 5 plasma cells per 20 high-power fields in endometrial samples
(Liu *et al.*, 2018)	None with in last 2 months	IHC	CD138[3]	Similar B cell count in control and reproductive failure groups including RPL, RIF and infertile groups (most samples have $CD138^+$ cell counts < 5 per $0.1mm^2$)

Table 3.4 *Continued.* : Study characteristics of papers examining endometrial B cells in infertility, RIF or RPL patients. [3]As discussed in the Chapter 3.4.5, CD138 staining is performed as a diagnostic criteria for CE.

3.4.5 Endometritis

Endometritis is defined as the inflammation of the lining of the uterus and may be in acute and chronic in presentation. Acute endometritis is manifested with fever, pelvic pain and vaginal discharge. CE, on the other hand, is usually asymptomatic or oligosymptomatic. CE has been linked with adverse reproductive outcomes including RIF and RPL (Huang et al. 2020). Our search retrieved 1 paper focused on endometritis (acute and chronic) (Disep et al. 2004) and 7 papers focused solely on CE (Cicinelli et al. 2019, Kitaya et al. 2014, Liu et al. 2018, Parks et al. 2019, Song et al. 2019, Toth et al. 2007, Kitaya and Yasuo 2010a). In the included papers there was no agreed definition or test for the diagnosis of CE, both hysteroscopic examination and histopathological assessment have been used. In histopathological assessment, CE is confirmed by the presence of plasma cells, identified by markers such as CD138 and multiple myeloma oncogene 1 (MUM1), or morphological assessment after standard histological staining with Hematoxylin Phloxine Saffron stain (HPS) or Hematoxylin and Eosin (H&E) (Table 3.5). Using different diagnostic methods to identify B cells, plasma cells or immunoglobulns, the prevalence of CE may differ (Cicinelli et al. 2019, Liu et al. 2018, Parks et al. 2019, Song et al. 2019, Toth et al. 2007, Zargar et al. 2020).

Endometrial B cells, plasma cells and immunoglobulin contents have been studied in endometritis by IHC (Table 3.5). Compared with controls, where $CD20^+$ B cells are found in the basal and stromal layers, in endometritis patients they are more abundant and in alternate locations such as in epithelium and glandular lumina (Disep et al. 2004, Kitaya and Yasuo 2010a). Disep et al. showed $CD20^+$ B cells comprise less than 1% of all $CD45^+$ cells in normal endometrium but up to 25% in endometritis samples (Disep et al. 2004). Kitaya and Yasuo showed on average there are 0.41 $CD20^+$ B cells per 20 gland lumina in controls and 47 B cells per 20 gland lumina in CE patients (Kitaya and Yasuo 2010a). Additionally, $CD20^+$ B cell counts also increased with endometrial inflammation severity (graded according to plasma cell and neutrophils presence) along with the size of lymphoid aggregates (Disep et al. 2004). In CE $CD138^+$ plasma cells

counts (>5) were statistically correlated with C. trachomatis infection (Toth et al. 2007). The densities of IgM^+, $IgA1^+$, $IgA2^+$, $IgG1^+$ and $IgG2^+$ during the follicular phase were significantly higher in CE patients with RIF compared with both RIF patients without CE and healthy controls. Among all five types of immunoglobulins assessed, IgM^+ had the highest density, followed by $IgG2^+$, $IgA1^+$ and $IgA2^+$, with each one significantly lower than the former. $IgG1^+$ density was significantly lower than $IgG2^+$, but significantly higher than $IgA2^+$ (Kitaya et al. 2014).

Citation	Study Type	Control Group		Endometritis Group		Age (yrs)	Menstrual Cycle Phase of the Samples Obtained
		Control Characteristics	Number of participants	Endometritis Diagnosis	Number of participants		
(Kitaya and Yasuo, 2010a)	Case-control	No sign of plasma cells by CD138 staining in endometrial samples	54	$CD138^+$ punctate staining in endometrial samples	22	Premenopausal	Mid-luteal phase
(Toth *et al.*, 2007)[1]	Case-control[1]	-	-	Surgical diagnosis	30 out of 92	16-46	-
				HPS staining and morphological plasma cell identification in endometrial samples	38 out of 92		
				H&E staining and morphological plasma cell identification in endometrial samples	72 out of 92		
				CD138 and HPS staining to find plasma cells in endometrial samples	76 out of 92		
(Liu *et al.*, 2018)[2]	Case-control[2]	-	-	1 or more plasma cells per 10 per 10 high power fields in endometrial samples, identified by CD138	12 out of 220	20-40	Mid-luteal phase
				1.95 or more plasma cells per 10 per 10 high power fields in endometrial samples, identified by CD138	36 out of 220		
				1 or more plasma cells per whole section in endometrial samples, identified by CD138	95 out of 220		
				2.95 or more plasma cells per whole section in endometrial samples, identified by CD138	42 out of 220		
				5.15 or more plasma cells per 0.1 mm^2 in endometrial samples, identified by CD138	20 out of 220		

Table 3.5: Study characteristics of papers examining endometrial B cells in endometritis patients. [1]A case-control study on Chlamydia trachomatis and abnormal uterine bleeding. In total 92 cases, Chlamydia trachomatis was detected in 44 cases, abnormal uterine bleeding was diagnosed in 65 cases (as detailed in Table 3.6), uterine fibroids and ovarian cysts were noted in 27 cases (Toth et al. 2007). [2]A case-control study on infertility, RIF and RPL (as detailed in Table 3.4), in total 220 cases, 40 were controls, 93 were RPL patients, 39 were RIF patients and 48 were infertile patients (Liu et al. 2018).

Citation	Study Type	Control Group		Endometritis Group			Age (yrs)	Menstrual Cycle Phase of the Samples Obtained
		Control Characteristics	Number of participants	Endometritis Diagnosis		Number of participants		
(Cicinelli *et al.*, 2019)[3]	Case-control[3]	-	-	Hysteroscopic examination based on the demonstration of micro-polyps, polypoid endometrium, stromal edema and focal or diffuse hyperemia		238 out of 480	Mean age, 33	Follicular phase
				1–5 plasma cells per high-power field or discrete clusters of <20 plasma cells endometrial samples identified by CD138		206 out of 480		
(Song *et al.*, 2019)	Cross-sectional	-	-	1 or more plasma cell identified per 10 high power fields in endometrial samples, identified by CD138		322 out of 1189	Mean age, 33	Follicular phase
				Endometrium with one or more hysteroscopic features, hyperemia, micro-polyps, and/ or interstitial edema		454 out of 1189		
(Zargar *et al.*, 2020)	Cross-sectional	-	-	More than 5 plasma cells per 20 high-power fields in endometrial samples identified by CD138	RPL patients[4]	14 out of 38	Mean age, 36	Follicular phase (3 to 5 days after menstruation)
					RIF patients[4]	11 out of 47		
				Hysteroscopy examination, direct observation of mucosal edema, focal or diffuse endometrial hyperemia, and the presence of micropolyps (<1 mm)	RPL patients[4]	12 out of 38		
					RIF patients[4]	10 out of 47		

Table 3.5 *Continued.* : Study characteristics of papers examining endometrial B cells in endometritis patients. [3]A case-control study on endometrial polyps (as detailed in Table 3.6), in total 480 cases, 50% of all participants have endometrial polyps (Cicinelli et al. 2019). [4]In total 38 RPL patients and 47 RIF patients were included. As detailed in Table 3.4, RPL is diagnosed when participants had 2 or more consecutive pregnancy losses or 3 or more alternate pregnancy losses (<20 weeks of gestational ages), RIF is diagnosed when participants failed to achieve a clinical pregnancy after 2 good-quality embryo transfers in fresh or frozen cycles (Zargar et al. 2020).

Citation	Study Type	Control Group		Endometritis Group			Age (yrs)	Menstrual Cycle Phase of the Samples Obtained
		Control Characteristics	Number of participants	Endometritis Diagnosis		Number of participants		
(Parks *et al.*, 2018)	Cross-sectional	-	-	1 or more plasma cells in endometrial samples, identified by MUM1, CD138, and H&E		55 out of 87	Median age, 36	Variable
				1 or more plasma cells in endometrial samples, identified by MUM1 and H&E		118 out of 224		
(Disep *et al.*, 2004)	Case-control	Histologically normal, no evidence of any endometrial pathology	22	Based on the presence of stromal plasma cells and/or neutrophils in endometrial samples, inflammation was graded as	Mild	25	Variable	Variable
					moderate	32		
					severe	22		
(Kitaya *et al.*, 2014)	Case-control	No CE, proven fertile women	22	RIF patients[5] with unusual plasmacyte infiltrates within the endometrial stromal compartment (histopathologic diagnosis)		28	Mean age, 37	Follicular phase
		No CE, consecutive negative pregnancy tests following transfer of 3 or more morphologically good embryos and/or blastocysts	23					

Table 3.5 *Continued.* : Study characteristics of papers examining endometrial B cells in endometritis patients. [5]As detailed in Table 3.4, RIF is diagnosed when participants had consecutive negative pregnancy tests following transfer of 3 or more morphologically good embryos and/or blastocysts (Kitaya et al. 2014).

Citation	Hormone Treatment	Experimental method	Marker for B cell (subset)	Key Findings
(Kitaya and Yasuo, 2010a)	-	IHC	CD138, CD20	B cells were detected in stroma as well as lymphoid aggregates in all samples. In CE, B cells were seen in greater numbers (around 0.41 B cells per 20 gland lumina in controls versus 47 B cells per 20 gland lumina in CE samples) and unusual locations. B cell aggregates were present with an increased size in CE samples.
(Toth *et al.*, 2007)	65% of participants named oral contraception as their primary method of birth control	IHC	CD138	More CE cases were reported using histopathological assessment compared with hysteroscopic examination. Significant correlation was reported between higher plasma cell counts (>5) and C. trachomatis infection.
(Liu *et al.*, 2018)	None with in last 2 months	IHC	CD138	Numbers of CE cases were different when different numbers of plasma cells were used as diagnostic criteria.
(Cicinelli *et al.*, 2019)	None within last 3 months	IHC	CD138	More CE cases were reported using hysteroscopic examination compared with histopathological assessment.
(Song *et al.*, 2019)	-	IHC	CD138	More CE cases were reported using hysteroscopic examination compared with histopathological assessment.
(Zargar *et al.*, 2020)	-	IHC	CD138	More CE cases were reported using histopathological assessment compared with hysteroscopic examination.
(Parks *et al.*, 2018)	-	IHC	CD138, MUM1	In histopathological assessment, CE prevalence was different when different markers were used for plasma cells identification.
(Disep *et al.*, 2004)	-	IHC	CD20	B cells were detected in stroma as well as lymphoid aggregates in all samples. In endometritis, B cells were seen in greater numbers (<1% of $CD45^+$ cells in controls versus up to 25% in endometritis samples) and unusual locations. Additionally, the sizes of B cell aggregates were increased with endometrial inflammation severity.
(Kitaya *et al.*, 2014)	Controlled ovarian stimulation protocol in most RIF patients	IHC	CD138, IgM, IgA1, IgA2, IgG1, IgG2, IgG3, IgG4, IgD, IgE	IgM^+ has the highest density among all assessed immunoglobulins. Significantly higher IgM^+, $IgA1^+$, $IgA2^+$, $IgG1^+$ and $IgG2^+$ densities in CE patients with RIF compared with both RIF patients without CE and controls.

Table 3.5 *Continued.* : Study characteristics of papers examining endometrial B cells in endometritis patients.

3.4.6 Other pathologies

$CD20^+$ endometrial B cells and $CD138^+$ endometrial plasma cells were also studied by IHC in patients suffering from abnormal uterine bleeding, endometrial polyps and uterine fibroids (Table 3.6). The $CD20^+$ B cell density was low in both controls and uterine fibroids patients (0–3 in 10 non-overlapping stromal areas) and no difference was observed throughout the menstrual cycle (Kitaya and Yasuo 2010b). Toth et al. examined the correlation between abnormal uterine bleeding and C. trachomatis CE (diagnosed by $CD138^+$ staining), and reported $CD138^+$ plasma cells were present in 80% of patients with abnormal uterine bleeding, compared to 41% in controls (Toth et al. 2007). Greater prevalence of $CD138^+$ plasma cells in the follicular phase was reported in patients with endometrial polyps compared with the controls (62% versus 24%). Moreover, 78% of endometrial polyps had $CD138^+$ staining, within this group 64% also had $CD138^+$ staining on their corresponding endometrial samples. Endometrial polyps that were $CD138^-$ had significantly less $CD138^+$ staining in the endometrium (31%) from the same patient (Cicinelli et al. 2019).

Citation	Study Type	Control Group		Pathological Group		Age (yrs)	Menstrual Cycle Phase of the Samples Obtained
		Control Characteristics	Number of Participants	Pathology and Patients' Characteristic (if stated)	Number of Participants		
(Toth *et al.*, 2007)[1]	Case-control	Without abnormal uterine bleeding diagnosis	27	Abnormal uterine bleeding	65	16-46	-
(Cicinelli *et al.*, 2019)	Case-control	Normal endometrium without evidence of endometrial polyps at hysteroscopy[2]	240	Endometrial polyps, diagnosed at hysteroscopy and histology, identified as localized overgrowths of endometrial mucosa	240[3]	Mean age, 33	Follicular phase
(Kitaya and Yasuo, 2010b)	Case-control	Normal endometrium without uterine fibroids	With benign ovarian tumours: 20	Uterine fibroids, classified into three categories according to the location within the uterine wall	Submucosal, causing cavity distortions: 24	37-45	Variable
					Intramural, with less than 50% extension outside the myometrium without any cavity distortions: 25		
			With uterine prolapse: 4		Subserosal, with 50% or more extension outside the myometrium without cavity distortions: 13		

Table 3.6: Study characteristics of papers examining endometrial B cells in controls and abnormal uterine bleeding, endometrial polyps and uterine fibroids patients. [1]In total 92 cases, Chlamydia trachomatis was detected in 44 cases, uterine fibroids, and ovarian cysts were noted in 27 cases. Additionally, CE was diagnosed by H&E, HPS and/ or CD138 staining, as detailed in Table 3.5 (Toth et al. 2007). [2]in total 240 cases, 136 women had a submucous/intramural uterine myoma. Additionally, CE was diagnosed by hysteroscopic examination or CD138 staining, as detailed in Table 3.5 (Cicinelli et al. 2019).[3]240 Endometrial polyps' samples from the same group of patients were also collected and analysed (Cicinelli et al. 2019).

Citation	Hormone Treatment	Experimental method	Marker for B cell (subset)	Key Findings
(Toth *et al.*, 2007)	65% of participants named oral contraception as their primary method of birth control	IHC	CD138	Greater prevalence of plasma cell presence was reported in the abnormal uterine bleeding patients compared with the controls (80% versus 41%).
(Cicinelli *et al.*, 2019)	None within last 3 months	IHC	CD138	Greater prevalence of plasma cell presence was reported in the endometrial polyps patients compared with the controls (62% versus 24%).
(Kitaya and Yasuo, 2010b)	None	IHC	CD20	Similar B cell count (0–3 in 10 non-overlapping stromal areas) in uterine fibroids patients and controls.

Table 3.6 *Continued.* : Study characteristics of papers examining endometrial B cells in controls and abnormal uterine bleeding, endometrial polyps and uterine fibroids patients.

3.5 Discussion

There have been a number of reviews on the role of B cells in benign gynaecological conditions. However, these articles mostly discussed peripheral B cells and antibody titres in one specific pathology, and no quality assessment was performed for the endometrial B cell data included (Muzzio et al. 2013, Riccio et al. 2017, Vallvé-Juanico et al. 2019). This systematic review is the first to summarise the evidence for endometrial B cell location, number, phenotype and function in normal endometrium and in benign endometrial pathologies with a comprehensive searching and grading process.

3.5.1 Summary of findings

This systematic review included 16 case-control and 7 cross-sectional studies; endometrial B cells were studied in healthy women, endometriosis, infertility, RIF, RPL, endometritis, abnormal uterine bleeding, endometrial polyps and uterine fibroids. 6 studies have mixed patient populations with more than 1 diagnosed condition, mostly to evaluate the prevalence of CE or endometriosis in patients with RPL. The experimental methods used were IHC alone (n=17), flow cytometry alone (n=3), single cell RNA-seq (n=1), and IHC combined with either an RNase protection assay or mass spectrometry (n=2). B cells were detected in the majority (n=12) by one of the commonly used B cell markers alone (CD19, CD20 or CD22), a combination of B cell markers, CD20 with either CD138 or HLA-DR and CD5 (n=2) or CD138 and MUM (n=1), or CD138 alone (n=5). In addition, 2 studies examined the immunoglobulin expression (1 study also included CD138), and only 1 single cell RNA-seq study performed an unbiased profiling on endometrial B cells.

Despite the commonly reported claim that B cells are rare or absent in the endometrium (Guzman-Genuino and Diener 2017, Lee et al. 2011, Schumacher et al. 2018, Ticconi et al. 2019), this review demonstrates that endometrial B cells are consistently present in normal cycling human endometrium and in endometrium from women with

endometriosis, infertility, RIF, RPL, endometritis and other pathologies including abnormal uterine bleeding, endometrial polyps and uterine fibrosis. B cells typically constitute less than 5% of total $CD45^+$ lymphocytes, and no more than 2% of total cells in normal endometrium. This is lower than that in other lymphoid mucosal tissues such as the lung and gut (Farstad et al. 2000, Weisel et al. 2020), but is similar to other tissues such as the stomach and liver. Gastric B cells account for 0 – 5% of all live cells in the antral mucosa biopsies from healthy stomach and hepatic B cells represent 1 - 8% of all lymphocytes in healthy liver (Goll et al. 2005, Norris et al. 1998, Robinson et al. 2016). Although B cells are not an abundant cell population in these organs, their proportional and phenotypical differences as well as functional importance have been noted in gastric and hepatic diseases such as peptic ulcer disease and hepatitis C infections (Curry et al. 2003, Goll et al. 2005, Racanelli et al. 2001). By comparison, the characterization of endometrial B cells in reproductive pathologies is limited and mainly focused on the proportional differences.

Results show the quantity of B cells within the endometrium is altered in certain pathologies. $CD20^+$ B cells are more abundant in patients with endometritis, but data are conflicting as to whether there are increased B cell numbers in endometriosis and patients with infertility, RIF or RPL. This is partially due to the different methodologies used for B cell identification: flow cytometric analysis involves tissue digestion, which might affect the surface expression of certain molecules, and cause skewed cell population retrieval (Autengruber et al. 2012, Skulska et al. 2019); IHC only detects the immune profile of a limited tissue area, thus reliable quantification can be difficult to obtain. Discrepancies also arise between studies' cases and control selection criteria, particularly in studies focused on RIF or RPL. Appropriate endometrial control tissue is often problematic in studies and this may be of relevance in the included studies in this review. Most studies used endometrium from women with proven fertility as controls. B cells present in the endometrium of these parous women may have acquired a distinct phenotype during pregnancy, therefore using fertile women as controls may be a reflection of pregnancy

induced changes in B cell populations rather than changes associated with the pathology of interest. Long-lived pregnancy induced immune cell changes have been previously identified in endometrial NK cells where pregnancy trained decidual NK cells (PTdNKs) have been reported (Gamliel et al. 2018, Nielsen 2011). The definitions of RPL and RIF are still debated and differ between international guidelines (Rinehart 2007, Youssef et al. 2019). For example, the most recent ESHRE guideline defined RPL as the loss of two or more pregnancies (ESHRE 2018), while most good quality studies presented in this systematic review defined RPL as the loss of three or more pregnancies. Similarly, for CE, there is no universally accepted standardized definition or established diagnostic guideline, typically the identification of plasma cells (CD138 immunohistochemistry staining) in the endometrial stroma is used. However, CD138 expression is not limited to plasma cells and cannot be considered a reliable marker alone, for example it is constitutively expressed on endometrial epithelial cells (Inki 1997, Kind et al. 2019, Moreno and Simon 2019). Other plasma cell markers, such as MUM1, have also been explored (Parks et al. 2019). Although MUM1 seems to have an improved sensitivity compared with CD138, MUM1 expression has been reported in 1-5% of tonsil and splenic T cells (largely GC T cells) as well as PHA activated T cells (Falini et al. 2000). We know T cells exhibit an activated phenotype in human endometrium (Feyaerts et al. 2017), therefore MUM1 expression alone might not be an ideal endometrial plasma cell marker and additional validation is required to ensure endometrial T cells do not express MUM1. Plasma cells do exhibit a distinct histological morphology, a round-to-ovoid shape and abundant cytoplasm, which might be useful as an additional criteria in IHC identification (Allen and Sharma 2020, Tellier and Nutt 2017).

3.5.2 Possible tertiary lymphoid structures in endometrium

In total, there are 11 IHC studies investigated endometrial B cells using pan-B cell markers such as CD19, CD20 or CD22. 8 of these studies described that B cells are present not only as single cell entities, but also in structures called 'lymphoid aggregates'

(LAs). Although the remaining papers did not report the presence of endometrial B cells in LAs, it is possible that a standard endometrial biopsy failed to aspirate the lower functional layer of the endometrium and/ or the basal layer of the endometrium, where LAs are found (Fernandez-Shaw et al. 1995, Mettler et al. 1997). LAs are predominantly found with a B cell core, surrounded by T cells and macrophages (Figure 3.2). These B cells have been documented in low but constant numbers throughout the menstrual cycle, however their phenotype and function are relatively unexplored (Mettler et al. 1997, Wira et al. 2014).

LAs resemble ectopic/ tertiary lymphoid structures (TLSs) that have been described in various tissues in response to chronic immune stimulation; their function can be both protective (in cancers and tumours) and destructive (largely in autoimmune conditions) (Pipi et al. 2018). TLS formation and structure are unique to the tissue in which they arise, however they may be generally described as organised B cell compartments containing GCs, with T cell compartments housing antigen presenting cells, and in many tissues, high endothelial venules allowing entry of lymphocytes from the peripheral circulation (Van De Pavert and Mebius 2010). In comparison, LAs are composed of a B cell core and surrounding spheroidal predominantly T cell mass, with a diffuse halo of macrophages (Mettler et al. 1997, Wira et al. 2014). There is debate in the literature as to the defining characteristics of TLSs; however, LAs may constitute a novel TLS, albeit after adopting a more inclusive definition than that which has been historically proposed (Table 3.7). Further evidence is needed to confirm their cellular phenotype, structure, and functional properties, for example, there has been little exploration into whether these B cells may constitute GC-like B cells; studies have investigated the presence of GC-like structures and associated cells have failed to use specific GC markers to support their findings (Morris et al. 1985, Wira et al. 2014).

The mechanism by which LAs grow across the menstrual cycle is not entirely understood, but it is possible that the aggregate structure is under hormonal control (Yeaman et al. 1997, 2001). In general, LAs express HLA-DR (Mettler et al. 1997), suggest-

Bona Fide Definition of Tertiary Lymphoid Structures *(Dieu-Nosjean et al. 2014)*	**Evidence from Endometrial Lymphoid Aggregates**	**References**
Ectopic and organised lymphoid tissue, contains distinct T and B cell zones	Yes	(Disep *et al.*, 2004; Klentzeris *et al.*, 1992; Mettler *et al.*, 1997; Wira *et al.*, 2014)
$PNAd^+$ high endothelial venules present surrounding, for extravasation of $CD26L^+$ immune cells	Addressins of the PNAd family have not been examined for endometrial LAs; however, other adhesion molecules including ICAM-1, VCAM-1 and E-selectin have been reported.	(Tabibzadeh *et al.*, 1994)
Evidence of B cell class switching and GC reactions in B cell follicles	Functional activity has not been studied.	-
$LAMP^+$ mature dendritic cells present in T cell zone	$LAMP^+$ dendritic cells have been reported in the endometrium; however, they have not been explicitly examined in LAs. Dendritic reticulum cells (DRC) have been noted in the LAs, with staining conducted using anti-DRC1 antibody.	(Maridas *et al.*, 2014; Schulke *et al.*, 2008)
Expression of major set of chemokines involved in SLO organisation	These chemokines' expression has not been studied.	-

Table 3.7: Comparison of the bona fide definition of tertiary lymphoid structures with evidence from endometrial lymphoid aggregates. The the bona fide definition of tertiary lymphoid structures was adopted from (Dieu-Nosjean et al. 2014). PNAd, peripheral node addressin; ICAM-1, intracellular adhesion molecule; VCAM-1, vascular cell adhesion molecule; LAMP, lysosome associated membrane protein.

ing they could play an active role in immune protection during menstruation, possibly through antigen presenting in a GC-like structure. This GC-like structure may contribute to the generation of class-switched B cells and plasmablasts found in the decidua (Huang et al. 2017, Leng et al. 2019). Additionally, the infiltration of plasma cells has been described in endometrial inflammatory conditions such as endometritis, there is a possibility that LA GC-like B cells are implicated in this process by providing the site of plasma cell generation. However, visualization of GC-like B cells and associated cells necessary for propagating their activation, including T-follicular helper cells, are needed to confirm this hypothesis. Visualization of these structures could further classify LAs

as a TLS, which may assist in their characterization by identifying common pathways and molecules documented as involved with various TLS formation and maintenance processes.

3.5.3 Future directions

Evidence from our systematic review has demonstrated that endometrial B cells are persistently present in normal human endometrium, accounting for no more than 5% of all $CD45^+$ lymphocytes. Their abundance and phenotype vary in benign gynaecological conditions, but the current evidence is inconsistent. Endometrial B cells are either scattered or surrounded by T cells and macrophages in LAs. LAs seem to be under hormone control throughout the menstrual cycle and are similar to TLSs that have been observed in other tissues.

This work synthesises the current evidence in our understanding of endometrial B cells and is a foundation for future research questions. Firstly, endometrial B cell subsets and their expressed tissue residency markers need to be determined, ideally through unbiased profiling such as RNA sequencing or combining flow cytometry and IHC. Single-cell RNA sequencing would also significantly advance our understanding in endometrial B cells, but for minority cell populations such as endometrial B cells, cell enrichment is a necessary step before sequencing in order to obtain sufficient amount of data to be able to define B cell sub-populations. Secondly, the functional properties and significance of endometrial LAs need further investigation, including the identification and spatial visualisation of the component cells, focusing on TLS related T follicular helper and GC B cells. Utilising spatial profiling techniques in profiling cellular protein between loose stromal cells and cells of the LA would help us understand the cellular component and function of endometrial LAs. Thirdly, the reliability of diagnosing endometritis using CD138 alone to define a plasma cell warrants further investigation. Addressing these questions would be important in understanding the role of B cells in normal endometrium and in benign endometrial pathologies, especially in autoimmune associated reproductive

pathologies such as endometriosis. For chronic endometritis, an advanced understanding of endometrial B cells and plasma cells would help to standardise its diagnosis and management in clinical practice.

Chapter 4

RNA-seq Analysis of Human Endometrial B Cells During the Mid-luteal Phase

4.1 Introduction

4.1.1 RNA and the transcriptome

RNA, along with DNA and proteins, are the three major biological macromolecules that are essential for all known forms of life. RNA is the main player in protein synthesis from DNA, which involves firstly transcription and then translation. Transcription describes the process of copying information from DNA to RNA, whereby a single stranded messenger RNA (mRNA) complementary to the corresponding DNA sequence is generated. Proteins are then synthesized in a process known as translation. Translation starts with the relocation of mRNA from cell nucleus to ribosomes, where amino acids chains are aligned and assembled using mRNA as the template. The assembly process is facilitated by transfer RNA (tRNA), which serves as the link between amino acids and nucleotide triplets (codons) encoded onto the mRNA (Schweet and Heintz 1966, Lodish et al. 2000, Crick 1970). mRNA are variable in size, and corresponding to the size of

the encoded protein, although the majority of mRNA fall in the range of 300 - 3000 nucleotides (Sommer and Cohen 1980). The transcriptome is the complete set of RNA molecules present in a cell. While the genome remains generally unchanged for any given cell (except somatic mutations), the transcriptome is highly variable under genetic regulation and environmental stimulation. One example of this gene expression variability is the transcriptomic alternations in murine bone marrow-derived B cells. Throughout murine B cell development in the bone marrow, 10.7% of all genes were differentially expressed among different B cell developmental stages, with 2.8% - 6.8% of all genes changing by at least two-fold upon differentiation from one cellular stage to the next (Hoffmann et al. 2002). Such alterations have also been observed in human B cell development. In healthy adults' bone marrow, there are over 700 differentially expressed genes, separating five B cell developmental stages (Hystad et al. 2009). Transcriptomic analysis also revealed distinct gene expression patterns in human spleen and liver B cells compared with peripheral B cells (Zhao et al. 2020), which corresponds to their GC enriched environment. Additionally, many immune regulatory pathways including those driven by infection and inflammation also result in altered mRNA expression in corresponding cells (Vernel-Pauillac and Merien 2006, Herman and Autieri 2017). Overall, mRNA transcriptomic analysis can serve as a useful tool to improve our understanding of the cellular compositions and the immune processes in a certain tissue.

4.1.2 RNA-seq workflow

4.1.2.1 RNA preparation

To define the transcriptome in a cell type or tissue, RNA needs to be extracted, purified and quantified. A number of RNA preparation methods are widely available including organic extraction, filter based spin basket, magnetic particle and direct lysis. The filter based spin basket format was used in this study due to its convenience, high yield, and the ability to enrich mRNA (Panthee et al. 2018). Specifically, RLT buffer (Qiagen, Germany) was used as the lysis buffer, followed by RNA purification using

a silica-membrane based method provided by RNeasy Micro Kits (Qiagen, Germany). RLT buffer contains a high concentration of guanidine isothiocycanate that supports RNA binding to the silica membrane. The use of RNeasy selectively excludes RNAs $<$ 200 nucleotides (such as tRNA, 5S rRNA and 5.8S rRNA), therefore resulting in an enrichment of mRNA.

4.1.2.2 Sequencing platforms

After mRNA extraction and purification, the transcriptome can be quantified using sequence-based approaches. Early stage sequencing-based approaches represented by Serial Analysis of Gene Expression (SAGE) enabled a more quantitative measure on RNA compared with cDNA microarray (a hybridization-based method for mRNA quantification) (Velculescu et al. 1995). However, SAGE and its variants are relatively expensive, labour intensive and unsuitable for large-scale studies. This limitation was overcome by the introduction of Next Generation Sequencing (NGS). By performing sequencing on a library of cDNA fragments simultaneously, millions of reads can be produced in parallel. NGS technologies like RNA-seq provides a high sensitivity, high precision, high throughput and relatively cheap method for transcriptomic quantification (Wang et al. 2009). A number of RNA-seq library preparation approaches have been developed, each with their own requirements and usages (e.g. polyA enriched mRNA-seq and small RNA-seq require good quality total RNA, 3' mRNA-seq is mainly used for expression quantification). A wide range of sequencing platforms are also commercially available. At present, the most commonly used platforms are developed by Illumina, among which NovaSeq 6000 represents the most powerful, simple, scalable, and reliable high-throughput sequencer to date, and is suitable for human immune cell transcriptomic quantification.

To best quantify the bulk mRNA from the limited number of B cells that can be isolated from endometrial biopsies, RNA-seq using Smart-seq2 and NovaSeq 6000 was used in my research. Smart-seq2 was developed for single-cell RNA-seq which enables transcriptome analysis from individual cells but works equally well for bulk RNA library

preparation (Picelli et al. 2014). This plate-based sequencing approach has been shown to be able to detect more genes, especially the low abundant transcripts and the alternative spliced transcripts, compared with droplet-based sequencing method like 10X Genomics Chromium (Wang et al. 2021). Smart-seq2 utilized the SMART reaction (Switching Mechanism At the end of the 5'-end of the RNA Transcript), and exploits the "Reverse Transcription" and "Template Switching" properties of Moloney Murine Leukemia Virus reverse transcriptase. Figure 4.1 provides details of the Smart-seq2 protocol (Picelli et al. 2014).

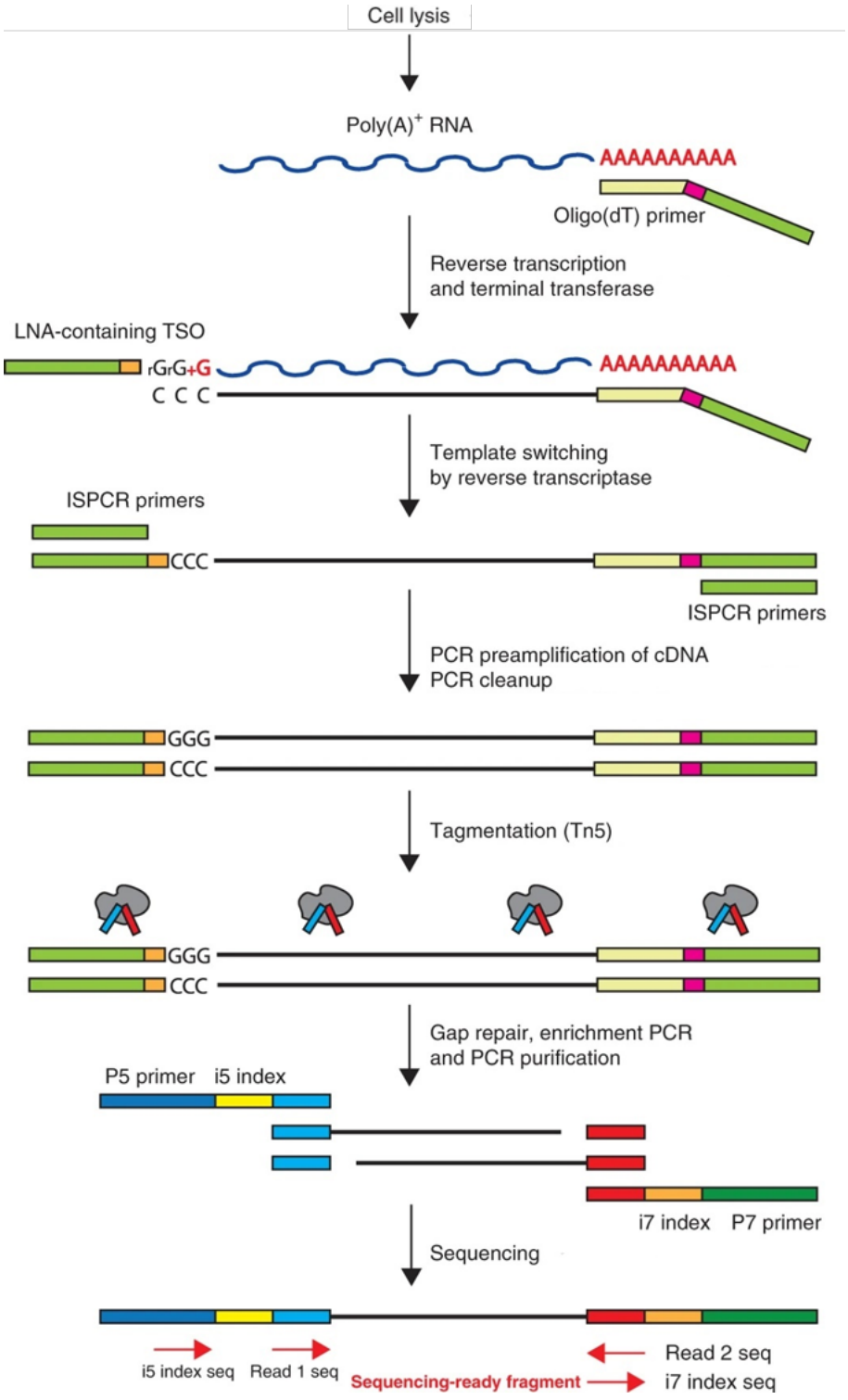

Figure 4.1: Outline of the Smart-seq2 protocol, adapted from (Picelli et al. 2014). TSO, template-switching oligos; LNA, locked nucleic acid; ISPCR primers refers to the PCR primer used in the amplification step after reverse transcription; primers that are used for tagmentation are included in the Nextera XT sample preparation and index kits.

4.1.2.3 Computational analysis

Millions to billions of raw reads generated by the sequencer are the starting materials of bioinformatic analysis. A typical computational workflow of RNA-seq analysis is presented in Figure 4.2. After a series of read processing steps, de novo assembly or reference-guided alignment is performed, followed by reads quantification, normalisation, QC and differential expression or splicing analysis (Conesa et al. 2016). Various tools have been developed for each step of the analysis.

To better visualise and understand the RNA-seq data, enrichment analysis is frequently performed. The most commonly used tools are Gene Ontology (GO) and Kyoto Encyclopedia of Genes and Genomes (KEGG) analysis. GO terms describe gene products' properties by providing an ontology of defined terms that covers cellular components, molecular function and biological processes (44,945 terms as of July 2019) (Ashburner et al. 2000, Consortium 2019). GO terms enrichment analysis could help to provide a functional profile of the gene sets generated via high-throughput experiments. KEGG pathway database is a collection of currently known pathway maps (537 pathways as of July 2020) focusing on the molecular interaction, reaction and relation networks (Kanehisa and Goto 2000). By mapping gene sets onto KEGG database, the interaction among genes of interest can be visualised and biological pathway of interest can be identified. Another commonly used enrichment analysis tool is Gene Set Enrichment Analysis (GSEA) (Subramanian et al. 2005). GSEA first identified signature genes in all pre-defined groups. Then, these genes can be mapped to one of the 8 major gene sets collections, including hallmark gene sets (50 gene sets as of July 2020), positional gene sets (299 gene sets as of July 2020), curated gene sets (5,529 gene sets as of July 2020), regulatory target gene sets (3,735 gene sets as of July 2020), computational gene sets (858 gene sets as of July 2020), GO gene sets (10,192 gene sets as of July 2020), oncogenic signatures (189 gene sets as of July 2020) and immunological gene sets (4,872 gene sets as of July 2020). Significantly enriched gene sets and their hierarchy as well as the interaction between gene sets can be visualised. GSEA pioneered the specific

knowledge-based approach in gene expression data analysis and has been shown to yield a good balance between sensitivity, performance and applicability as a bioinformatic tool (Huang et al. 2009). Apart from GO, KEGG and GSEA enrichment analysis, dozens of enrichment analysis tools have been developed over the past two decades, as reviewed here (Huang et al. 2009, Lu et al. 2015).

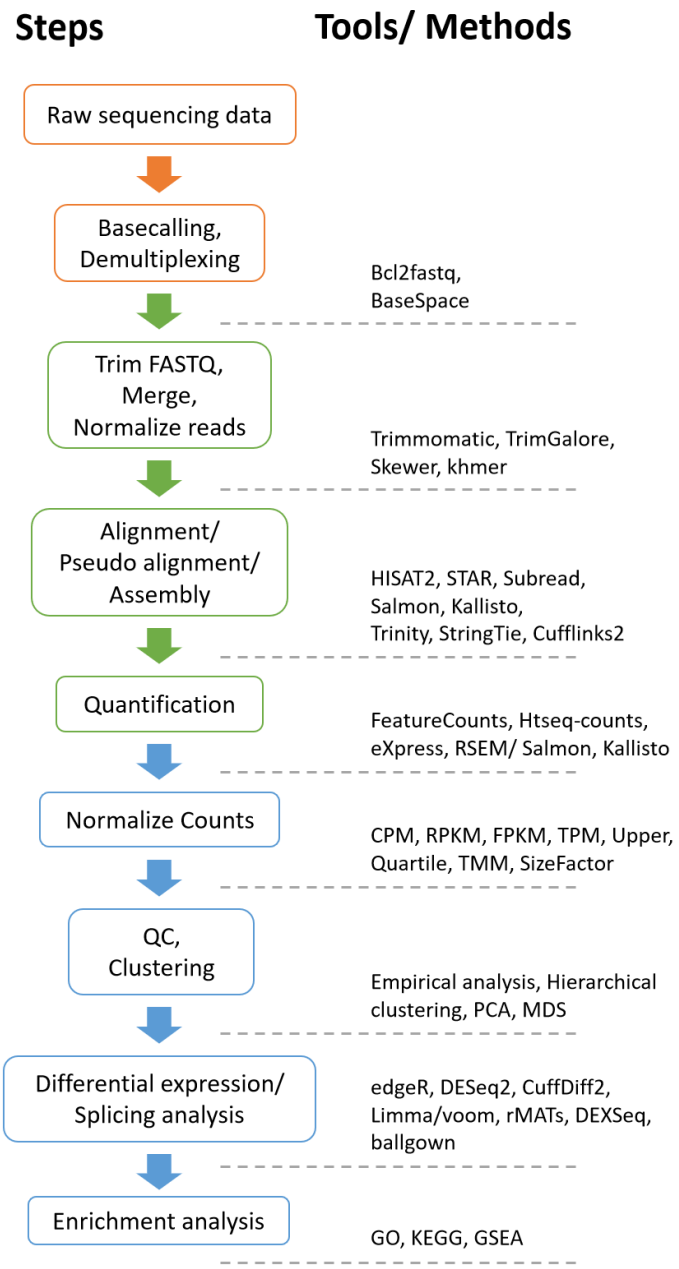

Figure 4.2: A typical computational workflow of RNA-seq data analysis. Computational tools/ methods are illustrated for each step. QC, quality control; HISAT2, hierarchical indexing for spliced alignment of transcripts 2; STAR, spliced transcripts alignment to a reference; RSEM, RNA-Seq by expectation maximization; CPM, counts per million reads mapped; RPKM, reads per kilobase of transcript per Million mapped reads; FPKM, fragments per kilobase of exon model per million reads mapped; TPM, transcripts per kilobase million; TMM, trimmed mean of M values; PCA, principal component analysis; MDS, multidimensional scaling; rMATs, replicate multivariate analysis of transcript splicing. GO, Gene Ontology; KEGG, Kyoto Encyclopedia of Genes and Genomes; GSEA, Gene Set Enrichment Analysis.

4.1.3 Transcriptomic characterization of human endometrium

4.1.3.1 Endometrial characteristics during the menstrual cycle

With the recent progress made in 'Omic' technologies, transcriptomic characterization has become available to decipher the molecular components and their mechanisms in human endometrium. Several microarray studies have shown endometrium undergoes extremely dynamic transcriptomic alternations between the follicular and luteal phase. Gene clusters under GO terms 'cell adhesion', 'cell proliferation', 'wound healing', etc. have been shown to alter significantly across the menstrual cycle (Messaoudi et al. 2019, Talbi et al. 2006). Differentially expressed genes involved in immune response have also been reported. For example, complement related genes (decay accelerated factor, adipsin, complement component 1, complement component 2, complement component 3, complement component 4 binding protein), innate immunity activation related genes (*TLR3*, *TLR4*, *HLA-A*), cytokines and receptors related genes (*IL-1R*, *IL-6R*, *IL-15*, *IL-15R*, Fc fragment of IgE I-receptor for gamma polypeptide) are upregulated in mid-luteal phase compared with early-luteal phase in endometrium (Talbi et al. 2006, Mirkin et al. 2005, Riesewijk et al. 2003, Haouzi et al. 2009). Moreover, Ig heavy constant gene, Fc-receptor related genes (Fc fragment of IgE high affinity I, receptor, Fc fragment of IgG Ia receptor, Fc fragment of IgG IIa, Fc fragment of IgG IIb receptor) and HLA-related genes (*CD74*, *HLA-DP*, *HLA-DQ*, *HLA-DR*) are upregulated in the late luteal phase compared with the mid-luteal phase (Talbi et al. 2006). Notably, *HLA-DOB* and *HLA-DPA2* have been shown to be downregulated in the mid-luteal phase compared with the early-luteal phase (Carson et al. 2002, Riesewijk et al. 2003).

More recently, single cell RNA-sequencing has been used to characterise molecular and cellular changes in endometrial tissue through the menstrual cycle. Wang et al. identified seven broad cell types, including lymphocytes, in human endometrium across the menstrual cycle, with altered NK and T cell phenotypes being extensively characterised (Wang et al. 2020). Lucas et al. identified five cell clusters, with naïve B cells present

in the immune population, constituting no more than 2% of total endometrial cell populations. Compared with monocytes, macrophage/dendritic cells and NK cells, naïve B cells have a higher mRNA expression level of *CD19*, *CD20*, *CD79A*, *LY9*, *CD83*, *BTG1*, *CXCR4* and moderate level of *CD74* and *HLA-DRA* (Lucas et al. 2020). However, for minor cell populations like endometrial B cells, the genetic profiles generated from single cell RNA-seq could be biased due to the limited number of cells being sequenced. For example, Lucas et al. only identified a maximum of three B cells in each sample, all presented a naïve B cell phenotype. It is possible that there are other B cell subsets present in the endometrium, and endometrial B cells could collectively present novel signature genes or enriched pathways that have yet to be discovered by transcriptomic analysis.

4.1.3.2 Endometrial characteristics in RPL patients

Microarray technology has also been applied to study endometrial gene expression in women with RPL. RPL patients have a distinct gene expression profile, represented by the dysregulation of leukocyte extravasation signalling, lipid metabolism and detoxification pathways (Altmäe et al. 2009). GSEA analysis has highlighted 'immune system process' along with other enriched GO terms that are differentially expressed between control and RPL group (Koot et al. 2016). A systematic review and meta-analysis on endometrial receptivity markers highlighted the importance of the inflammatory response, immunoglobulin-mediated immune responses and complement in facilitating implantation success (Altmäe et al. 2017). These findings contribute to the development of various diagnostic tools for human endometrial receptivity assessment. An eleven-marker transcriptomic expression method was proposed and subsequently commercialized as the 'Win-Test' (Hamamah and Haouzi 2013). A more comprehensive assessment called Endometrial Receptivity Analysis (ERA), which include 238 gene markers, has also become available. Within the selected 238 genes, immune related genes like complement component 3, *HLA-DOB*, *IL15* and *BCL6* are included (Vallés et al. 2018).

To date, no transcriptomic study has been performed on endometrial B cells. As a key player in the mucosal immune system, B cell dysfunction has been implicated in benign female reproductive pathologies including RPL (Chapter 3). Using RNA-seq, my research is the first to characterise endometrial B cells and to compare their transcriptomic profile between control and RPL patients.

4.2 Chapter Aims

This chapter presents transcriptome analysis by RNA sequencing of endometrial B cells identifying potential B cell phenotypes and function in control women and patients who have experienced RPL. To achieve this, endometrial B cells were isolated from 16 endometrial biopsies, and cDNA library preparation was performed for RNA sequencing. Bioinformatic analysis of sequencing data explores endometrial B cells phenotypes and functions associated with B cell development, endometrial decidualisation, previous exposure to pregnancy and RPL.

This chapter details human subject recruitment, cell isolation, library preparation and sequencing, pipeline developed for quality control (QC) assessment and subsequent data analysis. Data filtering was performed in response to QC results, investigating the transcriptomic signature of endometrial B cells in comparison with endometrial T cells. Differentially expressed genes were identified in different patient groups and computing enrichment analysis using GO term, KEGG and GSEA was undertaken. Lastly, I briefly conclude my findings and discuss the limitations of this study as well as the prospective direction of endometrial B cell research.

Objectives:

1) To undertake a comprehensive bioinformatic analysis pipeline of endometrial B cell RNA-seq data.

2) To determine the endometrial B cell signature genes and enriched pathways in comparison with endometrial T cells.

3) To determine if there is any differentially expressed genes and enriched pathways between healthy women, PRPL patients and SRPL patients.

4.3 Materials and Methods

4.3.1 Subject recruitment

The study was approved by the Oxford Research Ethics Committee C (ref:08/H0606/94). Methods were carried out in accordance to current guidelines and regulations. All participants gave written informed consent.

All recruits were patients attending Oxford Fertility or John Radcliffe Hospital Recurrent Miscarriage Clinic between 2016 to 2018. Both blood and endometrial samples were collected between 7–11 days post LH pre-ovulatory surge in the menstrual cycle before IVF commenced. The control group were patients undergoing IVF for male factor infertility, and all patients had proven fertility by either a previous live birth or had a pregnancy with live birth outcome in the following IVF cycle. RPL patients were at least three months post miscarriage or hormonal treatment at the time of sample collection. All women with RPL had normal thyroid function, negative antiphospholipid screen (cardiolipin Ab, anti-beta-2 glycoprotein and DRVVT), negative thrombophilia screen (including Factor V Leiden, prothrombin gene mutation, Antithrombin III, protein C, protein S) and no evidence of uterine structural abnormalities (identified by ultrasound scan or hysteroscopy). Maternal and paternal karyotypes were only carried out if an unbalanced translocation was identified in karyotyped miscarriage tissue as per Royal College of Obstetrics and Gynaecology guidelines (RCOG 2011).

In total 16 endometrial samples were obtained using an Endocell disposable endometrial cell sampler (Wallach Surgical devices, CT, USA). Among 10 RPL patients, 5 suffered from primary RPL (PRPL) and 5 are diagnosed as secondary RPL (SRPL). 6 control subjects were matched for age and previous live births, 4 were parous controls (PC), 2 were nulliparous controls (NULLPC). All patient details shown in Table 4.1.

Sample	Age	No. of Miscarriages	No. of Ectopic Pregnancy	No. of Previous Live Birth	Pregnancy Outcome in the Subsequent IVF Cycle
NULLPC.1	35	0	0	0	Live Birth
NULLPC.2	37	0	0	0	Live Birth
NULLPC.3	35	0	0	0	Live Birth
NULLPC.4	28	0	0	0	Live Birth
mean $\pm$ SD	34 ± 3	0 ± 0	0 ± 0	0 ± 0	-
PC.1	35	0	0	1	Live Birth
PC.2	33	0	0	1	Live Birth
mean $\pm$ SD	34 ± 1	0 ± 0	0 ± 0	1 ± 0	-
PRPL.1	38	3	0	0	n/a
PRPL.2	37	4	0	0	n/a
PRPL.3	36	5	0	0	n/a
PRPL.4	32	6	0	0	n/a
PRPL.5	35	3	0	0	n/a
mean $\pm$ SD	36 ± 2	4 ± 1	0 ± 0	0 ± 0	-
SRPL.1	39	5	0	1	n/a
SRPL.2	30	4	0	1	n/a
SRPL.3	34	9	0	1	n/a
SRPL.4	35	3	0	1	n/a
SRPL.5	41	7	0	1	n/a
mean $\pm$ SD	36 ± 4	6 ± 1	0 ± 0	1 ± 0	-

Table 4.1: Patient characteristics for RNA-seq samples. Mean $\pm$ SD values for each group are shown. NULLPC, nulliparous control; PC, parous control; PRPL, primary recurrent pregnancy loss; SRPL, secondary recurrent pregnancy loss.

4.3.2 RNA isolation and quantification

4.3.2.1 Sample processing

After collection, all endometrial samples were digested using 1X Liberase (Roche, Switzerland) as previously described in Chapter 2.3.5. Single cell suspensions were frozen in 10% DMSO/FCS using a Mr.Frosty Freezing chamber (Thermo Fisher, USA), before being transferred to liquid nitrogen for storage prior to use.

4.3.2.2 Cell sorting

Frozen endometrial cell digests were thawed into HS-media (RPMI1640 supplemented with 10%FCS, 1% Human Serum, 2mM glutamine, 100 IU/ml penicillin and 100 μg/ml streptomycin) at 37°C and centrifuged at 300 x g. Endometrial cells were re-suspended in HS-Media and transferred to a 25cm^2 flask for 30 minutes at 37°C/ 5% CO_2, then supernatants containing non-adherent cells were further transferred to a fresh flask for an additional 30 minutes incubation, for stromal and epithelial cell depletion. Supernatants were then removed and transferred onto a lymphoprep layer with centrifugation at 800 x g for 20 minutes. Cells in the interface were washed in PBS and prepared for cell sorting on an Aria III (BD Biosciences, USA) using 85 μm nozzle. Briefly, endometrial cells were stained with Zombie Aqua^{TM} Viability Dye (Biolegend, USA) then incubated with antibodies CD3 APC FIRE^{TM}750, CD45 BV650^{TM}, CD4 FITC, CD25 PE, CD8 BV711^{TM}, CD19 PE-Cy7 and CD127 APC (all from Biolegend, USA).

CD19$^+$ B cells were isolated as singlet cells (FSC-H vs FSC-A), Zombie Aqua^{TM-}, CD45$^+$, CD19$^+$. Endometrial T regulatory cells (CD45$^+$ CD3$^+$ CD4$^+$ CD25^{bright} CD127$^{dim/-}$), non T regulatory CD4 T cells (CD45$^+$ CD3$^+$ CD4$^+$ CD25$^{+/-}$ CD127$^+$) and CD8 T cells (CD45$^+$ CD3$^+$ CD4$^-$ CD8$^+$) were also isolated based on their respective surface markers. Sequencing data of T cells were only used for PCA (Chapter 4.4.3.3) and comparative analysis with B cells (Chapter 4.4.4.2).

4.3.2.3 RNA extraction

Immediately after sorting, cells were pelleted by centrifugation and re-suspended in RLT buffer (Qiagen, USA) and RNA was extracted using QIAGEN RNeasy Micro Kits (Qiagen, USA) according to the manufacturer's protocol 'Purification of Total RNA from Animal and Human Cells'. The procedure enriches for mRNA; all RNA molecules longer than 200 nucleotides are purified.

4.3.2.4 RNA quantification

RNA quantity and quality were accessed on Agilent 4200 TapeStation System (Agilent, USA) according to the manufacturer's protocol 'Agilent High Sensitivity RNA ScreenTape Assay'.

4.3.3 Library preparation and RNA sequencing

The RNA-seq library was prepared in collaboration with the Weatherall Institute of Molecular Medicine Single Cell Facility. Samples were treated as single cells using Smart-Seq2 protocol for cDNA conversion (Picelli et al. 2014). The library was prepared using Standard Nextera Illumina Library Prep kit according to manufacturer's protocol. Briefly, unique dual-index strategy was implemented to barcode the cDNA fragments. All samples were amplified for 16 cycles during DNA amplification, unless cDNA concentrations suggest a greater number of cycles. In library QC step, cDNA quantities were assessed using 2100 Bioanalyzer (Agilent, USA) and Quant-iT PicoGreen (Thermo Fisher, USA). cDNA masses ranged from 0.9 to 15 ng/μl.

Clustering and sequencing was carried out by Novogene Co., Ltd. Novogene Experimental Department. The clustering of the index-coded samples was performed on a cBot Cluster Generation System using PE Cluster Kit cBot-HS (Illumina) according to the manufacturer's instructions. After cluster generation, paired end RNA sequencing was performed using Novoseq 6000 platform, with 125 bp/150 bp read length and approximately 25 million reads per sample.

4.3.4 Early analyses (undertaken by Novogene Co., Ltd)

4.3.4.1 Quality control procedures

Raw reads of fastq format were firstly processed through Novogene Co., Ltd. in-house perl scripts. In this step, probability of an incorrect base call 1 in 100 times (Q20), probability of an incorrect base call 1 in 1000 times (Q30), raw reads number, error rate and A/T/G/C content distribution were calculated. Accordingly, clean data (clean reads) were obtained by removing reads containing adapter, reads containing ploy-N and low quality reads from raw data. Read trimming was also performed to remove bases towards read ends with high error rate and distorted GC contents. All the downstream analyses were based on the obtained clean data.

4.3.4.2 Read alignment and quantification

Raw reads were mapped to Ensembl Homo sapiens cDNA database release 94 (http://ftp.ensembl.org/pub/release-94/fasta/homo_sapiens/cdna/) using TopHat v2.0.12 (Kim et al. 2013). Appropriate parameters were also set (e.g. the longest intron length). Only filtered reads were used to analyse mapping status of RNA-seq data to the reference genome.

HTSeq v0.6.1 was used to count the reads numbers mapped to each gene (Anders et al. 2015). The non-normalised count table generated was then used for downstream analysis.

4.3.5 Sample variance visualization (undertaken by Mengni Shen)

To perform sample variance visualization, the count matrix was first generated using DESeq2 package in R (version 3.5.3) (Love et al. 2014) with no comparison groups applied. Briefly, the count matrix was generated through the following steps, estimation of size factors, estimation of dispersion, negative binomial generalised linear model fitting and wald statistics.

Either regularised logarithm (rlog) or variance stabilizing transformations (vst) was then used to generate the transformed version of the count data. Blind dispersion estimation was performed so that the comparison is unbiased with regards to the information about experimental groups. Four mathematical statistics were performed on the transformed data; 1) Correlation coefficient values across 16 endometrial B cell samples were calculated after rlog transformation, 2) Sample-to-sample distance matrix of 16 endometrial B cell samples was generated by euclidean distance measure after vst transformation, 3) Principal component analysis (PCA) plots of all T and B cell samples were generated with vst transformation whereas PCA plots of 16 B cell samples were generated using rlog transformed count data, 4) A diagnostic test for outliers called Cook's distance was used to measure how much a single sample is influencing the fitted coefficients for a gene. Through visual inspection, an outlier with a relatively high value of Cook's distance was identified.

4.3.6 Differentially gene expression analysis (undertaken by Mengni Shen)

Using the count matrices generated by the DESeq2 model, result tables of differential expression analysis between experimental groups were extracted with $\log_2$ fold changes, p values and adjusted p values. Adjusted p values were computed using the Benjamini and Hochberg's approach for controlling the false discovery rate. Genes with an adjusted p value < 0.01 were assigned as differentially expressed.

4.3.7 Pathway enrichment analysis (undertaken by Mengni Shen)

4.3.7.1 GO term and KEGG analysis

GO term enrichment analysis was performed using goseq package (Young et al. 2010). After count matrices were generated by the DESeq2 model, $\log_2$ fold change (usually > 1.5) was applied due to the large number of differentially expressed genes. The

dataset was then fitted to the probability weighting function, to obtain a weighting for each gene, depending on its length. Lastly, Wallenius approximation was performed to calculate the enriched GO terms among differentially expressed genes, with hg19 build of human genome used in GO annotation.

KEGG pathway enrichment analysis was performed using clusterProfiler package (Yu et al. 2012). After differentially expressed gene lists (Ensembl ID) were generated as previously described, they were mapped to Entrez database for KEGG enrichment. KEGG enrichment analysis was performed using Homo sapiens (human) reference source (ftp://ftp.ncbi.nlm.nih.gov/refseq/release/complete/) with a false discovery rate control returned. In a given pathway, rich factor was calculated by computing the ratio of the differentially expressed gene number to the background number.

4.3.7.2 GSEA analysis

Gene Set Enrichment Analysis (GSEA) was performed using GSEA software (version 4.0.2) (Subramanian et al. 2005), normalised read count table generated by DESeq2 model was loaded as input data. Signal to noise metric was generated and used for ranking genes. Hallmark gene sets (ftp.broadinstitute.org://pub/gsea/gene_sets/h.all.v7.0.symbols.gmt), curated gene sets (ftp.broadinstitute.org://pub/gsea/gene_sets/c2.all.v7.0.symbols.gmt), GO gene sets (ftp.broadinstitute.org://pub/gsea/gene_sets/c5.all.v7.0.symbols.gmt) and immunologic gene sets (ftp.broadinstitute.org://pub/gsea/gene_sets/c7.all.v7.0.symbols.gmt) were selected as mapping gene sets. Phenotype labels detailed different cell types and pathological groups. The number of permutations was set to 1000 on 'gene set' for all analyses. No collapse or remap was performed to gene symbols. No chip platform was selected. GSEA results were visualised in Cytoscape software (version 3.7.2) (Otasek et al. 2019).

4.4 Results

4.4.1 Cell sorting and RNA quantification

Endometrial B cells were isolated by flow cytometric cell sorting, a representative flow cytometry gating strategy is shown in Figure 4.3a-d. Sorting purity was over 97% for all samples (data not shown). On average, $CD19^+$ B cells comprise $5 \pm 5.5\%$ of all $CD45^+$ live single cells in endometrial digests (n=16) (Table 4.2). B cell proportions were not altered between NULLPC, PC, PRPL and SRPL groups (Figure 4.3e). MFI of CD25 and CD127, which are indicators of B cell activation and enhanced survival (Johnson et al. 2007, Amu and Brisslert 2011), were examined on endometrial B cells and the results are illustrated in Figure 4.4, no significant difference was observed between groups. Additionally, gating strategy of endometrial T cell sorting are shown in Appendix C.

Extracted RNA quantities vary among endometrial B cell samples, with the majority below 100 pg/μl. In general, the RNA quantity correlates with the cell input number (Figure 4.5). RNA concentrations were similar between groups. RINe values, as an objective assessment of eukaryotic RNA degradation, correlated with RNA concentrations and showed degraded RNA in most samples. This is likely due to the low input cell numbers. Endometrial T cell RNA concentrations and RINe values are shown in Appendix C.

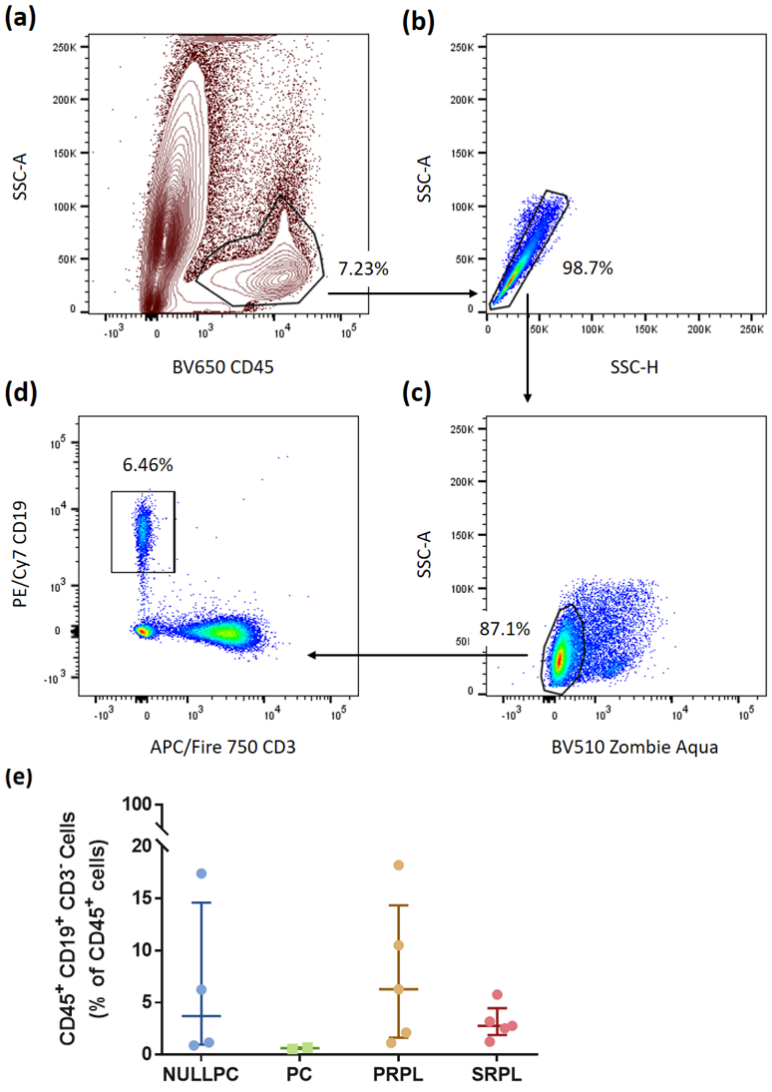

Figure 4.3: Gating strategy for endometrial B cell sorting and cell proportions of endometrial B cells acquired by sorting. B cells were obtained by cell sorting using an AriaIII (BD) from endometrial biopsy digests. (a)-(d) Representative gating strategy for B cells. (a) $CD45^{+}$ lymphocytes were gated on $BV650^{TM}$ (CD45) versus SSC-A; (b) Single cells were selected using SSC-H versus SSC-A parameters; (c) live cells were $BV510^{TM}$ Zombie $Aqua^{TMlow}$; (d) $CD3^{-}$ $CD19^{+}$ cells were acquired. (e) Percentages of sorted B cells of total $CD45^{+}$ lymphocytes among groups. NULLPC, nulliparous control; PC, parous control; PRPL, primary recurrent pregnancy loss; SRPL, secondary recurrent pregnancy loss. Error bar shows mean $\pm$ SD.

Sample	$CD45^+$ cell no. $\times(10^4)$	$CD19^+$ cell no. $\times(10^3)$	Proportion of $CD19^+$ cells in total $CD45^+$ population (%)
NULLPC.1	6.8	0.6	0.9
NULLPC.2	41.0	25.6	6.2
NULLPC.3	9.4	16.4	17.4
NULLPC.4	23.7	2.8	1.2
mean $\pm$ SD	20.2 $\pm$ 13.6	11.4 $\pm$ 10.2	6.4 $\pm$ 6.7
PC.1	0.9	0.06	0.7
PC.2	20.4	1.0	0.5
mean $\pm$ SD	10.7 $\pm$ 9.8	0.5 $\pm$ 0.5	0.6 $\pm$ 0.1
PRPL.1	7.3	1.5	2.1
PRPL.2	2.2	1.4	6.3
PRPL.3	17.5	18.3	10.5
PRPL.4	2.7	4.9	18.2
PRPL.5	6.2	0.7	1.1
mean $\pm$ SD	7.2 $\pm$ 5.5	5.4 $\pm$ 6.6	7.6 $\pm$ 6.2
SRPL.1	4.4	2.5	5.8
SRPL.2	8.5	2.7	3.2
SRPL.3	59.6	16.4	2.8
SRPL.4	12.0	1.5	1.2
SRPL.5	4.1	1.0	2.5
mean $\pm$ SD	17.7 $\pm$ 21.1	4.8 $\pm$ 5.8	3.1 $\pm$ 1.5
mean $\pm$ SD of all samples	14.2 $\pm$ 15.4	6.1 $\pm$ 7.9	5.0 $\pm$ 5.5

Table 4.2: Endometrial B cell numbers and proportions after cell sorting. Mean $\pm$ SEM values for each group and all samples are shown. NULLPC, nulliparous control; PC, parous control; PRPL, primary recurrent pregnancy loss; SRPL, secondary recurrent pregnancy loss.

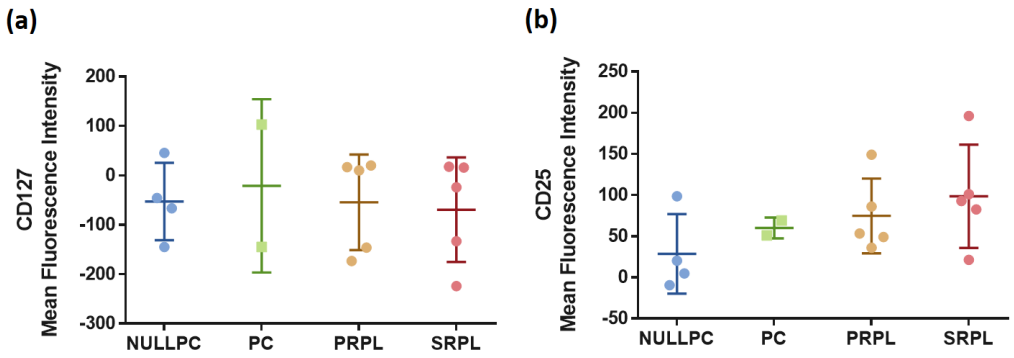

Figure 4.4: CD127 and CD25 expression on endometrial B cells. B cells were obtained by cell sorting from endometrial biopsy digests, CD25 and CD127 expression levels were determined at the time of cell sorting. (a)-(b) Endometrial B cell expression of CD127 (MFI of CD127 APC) and CD25 (MFI of CD25 PE). MFI, mean fluorescence intensity; NULLPC, nulliparous control; PC, parous control; PRPL, primary recurrent pregnancy loss; SRPL, secondary recurrent pregnancy loss. Error bar shows mean $\pm$ SD.

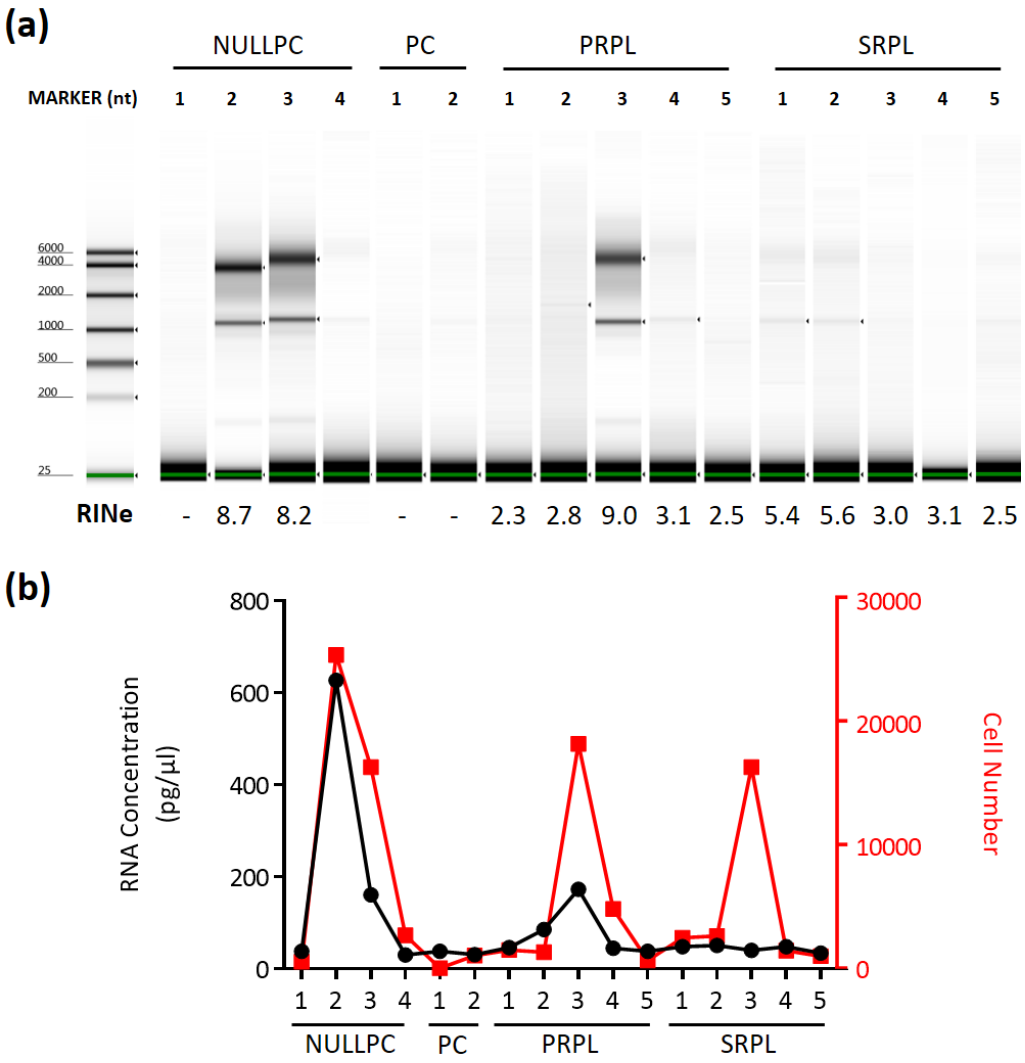

Figure 4.5: Endometrial B cell RNA quality assessment. B cells ($CD19^{+}$) were obtained from endometrial biopsy digests (n=16) by cell sorting and RNA was isolated using QIAGEN RNeasy Mini Kit. RNA quantity and quality were then accessed on Agilent 4200 TapeStation System, High Sensitivity RNA ScreenTape (a) Total RNA quality assessment based on 18S (1869nt) and 28S rRNA (5070nt). On the left side, MARKER lane shows electronic RNA ladder. RINe values are displayed below each lane. Sample numbers and groups are labelled above each lane. (b) B cell RNA concentrations and their corresponding cell numbers in all 16 samples. Cell input numbers (red squares) and RNA concentrations (black dots) of each sample are shown. NULLPC, nulliparous control; PC, parous control; PRPL, primary recurrent pregnancy loss; SRPL, secondary recurrent pregnancy loss.

4.4.2 Quality control (QC)

RNA sequencing resulted in a mean of 27 million reads and 8.1 billion bases per sample, ranging from 7 million to 43 million, 2.3 billion to 13.2 billion respectively. Sample "parous control.1" yield the lowest raw read counts and raw base counts. Although raw read counts varied more than expected, multiplex sequencing showed no sign of lane bias. The differences in read counts were most likely due to the inconsistency of sample RNA quality and quantity. QC report returned error rate were all $< 0.04\%$, and around 90% base count was assigned with Phred value > 20 or 30 (indicating the probability of incorrect base call is less than 1 in 100 or 1 in 1000), which are shown as quality scores Q20 and Q30 in Table 4.3. These QC data ensured the RNA sequencing data was of good quality, while it is noted that sample "parous control.1" had the lowest quality score (Q20 and Q30) (Table 4.3).

After raw data filtering was conducted to remove reads containing adapters, N $>$ 10% (N represents the base cannot be determined) and low quality (Qscore ≤ 5) base, all samples had $> 99.9\%$ clean reads. GC contents and error rate were higher towards the end of sequencing reads, read trimming was therefore conducted to remove reads of higher error rate and distorted GC contents. A summary of results metrics and representative QC figures are provided in Table 4.3 and Figure 4.6. All downstream analysis was performed on the obtained clean data.

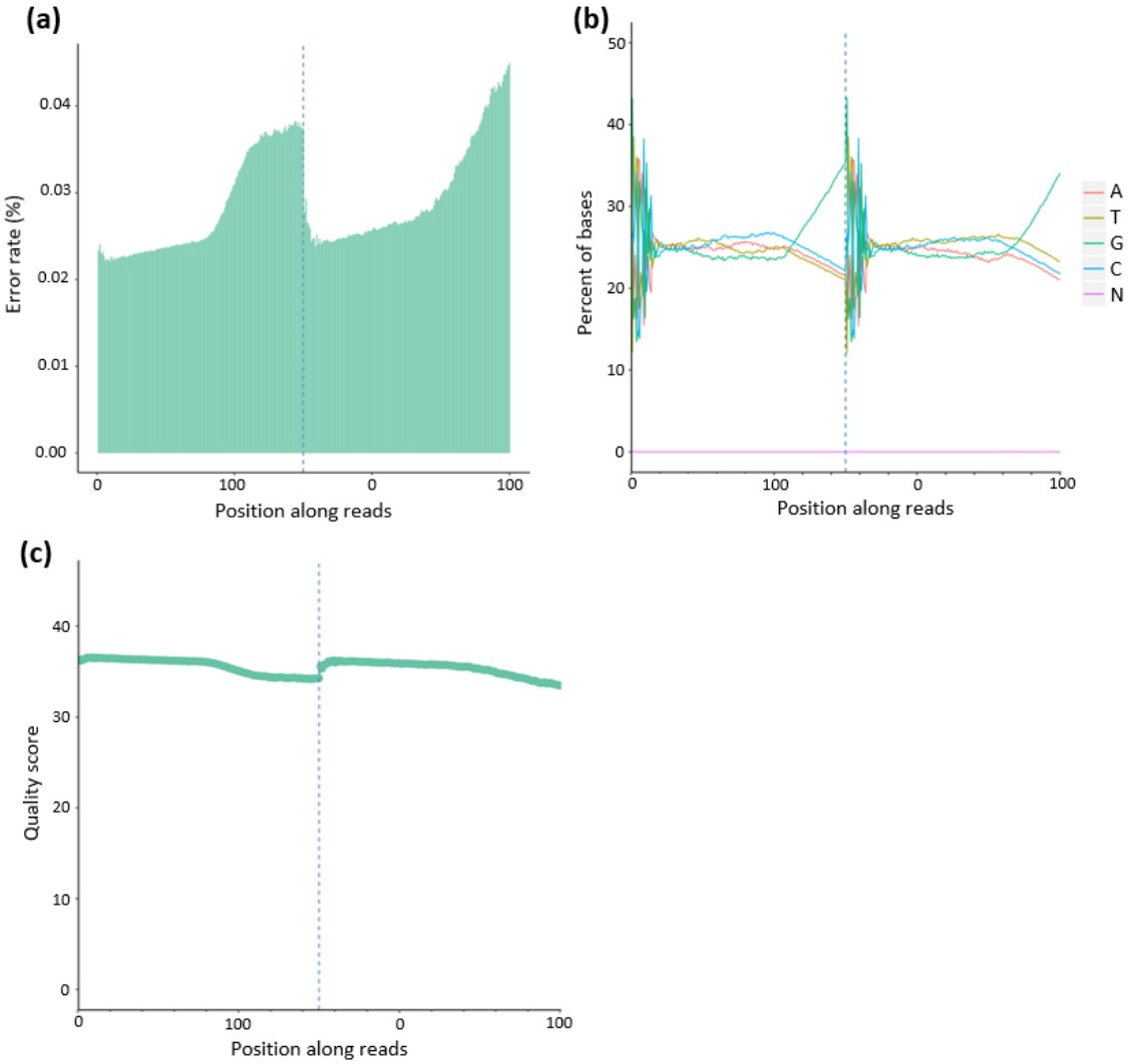

Figure 4.6: Representative figures of endometrial B cell RNA sequencing QC results (n=16). (a-c) Quality control of raw data. The base position is on the x-axis and the single base percentage is on the y-axis. The left part of the distribution is for reads1 and the right part is for reads2. (a) Distribution of sequencing error rate along reads, (b) distribution of A/T/G/C base along reads, (c) distribution of sequencing quality along reads, shown in quality score.

Sample	Raw reads No.	Raw bases No.	Error rate (%)	Q20 (%)	Q30 (%)	GC content (%)
NULLPC.1	12695111	3.8G	0.03	95.02	90.47	51.26
NULLPC.2	18134532	5.4G	0.03	96.19	96.19	50.67
NULLPC.3	24663885	7.4G	0.03	95.88	91.33	50.78
NULLPC.4	18921911	5.7G	0.03	95.39	90.55	50.95
PC.1	7581521	2.3G	0.03	89.40	82.97	46.28
PC.2	17608205	5.3G	0.03	95.08	90.41	52.03
PRPL.1	26114023	7.8G	0.03	95.86	91.36	50.45
PRPL.2	29267102	8.8G	0.03	95.63	91.03	50.87
PRPL.3	28825397	8.6G	0.03	94.92	90.22	51.66
PRPL.4	40360559	12.1G	0.03	94.91	90.30	51.38
PRPL.5	43975656	13.2G	0.03	93.10	88.22	52.95
SRPL.1	37160023	11.1G	0.03	96.15	91.67	50.62
SRPL.2	32652545	9.8G	0.03	95.80	91.07	51.16
SRPL.3	30931934	9.3G	0.03	95.91	91.11	49.67
SRPL.4	29176501	8.8G	0.03	95.15	90.27	51.54
SRPL.5	35582881	10.7G	0.03	95.69	90.55	51.18

Table 4.3: Summary of RNA sequencing QC results for 16 endometrial B cell samples. This table includes raw reads number, raw bases number: (total raw reads) x (sequence length), calculated in billion (G), error rate: base error rate, quality score Q20 and Q30: (Base count of Phred value $>$ 20 or 30) / (Total base count) and GC content: (G & C base count) / (Total base count). QC, quality control; NULLPC, nulliparous control; PC, parous control; PRPL, primary recurrent pregnancy loss; SRPL, secondary recurrent pregnancy loss.

4.4.3 Sample variance visualization

4.4.3.1 Correlation coefficient

A correlation coefficient was used as a statistical measure to calculate the strength of the relationship between the 16 endometrial B cell samples. Shown in Figure 4.7, sample PC.1 had the weakest correlation with other samples. Similarities in correlation values cannot serve as an indicator in separating RPL samples from controls. Apart from PC.1, all other correlation coefficient values are above 0.7, indicating a strong positive linear relationship via a firm linear rule. Therefore, sample PC.1 could be a potential outlier as the remaining 15 endometrial B cell samples had a similar RNA expression profile.

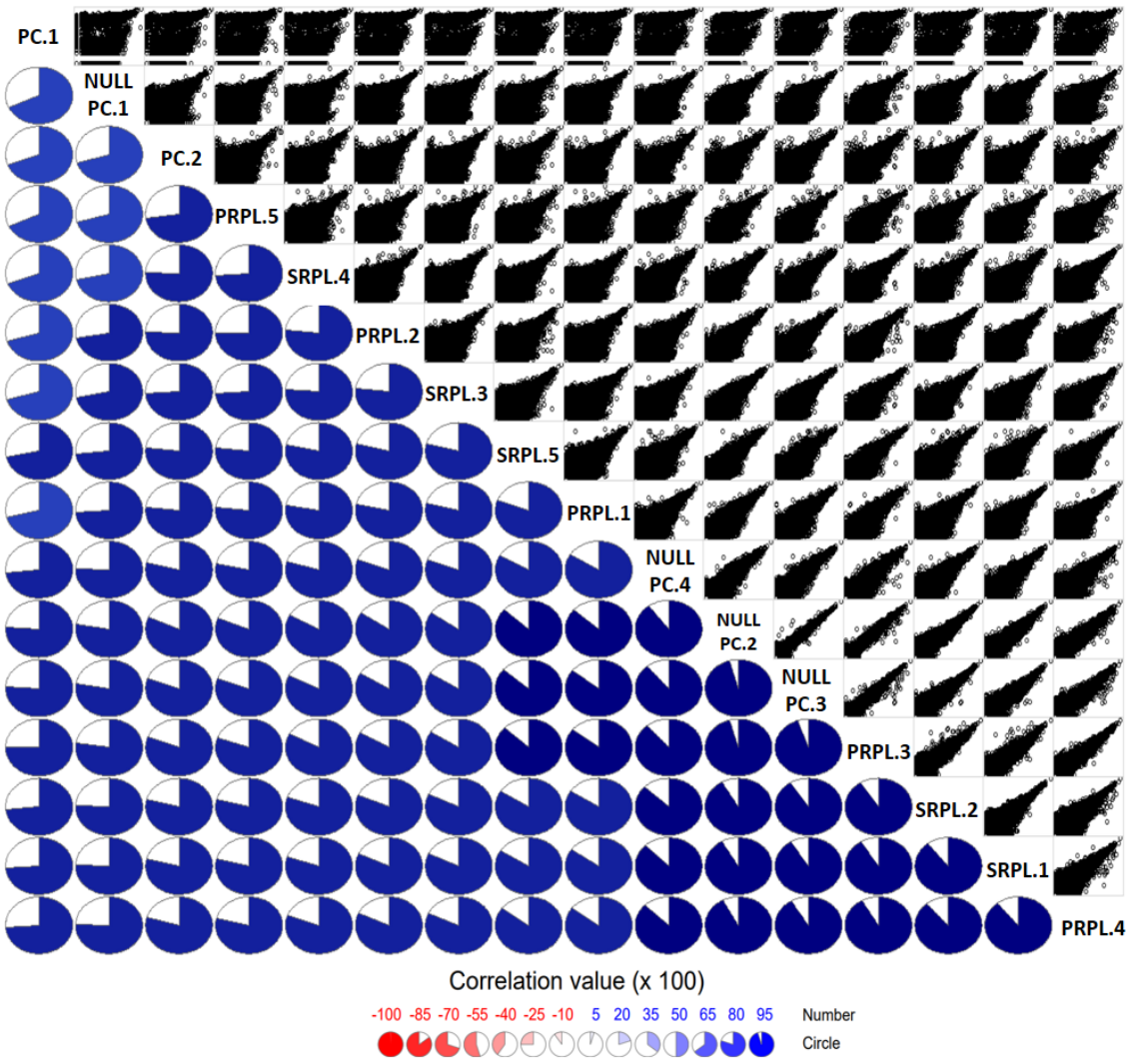

Figure 4.7: Correlation coefficient analysis between 16 endometrial B cell samples. Distances were calculated from regularized logarithm transformation. The upper panel shows correlation plots, the lower panel shows pie charts of correlation values. NULLPC, nulliparous control; PC, parous control; PRPL, primary recurrent pregnancy loss; SRPL, secondary recurrent pregnancy loss.

4.4.3.2 Dendrogram clustering

Sample variance is another way to visualise sample clustering. Figure 4.8 provides an overview of similarities and differences between 16 endometrial B cell samples. Hierarchical clustering based on sample distances formed one single leave in each clade, with no major clusters separating different groups. Similar to correlation coefficient, dendrogram did not cluster B cell transcriptome in different groups as different clusters, suggesting there was no major difference between groups. Sample PC.1 was separated from all other transcriptomic datasets and was a potential outlier.

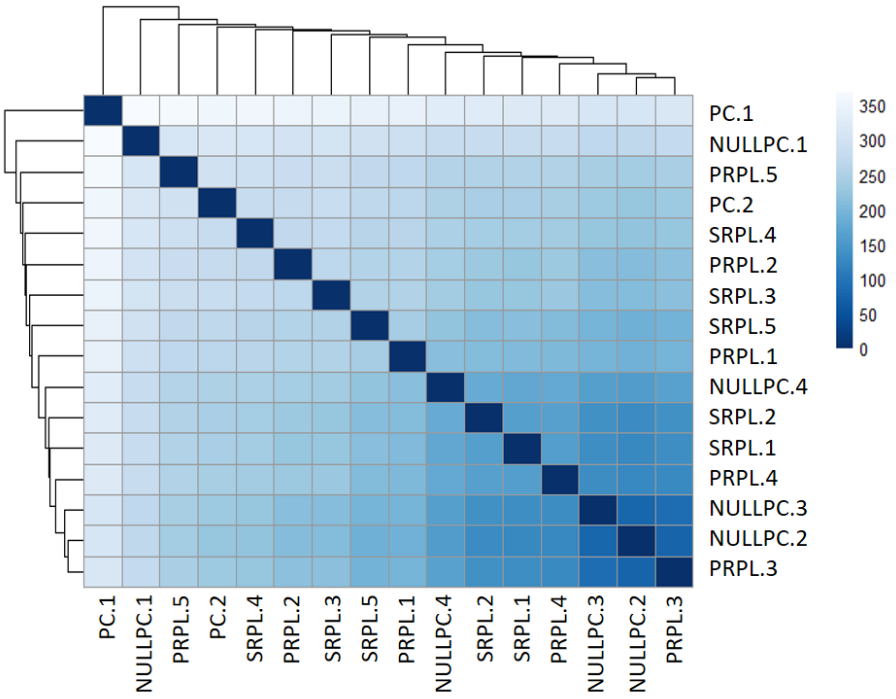

Figure 4.8: Heatmap of Euclidean distances between 16 endometrial B cell samples. Distances were calculated from variance stabilizing transformations. NULLPC, nulliparous control; PC, parous control; PRPL, primary recurrent pregnancy loss; SRPL, secondary recurrent pregnancy loss.

4.4.3.3 Principal component analysis (PCA)

PCA was performed using the expression count data of 16 endometrial B cell samples and matched endometrial T cell samples collected in this study. The PCA plot of all

samples were generated by dividing samples into 4 groups, endometrial B cells, endometrial T regulatory cells, endometrial CD4 T cell (all CD4 T cells excluding T regulatory cells) and endometrial CD8 T cells. The first principal component account for 48% of the variance, which is more than twice the value of second principal component (23%), suggesting the major difference separating the groups are between endometrial B cells and all endometrial T cells that included T regulatory cells, CD4 T cells, and CD8 T cells (Figure 4.9(a)). Auto clustering revealed four distinct clusters of endometrial B cells, endometrial non-T regulatory CD4 T cells, endometrial CD8 T cells and T regulatory cells (both circulating and endometrial). However, it did not segregate endometrial T regulatory cells from their circulating counterparts, with two endometrial T regulatory samples clustered together with circulating ones (Figure 4.9(b)). This reflects the differences among various immune cell subtypes and also illustrates the similarity between circulating and tissue resident T regulatory cells when compared to other immune cell types.

PCA of 16 endometrial B cells displayed a limited segregation between four experimental groups. Auto clustering was unable to identify any distinct groups, demonstrating that this transcriptomic-wide analysis was unable to provide evidence of transcriptomic B cell variations between RPL and fertile women (Figure 4.9(c-d)). The variances are likely to be a result of subject heterozygosity as well as RNA quality and quantity differences.

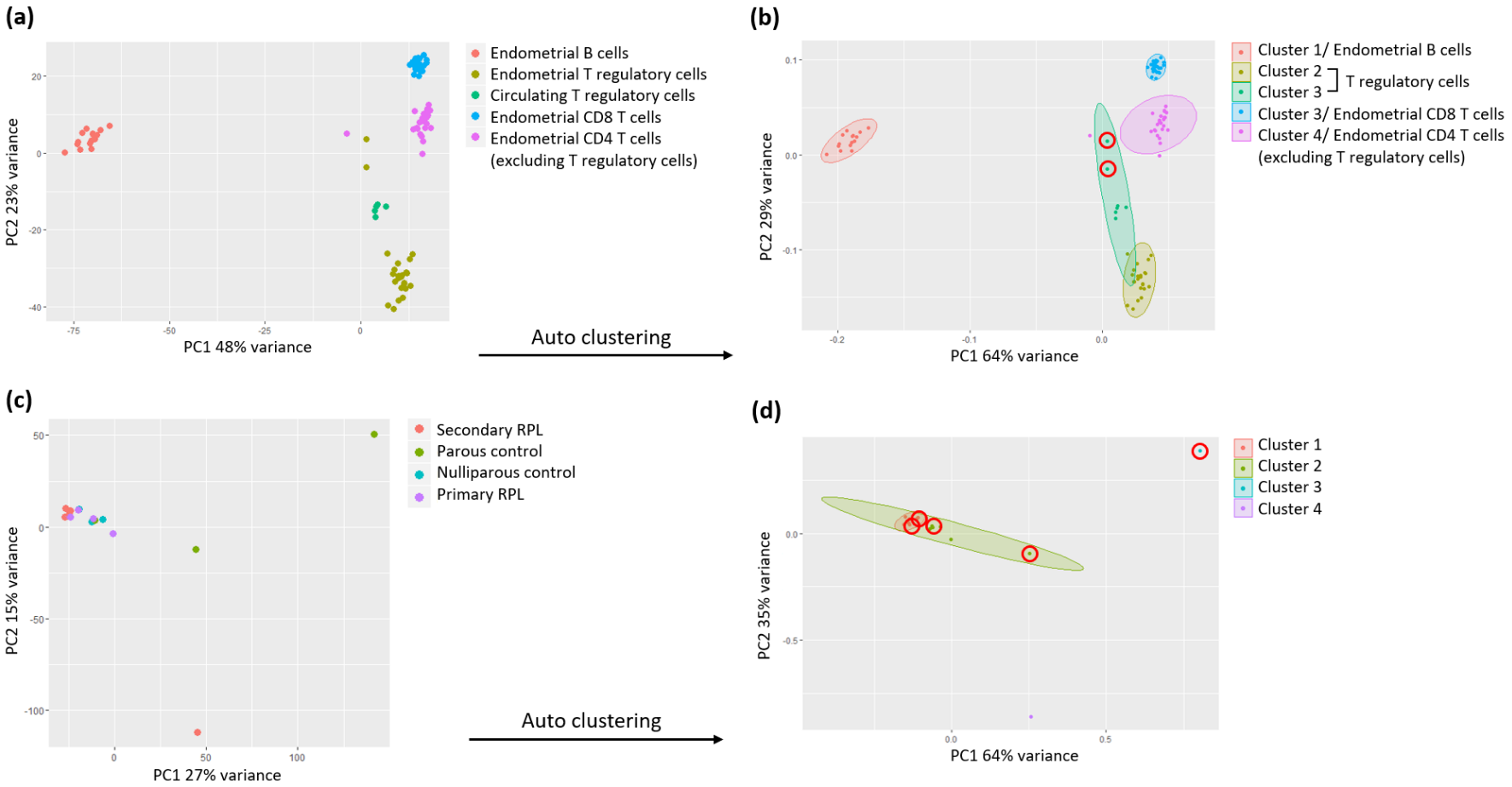

Figure 4.9: Visualization of principal component analysis (PCA) and auto clustering of T and B cells RNA-seq data. (a-b) PCA of all T and B cell RNA-seq data, variance stabilizing transformation was used for the calculation. Discrepancies between clustering groups and sample groups were manually circled in red. (c-d) PCA of 16 endometrial B cell RNA-seq data, regularized logarithm transformation was used for the calculation. Discrepancies between clustering groups and pathological groups were manually circled in red. (b),(d) Grouping was computed based on ellipses in normal probability of 95% confidence interval.

4.4.3.4 Cook's distance

The separation of sample PC.1 from other samples was further confirmed by Cook's distance. Cook's distance measures the influence of deleting a given observation and therefore can serve as a useful tool in identifying outliers in a defined dataset. Here, Cook's distance of 16 endometrial B cell RNA sequencing data was computed in R (Figure 4.10). Similar to previously described correlation coefficient, dendrogram clustering and PCA analyses, sample PC.1 shows the most significant Cook's distance compared to all other samples.

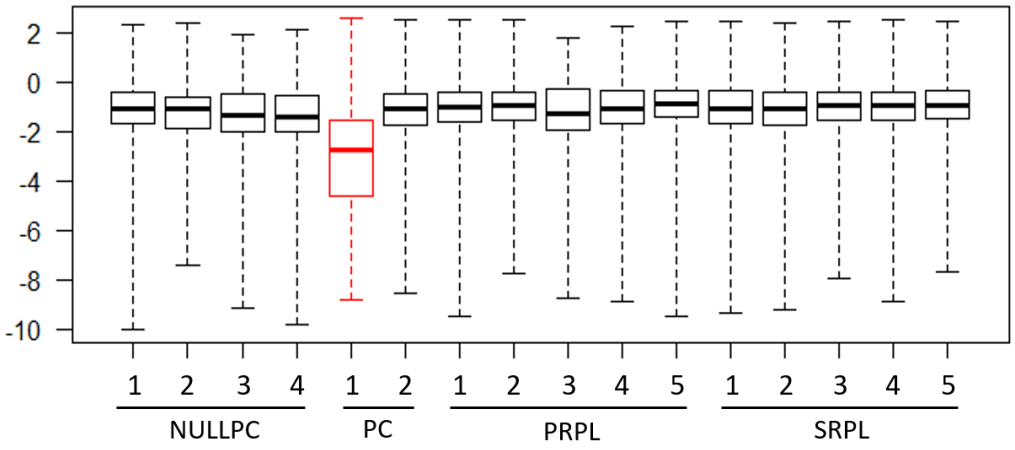

Figure 4.10: Cook's distance of 16 endometrial B cell RNA sequencing data. Distances were computed from the $\log_{10}$ of DESeq2 count matrix. Outlier is shown in red. NULLPC, nulliparous control; PC, parous control; PRPL, primary recurrent pregnancy loss; SRPL, secondary recurrent pregnancy loss.

Evidence presented showed that PC1 had the lowest raw read counts, raw read bases and quality score, therefore sample PC.1 was identified as an outlier with poor quality atypical data and discarded in the following analysis.

4.4.4 Endometrial B cells gene expression analysis

4.4.4.1 Top expression genes in endometrial B cells

Top expression gene analysis was used to examine the endometrial B cell gene expression profile from all women in this cohort.

DESeq2 analysis returned 60,448 encoding genes, and 27,346 displayed non-zero read counts in the endometrial B cell sample set. The heatmap shows the top 20 expressed genes in all B cell samples (n=15) (Figure 4.11). Due to the large variations in read count data, $\log_2$ was applied to the count matrix. As expected, most of these genes were housekeeping genes, e.g. mitocondrial functional related genes *MT-RNR2*, *MT-CYB*, *MT-ND4* and *MT-CO3*. Several B cell signature genes (*IGHM*, *IGHG1*, *HLA-DRA*) were also highly expressed, confirming the efficacy of cell sorting and RNA sequencing.

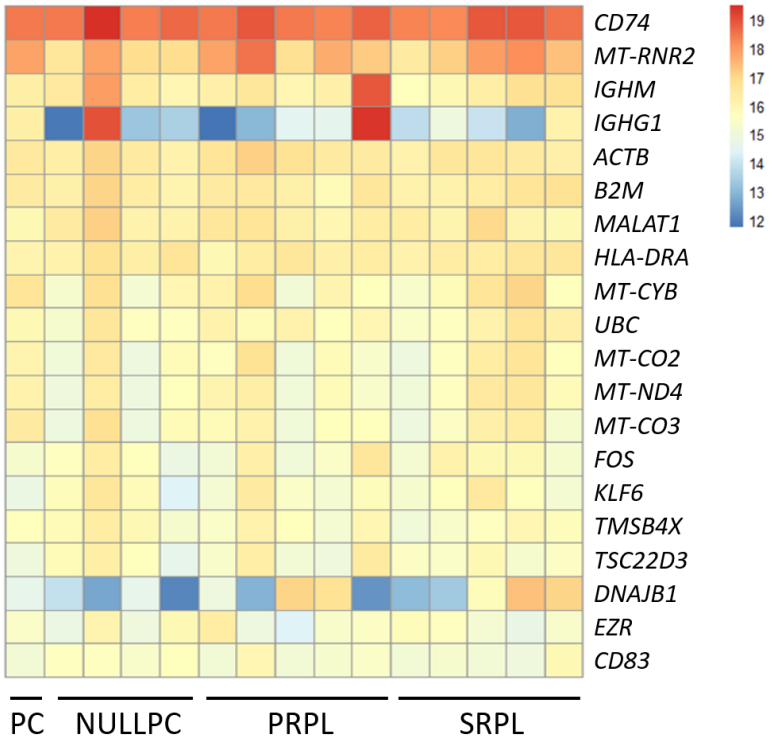

Figure 4.11: Heatmap of the top 20 expressed genes in endometrial B cells. The data is of $\log_2$ normalised counts generated using normalised count matrix. NULLPC, nulliparous control; PC, parous control; PRPL, primary recurrent pregnancy loss; SRPL, secondary recurrent pregnancy loss.

4.4.4.2 B cell specific genes in endometrial B cells

I combined the data from all endometrial samples, both controls and RPL, to perform comparative analysis between endometrial B cells and endometrial T cells (endometrial T regulatory cells, endometrial CD4 T cells and endometrial CD8 T cells were combined and viewed as one group) to determine B cell-specific genes expression profile.

The analysis returned 36,905 non-zero read counts genes. Of which, 4,295 genes were differentially expressed (Benjamin-Hochberg corrected $p < 0.01$), with 2,510 genes significantly higher in endometrial T cells and 1,785 genes significantly higher in endometrial B cells. The finding that only 11.64% were deferentially expressed emphasized the similarities between endometrial T and B cells but also illustrated the differences in these two immune cell types. A threshold of $\log_2$ fold change > 1.5 was applied to examine the highly expressed genes in endometrial B cells. The top 20 expressed genes, shown in Figure 4.12, included known B cell markers (*CD20*, *CD79A*), immunoglobulin related genes (*IGHM*, *IGHG1*, *IGHA1*, *IGLC2*), HLA related genes (*CD74*, *HLA-DRA*, *HLA-DPA1*, *HLA-DRB1*), various B cell pathway related genes (*IRF8*, *BUFF-R*), B cell activation marker (*CD83*) and chemokine receptor (*CCR7*). This result suggests an activated phenotype of endometrial B cells and this was further confirmed by GO term and KEGG enrichment analysis.

Analysis of 1,785 B cell specific genes returned 562 enriched GO terms (with over-represented p value < 0.01), the top 20 are shown in Figure 4.13. The most enriched GO term is 'HLA class II protein complex', corresponding to the B cell cellular component. Other GO terms are referring to B cell biological process (18/20), with half representing immune activation (9/18).

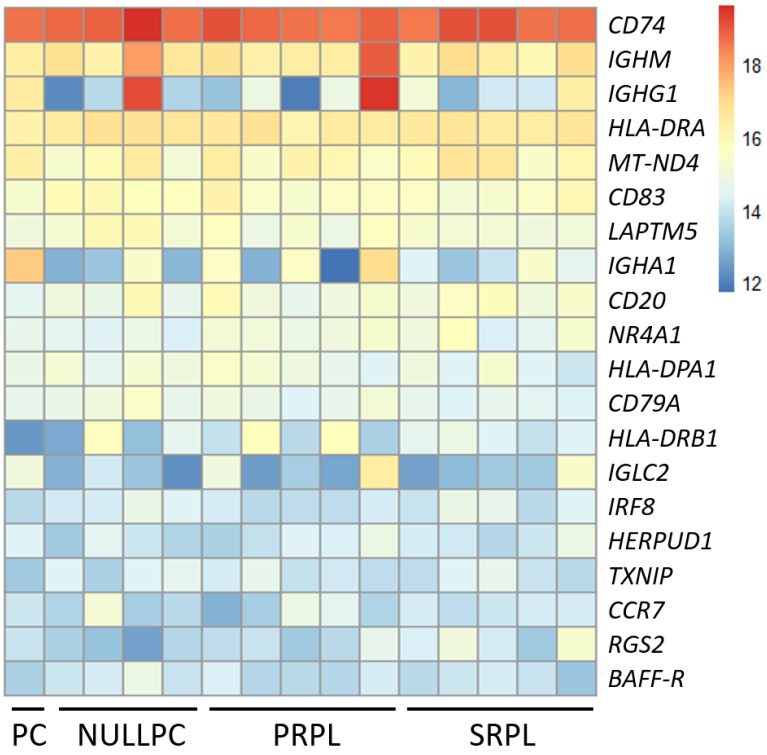

Figure 4.12: Heatmap of endometrial B cell-specific most highly expressed genes. Top 20 B cell-specific genes are illustrated. The data were generated by comparative analysis with endometrial T cells, $\log_2$ fold change > 1.5 was applied. NULLPC, nulliparous control; PC, parous control; PRPL, primary recurrent pregnancy loss; SRPL, secondary recurrent pregnancy loss.

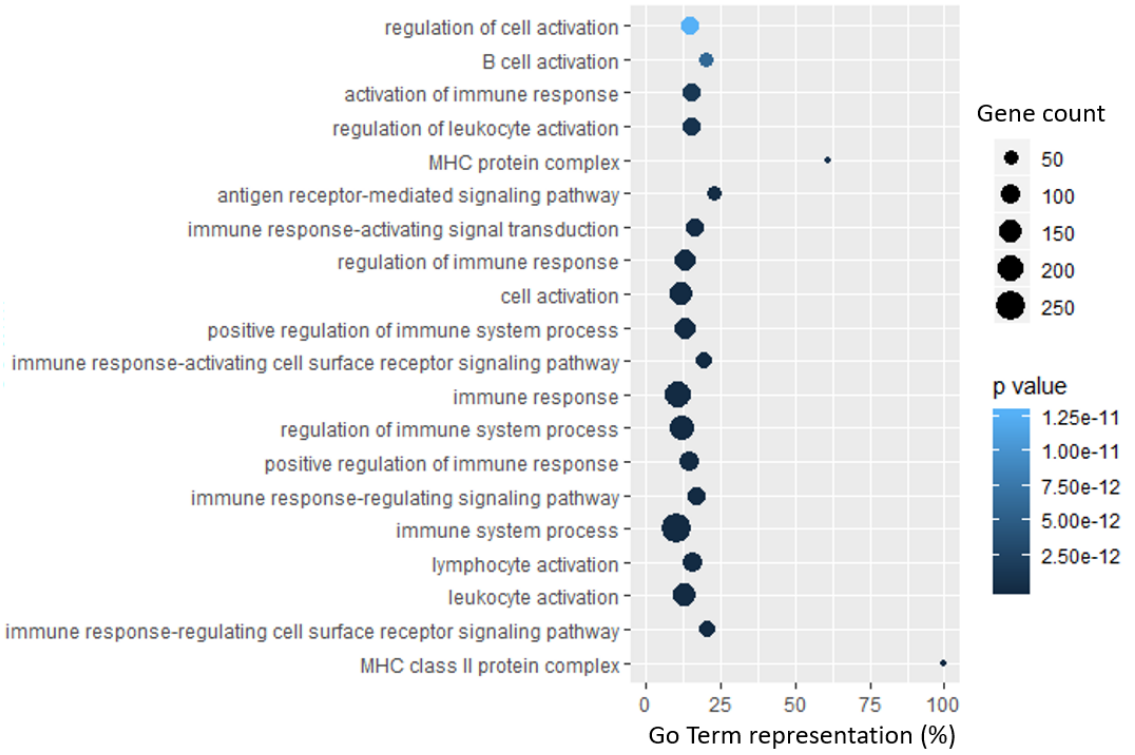

Figure 4.13: GO term enrichment analysis of endometrial B cell-specific genes. Top 20 Go terms enrichment are illustrated, ranked by p value from bottom to top. The data was generated by comparative analysis with endometrial T cells using probability weighting function calculation, $\log_2$ fold change > 1.5 was applied.

4.4.4.3 Pathway enrichment analysis of B cell specific genes

For KEGG enrichment analysis, 1,098 out of 1,785 B cell specific genes were mapped to the Entrez database. Analysis of these genes returned 26 enriched KEGG terms (with adjusted p value < 0.01), the top 10 is shown in Figure 4.14. The most enriched KEGG term was 'B cell receptor signaling pathway', following by 'intestinal immune network for IgA pathway'. Pathways like 'allograft rejection' and 'graft-versus-host disease' were also shown in the top 10, which could relate to endometrial B cell involvement during the embryo implantation phase. Other KEGG terms include 'antigen processing and presentation', 'autoimmune thyroid disease', etc.

Another tool to interpret B cell specific gene enrichment is GSEA. Based on normalised count table output by DESeq2, signal to noise metric was generated for ranking

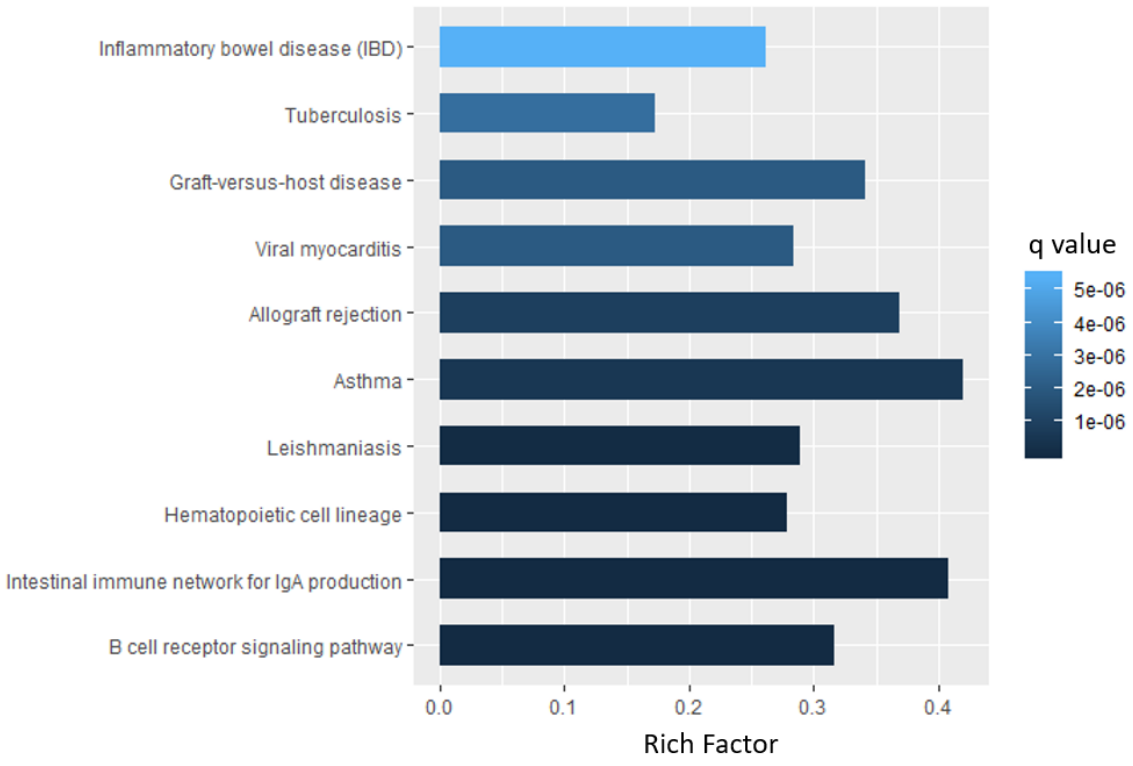

Figure 4.14: KEGG term enrichment analysis of endometrial B cell-specific genes. Top 10 KEGG terms enrichment are illustrated, ranked by q value from bottom to top. The data was generated by comparative analysis with endometrial T cells using Benjamini-Hochberg procedure.

Gene Name	Signal to Noise Score	Gene Description
BANK1	4.6	B cell scaffold protein with ankyrin repeats 1
HLA-DRA	4.5	HLA classes II-like antigen recognition protein
CD79A	3.9	Immunoglobulin-like domain
IGHD	3.8	Immunoglobulin heavy constant delta
PHACTR1	3.8	Phosphatase and actin regulator 1
WDFY4	3.8	Member of WDFY family, function in binding and phospholipid binding
HVCN1	3.6	Voltage-gated proton channel that has been shown to allow proton transport
TCF4	3.6	A basic helix-loop-helix transcription factor
CD74	3.6	HLA class II histocompatibility antigen gamma
CD83	3.5	A member of immunoglobulin (Ig) superfamily, able to influences B cell-surface HLA class II expression

Table 4.4: GSEA generated top 10 marker genes for endometrial B cells. By comparing RNA-seq data of endometrial B cells with endometrial T cells, a signal to noise metric was generated for ranking genes. The top 10 gene names, signal to noise score and gene descriptions are shown.

genes. This metric was subsequently used to determine the upregulation of B cell gene sets in GO gene sets, curated gene sets, hallmark gene sets and immunological gene sets by comparing endometrial B cells with endometrial T cells (endometrial T regulatory cells, endometrial CD4 T cells and endometrial CD8 T cells were combined and viewed as one group). Table 4.4 shows the top 10 genes for B cells and their signal to noise score. Genes including *HLA-DRA*, *CD79A*, *CD74*, *CD83* were also amongst the top 20 B cell-specific genes returned by DESeq2 analysis (Figure 4.12).

In GO gene sets, 2050 out of 9996 gene sets were upregulated in B cells. 1016 gene sets were significant at FDR < 0.25, 439 gene sets were significant at FDR < 0.1. 377 gene sets were significantly enriched at nominal p value < 0.01, 212 gene sets were significantly enriched at nominal p value < 0.001. Ranked by normalised enrichment score, a snapshot of top 9 gene set enrichment results is shown in Figure 4.15. Although the positions of genes in a given GO term gene set were scattered from B cell positively correlated to T cell positively correlated, a clear enrichment of B cell positively correlated

genes were illustrated in most gene sets (e.g. B cell mediated immunity). 186 gene sets with FDR < 0.1 and nominal p value < 0.001 were used in enrichment map visualization (Figure 4.16). After auto annotation, 11 clusters were generated and labeled with 'shared name' across all GO terms included (Figure 4.16b). Many clusters are not directly related to immune function hence are not discussed here. The largest cluster 'Immune response receptor' includes 37 GO terms is detailed in Figure 4.17. Shown in a tree layout, all the GO terms included are under 'Activation of immune response', indicating B cells contribute to immune response activation in human endometrium. A number of B cell functionally related GO terms are present, suggesting the activation of the immune response is mediated by B cell functional pathways like immunoglobulin production, and B cell activation, proliferation and differentiation.

In curated gene sets, 1646 out of 5529 gene sets were upregulated in B cells. 852 gene sets were significant at FDR < 0.25, 388 gene sets were significant at FDR < 0.1. 337 gene sets were significantly enriched at nominal p value < 0.01, 206 gene sets were significantly enriched at nominal p value < 0.001. Ranked by normalised enrichment score, a snapshot of top 9 gene set enrichment results are shown in Figure 4.18. Although the positions of genes in a given curated gene set were scattered from B cell positively correlated to T cell positively correlated, a clear enrichment of B cell positively correlated genes were illustrated in most gene sets (e.g. Genes up-regulated during differentiation from small pre-BII to immature B lymphocyte.). 192 gene sets with FDR < 0.1 and nominal p value < 0.001 were used in enrichment map visualization (Figure 4.19). After auto annotation, 7 clusters were generated and named with shared name across all curated gene sets included (Figure 4.19b). Curated gene sets include gene sets data from multiple databases, some of which have a particular focus on disease development. As a result, the resulting gene sets generated clusters like 'Squamous papilloma' and 'Serum rapamycin', which are not relevant in my research. The top 2 largest clusters 'BCR pathway' and 'IgA production' includes 13 and 10 curated gene sets that are the main focus, which are detailed in Figure 4.20. Shown in tree layout, all the curated gene sets

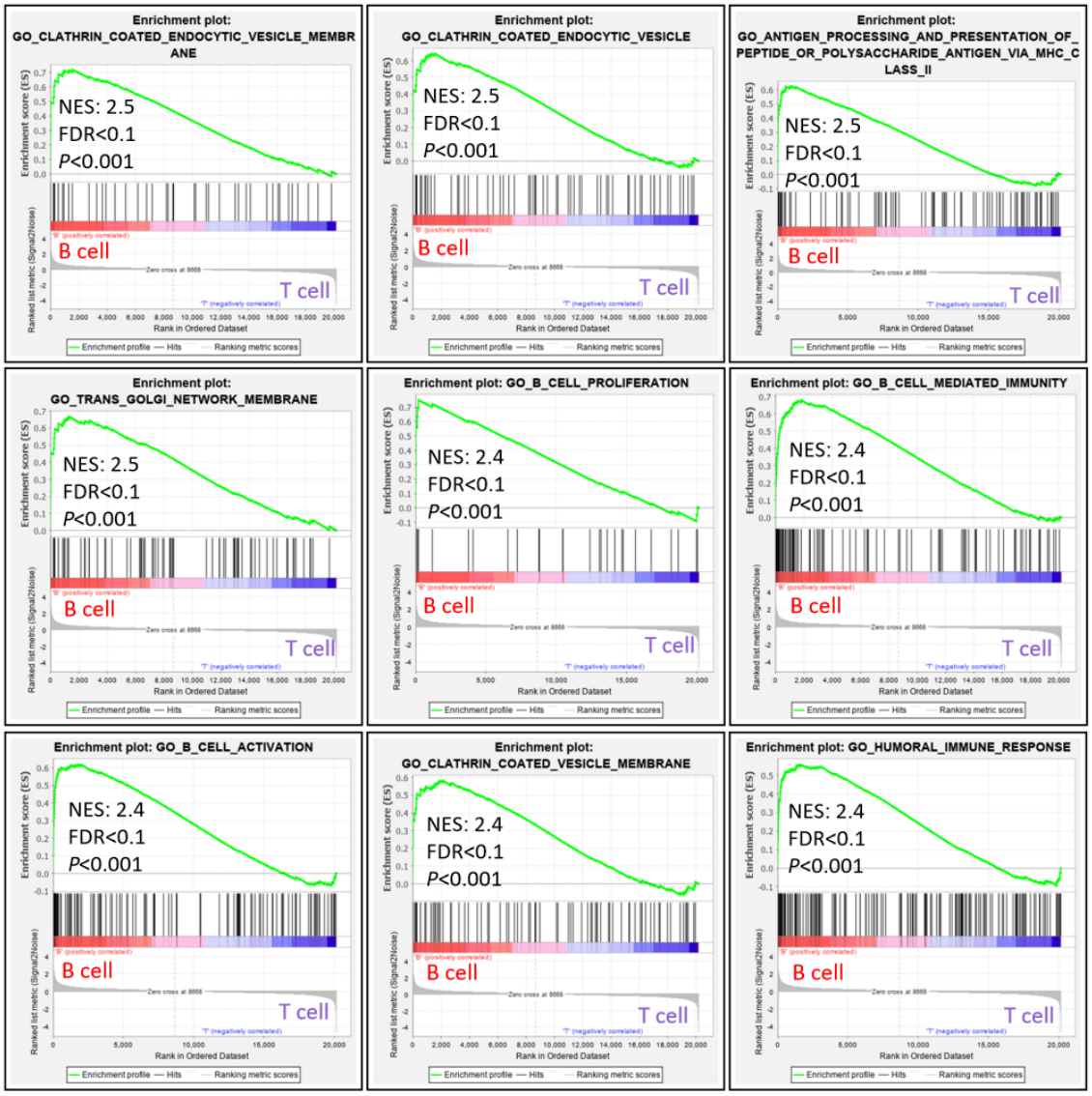

Figure 4.15: A snapshot of top 9 gene set enrichment plots generated by implemented by GSEA using GO term gene sets. Plots are selected based on normalised enrichment score ranking. Enrichment score for each gene sets is shown in the top portion of each plot. The position of genes in the GSEA ranked genes list is illustrated in the middle portion of each plot, each vertical line represents one gene. The correlations of genes in the GSEA ranked list is shown in the bottom portion of each plot, B cell on the left refers to B cell positively correlated, T cell on the right refers to T cell positively correlated. NES, normalised enrichment score. FDR, false discovery rate.

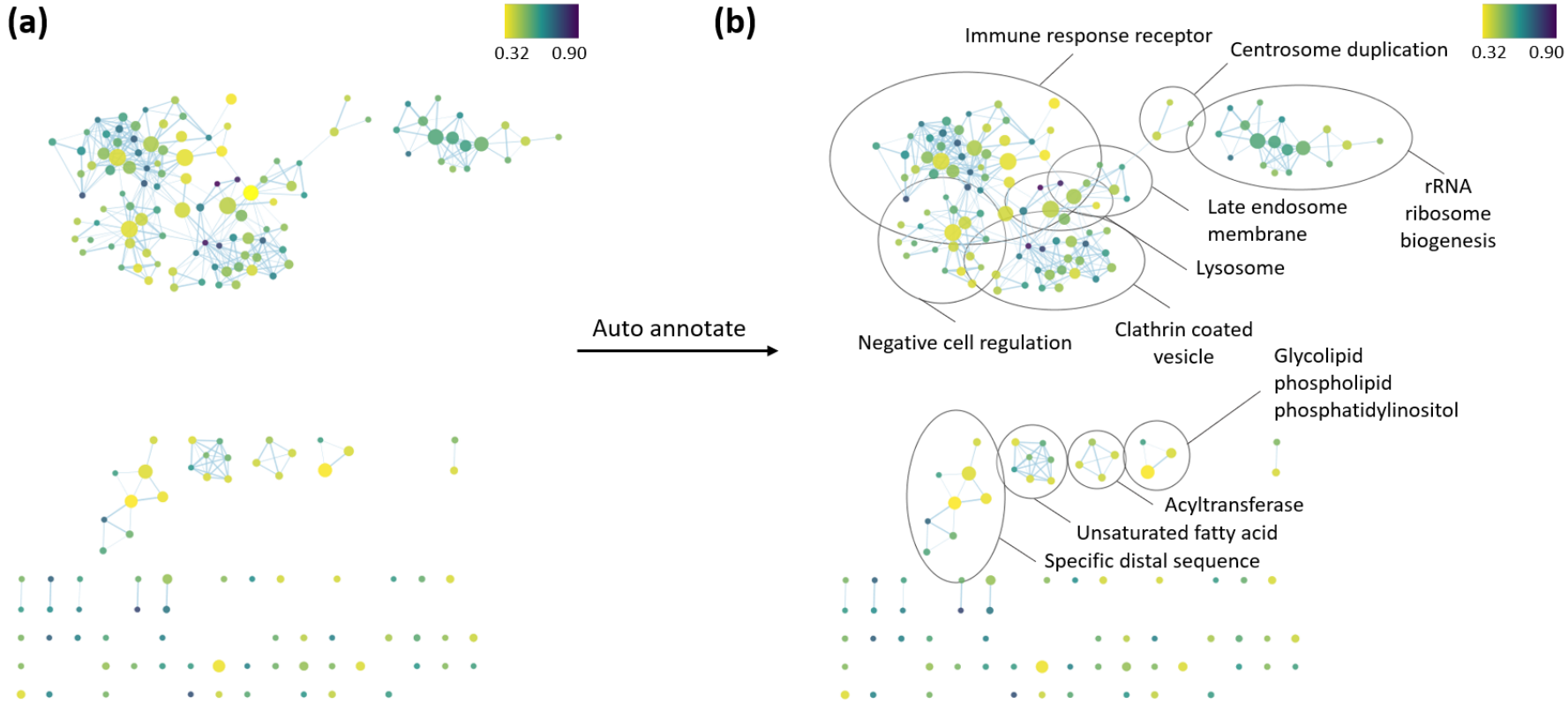

Figure 4.16: Visualization and auto annotation of upregulated GO terms in endometrial B cells implemented by GSEA and Cytoscape. All shown GO terms have FDR < 0.1 and nominal p value < 0.001. Node size indicates the size of gene set, node colour indicates the enrichment score. (a) Upregulated GO terms in endometrial B cells when compared with endometrial T cells. (b) Auto annotation of upregulated GO terms in endometrial B cells when compared with endometrial T cells. Cluster with over 2 nodes were generated. Clusters are labelled with shared name. GSEA, gene set enrichment analysis.

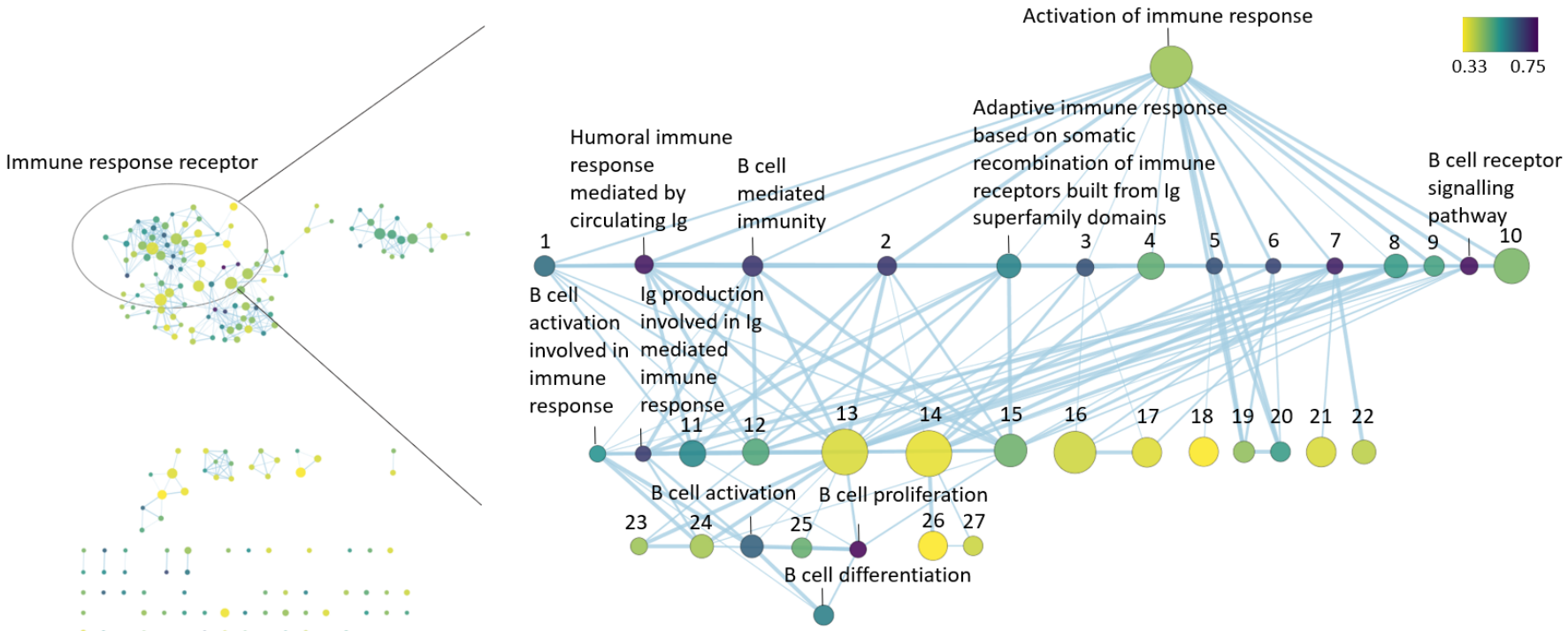

Figure 4.17: Visualization of the largest GO term annotation cluster upregulated in endometrial B cells implemented by GSEA and Cytoscape. Figure illustrates in a tree layout. Node size indicates the size of gene set, node colour indicates the enrichment score. 1, protein activation cascade; 2, complement activation; 3, membrane invagination; 4, phagocytosis; 5, myd88 dependent toll like receptor signalling pathway; 6, positive regulation of interferon alpha production; 7, phagocytosis recognition; 8, lymphocyte mediated immunity; 9, fc gamma receptor signalling pathway; 10, immune response regulating cell surface receptor signalling pathway; 11, humoral immune response; 12, leukocyte mediated immunity; 13, immune effector process; 14, endocytosis; 15, adaptive immune response; 16, side of membrane; 17, external side of plasma membrane; 18, positive regulation of sequence specific dna binding transcription factor activity; 19, pattern recognition receptor signaling pathway; 20, toll like receptor signaling pathway; 21, defence response to bacterium; 22, cell recognition; 23, myeloid cell activation involved in immune response; 24, cell activation involved in immune response; 25, leukocyte proliferation; 26, receptor mediated endocytosis; 27, receptor metabolic process. GSEA, gene set enrichment analysis.

included in cluster 'IgA production' are under 'Allograft rejection'. This correlates with findings in KEGG enrichment analysis, indicating possible endometrial B cell involvement during the embryo implantation phase. For cluster BCR pathway, all curated gene sets are directly linked to B cell related functional pathway, suggesting an activation of B cell function in human endometrium.

In Immunologic gene sets, 2447 out of 4872 gene sets were upregulated in B cells. 2225 gene sets were significant at FDR < 0.25, 1707 gene sets were significant at FDR < 0.1. 1029 gene sets were significantly enriched at nominal p value < 0.01, 731 gene sets were significantly enriched at nominal p value < 0.001. Ranked by normalised enrichment score, a snapshot of top 9 gene set enrichment results are shown in Figure 4.21. Although the positions of genes in a given immunologic gene set were scattered from B cell positively correlated to T cell positively correlated, a clear enrichment of B cell positively correlated genes were illustrated in most gene sets (e.g. Upregulated genes in B cells versus Th2 cells, Upregulated genes in B cells versus monocytes.). 728 gene sets with FDR < 0.1 and nominal p value < 0.001 were used in enrichment map visualization (Figure 4.22). After auto annotation, 9 clusters were generated and named with shared name across all immunologic gene sets included (Figure 4.22b). Immunologic gene sets include gene set data from published immunologic studies, all of which are specifically designed with experimental condition, cell type and target of interest. For example, cluster "B cell versus monocyte" looks at differences in B cell and monocyte gene expression profiles after 7 days flu vaccination. Although most clusters generated are related to B cell or T cell function, limited information is present in helping us understanding the differences between endometrial B and T cells as no similar sequencing data is available in published studies.

In hallmark gene sets, only 50 gene sets are available in the database. 13 out of 50 gene sets were upregulated in B cells. 5 gene sets were significant at FDR < 0.25, 1 is significant at FDR < 0.1. None of the gene sets were significantly enriched at nominal p value < 0.01. Ranked by normalised enrichment score, a snapshot of top 9

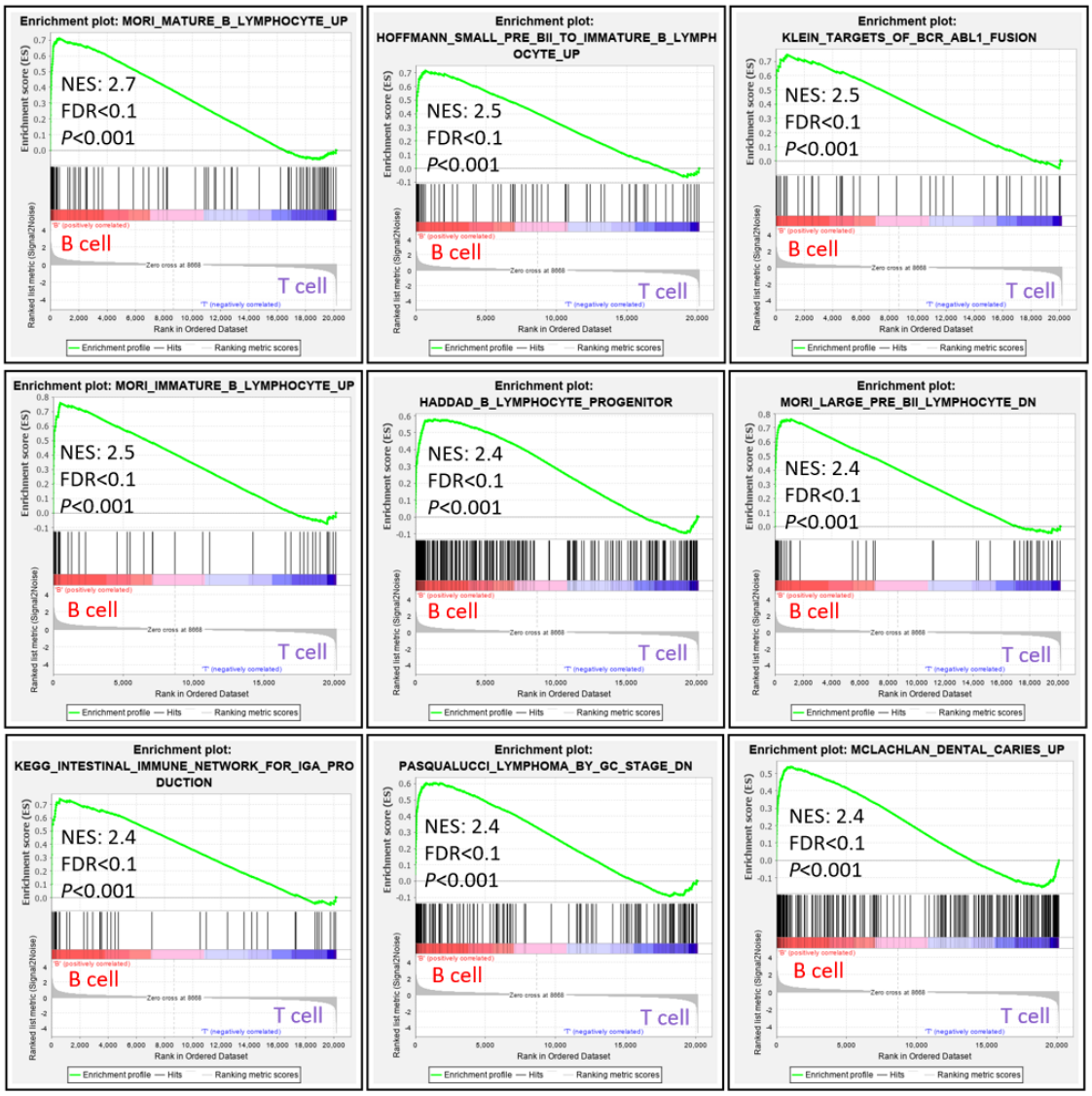

Figure 4.18: A snapshot of top 9 gene set enrichment plots generated by implemented by GSEA using curated gene sets. Plots are selected based on normalised enrichment score ranking. The position of genes in the GSEA ranked genes list is illustrated in the middle portion of each plot, each vertical line represents one gene. The correlations of genes in the GSEA ranked list is shown in the bottom portion of each plot, B cell on the left refers to B cell positively correlated, T cell on the right refers to T cell positively correlated. NES, normalised enrichment score. FDR, false discovery rate.

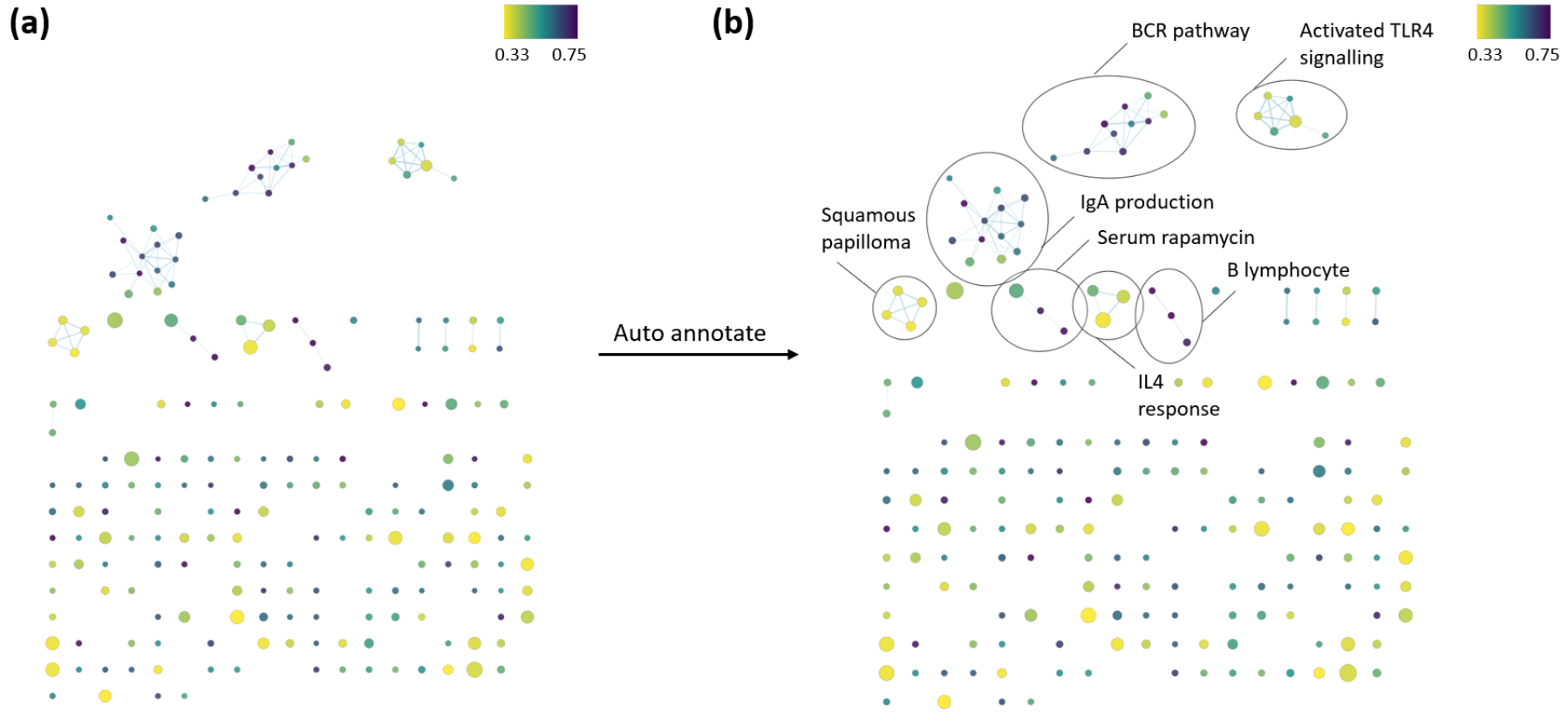

Figure 4.19: Visualization and auto annotation of upregulated curated gene sets in endometrial B cells implemented by GSEA and Cytoscape. All shown curated gene sets have FDR < 0.1 and nominal p value < 0.001. Curated gene sets include gene sets from BIOCARTA, KEGG, PID and REACTOME. Node size indicates the size of gene set, node colour indicates the enrichment score. (a) Upregulated curated gene sets in endometrial B cells when compared with endometrial T cells. (b) Auto annotation of upregulated curated gene sets in endometrial B cells when compared with endometrial T cells. Cluster with over 2 nodes were generated. Clusters are labelled with shared name. GSEA, gene set enrichment analysis. BCR, B cell receptors; TLR, Toll-like receptors.

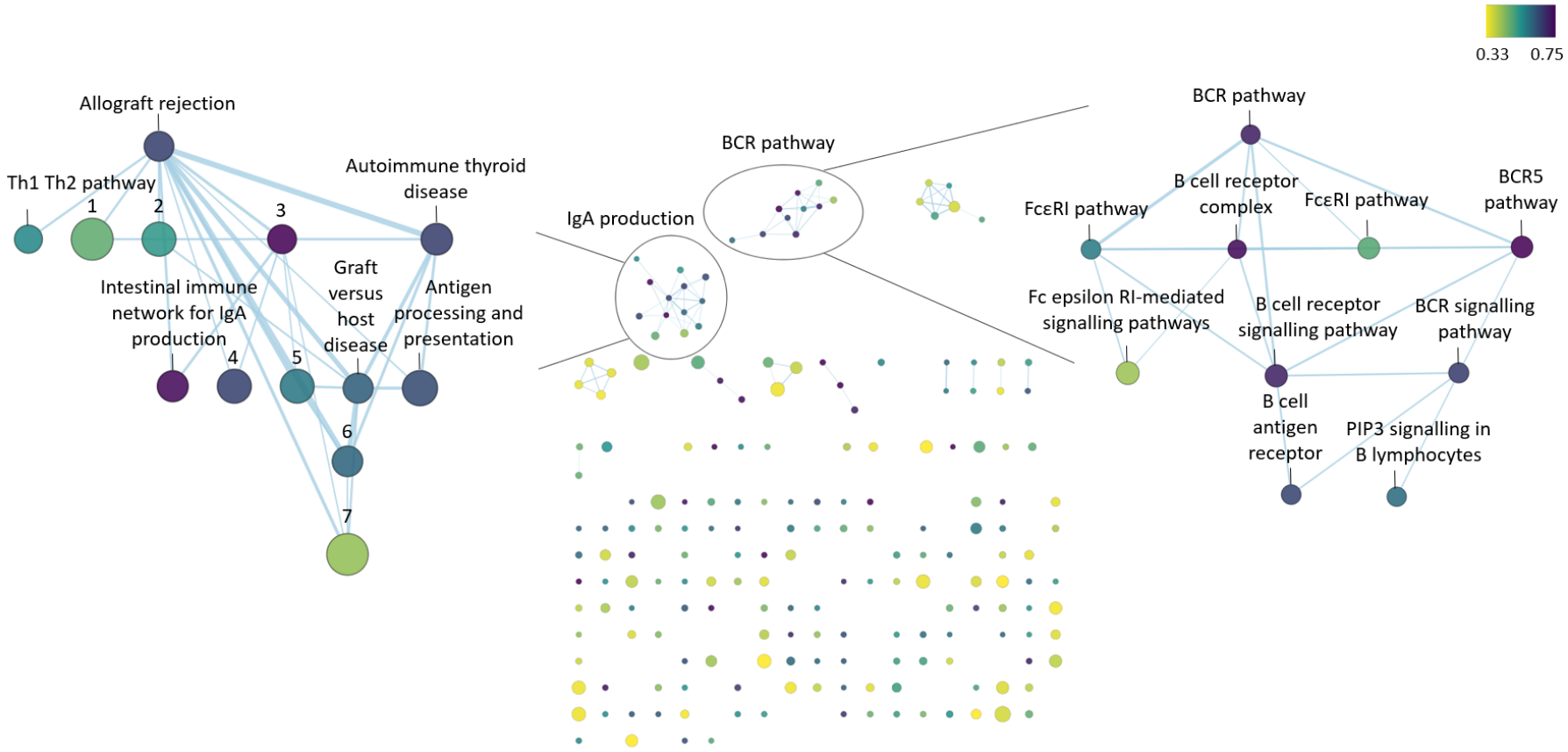

Figure 4.20: Visualization of the largest curated gene sets annotation cluster upregulated in endometrial B cells implemented by GSEA and Cytoscape. Figure illustrates as a tree layout. Curated gene sets include gene sets from BIOCARTA, KEGG, PID and REACTOME. Node size indicates the size of gene set, node colour indicates the enrichment score. 1, Systemic lupus erythematosus; 2, Proteasome 26S Subunit, Non-ATPase 4 targets; 3, Asthma; 4, Leishmania infection; 5, Viral myocarditis; 6, Type1 diabetes mellitus; 7, Cell adhesion molecules. GSEA, gene set enrichment analysis. Two gene sets named "FcϵRI pathway" are from BIOCARTA and PID, separately.



Figure 4.21: A snapshot of top 9 gene set enrichment plots generated by implemented by GSEA using immunologic gene sets. Plots are selected based on normalised enrichment score ranking. The position of genes in the GSEA ranked genes list is illustrated in the middle portion of each plot, each vertical line represents one gene. The correlations of genes in the GSEA ranked list is shown in the bottom portion of each plot, B cell on the left refers to B cell positively correlated, T cell on the right refers to T cell positively correlated. NES, normalised enrichment score. FDR, false discovery rate.

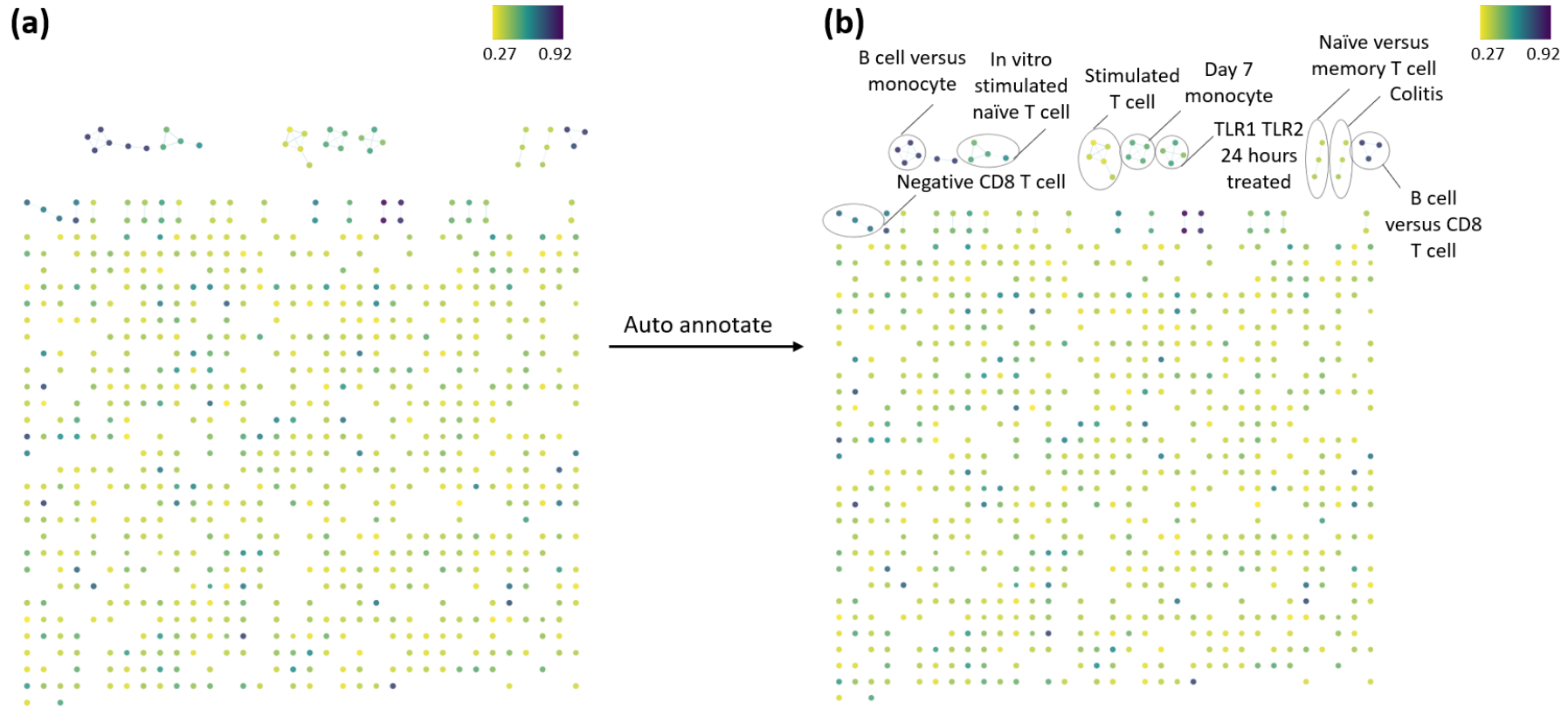

Figure 4.22: Visualization and auto annotation of upregulated immunologic gene sets in endometrial B cells implemented by GSEA and Cytoscape. All shown immunologic gene sets have FDR < 0.1 and nominal p value < 0.001. Immunologic gene sets include gene sets from published immunologic studies. Node size indicates the size of gene set, node colour indicates the enrichment score. (a) Upregulated immunologic gene sets in endometrial B cells when compared with endometrial T cells. (b) Auto annotation of upregulated immunologic gene sets in endometrial B cells when compared with endometrial T cells. Cluster with over 2 nodes were generated. Clusters are labelled with shared name. GSEA, gene set enrichment analysis. TLR, Toll-like receptors.

gene set enrichment results are shown in Figure 4.23. The positions of genes in a given hallmark gene set were scattered from B cell positively correlated to T cell positively correlated, without a clear enrichment towards B cell positively correlation in most gene sets. Not enough gene sets were present for visualization and auto annotation analysis. It is expected as hallmark gene sets only include well-defined biological process or states gene sets, with 50 gene sets condensed from 4000 gene sets from MSigDB. While the differences between endometrial B and T cells are less substantial, as both are human tissue immune cells.

Comparative analysis with endometrial T cells illustrates endometrial B cells are likely to possess an activated phenotype during the implantation phase, through high expression of various HLA related molecules and activation markers. The enrichment of IgA production, allograft reaction and autoimmune disease related pathways suggest B cells play an active role in endometrium during embryo implantation and the maintenance of successful pregnancy. Subsequent RNA-seq validation and functional analysis were conducted based on this hypothesis.

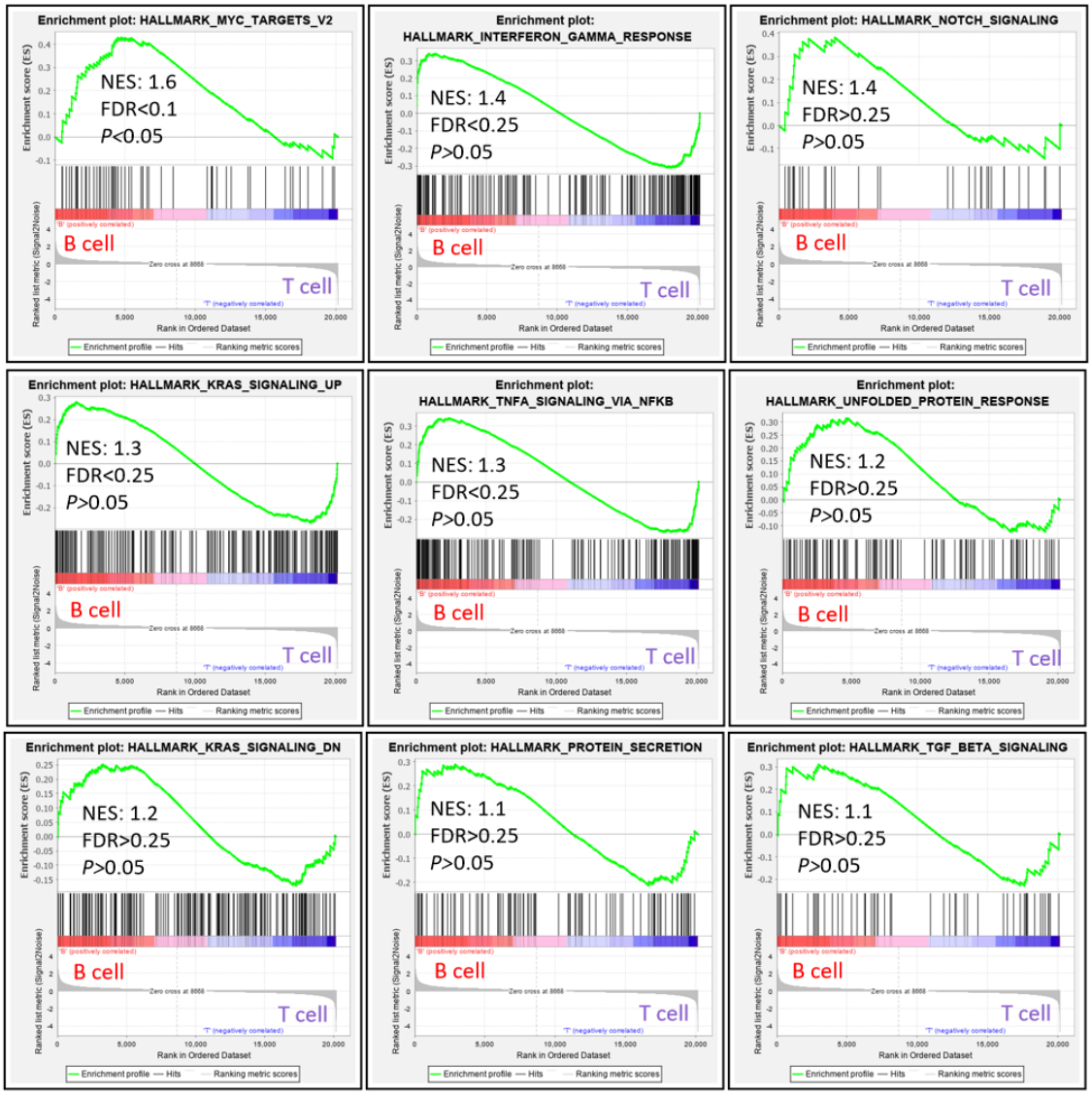

Figure 4.23: A snapshot of top 9 gene set enrichment plots generated by implemented by GSEA using hallmark gene sets. Plots are selected based on normalised enrichment score ranking. The position of genes in the GSEA ranked genes list is illustrated in the middle portion of each plot, each vertical line represents one gene. The correlations of genes in the GSEA ranked list is shown in the bottom portion of each plot, B cell on the left refers to B cell positively correlated, T cell on the right refers to T cell positively correlated. NES, normalised enrichment score. FDR, false discovery rate.

4.4.5 Differential gene expression analysis between controls and RPL groups

4.4.5.1 Control versus RPL

Previous DESeq2 analysis returned 27,346 non-zero read count genes in the endometrial B cell sample set, I next performed differential expression analysis comparing the controls (1 parous and 4 nulliparous control samples) with RPL group (5 PRPL samples and 5 SRPL samples): 27 genes were upregulated in the control group and 8 genes were upregulated in the RPL group. An adjusted p value < 0.05 and $\log_2$ fold changes $>$ 1 ($<$ -1) was applied due to the limited number of differentially expressed genes. A heatmap and volcano plot of differentially expressed genes are shown in Figure 4.24 and Figure 4.25.

Pathway enrichment analysis including GO terms, KEGG and GSEA were implemented. No enriched pathway passed p value < 0.05 and q value < 0.05.

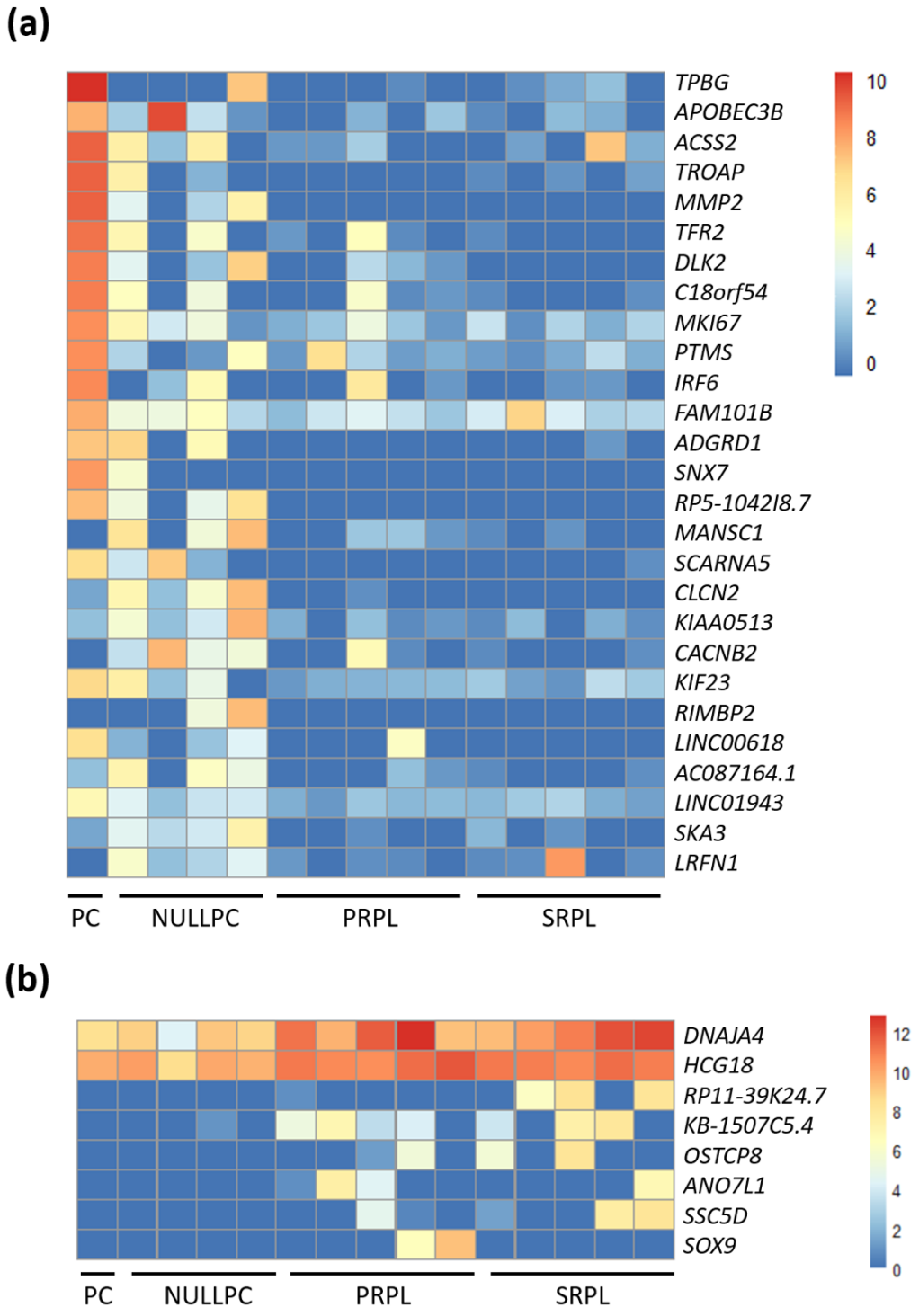

Figure 4.24: Heatmap depicting differentially expressed genes between control and RPL patients. Controls (PC and NULLPC) and RPL (PRPL and SRPL) groups were compared. Genes were ranked from top to bottom by expression base mean. (a) Upregulated genes in control group. (b) Upregulated genes in RPL group. The data was generated by DESeq2, adjusted p value < 0.05 and $\log_2$ fold change > 1 were applied. NULLPC, nulliparous control; PC, parous control; PRPL, primary recurrent pregnancy loss; SRPL, secondary recurrent pregnancy loss.

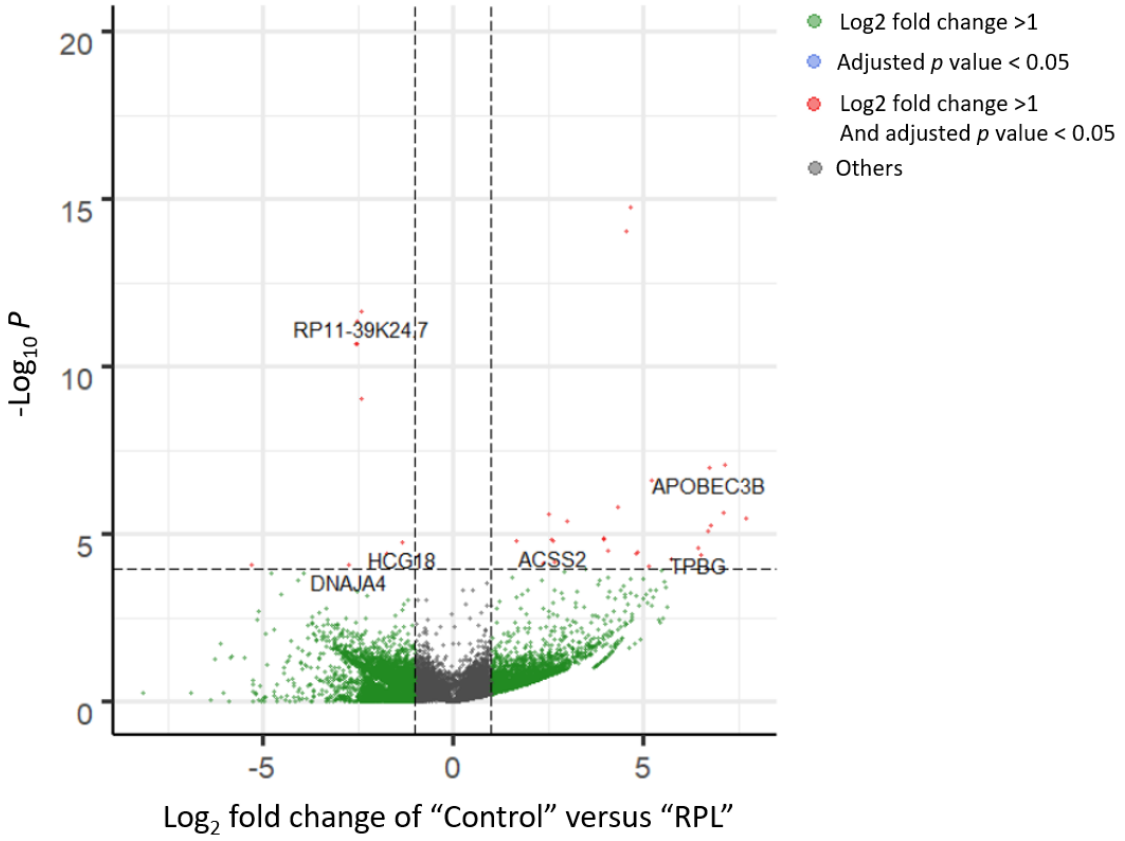

Figure 4.25: Volcano plot of differentially expressed genes between control and RPL patients. Controls (PC and NULLPC) and RPL (PRPL and SRPL) groups were compared. Each point represents one gene. Genes were coloured according to figure legend. Top 3 differentially expressed genes (ranked by expression base mean) in both groups were labeled. p value $<$ 0.05 and $\log_2$ fold change $>$ 1 were applied. NULLPC, nulliparous control; PC, parous control; PRPL, primary recurrent pregnancy loss; SRPL, secondary recurrent pregnancy loss.

4.4.5.2 Intersect of the expressed genes in study groups

Before performing differential gene expression analysis between study groups, the intersect of the expressed genes in NULLPC, PRPL, SRPL groups were visualised using a Venn diagram (Figure 4.26). The PC group was not included as there was only one sample in the group, which may be a biased representation of the transcriptome profile. To reduce the noise of the dataset, only genes with normalised count $>$ 10 were included, which leaves 20,636 genes (out of 60,448 genes) in the analysis. 66.4% of the genes (13,703/20,636) were shared between NULLPC, PRPL and SRPL groups, indicating the similarity between groups. The numbers of unique genes in all three groups were similar,

accounting for around 7% of all genes analysed. Differential gene expression was then analysed between NULLPC and PRPL, PRPL and SRPL. Comparison between NULLPC and SRPL was not performed as they differed not only in parity history, but also in subsequently pregnancy outcome.

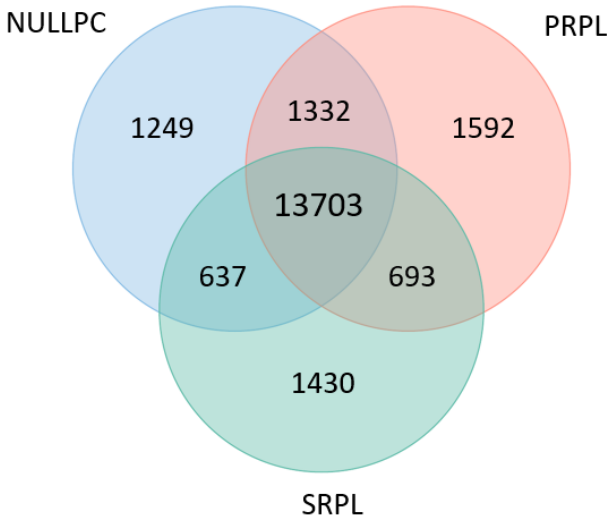

Figure 4.26: Venn diagram representing the intersect of the expressed genes in nulliparous controls and RPL groups. Only genes with normalised count $>$ 10 were included. NULLPC, nulliparous control; PRPL, primary recurrent pregnancy loss; SRPL, secondary recurrent pregnancy loss.

4.4.5.3 Nulliparous controls versus PRPL

DESeq2 differential expression analysis comparing NULLPC group with PRPL group was performed on non-zero read count genes. 13 genes were upregulated in the NULLPC group and 12 genes were upregulated in the PRPL group. An adjusted p value $<$ 0.05 and $\log_2$ fold changes $>$ 1 ($<$ -1) were applied due to the limited number of differentially expressed genes. A heatmap and volcano plot of differentially expressed genes are shown in Figure 4.27 and Figure 4.28.

Pathway enrichment analysis including GO terms, KEGG and GSEA were implemented. No enriched pathway reached a p value $<$ 0.05 and q value $<$ 0.05.

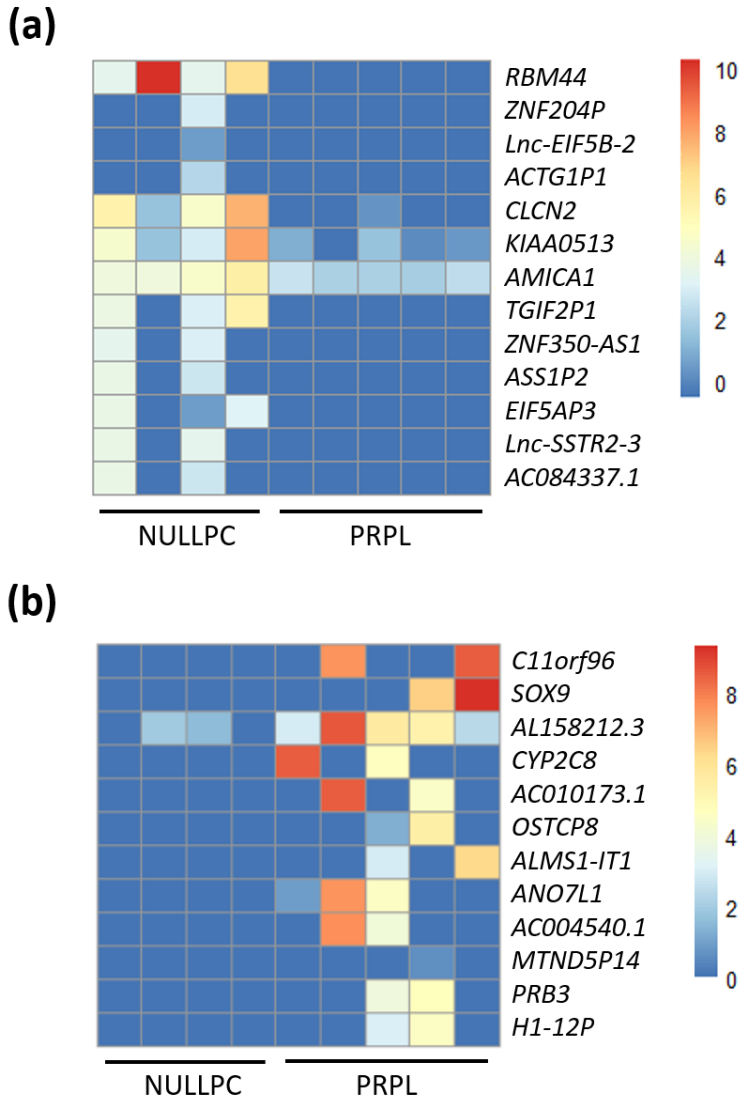

Figure 4.27: Heatmap depicting differentially expressed genes between NULLPC and PRPL patients. Genes were ranked from top to bottom by expression base mean. (a) Upregulated genes in NULLPC group. (b) Upregulated genes in PRPL group. The data was generated by DESeq2, adjusted p value < 0.05 and $\log_2$ fold change > 1 were applied. NULLPC, nulliparous control; PRPL, primary recurrent pregnancy loss.

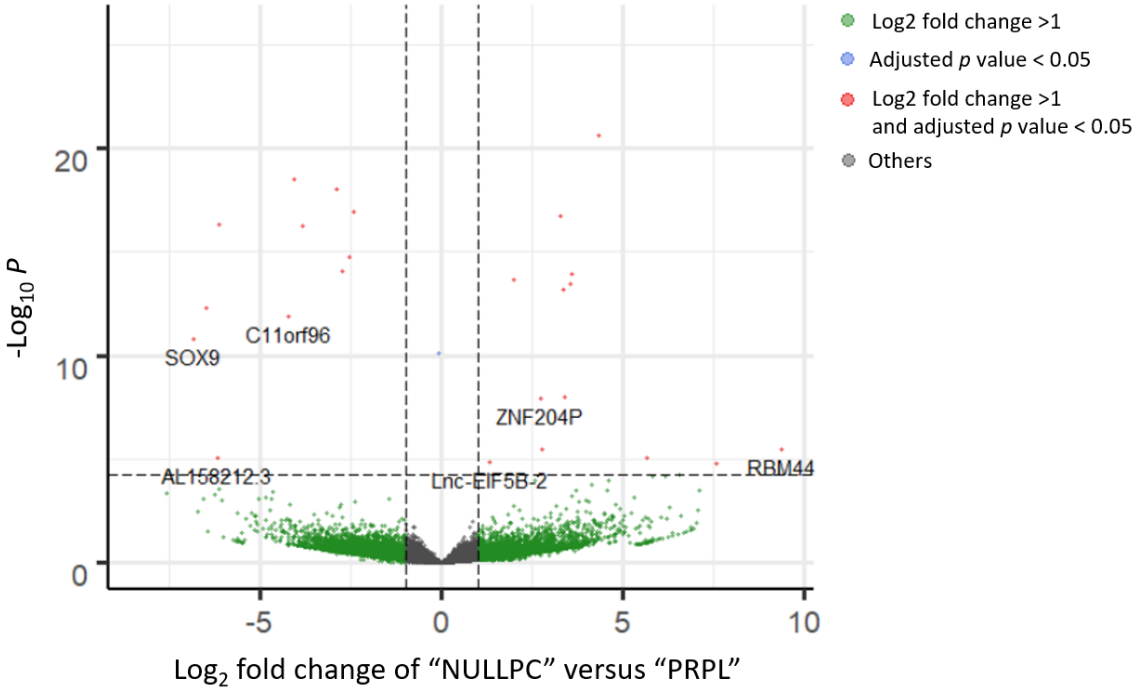

Figure 4.28: Volcano plot of differentially expressed genes between NULLPC and PRPL patients. Each point represents one gene. Genes were coloured according to figure legend. Top 3 differentially expressed genes (ranked by expression base mean) in both groups were labeled. Adjusted p value < 0.05 and $\log_2$ fold change > 1 were applied. NULLPC, nulliparous control; PRPL, primary recurrent pregnancy loss.

4.4.5.4 PRPL versus SRPL

DESeq2 differential expression analysis comparing PRPL group with SRPL group was performed on non-zero read count genes. 126 genes were upregulated in the PRPL group and 18 genes were upregulated in the SRPL group. An adjusted p value < 0.05 and $\log_2$ fold changes > 1 (< -1) were applied due to the limited number of differentially expressed genes. A heatmap and volcano plot of differentially expressed genes are shown in Figure 4.29 and Figure 4.30.

Pathway enrichment analysis including GO terms, KEGG and GSEA were implemented. No enriched pathway reached a p value < 0.05 and q value < 0.05.

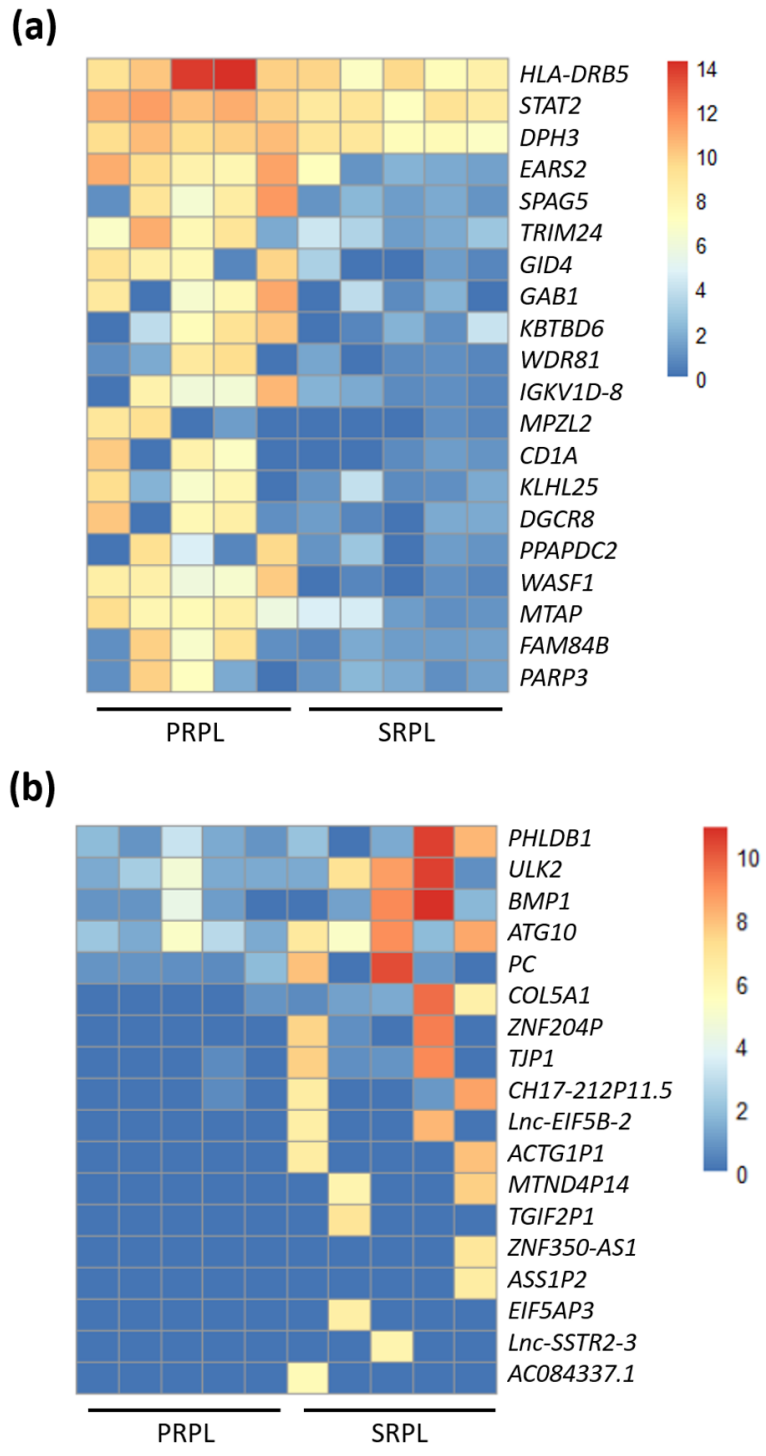

Figure 4.29: Heatmap depicting differentially expressed genes between PRPL and SRPL patients. Genes were ranked from top to bottom by expression base mean. (a) Top 20 upregulated genes in PRPL group. (b) Upregulated genes in SRPL group. The data was generated by DESeq2, adjusted p value < 0.05 and $\log_2$ fold change > 1 were applied. PRPL, primary recurrent pregnancy loss; SRPL, secondary recurrent pregnancy loss.

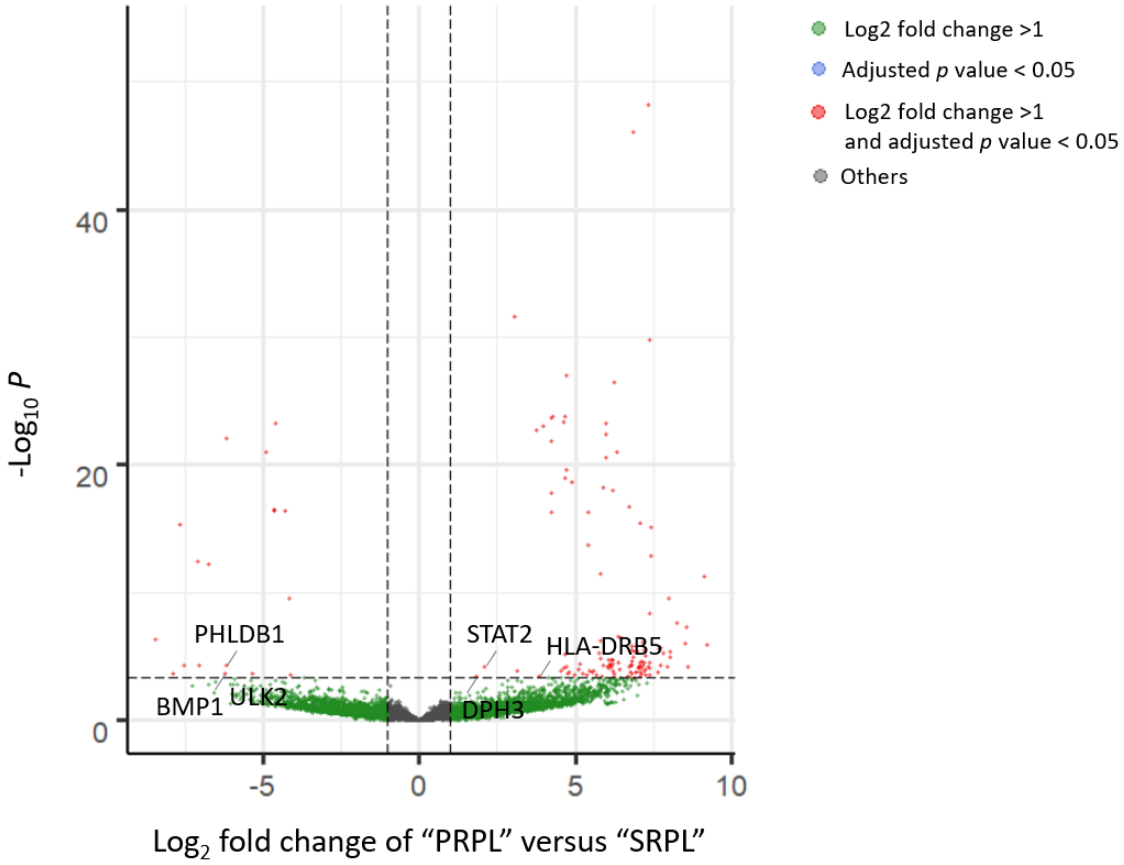

Figure 4.30: Volcano plot of differentially expressed genes between PRPL and SRPL patients. Each point represents one gene. Genes were coloured according to figure legend. Top 3 differentially expressed genes (ranked by expression base mean) in both groups were labeled. Adjusted p value < 0.05 and $\log_2$ fold change > 1 were applied. PRPL, primary recurrent pregnancy loss; SRPL, secondary recurrent pregnancy loss.

4.4.5.5 Intersect of differentially expressed genes in comparison groups

The intersect of differentially expressed genes between NULLPC versus PRPL and PRLP versus SRPL comparison groups was visualised using a Venn diagram (Figure 4.31). The number of differentially expressed genes in NULLPC versus PRPL group was smaller than that in PRPL versus SRPL group. There were 12 differentially expressed genes that overlapped between 'NULLPC versus PRPL' and 'PRPL versus SRPL' that might be related to previous pregnancy memory. However, 11 of them had normalised count < 1 in most samples, therefore were not selected as valid targets for endometrial B cell study (Figure 4.32). The remaining one was *AL158212.3*, a novel transcript overlapping

to VTI1A, that showed varied expression levels among samples, higher in NULLPC group when compared with PC group, and higher in PRPL group when compared with SRPL group. To date, the potential role of AL158212.3 has not yet been reported.

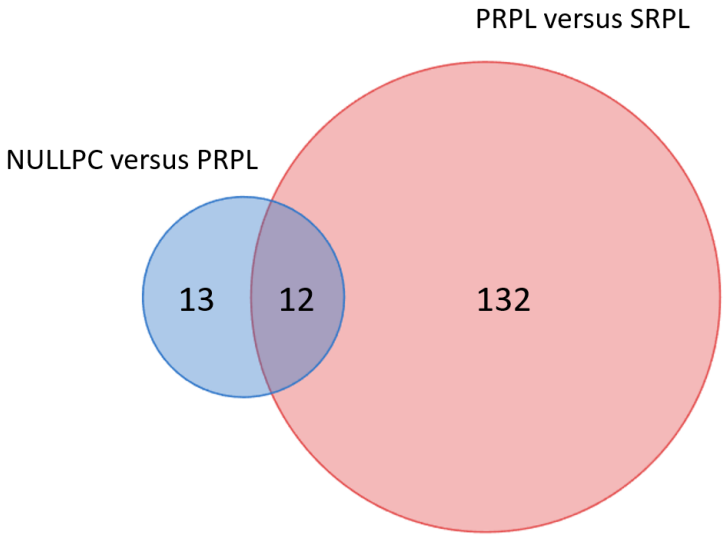

Figure 4.31: Venn diagram representing the intersect of differentially expressed genes between NULLPC versus PRPL and PRLP versus SRPL comparison groups. Differentially expressed genes were generated by DESeq2. Adjusted p value < 0.05 and $\log_2$ fold change > 1 were applied. NULLPC, nulliparous control; PRPL, primary recurrent pregnancy loss; SRPL, secondary recurrent pregnancy loss.

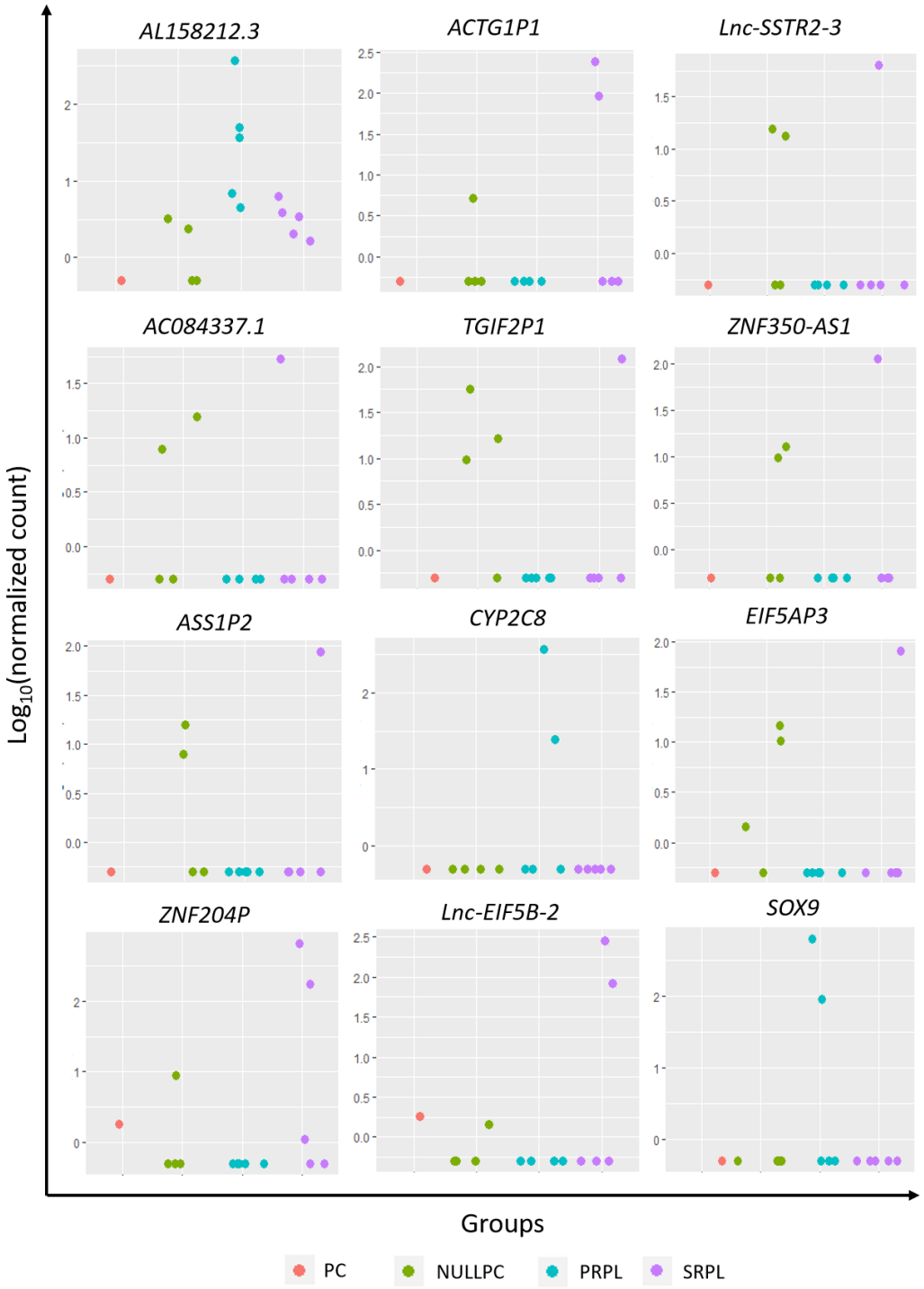

Figure 4.32: Gene expression level of 12 differentially expressed genes shared between NULLPC versus PRPL and PRLP versus SRPL comparison groups. Differentially expressed genes were generated by DESeq2. Adjusted p value < 0.05 and $\log_2$ fold change > 1 were applied. Each point represents one sample. Samples were coloured according to figure legend. Plots are present in jitter points to avoid overplotting. PC, parous control; NULLPC, nulliparous control; PRPL, primary recurrent pregnancy loss; SRPL, secondary recurrent pregnancy loss.

4.5 Discussion

4.5.1 Endometrial B cells have an activated gene expression profile

In this chapter I presented RNA-seq data for endometrial B cells. To my knowledge this is the first transcriptomic characterization of endometrial B cells, both in normal women and RPL patients.

RNA-seq analysis revealed all 16 endometrial B cell samples passed initial QC assessment and displayed a distinct gene expression profile compared with endometrial T cells (as illustrated in the PCA analysis). 15 endometrial B cell samples with higher quality scores shared strong correlation, limited sample variance and distance in their gene expression profiles (illustrated in the correlation coefficient analysis, dendrogram clustering analysis and Cook's distance analysis). These samples were included in the subsequent analysis.

Comparative analysis with endometrial T cells highlighted the upregulated genes and pathways in endometrial B cells. These included the highly expressed HLA related genes (*CD74*, *HLA-DRA*, *HLA-DPA1*, *HLA-DRB1*) along with the enriched GO terms 'MHC protein complex' and 'MHC class II protein complex'. Ig related genes (*IGHM*, *IGHG1*, *IGHA1*, *IGLC2*) along with the upregulated pathway 'Ig production involved in Ig mediated immune response' and 'IgA production' were also highly expressed. BCR related gene *CD79A* along with the upregulated pathways 'B cell receptor signalling pathway' and 'BCR pathway' were also highly expressed. Signaling and regulatory genes (*CCR7* and *IRF8*) along with the upregulated pathway 'immune response-activating signal transduction' were also highly expressed. Additionally, activation related genes (*BAFF-R* and *CD83*) were also highly expressed along with various B cell activation related pathways like 'B cell activation'. Taken together, it is very likely that endometrial B cells have an activated phenotype, mainly through Ig production and HLA activation. Although these results need to be interpreted with caution as the comparative analysis

was performed with endometrial T cells not peripheral B cells, meaning any genes and pathways constitutively expressed in B cells will likely to be upregulated.

Our data showed similarities with other endometrial transcriptomic study. Using single-cell sequencing, Lucas et al. sequenced the whole endometrial tissue and identified a maximum of three B cells in each sample, all presented a naïve B cell phenotype. These B cells have an increased expression of *CD79A*, *CD83*, *CD74* and *HLA-DRA* compared with endometrial NK cells (Lucas et al. 2020). In our research, all these genes are also shown to be upregulated when compared with endometrial T cells. As for the endometrial characteristics during the menstrual cycle, the expression levels of Ig and HLA related genes have been shown to fluctuate during the luteal phase (Carson et al. 2002, Riesewijk et al. 2003, Talbi et al. 2006). In theory, endometrial B cells could be contributing to these findings, however, considering the transcriptomic analyses were performed on whole tissue without B cell enrichment, stromal cells, epithelial cells and other types of immune cells are much more likely to be responsible for the RNA fluctuations.

4.5.2 Limited differences in gene expression profiles between study groups

Out of 27,346 non-zero read count genes in the endometrial B cell sample set, the differential gene expression analysis between NULLPC, PRPL and SRPL groups returned less than 0.1% of differentially expressed genes between NULLPC and PRPL groups, less than 0.6% of differentially expressed genes between PRPL and SRPL groups. Additionally, less than 0.2% differentially expressed genes were found when comparing controls (1 PC sample and 4 NULLPC samples) with RPL (5 PRPL samples and 5 SRPL samples) patients. In comparison, for T regulatory cells, which are also a minority cell population in human endometrial immune cells, 6.2% of genes were differentially expressed between NULLPC and PRPL groups, 8.5% of genes were found between PRPL and SRPL groups, 7.5% of genes were found between controls and RPL patients.

As shown above, endometrial B cells had a very limited number of differentially ex-

pressed genes between RPL and controls, and for these genes, their fold changes and expression levels were relatively low, with only a few B cell activation related genes like *HLA-DRB2* and *STAT2* (Gupta et al. 1999) significantly different to warrant experimental validation. As a result, there were no enriched GO terms and pathways found between experimental groups. This could due to the fact that the sample size in each group is small. Although 5 parous control samples were matched during the experimental design, there was an issue during sample processing and endometrial B cells were lost. The lack of parous controls may have meant real differences between parous controls and SRPL could not be identified, or it could be because endometrial B cells are not an active contributor to RPL. The differentially expressed immune related genes and enriched pathways reported in previous publications (Altmäe et al. 2009, 2017, Vallés et al. 2018, Koot et al. 2016) are more likely to be related to other lymphocytes like T cells and NK cells, which are much more represented in the endometrial immune environment (Fukui et al. 2011, Lee et al. 2012).

The number of differentially expressed genes between NULLPC, PRPL and SRPL groups were also illustrated with Venn diagram. Result shown that there are 10 times more genes being uniquely differentially expressed in PRPL versus SRPL compared with NULLPC versus PRPL. This counter-intuitive data could be suggesting that although endometrial B cells are not an active contributor to RPL, they could obtain an altered transcriptomic profile after previous exposure to pregnancy. This type of trained immunity has been described in dNK cells, where unique subsets of dNK cells exist after repeated pregnancies (Gamliel et al. 2018).

4.5.3 Future directions

4.5.3.1 Endometrial B cell subtyping

Using bulk RNA-seq, my research unraveled a key endometrial B cell phenotype during the mid-luteal phase. However, it was unable to illustrate which B cell subsets are present in the human endometrium. As discussed in Chapter 3, most published studies

used only pan-B cell markers like CD19, CD20 and CD22 to identify endometrial B cells. To date, there is only one study reported the presence of naïve B cells in the endometrium (Lucas et al. 2020). But due to the limited sample size, this study failed to determine the percentage of naïve B cells in the total endometrial B cell population, or whether there are any other B cell subsets. Naïve B cells are B cells that have not been exposed to antigens. Once exposed to antigens, naïve B cells could undergo germinal centre reactions, and either become memory B cells or antibody secreting plasma cells, both are functionally important in the tissue immune environment (Oleinika et al. 2019). Therefore, future studies could start with subtyping endometrial B cells, which will shed more light on endometrial B cell function, as well as the function of endometrial LAs described in Chapter 3.

4.5.3.2 Experimental validation of RNA-seq data

For RNA-seq data validation, protein level validation of B cell activation related genes would be the next step of research. Comparative analysis should be performed with peripheral B cells to ensure the B cell activation phenotype are specific to endometrial immune environment. For differentially expressed genes found between study groups, experimental validation could start at mRNA level, as the RNA-seq data alone could not serve as a strong indicator.

In the next chapter, some of the future experiments discussed above are addressed.

4.5.3.3 Future transcriptomic studies on endometrial B cells

As a pilot study, this chapter proved the feasibility of performing transcriptomic analysis of endometrial B cells. To maximize the usefulness of future transcriptomic data on endometrial B cells, it is crucial to perform cell enrichment before sequencing as endometrial B cells are a minority immune cell population. Additionally, instead of unexplained RPL, future studies could focus on autoimmune disorders (e.g. APS) that have been

linked to RPL where endometrial B cells are more likely to be playing an active role in the local immune environment.

Chapter 5

Analysis of Endometrial B Cell Subsets, Phenotypes and Cytokine Production

5.1 Introduction

5.1.1 B cell development

B cells, which are at the centre of the adaptive humoral immune system, display notable phenotypic and functional diversity between various known subsets (Figure 5.1). Early B cell development begins in the fetal liver before continuing in the bone marrow, where they arise out of the multipotential stem-cell pool. Developing B cells progress to the immature B cell stage when the B cell receptor (BCR) is expressed on the cell surface. At this stage, multiple checkpoints ensure that self-reactive B cells, which express BCR specific for self-antigens, undergo negative selection and are not released into the periphery. The subsequent B cell emigration from the bone marrow marks the transition of immature B cells to transitional B cells (Oleinika et al. 2019, Chung et al. 2003, Vossenkämper et al. 2012).

Upon entering into the periphery, B cells mature into antigen-naïve B cells. After

antigen exposure, naïve B cells are activated, and can either differentiate into short-lived plasmablasts, or enter into germinal centres (GCs) and differentiate into memory B cells or long-lived plasma cells. GCs are sites within secondary lymphoid organs and tertiary lymphoid structures (TLSs) (Pipi et al. 2018, LeBien and Tedder 2008). GC reactions represent the most dynamic phase of B cell development, where B cells undergo somatic hypermutation (SHM) and class switch recombination (CSR) to generate memory B cells or plasma cells that can produce a high affinity antibodies. Additionally, various regulatory B cell subsets have been identified. Immature, naïve and memory B cells all have the capacity to differentiate into regulatory B cells, however, it is yet to be confirmed whether there is any other developmental origin for regulatory B cells (Rosser and Mauri 2015, Mauri et al. 2017).

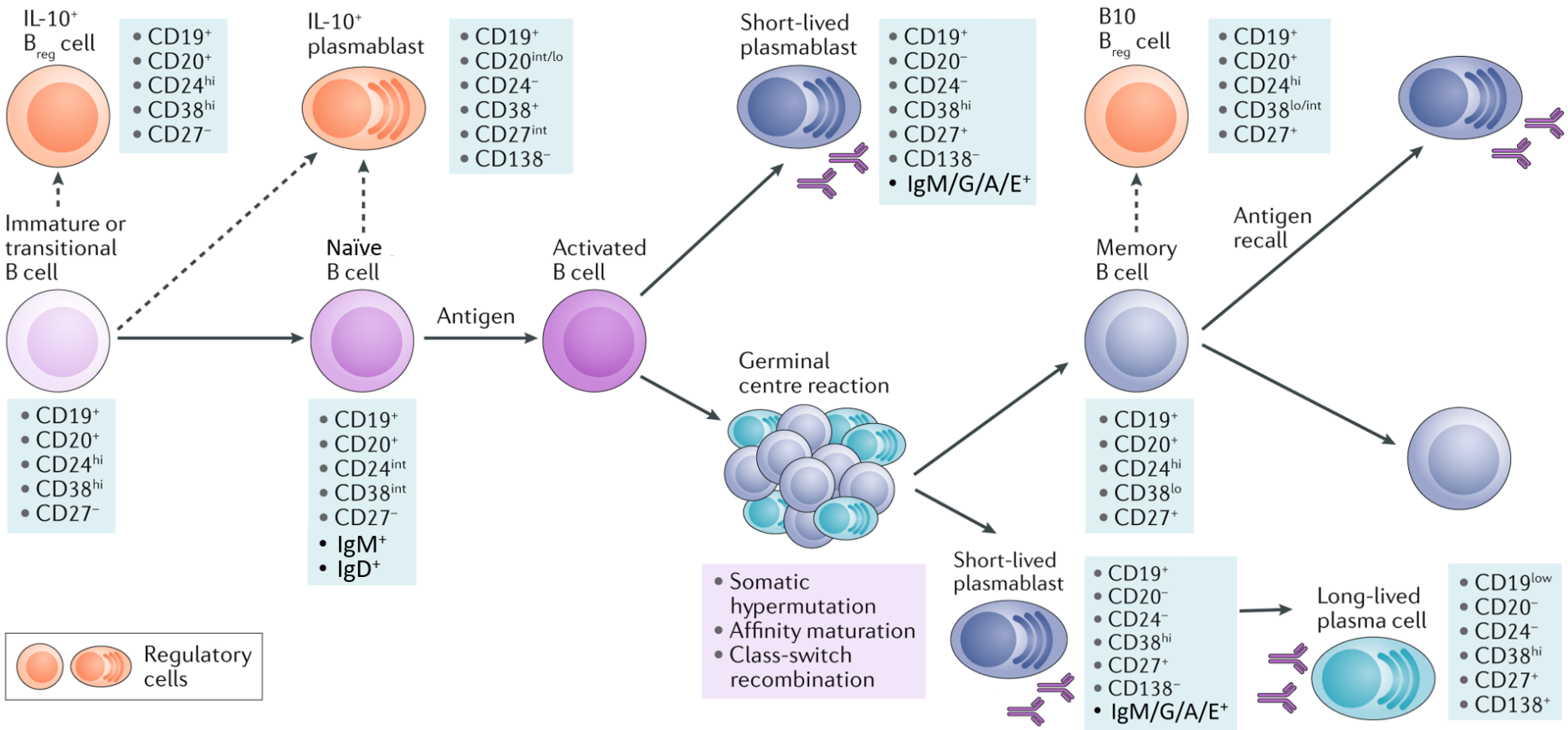

Figure 5.1: B cell development and differentiation pathways. Various B cell subsets, including immature/ transitional B cells, regulatory B cells, naïve B cells, memory B cells, plasmablasts (short-lived) and plasma cells (long-lived), are illustrated as B cells go through different developmental and differentiation stages. Markers for identifying different B cell subsets are illustrated. Figure is adapted from (Oleinika et al. 2019).

5.1.2 B cell subsets

The various B cell subsets are hereby discussed, and evidence for their involvement in the endometrial immune environment, endometrial pathologies or ongoing pregnancy are described.

5.1.2.1 Transitional B cells

Transitional B cells, defined by the expression of high levels of CD24 and CD38, typically account for 2-4% of all circulating B cells (Chung et al. 2003, Ziegler et al. 2018, Sims et al. 2005). As a crucial link between bone-marrow immature and peripheral mature naïve B cells, increased frequencies of transitional B cells have been reported in various autoimmune disorders such as systemic lupus erythematosus and primary Sjögren's syndrome. Researchers suggest that autoreactive transitional B cells arise when they are not removed during the tolerance checks that occur in the bone marrow, and may contribute to autoimmune disease development (Daridon et al. 2006, Mauri 2010, Vossenkämper et al. 2012). In pregnancy, the percentages of peripheral $CD24^{hi}CD38^{hi}IgD^{+}IgM^{+}$ transitional B cells are significantly lower in the third trimester and on the day of delivery compared with those in non-pregnant and post-partum women (Ziegler et al. 2018, Lima et al. 2016). In decidual tissues, $CD19^{+}CD24^{hi}CD38^{hi}$ transitional B cells represent approximately 20% of all B cells in the decidua basalis collected at term, and their frequencies are significantly reduced in women with preterm labour compared to those without labour (Leng et al. 2019). However, the proportion of transitional B cells in human endometrium has never been characterised.

Recently, there has been interest in the potential involvement of B regulatory cells in maintaining successful pregnancy. A subset of these B regulatory cells share a similar phenotype with transitional cells ($CD19^{+}CD24^{hi}CD38^{hi}$), and were reported to be immunosuppressive (Wortel and Heidt 2017, Ding et al. 2015). The phenotype and function of B regulatory cells is introduced in the next section.

5.1.2.2 Regulatory B cells

Regulatory B cells are a rare B cell subset with regulatory/suppressor functions, representing $<10\%$ of circulating B cells and their regulatory activity is mostly but not solely achieved through the production of IL-10 (Ding et al. 2015, Rosser and Mauri 2015, Esteve-Solé et al. 2018). As a suppressor cytokine, IL-10 is able to inhibit the effector mechanisms of the immune system through the inhibition of chemokine and pro-inflammatory cytokine production. Other anti-inflammatory mechanisms of regulatory B cells include the production of IL-35 and TGF-β (Rosser and Mauri 2015, Egwuagu and Yu 2015). Regulatory B cells are, however, still a relatively understudied cell type and it is not yet confirmed whether regulatory B cells are developed through a specific lineage under the control of a specific transcription factor, or by certain stimuli that cause B cells to take on a regulatory phenotype (Rosser and Mauri 2015, Mauri et al. 2017). Additionally, there is no consensus reached regarding which markers should be used to identify regulatory B cells. The most commonly proposed markers are $CD24^{hi}CD38^{hi}$ and $CD24^{hi}CD27^{+}$, other markers such as CD73, CD25 and CD1d have also been used (Mauri and Menon 2015, Floudas et al. 2016, Rosser and Mauri 2015, Egwuagu and Yu 2015, Esteve-Solé et al. 2018).

The functional importance of B regulatory cells has been described in various autoimmune diseases, cancer development and allotransplants, mostly through their ability to suppress immune responses (Egwuagu and Yu 2015, Fillatreau et al. 2002, Schioppa et al. 2011, Oleinika et al. 2019). More recently, their role in maintaining successful pregnancy have also been recognized. In mice models, an increased number of regulatory B cells are observed in pregnant mice compared with abortion-prone mice, and $CD5^{+}CD1d^{hi}$ regulatory B cells are able to restore pregnancy tolerance by promoting the generation of regulatory T cells (Jensen et al. 2013). Additionally, IL-10 producing B cells are able to rescue mice fetuses from inflammation-driven fetal death by modulating T cell immune responses (Busse et al. 2019). In mice uteri, an expanded pool of IL-10-producing B cells are observed during the implantation phase. These uterine B cells

are able to effectively suppress the proliferation and activation of $CD4^+$ T cells, thereby potentially contributing to the successful establishment of maternal immunological tolerance in early pregnancy (Guzman-Genuino et al. 2019). In humans, IL-10 producing B cells have also been found in the first trimester decidua and the frequencies of these IL-10 producing B cells are significantly higher in the decidua compared with peripheral samples (Benner et al. 2020). Additionally, an increase in the peripheral $CD24^{hi}CD27^+$ regulatory B cell frequency has been reported in first trimester pregnant women compared with non-pregnant subjects (Rolle et al. 2013). Such an increase was not observed in RPL and RIF patients, and RIF patients actually had decreased IL10 producing B cells (Rolle et al. 2013, Koushaeian et al. 2019, Guzman-Genuino and Diener 2017). Moreover, a decreased frequency of peripheral $CD24^{hi}CD38^{hi}$ regulatory B cells is observed in late pregnancy compared with non-pregnant women (Lima et al. 2016). In the human endometrium there are no published data regarding the frequency of regulatory B cells, or the IL-10 production capacity of endometrial B cells.

5.1.2.3 Naïve B cells

Before antigen exposure, B cells are naïve cells that co-express IgM and IgD on their surface. Naïve B cells also express moderate level of CD38 and CD24, comprising about 60–70% of all B cells in peripheral blood (Perez-Andres et al. 2010, Kaminski et al. 2012, Clavarino et al. 2016). During late gestation, the percentages of peripheral IgD^+CD38^+ naïve B cells are significantly higher compared with non-pregnant and post-partum women (Lima et al. 2016). In human endometrium, single-cell analysis of luteal phase endometrium identified a naïve B cell population in four out of six samples, which were no more than 2% of the total endometrial cell population. Compared with monocytes, macrophage/dendritic cells and NK cells, naïve B cells have a higher expression level of *CD19*, *CD20*, *CD79A*, *LY9*, *CD83*, *BTG1*, *CXCR4* and a moderate level of *CD74* and *HLA-DRA* (Lucas et al. 2020). However, the frequencies of naïve B cells in human endometrium has not yet been characterised.

5.1.2.4 GC B cells

GC B cells are a subset of B cells that have been activated by antigens and migrate to the GC to undergo GC responses. As shown in Figure 5.2, GCs are divided into two distinct compartments known as the dark zone and the light zone. In the dark zone, GC B cells are rapidly dividing B cells that undergo SHM and CSR, allowing B cells to diversify their BCR repertoire, thereby acquiring the capacity to bind to a wider range of antigens. Next, GC B cells migrate to the light zone, where B cells that have successfully gained mutations that confer a higher affinity surface antibody are selected. These GC B cells later develop into plasma cells or memory B cells and exit the GC. Lower affinity B cells re-enter into the dark zone for SHM in order to improve affinity towards the antigen (Niessl and Kaufmann 2018, Stebegg et al. 2018, King 2011).

A number of surface markers have been proposed to identify different stages of GC B cells, positive GC B cell markers include CD10, CD71, CD77, FAS (CD95), *etc.* (Kolar et al. 2007, Hao et al. 2008, Victora et al. 2012). FAS is highly expressed in GC B cells and is required for clonal selection of GC B cells as well as the subsequent establishment of the memory B cell repertoire. Additionally, FAS-FAS ligand signaling plays a key role in maintaining immune cell homeostasis as well as being involved with the pathogenesis of autoimmunity (Hueber and Koncz 2012, Victora et al. 2012, Siegel et al. 2000). In terms of surface immunoglobulin, IgD expression is downregulated when naïve B cells are activated and become GC B cells, therefore IgD has been used as a negative marker for GC B cells (Sabouri et al. 2016, Vinuesa et al. 2010). Apart from surface markers, the intracellular expression of the transcriptional repressor factor BCL6 has been described as the critical regulator of GCs (Basso and Dalla-Favera 2010). During B cell development, BCL6 expression is restricted to GC B cells and BCL6 knockout mice are characterised by the inability to form GCs and the lack of high-affinity antibody production (Fukuda et al. 1997). In the human endometrium, the BCL6 protein level is significantly higher in RPL and patients with unexplained infertility. However, BCL6 expression levels in endometrial B cells have not been assessed (Almquist et al. 2017, Fox et al. 2020).

Apart from GC B cells, a productive GC response also requires the involvement of multiple cell types including follicular dendritic cell, follicular T regulatory cell and T follicular helper cell (Tfh cells) (Figure 5.2). Tfh cells are mainly found in the GC light zone, and by interacting with GC B cells migrated from the dark zone, they are essential in B cell affinity maturation, and the development of high affinity antibodies and the generation of memory B cells (Crotty 2014, King 2011, Crotty 2011). Tfh cells can be identified by high surface expression of PD1, ICOS and CXCR5 (Shekhar and Yang 2012, Moser 2015, Crotty 2011). Additionally, intracellular BCL6 is also highly expressed by Tfh cells, and can help to control inflammation and autoimmunity by directly regulating the function and differentiation of Tfh cells (Crotty 2014, Shekhar and Yang 2012, Crotty 2011). To date, no attempt has been made to identify GC B cells and Tfh cells in the human endometrium, despite the existence of endometrial LAs that resembles TLSs with GC structures (as discussed in Chapter 3).

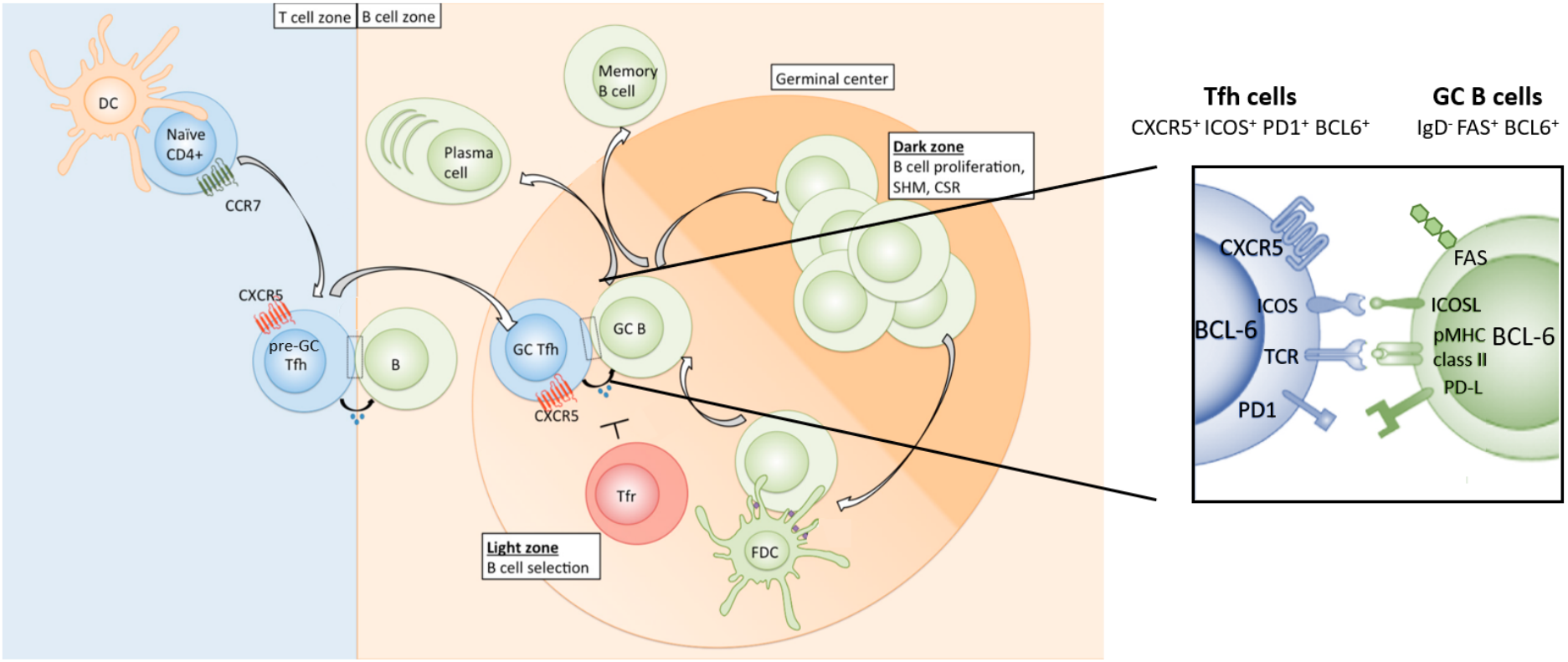

Figure 5.2: Overview of GC reactions and the phenotypic features of GC B cells and Tfh cells. In GCs, GC B cells undergo somatic hypermutation (SHM) and class switch recombination (CSR), and could later develop into plasma cells or memory B cells that exit the GC. Apart from GC B cells, a productive GC response also requires the involvement of multiple cell types including follicular dendritic cell (FDC), follicular T regulatory cell (Tfr) and T follicular helper cell (Tfh). The phenotypic features of GC B cells and Tfh cells are shown. Figure is adapted from (Niessl and Kaufmann 2018, King 2011).

5.1.2.5 Memory B cells

Identified by CD27 expression, memory B cells represent around 20-30% of all peripheral B cells (Perez-Andres et al. 2010, Sims et al. 2005, Agematsu et al. 2000). Memory B cells play a key role in the secondary immune response as they are able to generate an accelerated and robust antibody-mediated immune response in re-infection (Akkaya et al. 2020). In decidual tissues, $CD27^+$ memory B cells typically represent $> 20\%$ of all B cells in the first and second trimester, and $>40\%$ at term. This increased frequencies of memory B cells indicates pregnancy is accompanied by a gain in decidual B cell memory (Benner et al. 2020). However, the frequencies of memory B cells in the human endometrium have not yet been characterised.

5.1.2.6 Plasmablasts and plasma cells

Typically identified by $CD19^+CD24^-CD38^{hi}$, plasmablasts are a short-lived B cell differential stage after the GC reaction but before the generation of plasma cells. Plasmablasts can also be induced from activated B cells before entering into GCs (Nera et al. 2015, Balagué and Martínez 2015, Lin et al. 2017) (Figure 5.1). Compared with plasma cells, plasmablasts are capable of proliferation and antigen presentation. Plasma cells, on the other hand, are terminally differentiated B cells capable of secreting large quantities of antibodies in response to activation by antigens. Plasma cells express surface CD138, but decrease the expression of the pan-B cells markers CD19 and CD20 (O'Connell et al. 2004, Clavarino et al. 2016, Kaminski et al. 2012). The frequencies of plasma cells have been investigated by IHC studying CD138 expression in the endometrium of healthy women and patients with reproductive pathologies (see Chapter 3). However, these studies might be flawed considering CD138 is also constitutively expressed on endometrial epithelial cells (Inki 1997, Kind et al. 2019, Moreno and Simon 2019). To date, the frequency of plasmablast and plasma cells have never been investigated in the human endometrium by flow cytometry.

5.1.3 Endometrial B cells

The frequencies of B cells have been studied in the endometrium of healthy women and patients with reproductive pathologies (Chapter 3). However, evidence for endometrial B cell subsets, phenotype and cytokine production are very limited. To better understand the role of B cells in the endometrial immune environment, we need to first understand what B cell subsets are in the human endometrium and whether endometrial B cells are phenotypically different from peripheral B cells. RNA-seq analysis of endometrial B cells showed that B cells have an activated gene expression profile with the high expression of MHC related genes such as *CD74*, *CD83* and *HLA-DR* (Chapter 4) This data provided a starting point for endometrial B cell profiling. Additionally, it is unknown if endometrial B cells are tissue resident or infiltrating; tissue resident marker such as CD69 (Chapter 2.1.4) and CD62L could be used to investigate B cell tissue residency. CD62L is a homing receptor for lymphocytes and the decrease in its expression level has been associated with B cell migration from peripheral circulation to specific tissues (Pattanapanyasat et al. 2018, Morrison et al. 2010),

Apart from phenotypic studies, research into the cytokine production capability of endometrial B cells would also help us to better understand the role of B cells in human endometrium. Considering the emerging concept of regulatory B cell involvement in pregnancy, I investigated the endometrial B cells ability to produce IL-10 and TGF-β.

5.2 Chapter Aims

This chapter presents flow cytometric analysis of endometrial B cell subsets, detailing their phenotypes and cytokine production capabilities. To achieve this, both peripheral blood and endometrial samples were collected from women during their mid-luteal phase of the menstrual cycle, and were processed to obtain single cell digests. Flow cytometric analysis was performed to identify endometrial B cell subsets, the phenotypic differences between endometrial and circulating B cells, and the IL-10 and TGF-β expression levels of stimulated B cells. Additionally, a flow cytometric panel was devised to identify if Tfh cells are present in the endometrium.

Objectives:

1) To determine the B cell subsets present in the endometrium by analysis of common B cell marker expression.

2) To compare the phenotypic differences between endometrial and circulating B cells, specifically focusing on tissue resident markers as well as the top expressed genes that were identified in Chapter 4.

3) To identify if GC B cells and Tfh cells are present in the human endometrium.

4) To investigate whether peripheral versus endometrial B cells express IL-10 and TGF-β after stimulation.

5) To identify if B regulatory cell subsets are present in the endometrium, and to determine whether IL-10 expression is enriched in B regulatory cell subsets.

5.3 Materials and Methods

5.3.0.1 Subject recruitment

All recruits were patients attending Wolfson Fertility Centre, Oxford Fertility or John Radcliffe Hospital Recurrent Miscarriage Clinic from 2018 to 2020. Peripheral blood and/or endometrial samples were collected between 7–11 days post LH pre-ovulatory surge, in the menstrual cycle before IVF commenced. All women had negative antiphospholipid screen (cardiolipin Ab, anti-beta-2 glycoprotein and DRVVT), thrombophilia screening (including Factor V Leiden, prothrombin gene mutation, antithrombin III, protein C, protein S) and normal uterine structure (identified by ultrasound scan or hysteroscopy).

For endometrial B cell subset analysis, 7 endometrial samples were obtained. Patient details are shown in Table 5.1.

For endometrial B cell residency and activation profile analysis, 6 matched peripheral blood and endometrial samples were obtained. Patient details are shown in Table 5.2.

For the identification of endometrial Tfh cells and GC B cells, 6 endometrial samples were obtained. Patient details are shown in Table 5.3.

To assess B cell IL-10 and TGF-β production capabilities, 3 matched peripheral blood and endometrial samples were obtained. Patient details are shown in Table 5.4.

Sample	Age	BMI	No. of Miscarriages	No. of Ectopic Pregnancy	No. of Previous Live Birth
A	37	21.9	0	0	0
B	37	-	7	-	0
C	40	-	0	0	$\geq$1
D	35	-	1	0	$\geq$1
E	35	-	0	0	$\geq$1
F	38	-	0	0	0
G	38	21	0	0	0
mean $\pm$ SD	36.1 $\pm$ 3.2	-	1.1 $\pm$ 2.6	-	-

Table 5.1: Clinical characteristics of patients recruited for endometrial B cell subsets analysis. Mean $\pm$ SD values for each patient are shown.

Sample	Age	BMI	No. of Miscarriages	No. of Ectopic Pregnancy	No. of Previous Live Birth
A	31	27.6	0	0	0
B	35	21.5	0	0	0
C	37	21.9	0	0	0
D	38	-	4	-	1
E	33	-	3	0	0
F	32		3	0	0
mean $\pm$ SD	34.3 $\pm$ 2.6	-	1.7 $\pm$ 1.7	-	0.2 $\pm$ 0.4

Table 5.2: Clinical characteristics of patients recruited for endometrial B cell residency and activation profile analysis. Mean $\pm$ SD values for each patient are shown.

Sample	Age	BMI	No. of Miscarriages	No. of Ectopic Pregnancy	No. of Previous Live Birth
A	40	25.4	0	0	0
B	34	-	0	0	0
C	38	21.1	0	0	0
D	42	-	1	0	$\geq$1
E	35	-	1	0	$\geq$1
F	34	-	3	-	$\geq$1
mean $\pm$ SD	37.2 $\pm$ 3.4	-	0.8 $\pm$ 1.2	-	-

Table 5.3: Clinical characteristics of patients recruited for endometrial B cells and Tfh cells identification. Mean $\pm$ SD values for each patient are shown.

Sample	Age	BMI	No. of Miscarriages	No. of Ectopic Pregnancy	No. of Previous Live Birth
A	40	25.4	0	0	0
B	36	28.3	0	1	0
C	37	26.4	0	0	0
mean $\pm$ SD	38 $\pm$ 2	26.7 $\pm$ 1.2	0 $\pm$ 0	0.3 $\pm$ 0.5	0 $\pm$ 0

Table 5.4: Clinical characteristics of patients recruited for endometrial B cells IL-10 and TGF-β production analysis. Mean $\pm$ SD values for each patient are shown.

5.3.0.2 Sample processing

For peripheral blood samples, PBMCs were isolated according to the method described in Chapter 2.3.2. For endometrial biopsies, single cell digests were obtained either by mechanically digestion (for the identification of Tfh and GC B cells), or according to the

method described in Chapter 2.3.3 (for the analysis of B cell subsets, B cell residency and activation profile and the IL-10 and TGFβ production capabilities). In mechanical digestion, endometrial biopsies were cut into 1mm^3 fragments and transferred to 10ml Digestion Medium (Dulbecco's Modified Eagle's Medium + 10% Fetal bovine serum) with 100 μg/ml DNase I. Then, endometrial tissues were mechanically digested by grinding, the digests were passed through sequential 70 μm and 40 μm cell strainers. All the run-though was collected and centrifuged for 10 minutes at 300 x g. Supernatant was aspirated and cell pellet was re-suspended in 1 ml PBS. Cell counting was performed using a hemocytometer. All PBMCs samples and endometrial single-cell digests were stored in liquid nitrogen until further use.

After all samples were collected and processed, cells were thawed by placing the cryovials into a 37°C water bath. When the cells were almost thawed, the content was transferred to a 15ml falcon tube containing 9ml Dulbecco's Modified Eagle's Medium + 10% Fetal bovine serum. Falcon tubes were centrifuged for 5 minutes at 300 x g. All the supernatant was aspirated and cell pellets were re-suspended in 1 ml PBS.

5.3.0.3 Heatmap analysis of endometrial B cell RNA-seq data

Heatmaps of endometrial B cell genes expression levels were generated according to methods and materials described in Chapter 4.3.

5.3.0.4 Cell sorting

For analysis of endometrial B cell IL-10 and TGFβ production, cell sorting was performed according to the method described in Chapter 4.3.2.2.

5.3.0.5 B cell stimulation assay

After cell sorting, CD19$^+$ B cells were placed in a 96 well U bottom plate (Eppendorf, Germany) with 100 μl Culture Medium (RPMI 1640 Medium + 10% Fetal bovine serum + 1% human serum + 1% penicillin-streptomycin) overnight. Cell numbers in each well

did not exceed 5000. After overnight culture, cells were treated with 1 mg/ml PMA + 1 mg/ml LPS + 1mM ionomycin in 100 μl Culture Medium in a 96 well U bottom plate for 43 hours. Non stimulated controls were also established. Brefeldin A (Biolegend, USA) was added to the 96 well plate with 1 in 1000 dilution. After 5 hours of incubation, the 96 well plate was centrifuged at 300 x g for 2 mins. All the supernatant was aspirated and the cell pellet was re-suspended in 100 μl PBS for flow cytometric staining.

5.3.0.6 Flow cytometry analysis

PBMCs and/or endometrial cells were stained for flow cytometry analysis after they were thawed and re-suspended in PBS. Fc receptors were blocked using FcR Blocking Reagent (Miltenyi, Germany).

For endometrial B cell subset analysis, a 10-colour panel shown in Table 5.5 was used. This flow panel will be referred as "B cell subset analysis flow panel" in the following sections.

For endometrial B cell residency and activation profile analysis, an 8-colour panel shown in Table 5.6 was used in the B cell residency and activation profile analysis. This flow panel will be referred as "B cell residency and activation flow panel" in the following sections.

For the identification of endometrial Tfh and GC B cells, a 12-colour panel shown in Table 5.7 was used. All reagents, apart from BV785 CD69, were included in the staining of all six endometrial samples, BV785 CD69 was included in the staining for three endometrial samples. BCL6 intracellular staining was performed using Cytofix/Cytoperm Kit (BD, USA) according to the manufacturer's protocol after incubation with the cell surface markers. This 12-colour flow panel will be referred as "Tfh and GC B cell flow panel" in the following sections.

To assess B cell phenotypes and their IL-10 and TGF-β secreting capabilities, an 8-colour panel shown in Table 5.8 was used. IL-10 and TGF-β intracellular staining was performed using Cytofix/Cytoperm Kit (BD, USA) according to the manufacturer's

protocol after incubation with the cell surface markers. This 8-colour flow panel will be referred as "IL-10 and TGF-β flow panel" in the following sections. After staining and flow acquisition, flow data was analysed using FlowJo v10.

Reagents	Clone	Fluorophore	Concentration (μg/ml)
anti-CD45	HI30	BV650™	0.5
anti-CD19	HIB19	FITC	4
anti-CD27	O323	PE/DAZZLE™ 594	5
anti-CD38	HB-7	PE	4.5
anti-CD24	ML5	APC	4
anti-CD138	MI15	BV711™	5
anti-IgM	MHM-88	PE/Cy7	3
anti-IgG	M1310G05	BV421™	3.5
anti-IgA	REA1014	APC-Vio 770	1 : 50
Zombie Aqua™	-	BV510™	0.1μl/ 2 x 10^6 cells

Table 5.5: 10-colour flow cytometry panel for endometrial B cell subset analysis. anti-IgA is from Miltenyi Biotec, Germany. All others reagents are from Biolegend, USA.

Reagents	Clone	Fluorophore	Concentration (μg/ml)
anti-CD45	HI30	Alexa Fluor 700	4
anti-CD83	HB15e	BV785™	3
anti-CD74	LN2	PE	4
anti-HLA-DR	L243	APC	4.5
anti-CD69	FN50	BV711™	2.5
anti-CD19	HIB19	PE/Cy7	4
anti-CD62L	DREG-56	BV650™	3
Zombie Aqua™	-	BV510™	0.1μl/ 2 x 10^6 cells

Table 5.6: 8-colour flow cytometry panel for endometrial B cell residency and activation analysis. All reagents are from Biolegend, USA.

Reagents	Clone	Fluorophore	Concentration (μg/ml)
anti-CD45	HI30	Alexa Fluor 700	4
anti-CD19	HIB19	PE/Cy7	4
anti-CD3	UCHT1	APC/Fire™ 750	12
anti-CD4	OKT4	FITC	16
anti-ICOS	C398.4A	BV650™	7.5
anti-CXCR5	J252D4	BV421™	5
anti-PD1	EH12.2H7	APC	4
anti-BCL6	IG191E/A8	PE	5
anti-IgD	IA6-2	PE/DAZZLE™ 594	3.5
anti-FAS	DX2	BV711™	4.5
anti-CD69		BV785™	3
Zombie Aqua™	-	BV510™	0.1μl/ 2 x 10^6 cells

Table 5.7: 12-colour flow cytometry panel for TFH and GC B cells identification. All reagents are from Biolegend, USA.

Reagents	Clone	Fluorophore	Concentration (μg/ml)
anti-CD45	HI30	BV650™	0.5
anti-CD19	HIB19	PE/Cy7	4
anti-CD27	O323	BV785™	12
anti-CD38	HB-7	APC/Fire™ 750	4
anti-CD24	ML5	BV421™	5
anti-IL10	JES3-9D7	Alexa Fluor 488	5
anti-TGFβ	TW4-6H10	APC	5
Zombie Aqua™	-	BV510™	0.1μl/ 2 x 10^6 cells

Table 5.8: 8-colour flow cytometry panel assessing B cell phenotype and their IL-10 and TGF-β production capacity. All reagents are from Biolegend, USA.

5.3.0.7 Statistical analysis

Statistical analysis was performed using GraphPad Prism 7.03. Normality of the data were confirmed again using Shapiro-Wilk tests. Parametric data were then analysed using paired Student's t-test. Data were represented as mean $\pm$ SD. Differences were considered significant if $p < 0.05$.

5.4 Results

5.4.1 endometrial B cell subset analysis

Despite clear evidence of the presence of B cells in human endometrium (Chapter 2) and evidence that endometrial B cells may be implicated in various reproductive pathologies (Chapter 3), which B cell subsets are present in human endometrium has not been investigated. Data generated from the RNA-seq study (Chapter 4) revealed the expression levels of various B cell markers in the endometrium. As shown in Figure 5.3(a), high levels of pan-B cell markers *CD19* and *CD20* expression, moderate levels of *CD24*, *CD38* and *CD27* expression were observed in all 15 endometrial B cell samples, while the expression level of *CD138* was close to 0 in most samples. For *IGH* genes, the expression level of *IGHM* was higher than *IGHG*, *IGHA*, *IGHD* and *IGHE* in most samples (Figure 5.3(b)).

However, bulk RNA-seq analysis could only offer an overview of B cell markers expression levels in all B cells, nor a direct indication of which B cell subsets are present in the human endometrium. To achieve that, single cell suspensions of endometrial samples were stained with the "B cell subset analysis flow panel" (Table 5.5). As shown in Figure 5.4, the flow cytometric analysis showed a similar B cell profile to the RNA-seq data. Flow cytometry demonstrated that the majority (around 72%) of endometrial B cells were $IgM^{+}IgG^{-}IgA^{-}$ and thus naïve B cells, 9% and 7% of all endometrial B cells were $IgM^{-}IgG^{+}$ and $IgM^{-}IgA^{+}$ respectively. Around 30% of all endometrial B cells were $CD27^{+}$ and therefore designated memory B cells, $CD138^{+}$ plasmablasts were scarce ($<$ 2%) in most endometrial B cell samples. In addition, around 2% of all endometrial B cells were $CD24^{hi}CD38^{hi}$, indicating transitional B cells in the endometrial compartment.

The proportional distribution of endometrial B cell subsets is similar to that in the peripheral B cells. In peripheral blood, naïve B cells comprise about 60–70% of all B cells, memory B cells account for 20-30% of all B cells, and transitional B cells typically account for 2-4% of all B cells (Perez-Andres et al. 2010, Sims et al. 2005, Kaminski

et al. 2012, Clavarino et al. 2016).

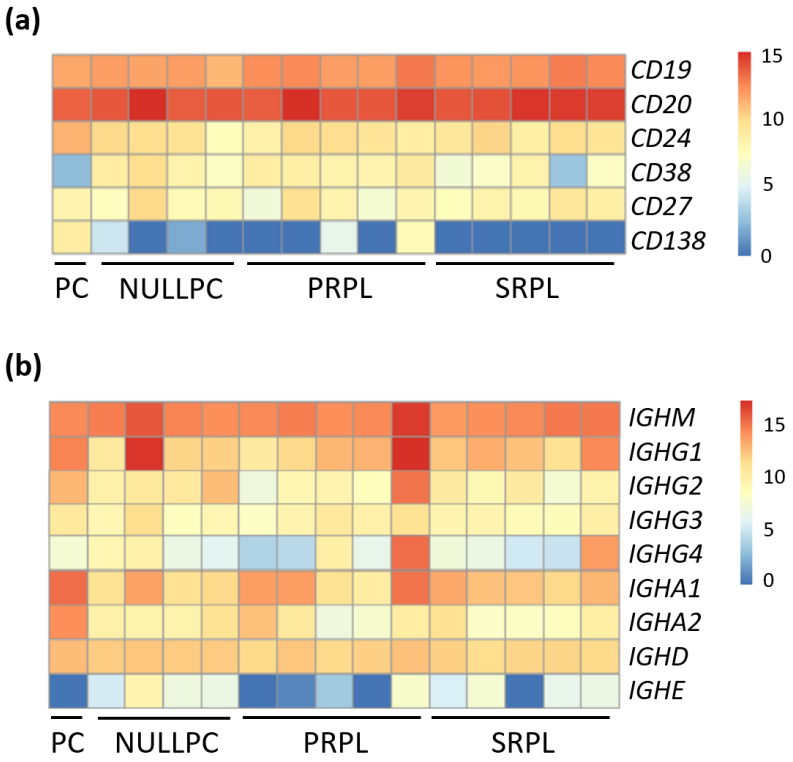

Figure 5.3: Heatmaps of endometrial B cell markers genes expression levels. B cell RNA was extracted from the sorted endometrial B cells, data was generated by RNA-seq, followed by DESeq2 analysis. Marker genes were selected according to key B cell markers presented in Figure 5.1. (a) The expression levels of 5 endometrial B cells markers used in the B cell subset analysis panel. (b) The expression levels of IGH genes. PC, parous control; NULLPC, nulliparous control; PRPL, primary recurrent pregnancy loss; SRPL, secondary recurrent pregnancy loss. n = 15.

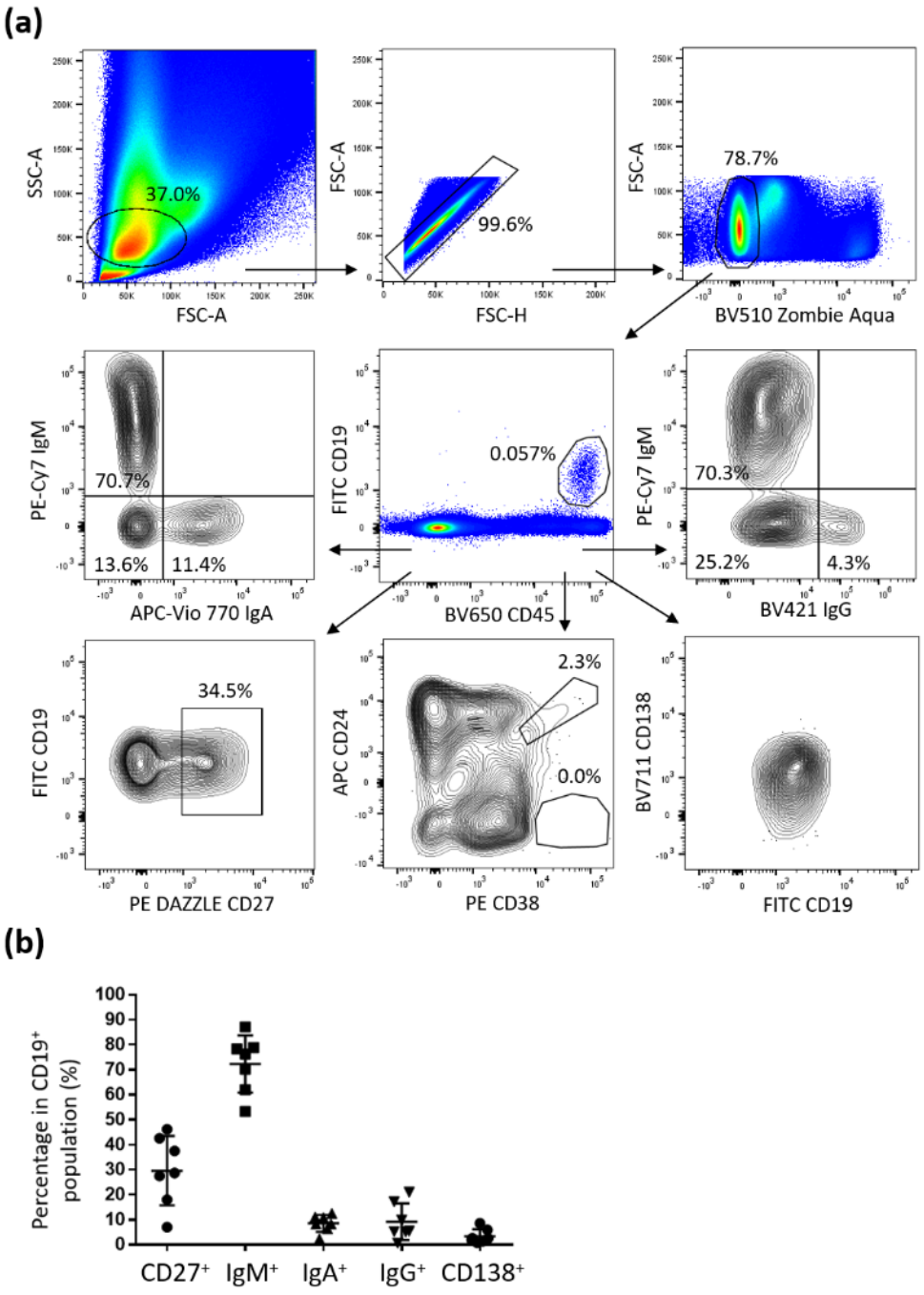

Figure 5.4: Flow cytometry analysis of endometrial B cell phenotype. Endometrial cells were isolated by Collagenase D treatment. Staining on endometrial B cells was undertaken using the "B cell subset analysis flow panel" (Table 5.5). (a) Representative figures of gating strategies for endometrial B cells. (b) Scatter plot of the expression levels of 5 endometrial B cell markers used in the flow analysis. Error bars represent mean $\pm$ SD. n $= 7$

5.4.2 Endometrial B cell residency, assessed by CD69 and CD62L expression levels

To determine whether endometrial B cells are tissue resident B cells, endometrial samples were digested with collagenase D and stained with "B cell residency and activation flow panel" (Table 5.6). Shown in Figure 5.5, there was a significant increase in CD69 expression in endometrial B cells compared with peripheral B cells ($p < 0.001$), when analysing both CD69 MFI and the percentage of $CD69^+$ B cells. While for CD62L, there was no significant difference in the expression level between endometrial B cells and peripheral B cells. Additionally, to ensure collagenase D digestion would not influence the detection of CD69 and CD62L on endometrial B cells, mechanical digestion was also performed on endometrial samples. There was no significant difference in CD69 and CD62L MFI in mechanically digested samples compared with collagenase D digested samples (data not shown). Negative controls for CD69 and CD62L staining are shown in Appendix D.

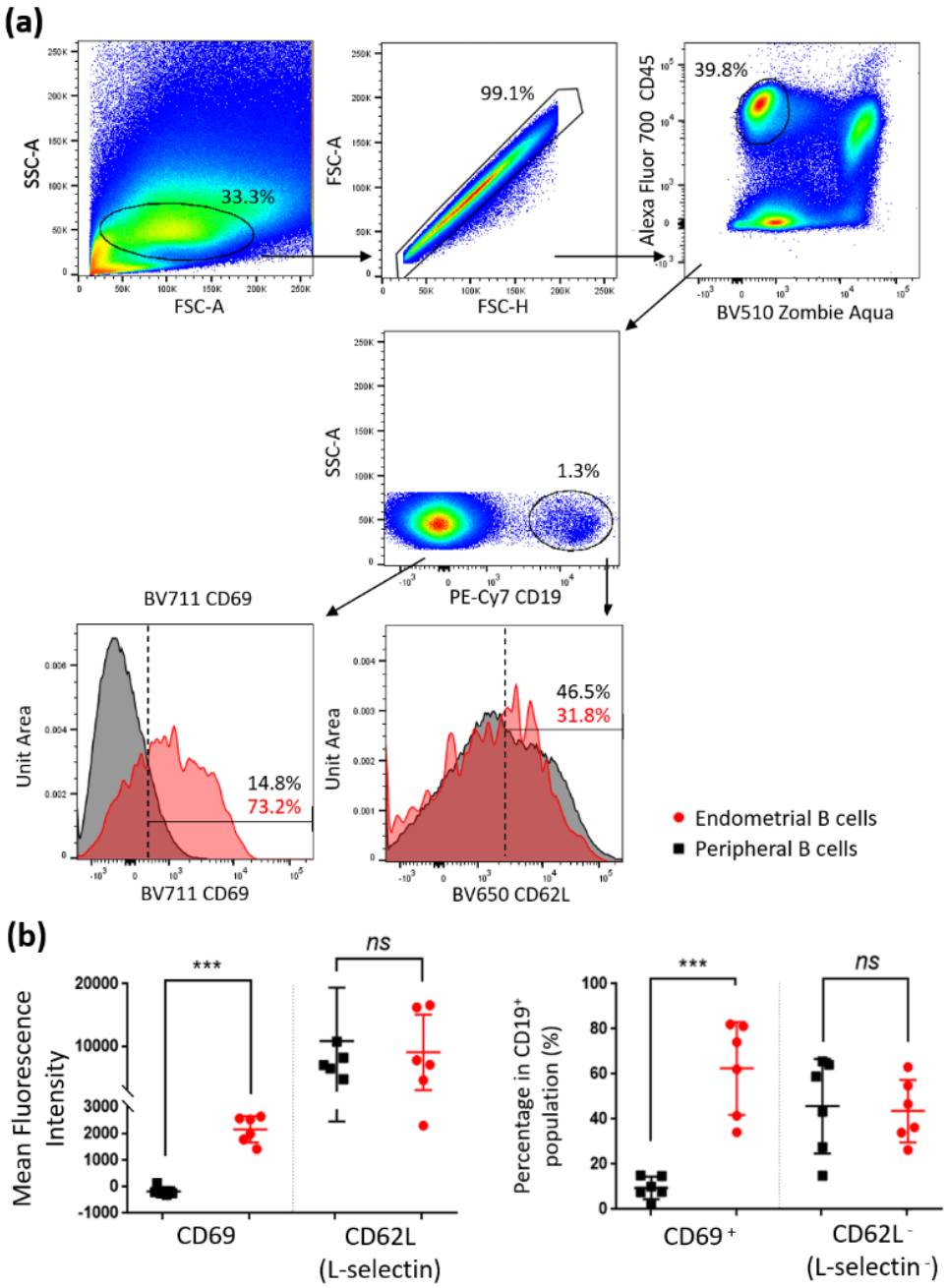

Figure 5.5: Flow cytometric analysis of endometrial B cell residency, assessed by CD69 and CD62L expression levels. Matched peripheral blood and endometrial samples were collected during the mid-luteal phase. PBMCs were isolated by Lymphoprep^{TM}, endometrium samples were digested by Collagenase D. Flow cytometric staining was undertaken using the "B cell residency and activation flow panel" (Table 5.6). (a) Representative figures of gating strategies for endometrial B cells, and representative histograms of CD69 and CD62L. (b) Scatter plots of CD69 and CD62L expression in endometrial B cells and peripheral blood B cells, MFI as well as the percentages of $CD69^{+}$ or $CD62L^{-}$ B cells were shown. Statistical analysis: paired t-test was performed between endometrial B cells and peripheral B cells. $\star\star\star$ $p \leq 0.001$. Error bars represent mean $\pm$ SD. $n = 6$.

5.4.3 The activation status of endometrial B cells, assessed by CD74, CD83 and HLA-DR expression levels

As discussed in Chapter 4.5.1, B cell RNA-seq data showed endometrial B cells have an activated gene expression profile, with *CD74*, *CD83* and *HLA-DR* highly expressed in all 15 endometrial B cell samples (Figure 4.12). To validate this activated gene expression profile in endometrial B cells, matched peripheral and endometrial B cell samples were collected during the mid-luteal phase. PBMCs were isolated by Lymphoprep^{TM}, endometrium samples were digested by Collagenase D. Matched samples were stained with the "B cell residency and activation flow panel" (Table 5.6). Shown in Figure 5.6, there was a significant increase in CD74, CD83 and HLA-DR expression in endometrial B cells compared with peripheral B cells ($p< 0.01$, $p< 0.05$, $p< 0.05$ respectively), in terms of their MFI as well as the percentages of $CD74^+$, $CD83^+$ or $HLA-DR^+$ B cells.

Additionally, to ensure collagenase D digestion would not influence the detection of CD74, CD83 and HLA-DR on endometrial B cells, mechanical digestion was also performed on endometrial samples. There was no significant difference in CD74, CD83 and HLA-DR MFI in mechanically digested samples compared with collagenase D digested samples (data not shown). Negative controls for CD74, CD83 and HLA-DR staining are shown in Appendix D.

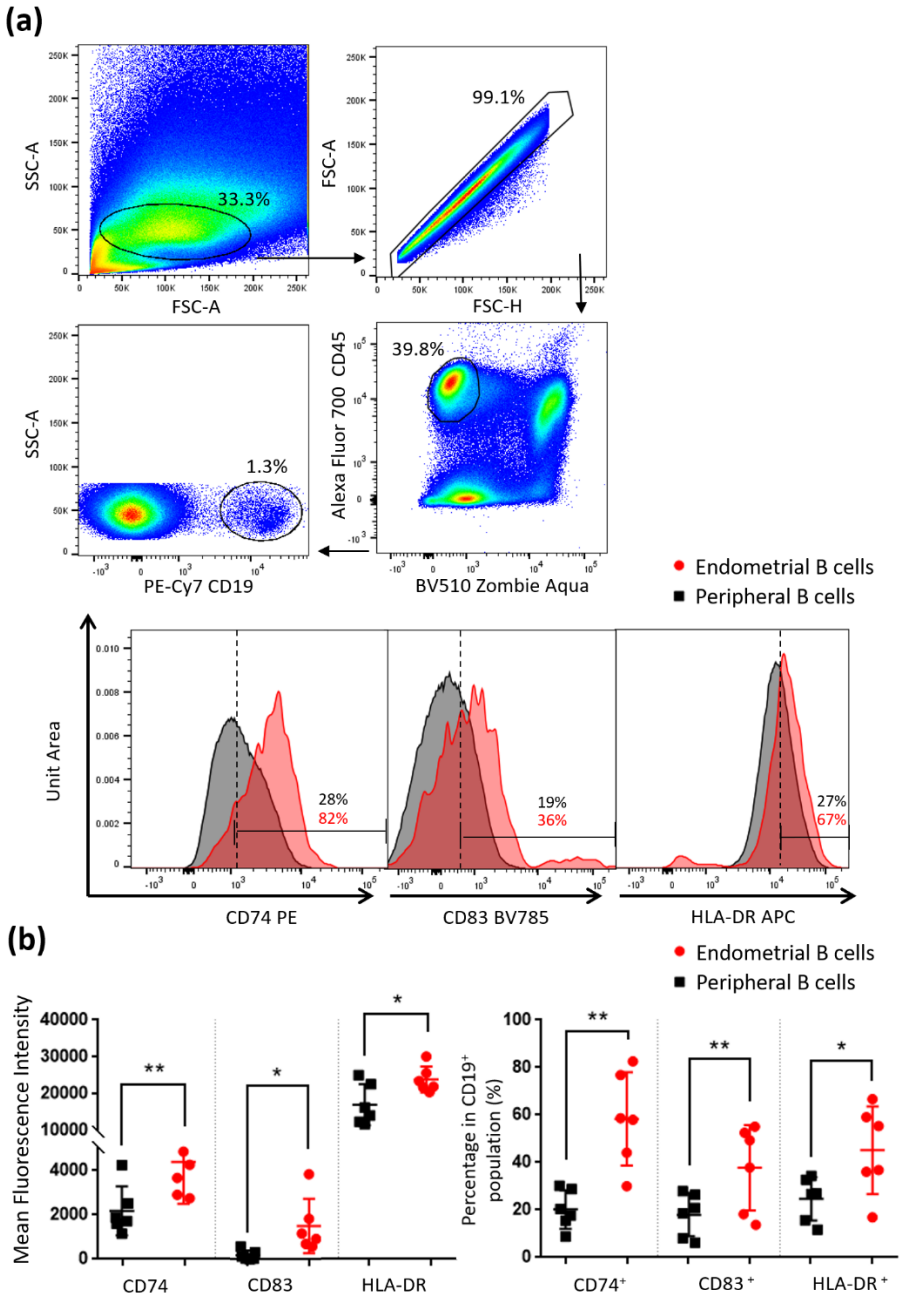

Figure 5.6: Flow cytometric analysis of the activation profile of endometrial B cells, assessed by CD74, CD83 and HLA-DR expression levels. Matched peripheral blood and endometrial samples were collected during the mid-luteal phase. PBMCs were isolated by Lymphoprep^{TM}, endometrium samples were digested by Collagenase D. Flow cytometric staining was undertaken using the "B cell residency and activation flow panel" (Table 5.6). (a) Representative figures of gating strategies for endometrial B cells, and representative histograms of CD74, CD83 and HLA-DR expression. (b) Scatter plots of CD74, CD83 and HLA-DR expression in endometrial B cells and peripheral blood B cells, MFI as well as the percentages of $CD74^{+}$, $CD83^{+}$, or $HLA-DR^{+}$ B cells are shown. Statistical analysis: paired t-test was performed between endometrial B cells and peripheral B cells. $\star$ $p \leq 0.05$. $\star\star$ $p \leq 0.01$. $\star\star\star$ $p \leq 0.001$. Error bars represent mean $\pm$ SD. $n = 6$.

5.4.4 Identification of endometrial Tfh cells and GC B cells

Considering the functional importance of GCs in B cell development, and that other mucosal tissues can contain GC-like structures (Chapter 3.5.2), flow cytometry was performed to detect if Tfh or GC B cells are present in the endometrium. Endometrial samples were mechanically digested and stained with "Tfh and GC B cell flow panel" (Table 5.7).

5.4.4.1 Identification of GC B cells

FAS^+IgD^- GC B cells were found in all 6 endometrial samples, accounting for approximately 12.2% of all $CD19^+$ B cells (12.2% $\pm$ 8.6%, mean $\pm$ SD, n = 6). These GC B cells also had a significantly higher level of intracellular BCL6 expression compared with FAS^- B cells ($p \leq 0.01$, Figure 5.7). Additionally, FAS^+IgD^- GC B cells had a moderate level of CD69 expression (Figure 5.7(a)). Compared with FAS^- B cells, GC B cells had a higher level of CD69 (MFI) in all 3 samples examined, however, no significant difference was found between these two B cell subsets ($p = 0.07$, Figure 5.7(b)). Negative controls for FAS, IgD and BCL6 staining are shown in Appendix D.

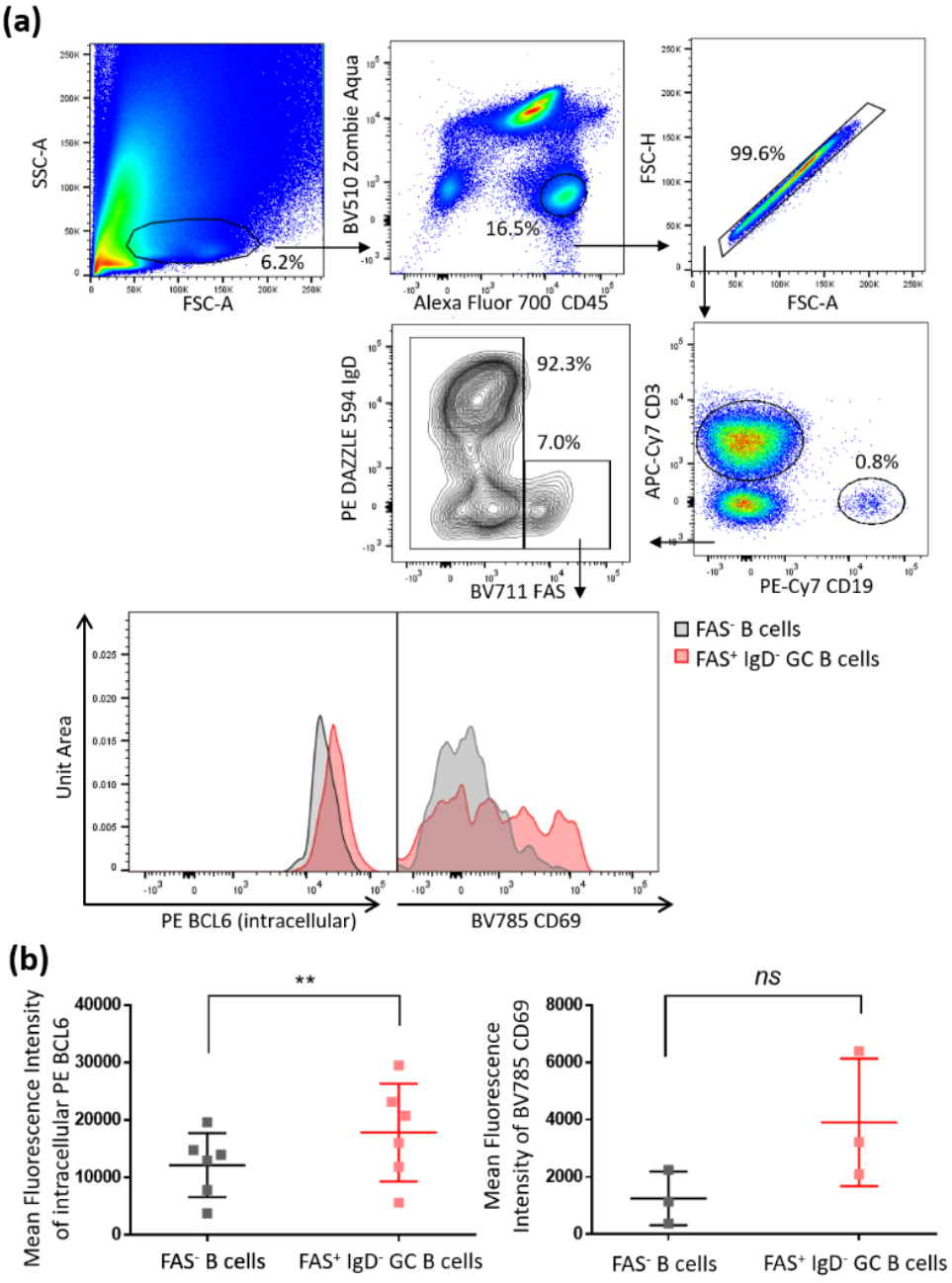

Figure 5.7: Flow cytometric identification of endometrial GC B cells. Endometrium samples were mechanically digested. Flow cytometric staining was undertaken using the "Tfh and GC B cell flow panel" (Table 5.7). (a) Representative figures of gating strategies for endometrial B cells, and representative histograms of BCL6 and CD69. (b) Scatter plots of BCL6 and CD69 MFI in $FAS^{+}IgD^{-}$ GC B cells and FAS^{-} B cells. Statistical analysis: paired t-test was performed between $FAS^{+}IgD^{-}$ GC B cells and FAS^{-} B cells. $\star\star$ $p \leq 0.01$. Error bars represent mean $\pm$ SD. n = 6 for BCL6 MFI, n = 3 for CD69 MFI. MFI, mean fluorescence intensity.

5.4.4.2 Identification of Tfh cells

$PD1^+ICOS^+CXCR5^+$ Tfh-like cells were found in all 6 endometrial samples, they accounted for approximately 4.1% of all $CD4^+$ T cells (4.1% $\pm$ 2.8%, mean $\pm$ SD, n = 6). However, these Tfh-like cells did not have a higher level of intracellular BCL6 expression compared with $PD1^-ICOS^-CD4^+$ T cells (p = 0.3, Figure 5.8). Additionally, the majority of $CD4^+$ T cells appear to be $CD69^+$ (Figure 5.8(a)), including $PD1^+ICOS^+CXCR5^+$ Tfh-like cells and $PD1^-ICOS^-CD4^+$ T cells. The frequency of $CD69^+CD4^+$ T cells is similar to data presented in Chapter 2.4.2.

Additionally, collagenase D digestion was shown to significantly decrease the CXCR5 MFI on $CD4^+$ T cells (data not shown), therefore all endometrial samples were mechanically digested for the identification of Tfh cells. Negative controls for PD1, ICOS, CXCR5 and BCL6 staining are shown in Appendix D.

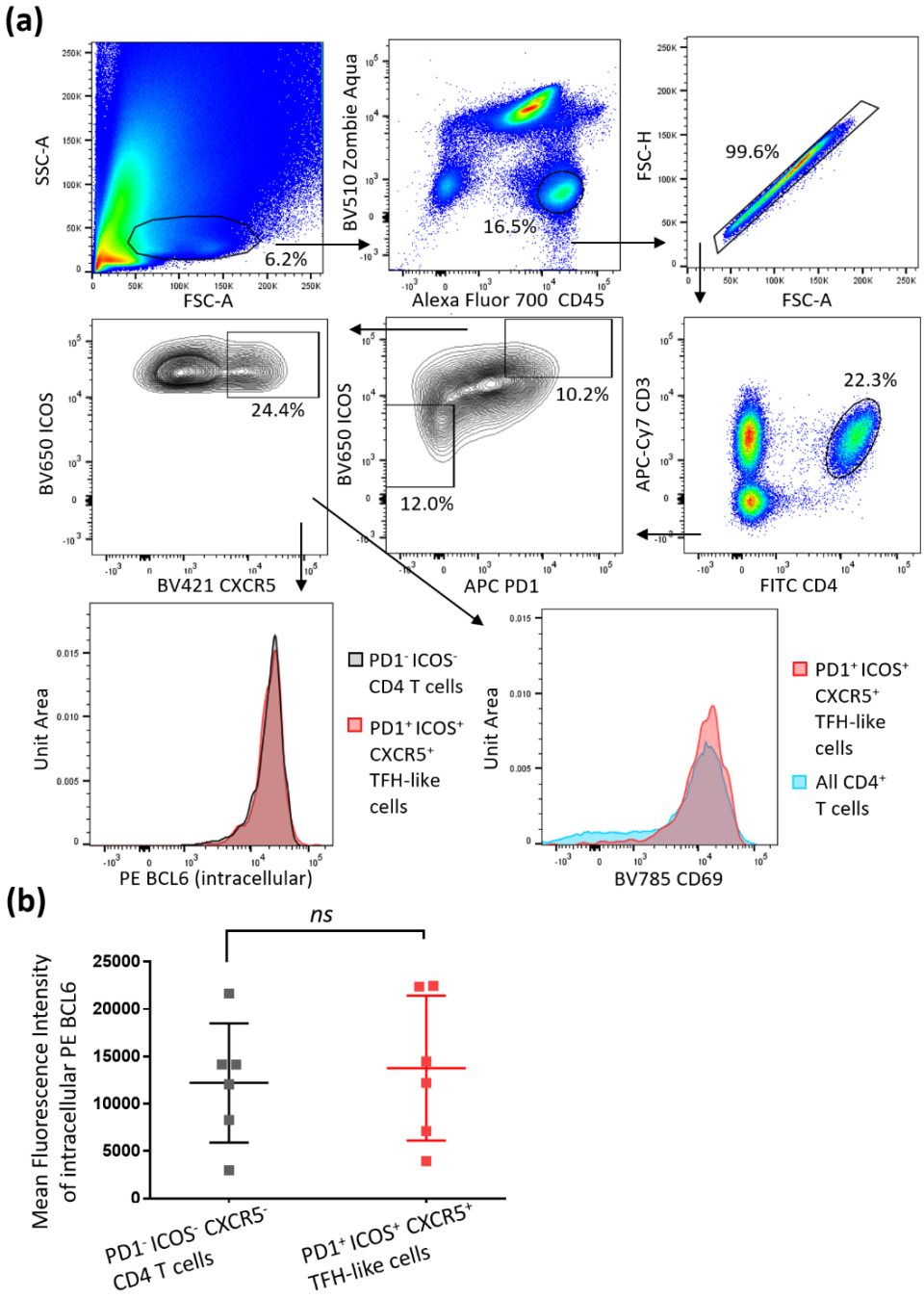

Figure 5.8: Flow cytometric identification of endometrial Tfh cells. Endometrium samples were mechanically digested. Flow cytometric staining was undertaken using the "Tfh and GC B cell flow panel" (Table 5.7). (a) Representative figures of gating strategies for endometrial Tfh cells, and representative histograms of BCL6 and CD69. (b) Scatter plots of BCL6 MFI in $PD1^{+}ICOS^{+}CXCR5^{+}$ Tfh-like cells and $PD1^{-}ICOS^{-}CD4^{+}$ T cells. Statistical analysis: paired t-test was performed between $PD1^{+}ICOS^{+}CXCR5^{+}$ Tfh-like cells and $PD1^{-}ICOS^{-}CD4^{+}$ T cells. Error bars represent mean $\pm$ SD. n $=$ 6. MFI, mean fluorescence intensity.

5.4.5 IL-10 and TGF-β production capabilities of peripheral and endometrial B cells

5.4.5.1 Cell sorting

Peripheral and endometrial $CD19^+$ B cells were obtained by flow cytometric cell sorting, a representative flow cytometry gating strategy is shown in Figure 5.9. Sorting purity was over 98% for all 6 samples (data not shown). A minimum of 68,000 $CD19^+$ B cells were obtained from PBMCs, and a minimum of 470 $CD19^+$ B cells were obtained from the endometrial samples. On average, $CD19^+$ B cells represented 7.2 $\pm$ 1.7% of all $CD45^+$ live single cells in the peripheral blood samples (mean $\pm$ SD, n = 3) , and 9.0 $\pm$ 4.9% in the endometrial samples (mean $\pm$ SD, n = 3).

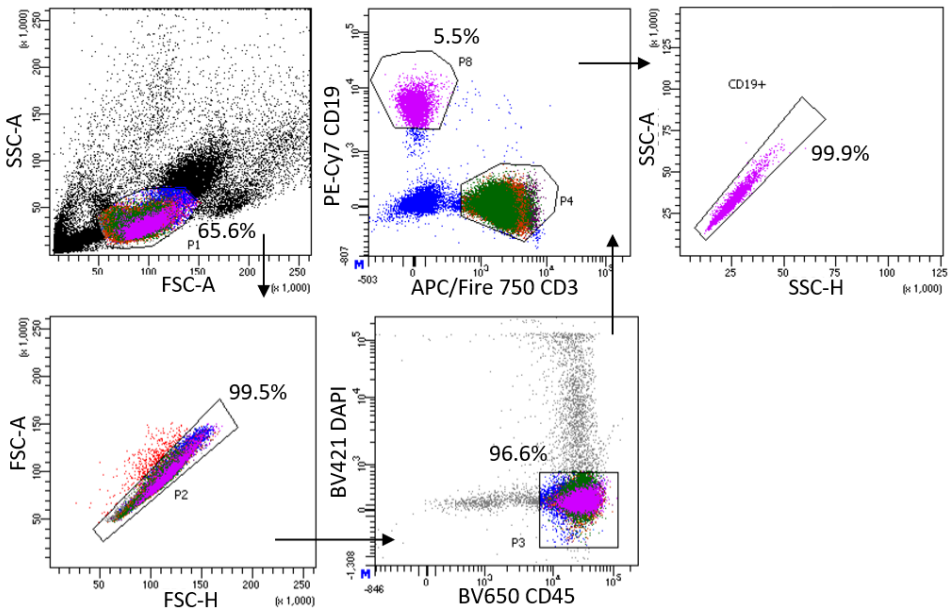

Figure 5.9: Representative figure of the gating strategy for peripheral and endometrial B cell sorting. $CD19^+$ B cells were obtained by cell sorting using an AriaIII (BD, USA) from PBMCs and endometrial biopsy digests.

5.4.5.2 IL-10 and TGF-β production capabilities of peripheral and endometrial B cells

To assess the IL-10 and TGF-β production capabilities of peripheral and endometrial B cells, $CD19^+$ B cells were either sorted and stimulated with PMS+LPS+ionomycin, or sorted and cultured without stimulation for 48 hours. The length of stimulation was optimized using sorted peripheral $CD19^+$ B cells for the optimal detection of intracellular IL-10 (data not shown). As shown in figure 5.10, all peripheral and endometrial $CD19^+$ B cells displayed a significantly higher level of IL-10 MFI after stimulation ($p \leq 0.05$). They also exhibited a higher level of TGF-β after stimulation, but no significant difference was observed between stimulated and unstimulated groups ($p = 0.1$). Additionally, the expression level of IL-10 and TGF-β was similar between peripheral and endometrial $CD19^+$ B cells after stimulation.

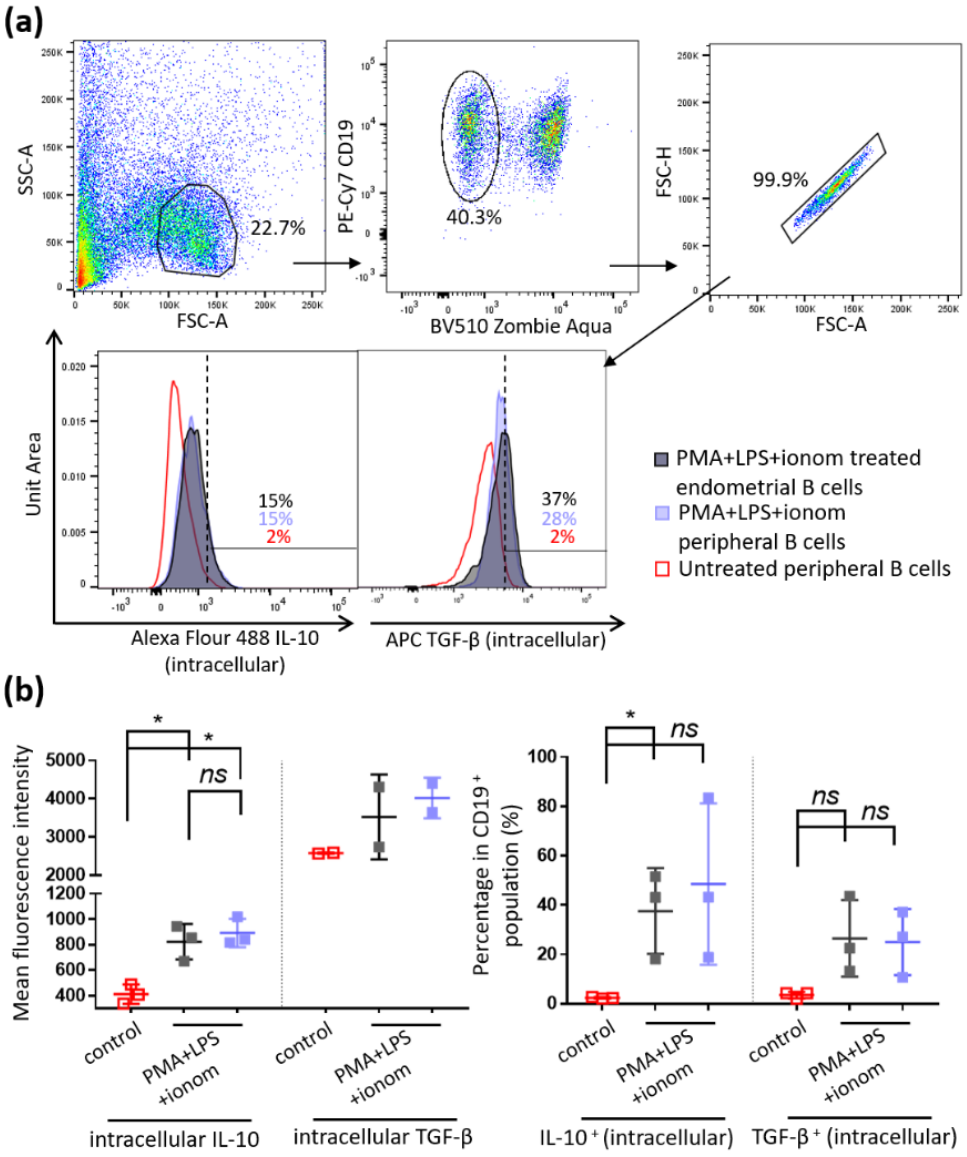

Figure 5.10: Flow cytometric analysis of IL-10 and TGF-β expression levels in peripheral and endometrial B cells after stimulation. Matched peripheral blood and endometrial samples were collected during the mid-luteal phase. PBMCs were isolated by Lymphoprep^{TM}, endometrium samples were digested by Collagenase D and CD19^{+} B cells were obtained by cell sorting. Sorted CD19^{+} B cells were either treated with PMS+LPS+ionomycin for 48 hours or cultured without stimulation for 48 hours. Flow cytometric staining were performed using the "IL-10 and TGF-β flow panel" (Table 5.8). (a) Representative figures of gating strategies for endometrial B cells, and representative histograms of IL-10 and TGF-β. (b) Scatter plots of IL-10 and TGF-β expression levels in all sample groups. Data is displayed as MFI of antibody binding as well as percentages of $IL-10^{+}$ or $TGF\beta^{+}$ cells. Statistical analysis: paired t-test was performed between all sample groups. $\star$ p $\leq$ 0.05. Error bars represent mean $\pm$ SD. n = 3 for endometrial samples, n = 3 for peripheral blood samples. MFI, mean fluorescence intensity.

5.4.5.3 IL-10 production capacity of peripheral and endometrial $CD27^{+}CD24^{hi}$ and $CD38^{hi}CD24^{hi}$ B regulatory cells

In circulating $CD19^{+}$ B cells, IL-10 production capacity has been reported to be enriched in the B regulatory cell populations, which can be identified by flow cytometry as $CD27^{+}CD24^{hi}$ or $CD38^{hi}CD24^{hi}$ (Lin et al. 2019, Hasan et al. 2019). To examine whether peripheral and endometrial B regulatory cells have an enhanced capability for IL-10 production, $CD19^{+}$ B cells were sorted and stimulated with PMS + LPS + ionomycin for 48 hours. IL-10 expression, combined with CD24, CD27 and CD38 levels, were measured by flow cytometry using the flow panel detailed in Table 5.8. In the peripheral blood samples, $CD27^{+}CD24^{hi}$ B regulatory cells accounted for around 10.6% (10.6% $\pm$ 4.5%, mean $\pm$ SD, n = 3) of all $CD19^{+}$ B cells, with an average cell count of 263, $CD38^{hi}CD24^{hi}$ B regulatory cells represented approximately 6.2% (6.2% $\pm$ 2.0%, mean $\pm$ SD, n = 3) of all $CD19^{+}$ B cells, with an average cell number of 167. In the endometrial samples, $CD27^{+}CD24^{hi}$ B regulatory cells were around 16.9% (16.9% $\pm$ 0.9%, mean $\pm$ SD, n = 3) of all $CD19^{+}$ B cells, with an average cell count of 79, $CD38^{hi}CD24^{hi}$ B regulatory cells represented approximately 11.0% (11.0% $\pm$ 2.0%, mean $\pm$ SD, n = 3) of all $CD19^{+}$ B cells, with an average cell number of 51.

As shown in figure 5.11, in peripheral $CD19^{+}$ B cells, IL-10 expression was significantly enriched in $CD27^{+}CD24^{hi}$ B regulatory cells ($p \leq 0.05$), and was also enriched in $CD38^{hi}CD24^{hi}$ B regulatory cells ($p = 0.07$). While for endometrial $CD19^{+}$ B cells, IL-10 expression was not enriched in either $CD27^{+}CD24^{hi}$ or $CD38^{hi}CD24^{hi}$ B regulatory cell types ($p = 0.1$).

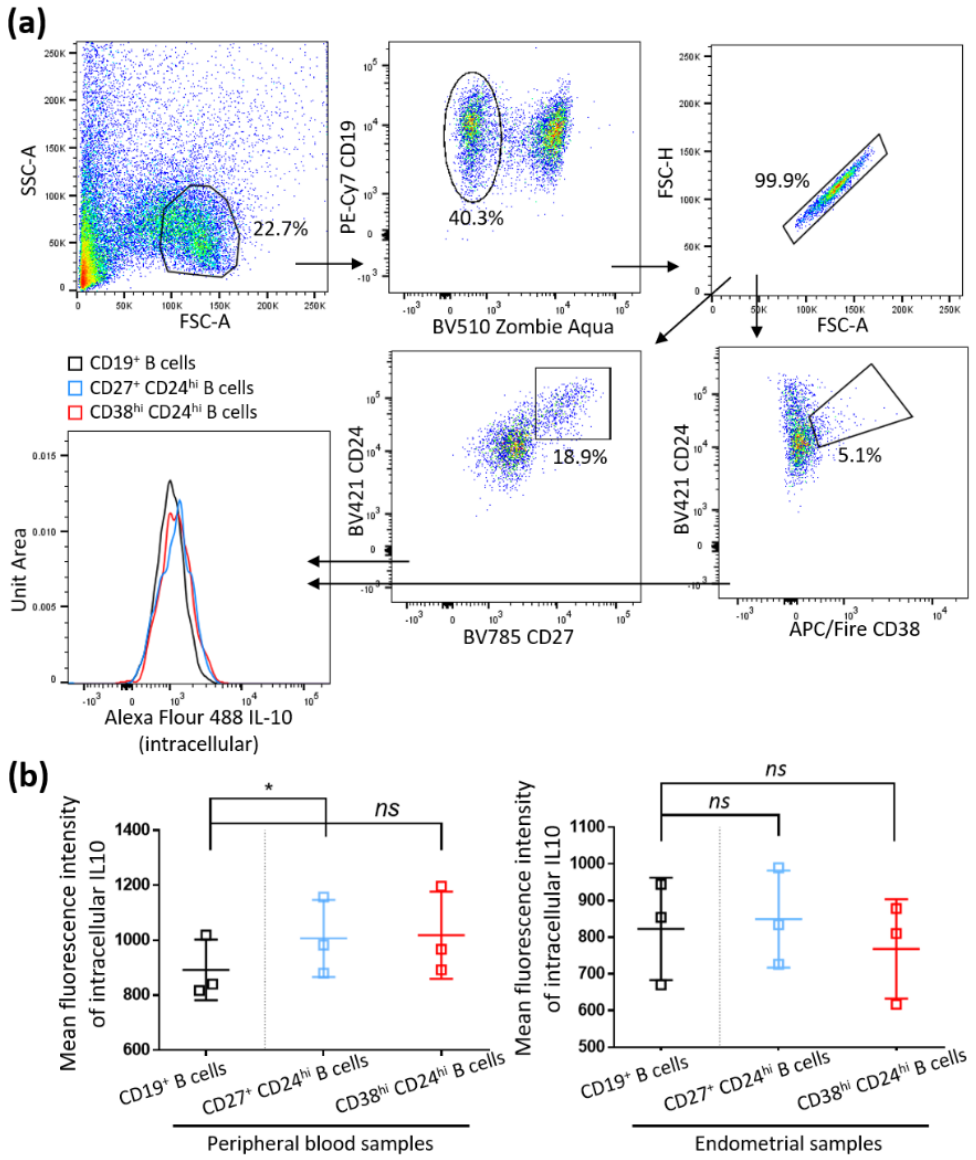

Figure 5.11: Flow cytometric analysis of IL-10 expression levels in stimulated peripheral and endometrial B regulatory cells. Matched peripheral blood and endometrial samples were collected during the mid-luteal phase. PBMCs were isolated by Lymphoprep^{TM}, endometrium samples were digested by Collagenase D. $CD19^+$ B cells were obtained by cell sorting. Sorted $CD19^+$ B cells were treated with PMS+LPS+ionomycin for 48 hours. Flow cytometric staining were performed using the "IL-10 and TGF-β flow panel" (Table 5.8). (a) Representative figures of gating strategies for $CD27^+CD24^{hi}$ and $CD38^{hi}CD24^{hi}$ B regulatory cells, and representative histograms of IL-10 in $CD19^+$ B cells, $CD27^+CD24^{hi}$ B regulatory cells, and $CD38^{hi}CD24^{hi}$ B regulatory cells. (b) Scatter plots of IL-10 expression levels in peripheral and endometrial $CD19^+$ B cells, $CD27^+CD24^{hi}$ B regulatory cells, and $CD38^{hi}CD24^{hi}$ B regulatory cells. Data was displayed as MFI. Statistical analysis: paired t-test was performed between sample groups. $\star$ $p \leq 0.05$. Error bars represent mean $\pm$ SD. $n = 3$ for endometrial samples, $n = 3$ for peripheral blood samples. MFI, mean fluorescence intensity.

5.5 Discussion

5.5.1 A distinct phenotype of endometrial B cells compared with peripheral blood B cells

In this chapter I have presented for the first time that endometrial B cells have an activated phenotype compared with peripheral blood B cells, with a significant increase in CD74, HLA-DR and CD83 expression levels. This finding corelates with the RNA-seq data presented in Chapter 4.4, where *CD74*, *HLA-DR* and *CD83* are among the top 20 genes expressed in endometrial B cells, and various B cell activation related pathways are significantly upregulated in endometrial B cells when compared with T cells. To my knowledge, this is the first evidence of endometrial B cells present an activated phenotype compared with circulating B cells.

Both CD74 and HLA-DR have a well established function in antigen presentation. CD74 is also known as the MHCII invariant chain that forms nonameric complexes with nascent MHCII molecules (Gil-Yarom et al. 2017), HLA-DR is a MHC class II cell surface receptor. The increased expression levels of CD74 and HLA-DR suggest an activated MHC class II signaling pathway in endometrial B cells, which could lead to tyrosine phosphorylation, calcium mobilization, AKT, ERK, JNK activation (Bouillon et al. 2003, Guo et al. 2003, Mooney et al. 1990, Katikaneni and Jin 2019). Studies have also shown that, in comparison to $MHCII^{-}$ B cells, $MHCII^{+}$ B cells had a substantial advantage in proliferation, differentiation into plasmablasts, or GC B cells, and isotype switching (Giles et al. 2015, Katikaneni and Jin 2019). Similarly, CD83 has also shown to be a modulator for B cell maturation, activation and GC responses (Li et al. 2019, Krzyzak et al. 2016). Therefore, the upregulation of CD74, HLA-DR and CD83 suggest endometrial B cells could undergo dynamic developmental processes such as GC reactions, and may playing an active role in the human endometrial immune environment.

Additionally, an increased expression of tissue resident marker CD69 (see Chapter 2.1.4) is observed on endometrial B cells compared with their peripheral counterparts.

This data is similar to results present in Chapter 2.4.2, and confirmed that the majority of endometrial B cells (approximately 62%) are tissue resident like B cells. However, there is no significant difference in CD62L expression, which is a homing receptor for lymphocytes and the decrease in its expression level has been associated with B cell migration from peripheral circulation to specific tissues (Pattanapanyasat et al. 2018, Morrison et al. 2010). This could due to the fact that CD62L is inherently unstable following cryopreservation, several studies have reported the loss of CD62L expression on cell surface following freeze-and-thaw (Sovalat et al. 2000, Lieberman et al. 2016, Florek et al. 2014). To properly investigate CD62L expression on endometrial B cells, samples may need to be freshly collected and processed in future studies.

5.5.2 Potential GC reactions in the human endometrium

In this chapter I have shown for the first time that GC B cells ($CD19^+FAS^+IgD^-BCL6^+$) and Tfh-like cells ($CD4^+PD1^+ICOS^+CXCR5^+$) exist in the human endometrium by flow cytometry. I also demonstrated the moderate to high expression of CD69 on these cells. To my knowledge this is the first evidence of tissue resident GC B and Tfh-like cells in the human endometrium in the literature.

Flow cytometry analysis revealed that approximately 12.2% of all endometrial B cells are FAS^+IgD^-, with a higher BCL6 and CD69 expression compared with FAS^- B cells. This indicates the presence of tissue resident GC B cells, which could be the precursors for endometrial memory B cells that represent around 30% of all endometrial B cells (Chapter 5.4.1). Additionally, it also demonstrates that compared with non-GC B cells, GC B cells are more likely to be tissue resident B cells, suggesting endometrial B cells are likely to be an active player in the endometrial immune environment, possibly through GC reactions. The presence of GC B cells also correlates with the upreuglation of CD74, HLA-DR and CD83 on endometrial B cells (as discussed in Chapter 5.5.1). Higher levels of CD74 and HLA-DR expression have been shown in GC B cells compared with naïve and memory B cells, indicating the synthesis of new MHCII molecules that could enhance

B cell antigen presentation capacities (Chalouni et al. 2003). CD83 is also expressed on GC B cells. In murine studies, CD83 is used as a marker for light zone B cells and might be involved in the antigen presentation to Tfh cells in the light zone (Krzyzak et al. 2016, Li et al. 2019).

Apart from GC B cells, $CD4^+PD1^+ICOS^+CXCR5^+$ Tfh-like cells were also identified in the human endometrium, accounting for approximately 4.1% of all $CD4^+$ T cells. However, compared with $CD4^+PD1^-ICOS^-CXCR5^-$ T cells, Tfh-like cells do not have a higher expression of BCL6, which is a defining marker for Tfh cells (Crotty 2014). Although BCL6 expression levels fluctuate during Tfh cell development, Tfh cells should express higher level of BCL6 compared with $CD4^+PD1^-ICOS^-CXCR5^-$ T cells (Li and Pauza 2015, Baumjohann et al. 2011). Considering the existence of tissue resident GC B cells in the endometrium, it might be possible that during the mid-luteal phase, the induction and initial development of GC-like reaction was formed independent of Tfh cells (Lentz and Manser 2001). This GC-like reaction could later be developed into a Tfh-dependent GC, which may contribute to the generation of class-switched B cells and plasmablasts found in the decidua (Huang et al. 2017, Leng et al. 2019). Additionally, the infiltration of plasma cells has been described in endometrial inflammatory conditions such as endometritis (see Chapter 3.4.5), there is a possibility that these GC B cells and Tfh-like cells are implicated in this process by providing the site of plasma cell generation.

This proposed GC-like reaction could be linked to the LAs structure discussed in Chapter 3.5.2. However, since we could not obtain any spatial information for these GC B cells and Tfh-like cells using flow cytometry, further research (e.g. spatial profiling through tissue microscopy) is needed to investigate whether GC B cells and Tfh cells are presented in the endometrial LAs, which could help to confirm whether endometrial LAs are TLSs.

5.5.3 Peripheral and endometrial B cells are capable of IL-10 production

In this chapter I have shown that after stimulation, peripheral blood B cells are capable of IL-10 production. Similar to previous studies, IL-10 expression is enriched in the $CD27^{+}CD24^{hi}$ and $CD38^{hi}CD24^{hi}$ B regulatory subsets (Koushaeian et al. 2019, Rolle et al. 2013).

In addition, I have shown that endometrial B cells are also capable of IL-10 production after stimulation, with a similar IL-10 expression level compared with matched peripheral blood samples. To my knowledge this is the first evidence of endometrial B cells IL-10 production in the literature. Considering the functional importance of IL-10 producing B cells in early pregnancy (Guzman-Genuino and Diener 2017, Jensen et al. 2013, Busse et al. 2019, Esteve-Solé et al. 2018), this findings could help us to better understand the B cell role in the endometrial immune environment, and how different cellular components are interacting with each other. However, the IL-10 expression does not seem to be enriched in $CD27^{+}CD24^{hi}$ and $CD38^{hi}CD24^{hi}$ B regulatory subsets in endometrial samples. This may be because of the limited cell counts (< 100 for both B regulatory subsets), larger biopsy samples are needed for future studies.

Apart from IL-10, the expression level of another anti-inflammatory signal, TGF-β, was also examined in the peripheral and endometrial B cells. TGF-β plays a key role in T regulatory induction, thereby is crucial during implantation (Li 2014, Guzeloglu-Kayisli et al. 2009). My data showed that B cells could be a source for TGF-β secretion, both in the peripheral blood and endometrium. However, no significant increase of TGF-β is observed between stimulated and unstimulated groups, more samples are needed to validate this finding. Additionally, it is important to note that the control I used in the IL-10 and TGF-β production assay was unstimulated peripheral B cells, which may have a different cytokine secretion profile compared with unstimulated endometrial B cells. Larger endometrial biopsy samples are needed to establish an unstimulated B cell control to further understand endometrial B cell IL-10 and TGF-β production capacities.

Chapter 6

Summary and Future Perspectives

This thesis covers two topics in reproductive immunology. Firstly it proposed the PIP study, a large scale clinical research project hoping to describe in detail endometrial and peripheral immune cell parameters in fertile controls and patients with infertility, RIF and RPL. Although participant recruitment was a major challenge, a SOP was established, and preliminary data demonstrated the proportional and phenotypic differences (in terms of CD69 expression) between endometrial and peripheral immune cell subsets, include $CD56^{bright}$ $CD16^{-}$ NK, $CD56^{bright}$ $CD16^{dim}$ NK, $CD56^{dim}$ $CD16^{bright}$ NK, $CD4^{+}$ T, $CD8^{+}$ T, CD4CD8 DP T, CD4CD8 DN T, $CD25^{bright}$ $CD127^{dim/-}$ Treg and $CD56^{+}$ $CD3^{+}$ NKT cells. With an increased sample size, we hope to firstly establish a dataset of normal endometrial immune cell parameters and secondly, using this extensive immune profiling, establish if there is an altered immune phenotype in patients with subfertility, RIF and RPL. Although many clinicians already undertook immune cell testing, to date we do not know the normal parameters of endometrial immune cells. This study will provide reference range for various immune cell parameters of interest. Furthermore, we hope the PIP study could provide clear evidence as to whether blood or endometrial immune cell testing identifies a population of patients who have immune mediated subfertility, implantation failure or miscarriage. These results could provide a basis for hypothesis driven RCT of immunomodulators in patient groups that may provide new and effective

treatments for these patients.

Secondly, the role of B cells in the endometrial immune environment was investigated. A systematic review on endometrial B cells was undertaken. Although it identified a lack of data regarding B cell phenotype or function in either normal cycling human endometrium or in endometrium from women with reproductive pathologies, there is evidence of B cell presence in the endometrium, either scattered or in the centre of LAs, and altered B cell numbers have been observed in reproductive pathologies such as RPL. The lack of a detailed understanding of endometrial B cells and the known importance of decidual B cells during pregnancy (Huang et al. 2017, Leng et al. 2019) lead me to further study endometrial B cells. RNA-seq and flow cytometric analysis were performed on endometrial B cells. B cells comprised 1-5% of endometrial immune cells and were found to mainly exist as naïve or memory B cells in the endometrium. Endometrial B cells were shown to exhibit an activated phenotype, with increased expression of CD69, HLA-DR, CD74 and CD83 compared with circulating counterparts. Upon stimulation, they were able to produce IL-10. Additionally, I reported the presence of $PD1^{+}CXCR5^{+}ICOS^{+}$ Tfh -like cells and $FAS^{+}IgD^{-}$ GC-like B cells in the endometrium, both are markers of TLSs and could be linked with the previously reported endometrial LAs. However, it is unclear whether these Tfh-like cells and GC-like B cells are within the LAs as no spatial information was obtained. A comprehensive analysis of LAs, first by visualisation of the TFh-like cells and GC-like B cells through immunofluorescence, then using spatial profiling techniques like GeoMX Digital Spatial Profiling to determine differences in cellular protein profile between loose stromal cells and cells of the LA, would help us understand the cellular component and function of endometrial LAs. Additionally, to understand the formation of LAs, a multiplex cytokine assay can be performed on key cytokines involved in TLS formation and function (LTα, CXCL13, CCL21, CCL19, IL-17, IL-23, IL-7, IL -27, and CCL3/MIP1-a), followed by western blot to detect levels of adhesion molecules involved in TSL formation (ICAM-1 and VCAM-1), as well as verify levels of MIP-1a obtained from the multiplex cytokine assay.

My research on endometrial B cells is to my knowledge the first flow cytometric and RNA-seq analysis focusing on the endometrial B cell population. It provided the first evidence of multiple B cell subsets existence within the human endometrium. It also showed for the first time that endometrial B cells display a different phenotype compared with peripheral B cells, in addition to their IL-10 producing capacity.

This level of B cell characterisation has not been undertaken previously in the field of reproductive immunology or endometrial research, and may, with the work planned following on from this thesis, enhance our understanding of the known link between autoimmune diseases and reproductive pathologies such as endometriosis. Endometriosis has been associated with a range of autoimmune diseases, which typically result from an expanded population of autoreactive B cells (Shigesi et al. 2019, Rawlings et al. 2017, Hershberg and Luning Prak 2015). However, whether B cell clonal expansion occurs in the endometrium is still unclear. Single-cell RNA-seq, BCR repertoire analysis and antigen specificity analysis of endometrial B cells are needed to better understand the immune aetiology of autoimmune associated reproductive pathologies.

To date, no single-cell level study has been performed on endometrial B cells in either normal endometrium or in pathology-focused patient groups. Existing studies have sequenced cells from whole endometrial tissue, in which the cell populations are dominated by stromal and epithelial cells (Lucas et al. 2020, Wang et al. 2020). For minority cell populations such as endometrial B cells, cell enrichment is a necessary step before sequencing in order to obtain sufficient amount of data to be able to define B cell sub-populations. This single-cell level data on endometrial B cells would also illustrate the immune cell-cell interaction network in the endometrium. Combined with the spatial transcriptomic analysis of LAs, this would provide a complete view of endometrial B cell phenotype and function at a high resolution.

Appendix A

PIP study patient data collection template

The PIP Study

Please complete the survey below.

Thank you!

Center Study ID (e.g IVI Ox 001, IVI Tam 001, WFC 001)	_____

Female Demographics

Age(years)	_____
Height (meters in 2 decimal places)	_____
Weight (kg in 1 decimal place)	_____
BMI	_____
Last day of the menstrual period in this cycle	_____
Date of endometrial Scratch	_____
Day of Endometrial Scratch	_____
Date of LH Surge	_____
Day of LH surge	_____
Cycle length min	_____
Cycle length max	_____
Type of Subfertility	☐ Anovulatory ☐ Male Factor ☐ Tubal Factor ☐ Unexplained
Duration of subfertility	_____
Previous pregnancies	_____

Previous Miscarriages	_____
Previous TOP	_____
Previous Live Births	_____
Number of Previous ART cycle	_____
Current Medications	☐ Prednisolone ☐ Immunomodulators ☐ Hydroxychloroquine
Medical History	☐ Antiphospholipid Syndrome ☐ Hyperthyroidisim ☐ Hypothyroidism
Known Endometriosis	◯ Yes ◯ No
Known Adenomyosis	◯ Yes ◯ No
Known submucosal fibroids	◯ Yes ◯ No
Known hydrosalpinx	◯ Yes ◯ No

Male Demographics

Male Age (years)	_____
Height (meters, in 2 decimal places)	_____
Weight (kg, number 1 decimal place)	_____
BMI Male	_____

Semen Analysis on Day of Insemination

Semen Volume (mls, number 2 decimal places)	_____
Semen Concentration (million per ml)	_____
Semen Motility (A+B) (Percentage)	_____
Semen Morphology (Percentage)	_____

Current Treatment Details

Cycle Number	_____
AMH	_____
Total Antral follicle count	_____
Type of protocol	◯ Agonist (Long protocol) ◯ Antagonist (Short protocol)
Duration of stimulation (days)	_____
Type of Cycle	◯ Fresh cycle ◯ Frozen cycle
Frozen cycle (Type)	◯ Natural ◯ Medicated
Endometrial Thickness (Last recorded (mm))	_____
Type of Insemination	☐ IVF ☐ ICSI ☐ Split
Estradiol Level (last recorded)	_____
Progesterone Level (Last collected (ng/ml))	_____
Number of oocytes collected	_____
Insemination Method	☐ IVF ☐ ICSI

Number fertilised IVF	_____
Number fertilised ICSI	_____
Number of embryo transferred	_____
Grade of embryo transferred (1)	_____
Grade of embryo transferred (2)	_____
Grade of embryo transferred (3)	_____
No of frozen embryo(s)	_____
Luteal Phase support medication	☐ Oestradiol Valerate 2mg (TDS) (Oral) ☐ Utrogestan 200mg (TDS) (PV) ☐ Cyclogest 400mg (BD) (PV) ☐ Lubion 25mg (OD) (IM) ☐ Lubion 25mg (BD) (IM) ☐ Gestone 100mg (OD) (IM)
Additional Medications	☐ Clexane ☐ Aspirin ☐ Prednisolone ☐ Dalteparin
Preimplantation Genetic Screening	☐ Yes ☐ No

Outcome Data

Urine pregnancy test	◯ Positive ◯ Negative
Ongoing Pregnancy (USS between 6-8 weeks with presence of Fetal Heart Activity)	◯ Pregnancy of Unknown Location ◯ Ectopic Pregnancy ◯ Single live intrauterine pregnancy ◯ Twin live intrauterine pregnancy ◯ Triplets live intrauterine pregnancy ◯ Miscarriage
Live birth (any live birth after 24 weeks gestation)	◯ Yes ◯ No
No of live birth	_____
First Live birth	◯ Yes ◯ No

Gestation at Delivery (Fetus1)	_____
Birth weight of baby 1	_____
Second Live birth	◯ Yes ◯ No
Gestation at Delivery (Fetus2)	_____
Birth weight of baby 2	_____
Third Live birth	◯ Yes ◯ No
Gestation at Delivery (Fetus3)	_____
Birth weight of baby 3	_____
Miscarriage	◯ Yes ◯ No
Number of Miscarriages	_____
Gestation at miscarriage	_____
Miscarriage Singleton	◯ Yes ◯ No
Miscarriage Twins	◯ Yes ◯ No
Miscarriage Triplets	◯ Yes ◯ No
Termination for anomaly	◯ Yes ◯ No

Appendix B

Isolation and Flow Cytometry Analysis of Various Immune Cells from Human Peripheral Blood and Endometrium: an SOP that Describes the Procedures for Assessing the Feasibility of the PIP Study.

Isolation and Flow Cytometry Analysis of Various Immune Cells from Human Peripheral Blood and Endometrium

Materials and Reagents

For Blood and endometrial sample

1. 1.5 ml Micro tube (SARSTEDT, catalogue number: 72.690.001)
2. 15 ml tubes (CELLSTAR, catalogue number: 188 261)
3. 25 ml tube (SARSTEDT, catalogue number: 63.9922.248)
4. 50 ml tubes (SARSTEDT, catalogue number: 62.547.004)
5. Sterile pipette filter-tips 10 µl (TipOne, catalogue number: S1111-3800)
6. Sterile pipette filter-tips 200 µl (TipOne, catalogue number: S1122-1830)
7. Sterile pipette filter-tips 1,000 µl (TipOne, catalogue number: S1122-8810)
8. Sterile serological pipettes 5 ml (COSTAR, catalogue number: 4487)
9. Sterile serological pipettes 10 ml (COSTAR, catalogue number: 4488)
10. Sterile serological pipettes 25 ml (COSTAR, catalogue number: 4488)
11. Pipettes 10 µl (Gilson)
12. Pipettes 200 µl (Gilson)
13. Pipettes 1000 µl (Gilson)
14. Transfer pipette (SARSTEDT, catalogue number: 86.1171.001)
15. Pipette controller (INTEGRA PIPETBOY 2)
16. PBS/2% FCS
    a) Phosphate-buffered saline, PBS (SIGMA, catalogue number: D8537)
    b) Fetal bovine serum (Sera Laboratories International Ltd, catalogue number: EU-000-F)
17. Mini cell strainer 40 µm (pluriStrainer, catalogue number: 43-10040-60)
18. Trypan blue solution, for microscopy (Sigma, catalogue number: 93595-50ML)
19. Zombie Aqua™ Fixable Viability Kit (Biolegend, catalogue number: 423101)
20. FluoroFix™ Buffer (Biolegend, catalogue number: 422101)
21. Freezing Medium (10% Dimethyl sulfoxide in FBS)
    a) Fetal bovine serum (Sera Laboratories International Ltd, catalogue number: EU-000-F)
    b) Dimethyl sulfoxide (Sigma)
22. Cryotube Vials (Thermo Fisher Nunc, catalogue number: 368632)
23. Cryo Freezing Container (NALGENE) containing isopropyl alcohol

24. Antibodies (Table 1):

Antibody	Clone	Fluorophore	Source	Cat No.
anti-CD45	HI30	BV650™	Biolegend	304044
anti-CD3	UCHT1	APC/Fire™ 750		300470
anti-CD56	HCD56	BV421™		318328
anti-CD4	OKT4	FITC		317408
anti-CD8a	RPA-T8	BV711™		301044
anti-CD16	3G8	BV785™		302046
anti-CD25	BC96	PE		302606
anti-CD127	A019D5	APC		351316
anti-CD19	HIB19	PE/Cy7		302216
anti-CD69	FN50	PE/DAZZLE™ 594		310942

Table 1. Antibodies used for flow cytometry analysis.

For blood sample only

1. 2 ml Screw Cap Micro Tube (SARSTEDT, catalogue number: 72.694.006)
2. Lymphoprep™ (Alere Technologies, catalogue number: 04-03-9391/01)
3. FACS™ Lysing Solution (BD, catalogue number: 349202)
4. Precision Count Beads™ (Biolegend, catalogue number: 424902)

For endometrial biopsy only

1. Petri-dish 92 x 16 mm (SARSTEDT, catalogue number: 82.1473)
2. Disposable scalpels (Swann-Morton, catalogue number: 0503)
3. Digestion Medium
   a) Dulbecco's Modified Eagle's Medium/Nutrient Mixture F-12 Ham (Sigma, catalogue number: D-6421)
   b) Fetal bovine serum (Sera Laboratories International Ltd, catalogue number: EU-000-F)
4. Collagenase D (SIGMA, catalogue number: 11088858001)
5. Deoxyribonuclease I from bovine pancreas (Merck, catalogue number: D5025)
6. Cell Strainers, 40 μm (Corning, catalogue number: 431750)
7. Cell Strainers, 70 μm (Corning, catalogue number: 431751)

Equipment

1. Thermo centrifuge (Thermo SCIENTIFIC MULTIFUGE X3R)
2. Bench-top centrifuge (Micro Centaur SANYO MSE)
3. Vacuum aspirator
4. Cell counting haemocytometer
5. High Performance Shaking Incubator (Labnet, model: 311DS)
6. -4°C Premium Frost-Free Fridge (Liebherr)
7. -80°C Ultra Low Temperature Freezer (New Brunswick Scientific)
8. Milli-Q™ NANOpure Diamond ™ Water System (Barnstead)
9. BD LSR II Flow Cytometer/ BD LSR Fortessa (BD)

Software

1. Flow cytometry acquisition software: BD FACSDiva™ version 8.0.1
2. Flow cytometry analysis software: Flowjo version 10.4.2

Procedure

A. Collection of human peripheral blood and endometrial biopsies

Take 3 x 4.5 ml blood (1 x 4.5 ml in Ethylenediaminetetraacetic acid (EDTA) vacutainer, 2 x 4.5 ml in Lithium/Sodium Heparin vacutainer) and an endometrial biopsy in the mid-luteal phase of the cycle preceding assisted reproductive technology, 7-10 days after the ovulatory LH-surge. Sample collection takes place between 8am and midday. All samples are couriered to the Nuffield Department of Women's and Reproductive Health. Sample processing takes place immediately after arriving in Nuffield Department of Women's and Reproductive Health. Sample acquisition by flow cytometry takes place the following morning, 9 a.m.

Data pertaining to participant baseline characteristics (duration and cause of subfertility, number of previous IVF cycles, number of previous implantation failure, whether intracytoplasmic sperm injection (ICSI) is involved, *etc.*) will be obtained with consent from the patient records, as well as pregnancy outcome data.

B. Preparation for absolute cell count determination

1. Aliquot 50 μl blood from Lithium/Sodium Heparin vacutainer using a reverse pipetting technique, transfer to an Eppendorf.
2. Add 1 μl (4 μg/ml) APC/Fire™ 750 anti-CD3 and 1 μl (8 μg/ml) FITC anti-CD4 to the Eppendorf, incubate for 15 minutes at room temperature in the dark.
3. Add 500 μl 1:10 Milli-Q water diluted 10x FACS™ Lysing Solution to the Eppendorf, mix well by pipetting. Incubate for 15 minutes at room temperature in the dark.
4. Wash
5. Store the Eppendorf at 4°C in dark overnight, proceed to step 5 before flow acquisition.
6. Vortex Precision Count Beads™ thoroughly, add 50 μl to the Eppendorf, mix well by pipetting. Start flow acquisition (Section E).

C. Isolation of peripheral blood mononuclear cells (PBMCs) and Human Endometrial Cells (HECs).

(a) Isolation of PBMCs

1. Prepare PBS/2% FCS, place at room temperature (15–25°C).
2. Spin EDTA vacutainer with collected blood for 2000 *x g*, 10 minutes at room temperature.
3. Transfer 1 ml of the upper plasma layer to 2 x 1 ml screw cap micro tube, label the date and sample number, stored at -80°C.
4. Transfer the remaining 9 ml blood from Lithium/Sodium Heparin vacutainer to a 25 ml tube, dilute with 9 ml of PBS.

For two Heparin vacutainers, spin at 2000g 10 minutes at room temperature/ Spin at 2500g for 10 min at 4C.

5. Take out 100ul plasma, 3 eppendorfs, put in -80 freezer.
6. Add 3 ml Lymphoprep™ in 2 separate 15 ml tubes.
7. Gently lay 9 ml of diluted blood on top of Lymphoprep™ in each 15 ml tube.
8. Centrifuge both 15 ml tubes at 800 *x g*, room temperature for 20 minutes with brake off.
9. After centrifugation, carefully remove the peripheral blood mononuclear cells (PBMCs) layer in the Lymphoprep™/plasma interface (Figure C1) with transfer pipette into a 50 ml tube.
10. Top up the 50 ml tube to 30 ml with PBS/2% FCS. Centrifuge for 10 minutes at 300 *x g*, room temperature. Aspirate the supernatant
11. Top up again to 30 ml with PBS/2% FCS. Centrifuge for 10 minutes at 200 *x g*, room temperature. Aspirate the supernatant.
12. After centrifugation, re-suspend cell pellet in 1 ml PBS.
7. Transfer 10 μl of collected cell suspension (in 50 ml tube) to 1.5 ml Eppendorf. Keep the 50 ml tube with cell suspension on ice.
13. Add 90 μl PBS to the Eppendorf, mix well by pipetting.
14. Dilute cell sample in Trypan Blue by preparing a 1:1 dilution of the cell suspension using a 0.4% Trypan Blue solution.
15. Carefully and continuously fill the haemocytometer chamber.
16. Incubate the haemocytometer and cells for 1 – 2 minutes at room temperature.
17. Perform cell counting.
18. Proceed to section D.

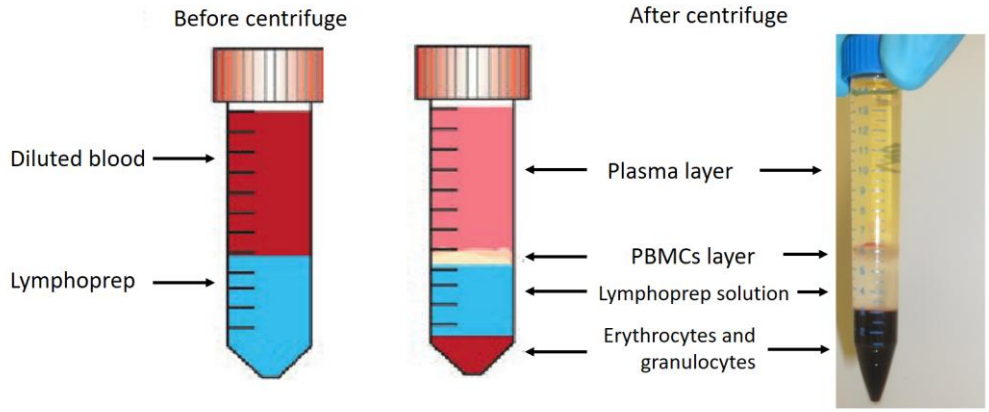

Figure C1. Illustration of Lymphoprep before and after centrifuge.

(b) Tissue digestion and isolation of HECs

Note: Ensure sterility. Work in a Class II microbiological safety cabinet and ensure full aseptic technique.

1. Prepare Digestion Buffer and warm to 37°C .Turn on the shaking incubator and set the temperature to 37°C.
2. Transfer endometrial tissue with PBS to a Petri-dish. Record shape, size and patient number of the biopsy
3. Take 5 mm^3 ES tissue, cut into 1 mm^3 fragments using scalpel and pipette and remove mucus. Ensure tissue fragments are small enough to fit through the tip of the transfer pipette (excess ES with good structure will be snap-freezed for immunohistochemistry).
4. Transfer all the tissue fragments into 15 ml tubes, maximum 20 mm^3 per tube. If blood contamination exchange solution to PBS. Remove supernatant to 1 ml solution of PBS with endometrial tissue.
5. Add 10 ml Digestion Buffer to each 15 ml tubes. Remove the excess buffer with only 1 ml left in each tube.
6. Add 10 μl (>= 2 Kunitz units, concentration: 100 μg/ml) DNase I and 100 μl (>0.3U/mg, concentration: 2mg/ml) Collagenase D aliquot to each 15 ml tube, vortex for 20 seconds.
7. Place all 15 ml tubes in 37°C shaking incubator for 30 minutes.
8. After incubation, add 10 ml Digestion Buffer to each 15 ml tubes and pass through sequential 70 μm and 40 μm cell strainers, wash the cell strainers twice with 3 ml Digestion Buffer, collect all the run-through in a new 50 ml Falcon tube.
8. Centrifuge the collected run-through for 10 minutes at 300 *x g*, room temperature, aspirate the supernatant then re-suspend cell pellet in 1 ml PBS.
9. Transfer 10 μl of collected cell suspension (in 50 ml tubes) to 1.5 ml Eppendorf. Keep the 50 ml tube with cell suspension on ice.
10. Add 40 μl PBS to the Eppendorf, mix well by pipetting.
11. Dilute cell sample in Trypan Blue by preparing a 1:1 dilution of the cell suspension using a 0.4% Trypan Blue solution.
12. Carefully and continuously fill the haemocytometer chamber.
13. Incubate the haemocytometer and cells for 1 – 2 minutes at room temperature.
14. Perform cell counting.
15. Proceed to section D.

D. Flow cytometry staining (11 colours), cell fixation and cell storage

Note: Ensure sterility for step 13. Work in a Class II microbiological safety cabinet and ensure full aseptic technique.

1. Prepare Freezing Medium, store in 4°C tissue culture room.
2. Dilute 1µl Zombie Aqua™ aliquot with 1 ml PBS. Placed on ice, in the dark.
3. Aliquot 2 million cells in an Eppendorf, centrifuge at 13,000 *x g* for 1 second, aspirate all supernatant. For the rest of cells, proceed to step 13 for storage.
4. Re-suspend the cell pellet in the Eppendorf with 100 µl diluted Zombie Aqua™ aliquot.
5. Incubate the Eppendorf for 15 minutes in dark, room temperature.
   During incubation, prepare antibody master mix according to Table D1.
6. Add antibody master mix to the Eppendorf, mix well by pipetting. Incubate for 15 minutes in dark, room temperature.
7. After incubation, wash cells with 1 ml PBS/2% FCS, mix well by pipetting. Centrifuge with 13,000 *x g* for 1 second. Aspirate all supernatant.
8. Repeat step 8.
9. Re-suspend cell pellet with 250µl Fluorofix™ in the Eppendorf, mix well by pipetting.
10. Incubate for 10 minutes in dark, room temperature.
11. Centrifuge the Eppendorf for 5 minutes at 300 *x g*. Aspirate supernatant and re-suspend with 400 µl PBS/2% FCS.
12. Store the Eppendorf at 4°C in dark overnight, proceed to section E next morning.
13. Cell storage:
    1) Transfer the rest of cells to one Eppendorf, centrifuge for 5 minutes at 300 *x g*. Aspirate all supernatant then re-suspend cell pellet with 1 ml Freezing Medium.
    2) Transfer 1 ml cell suspension to one labelled Cryo tube vial (sample name, cell number, date and name), place the vial in Cryo Freezing container with isopropyl alcohol, stored in -80°C overnight.
    3) Transfer the Cryo tube vials to vapour phase nitrogen tank, update the cell bank record.

Antibody	Fluorophore	Concentration (µg/ml)		Amount (in 50 µl)	
		PBMCs	HECs	PBMCs	HECs
anti-CD45	BV650™	0.5		0.5	
anti-CD3	APC/Fire™ 750	12		3	
anti-CD56	BV421™	3.6	1.8	3	1.5
anti-CD4	FITC	16		2	
anti-CD8a	BV711™	1.5		3	
anti-CD16	BV785™	7.2		3	
anti-CD25	PE	3	1	3	1
anti-CD127	APC	3		3	
anti-CD19	PE/Cy7	4		2	
anti-CD69	PE/DAZZLE™ 594	4		2	
Top up to 50 µl with PBS/ 2%FCS					

Table D1. List of antibodies and their usage per sample for PBMCs and HECs.

E. Flow cytometry acquisition

Book the time slot from 9.a.m. to 10 a.m. on flow calendar

Power on PC and log into Windows, Once boot up completed, launch Diva. Allow the laser to warm up for at least 30 minutes then run the CS&T.
For PBMCs sample, filter through 40 μm cell strainer, wash the cell strainer with 100 μl PBS/2%FCS and collect all the run-through in flow tube.

On BD FACSDiva Software,

1. Create experiment from following templates accordingly:
   i. For absolute cell counting, create experiment from template "PIPstudy_Countbeads_Monica", its global worksheet is shown in Figure E1.
   ii. For 11-color stained patient sample, create experiment from template "PIPstudy_ _Monica", its global worksheet is shown in Figure E2 and Figure E3 (due to lack of space, only part of analysis template PIPstudy_Compensation_Monica is shown).
2. Start acquisition on low rate, set the voltage for SSC vs. FSC to allow the majority of immune cells locate in the middle of FSC-A vs. SSC-A plot. Adjust the gating in worksheet accordingly.
3. Start acquisition on medium speed. Allow sample acquisition to stabilize before recording, record events accordingly:
   i. For determination of absolute count of cells, record 2,000 events on "beads" gate. *Allow PBS to run for 5 minutes after count beads acquisition, eliminate beads and red blood cell lysis contamination on following samples.*
   ii. For 11-color stained patient sample, record all events.
   During acquisition, ensure same voltage and compensation matrix were applied.
4. Export date in .fcs 3.1 format, save to 2 separate external hard drives.

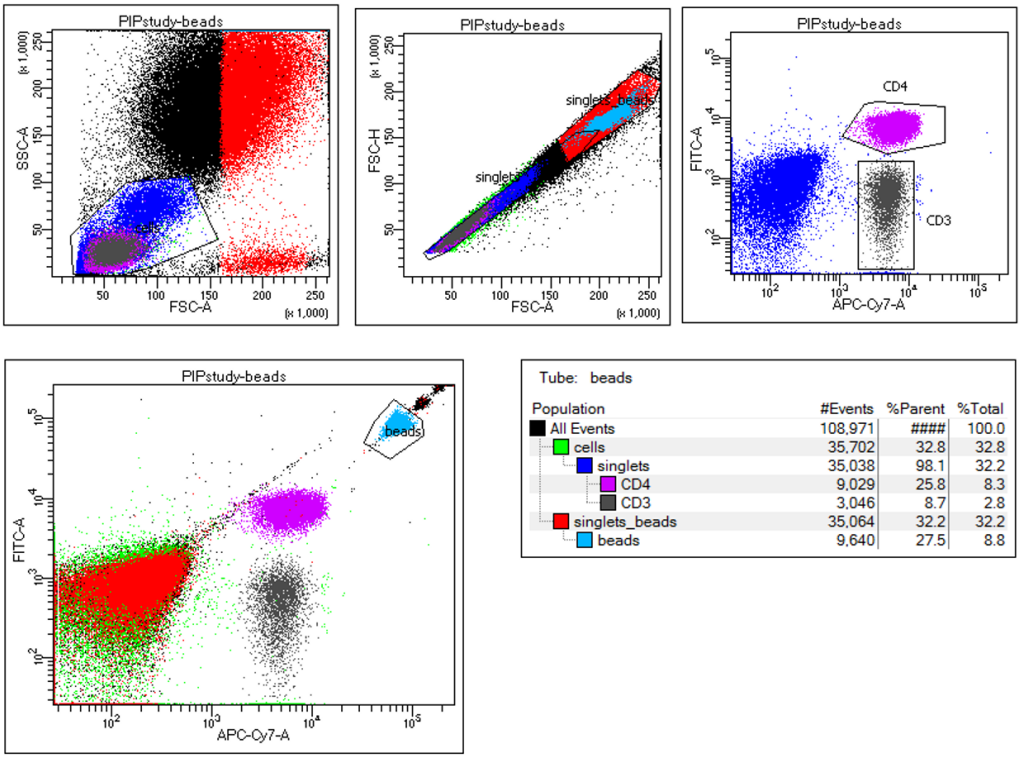

Figure E1. Analysis template PIPstudy_Countbeads_Monica .

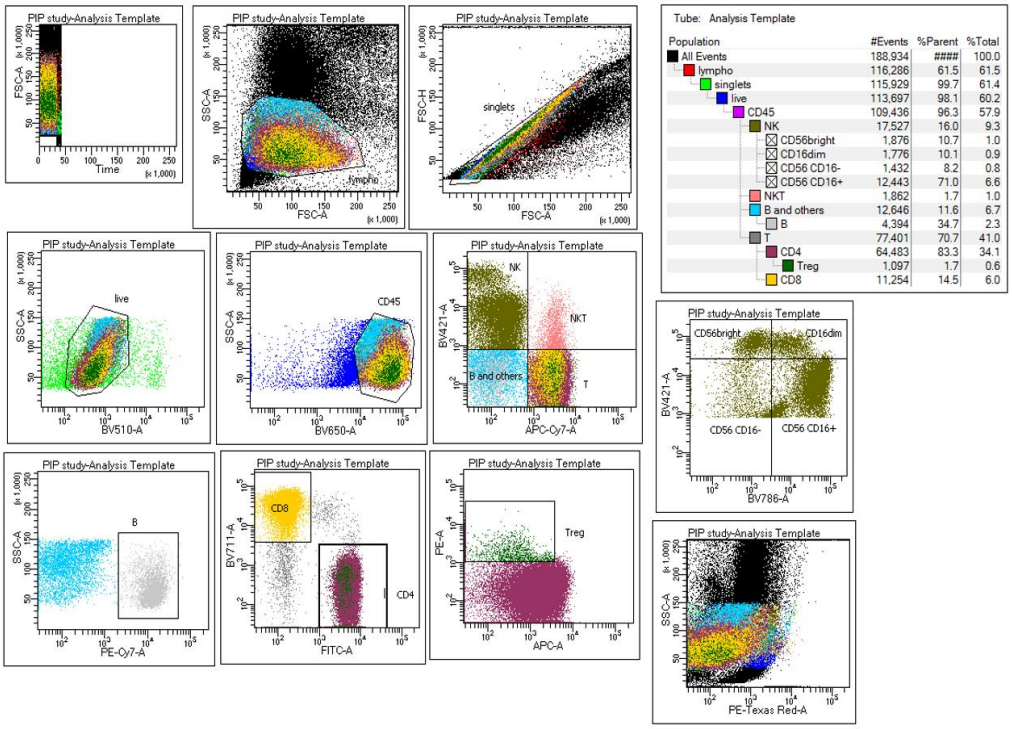

Figure E2. Analysis template PIPstudy_Monica .

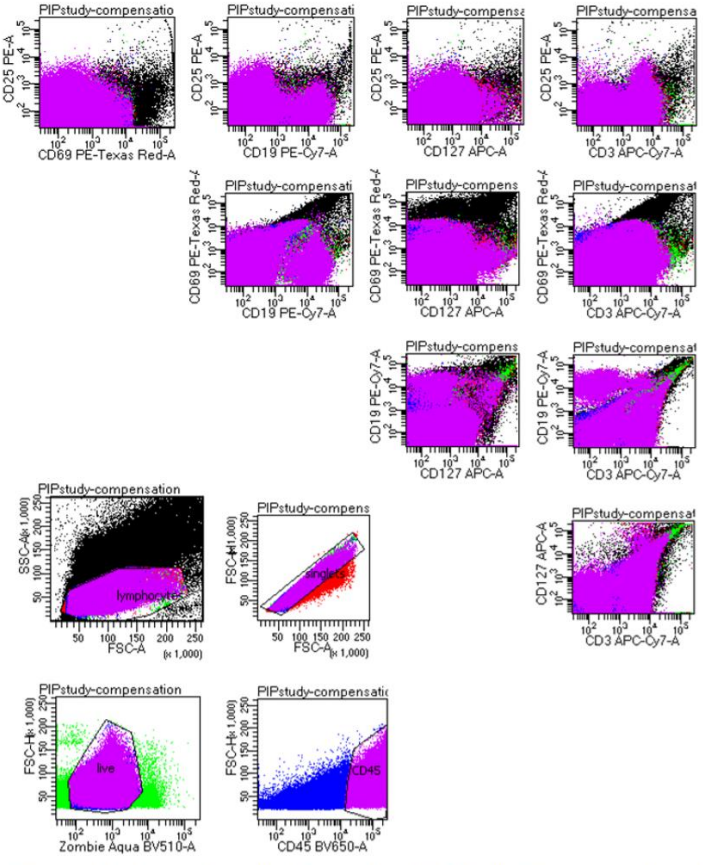

Figure E3. Part of analysis template PIPstudy_Compensation_Monica.

F. Flow cytometry analysis

The concentration of PBMC or CD3 positive T cells per ml blood was calculated using the formula,

$$\text{Absolute count (cells/ml blood)} = \frac{\text{number of the target sub-population counted x number of Perfect-Count/µl x 1000}}{\text{Total number of the microspheres counted}}$$

(a) Data cleaning steps for PBMCs (Figure F1)

Original flow data
↓ *Time vs. FSC-A*
i. Select the "clean" time data
↓ *FSC-A vs. SSC-A*
ii. Select small lymphocytes population
↓ *FSC-A vs. FSC-H*
iii. Select singlets
↓ *BV510™ (Zombie Aqua™) vs. SSC-A*
iv. Select live cells
↓ *BV650™ (CD45) vs. SSC-A*
v. Select $CD45^+$ population

Figure F1. Gating hierarchy of data cleaning steps for PBMCs analysis.

i. Plot Time vs. FSC-A, select data segments with continuous time gate centroids.

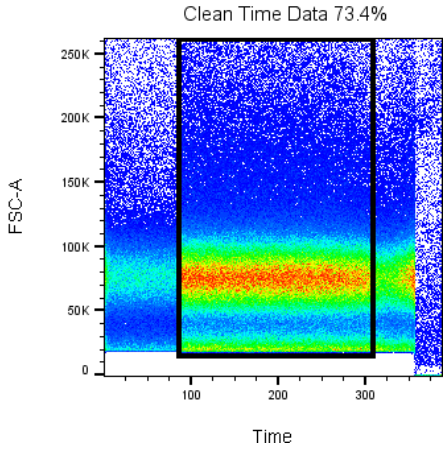

ii. Plot FSC-A vs. SSC-A, gate on small lymphocytes population, being careful to avoid 1) the debris field in the lower left corner; 2) granulocytes and monocytes population.

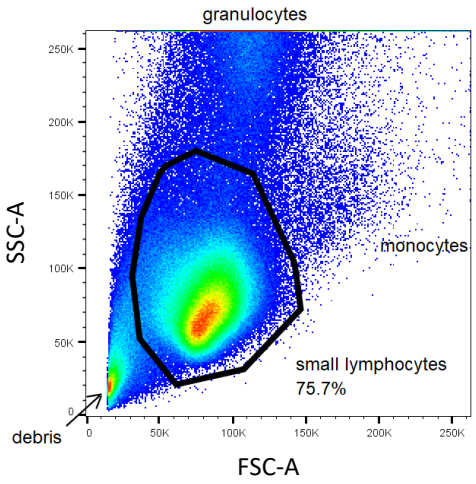

iii. Plot FSC-A vs. FSC-H, gate on singlets that clustered along the diagonal. The subpopulations are shown more clearly in the stylized illustration (right).

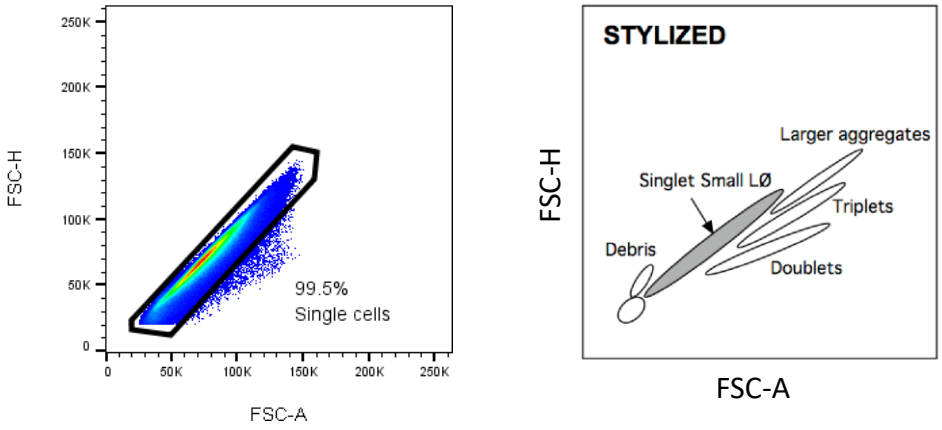

iv. Plot BV510™ (Zombie Aqua™) vs. SSC-A, zebra plot with outliers shown (right) is preferred. Gate on BV510^{-} population, excluding the BV510^{dim} as well as the BV510^{+}.

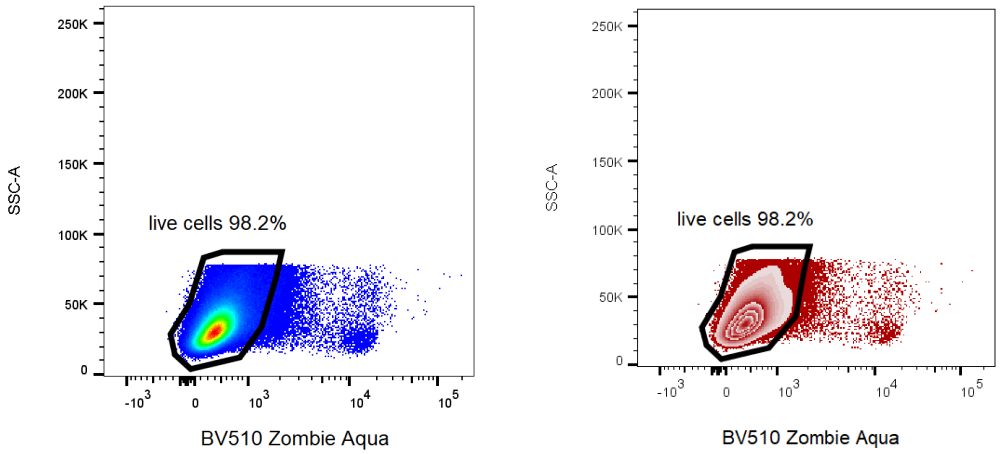

v. Plot BV650^{TM} (CD45) vs.SSC-A, zebra plot with outliers shown (right) is preferred. Gate on BV650^{+} population, excluding the BV650^{dim} (immature immune cell/ platelets, *etc.*) as well as the BV650^{-} (plasma cells, erythroid, *etc.*).

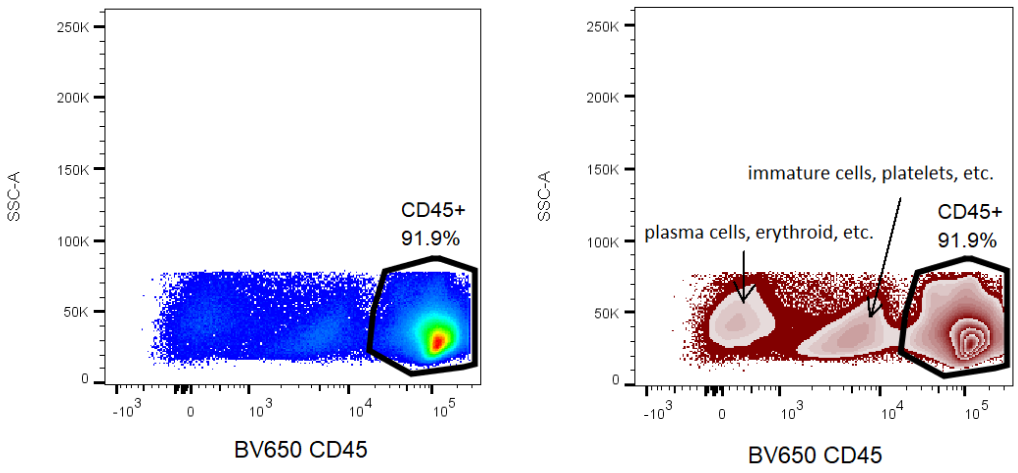

(b) Data cleaning steps for HECs (Figure F2)

Original flow data

↓ *Time vs. FSC-A*

i. Select the "clean" time data

↓ *FSC-A vs. FSC-H*

ii. Select singlets

↓ *BV650™ (CD45) vs. SSC-A*

iii. Select CD45⁺ population

↓ *BV510™ (Zombie Aqua™) vs. SSC-A*

iv. Select live cells

↓ *FSC-A vs. SSC-A*

v. Select small lymphocytes population

Figure F2. Gating hierarchy of data cleaning steps for HECs analysis.

i. Plot Time vs. FSC-A, select data segments with continuous time gate centroids.

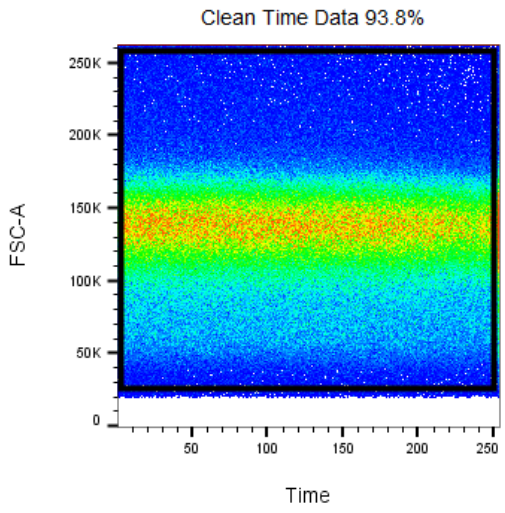

ii. Plot FSC-A vs. FSC-H, gate on singlets that clustered along the diagonal. The subpopulations are shown more clearly in the stylized illustration in Section E.a.iii.

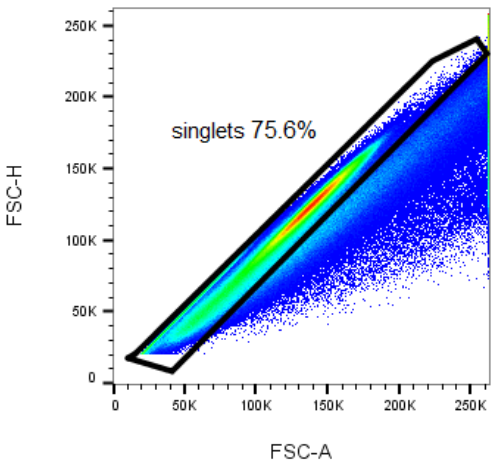

iii. Plot BV650™ (CD45) vs. SSC-A, zebra plot with outliers shown (right) is preferred. Excluding stromal cells which are BV650$^-$, gate on BV650$^+$ population, being careful to avoid debris in the bottom.

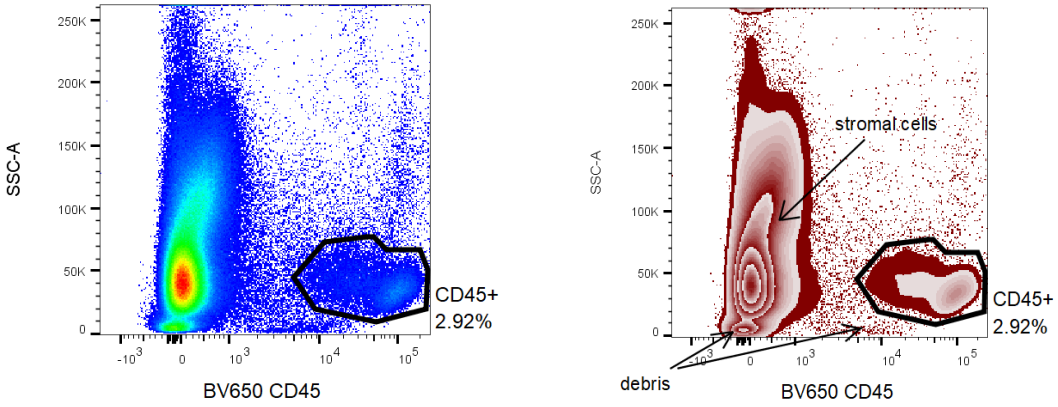

iv. Plot BV510™ (Zombie Aqua™) vs. SSC-A, dot plot (right) is preferred. Gate on BV510$^-$ population, excluding the BV510^{dim} as well as the BV510$^+$.

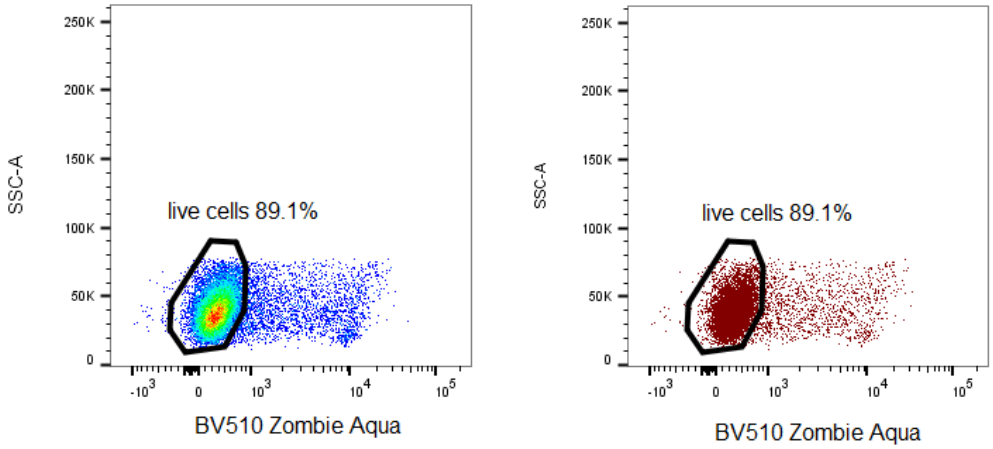

v. Plot FSC-A vs. SSC-A, gate on lymphocytes population in the middle, excluding outliers in 1) the lower left corner; 2) the right side.

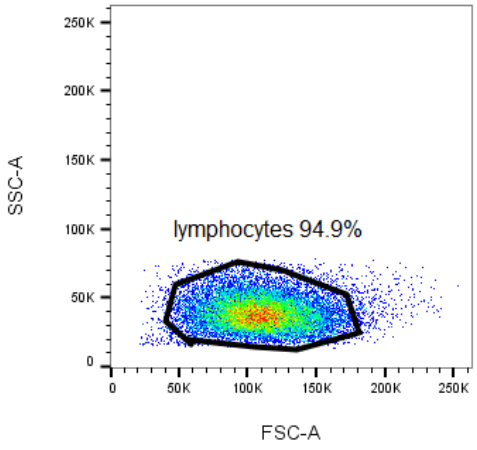

(c) Division into different immune cells subsets (Figure F3)

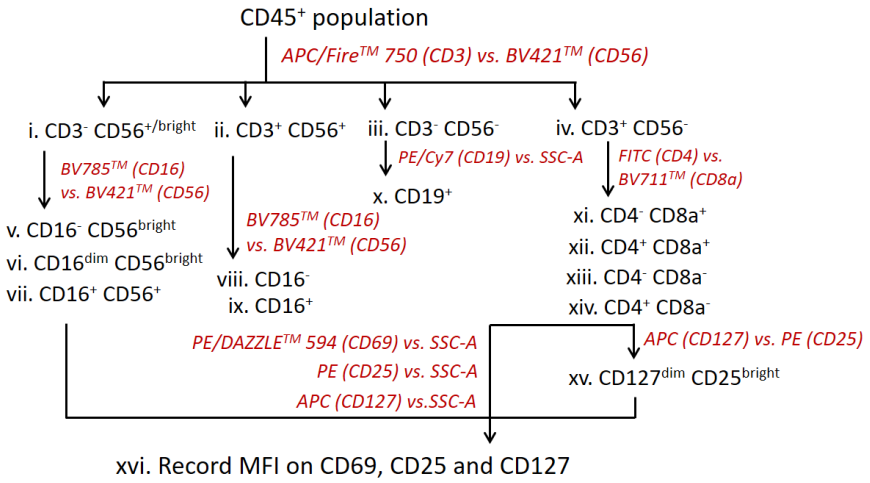

Figure F3. Gating hierarchy for PBMCs and HECs analysis, division into different immune cell subsets.

i, ii, iii, iv. Plot APC/Fire™ 750 (CD3) vs. BV421™ (CD56), apply quad as illustrated below. i, $CD3^{-}$ $CD56^{+/bright}$ population is located on the upper left; ii, $CD3^{+}$ $CD56^{+}$ population is located on the upper right; iii, $CD3^{-}$ $CD56^{-}$ population is located on the bottom left; iv, $CD3^{+}$ $CD56^{-}$ population is located on the bottom right.

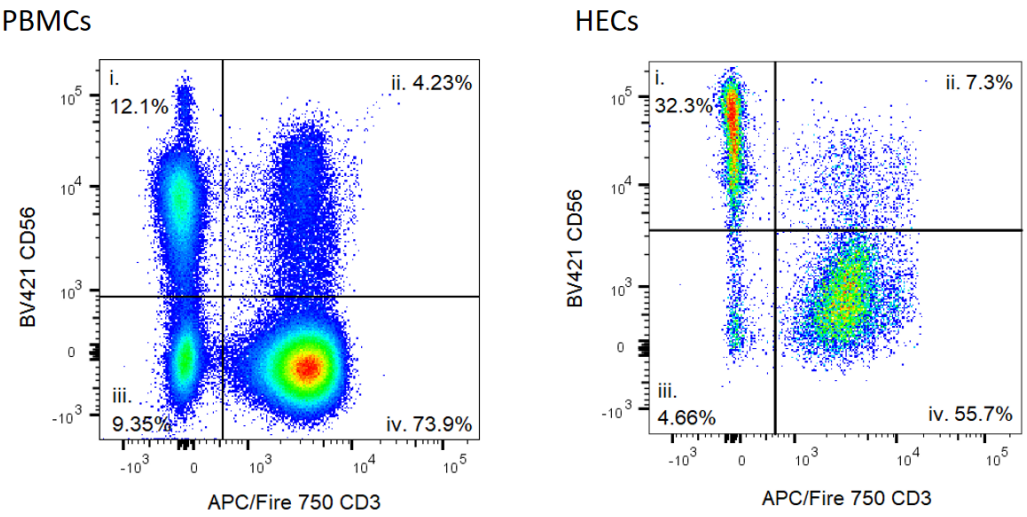

For i, CD3^{-} CD56$^{+/bright}$ population,

v, vi, vii. Plot BV785^{TM} (CD16) vs. BV421^{TM} (CD56). Apply quad and a subsequent gate to separate CD16^{dim} CD56^{bright} and CD16^{+} CD56^{+} as illustrated below.

v, CD16^{-} CD56^{bright} population is located on upper left; vi, CD16^{dim} CD56^{bright} population is located on upper middle; vii, CD16^{+} CD56^{+} population is located on middle right.

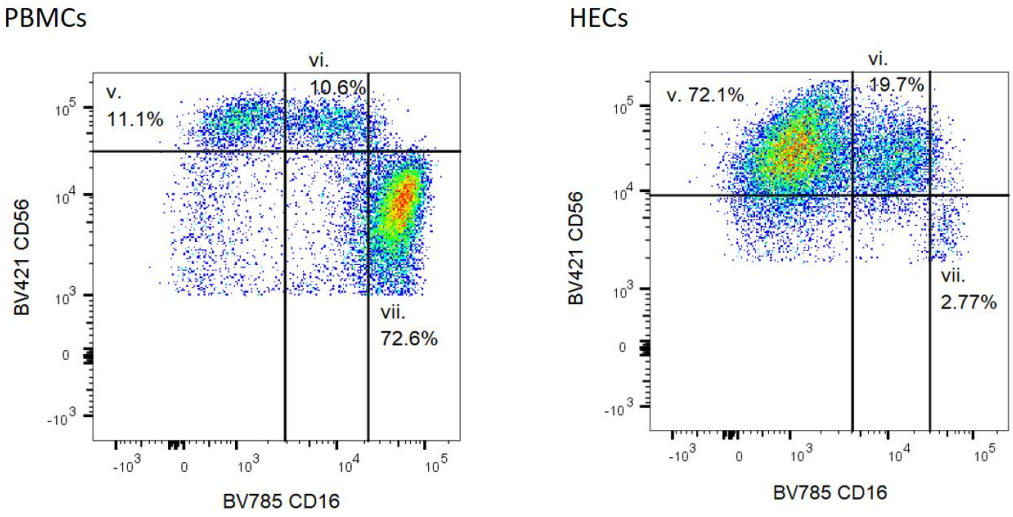

For iii, CD3^{-} CD56^{-} population,

x. Plot PE/Cy7 (CD19) vs. SSC-A, gate on CD19^{+} population located on the right.

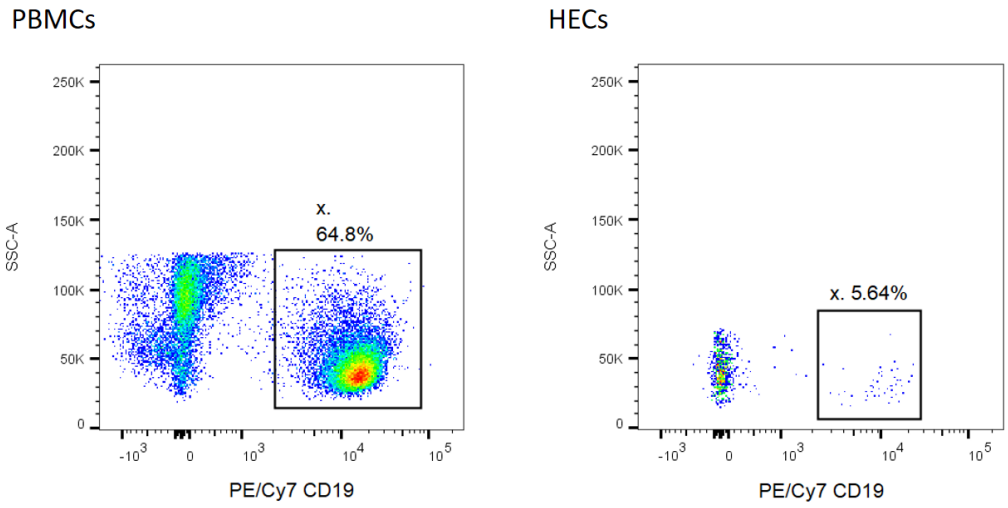

For iv, CD3$^+$ CD56$^-$ population,

xi, xii, xiii, xiv. Plot FITC (CD4) vs. BV711^{TM} (CD8a), apply quad as illustrated below.

xi, CD4$^-$ CD8a$^+$ population is located on the upper left; xii, CD4$^+$ CD8a$^+$ population is located on the upper right; xiii, CD4$^-$ CD8a$^-$ population is located on the bottom left; xiv, CD4$^+$ CD8a$^-$ population is located on the bottom right.

PBMCs

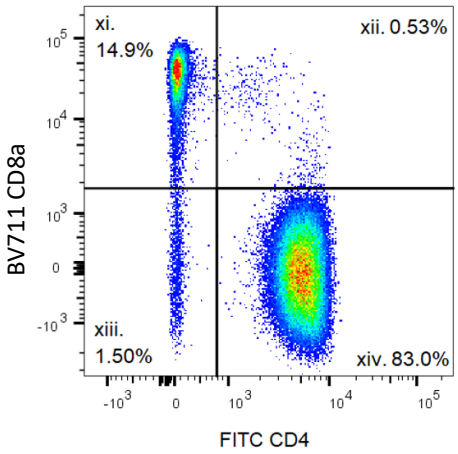

HECs

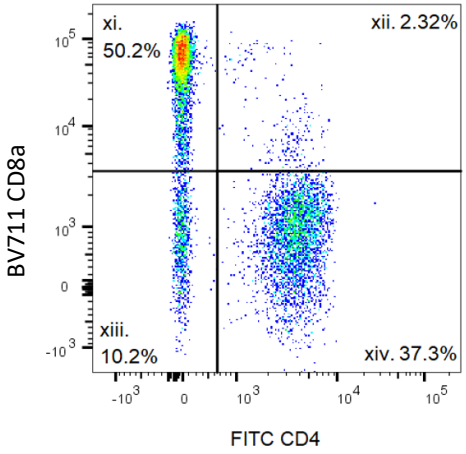

For xiv, CD4$^+$ CD8a$^-$ population,

xv. Plot APC (CD127) vs. PE (CD25), gate on CD127^{dim} CD25$^+$ population located on upper left. Avoid the population with greatest event density.

PBMCs

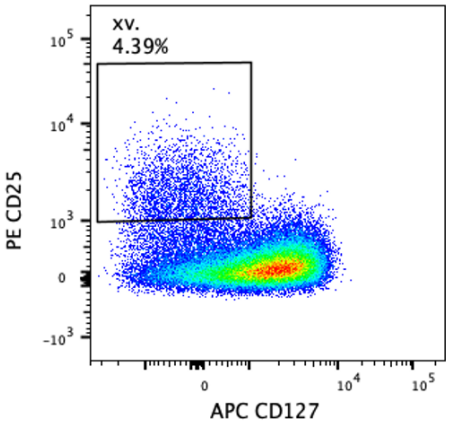

HECs

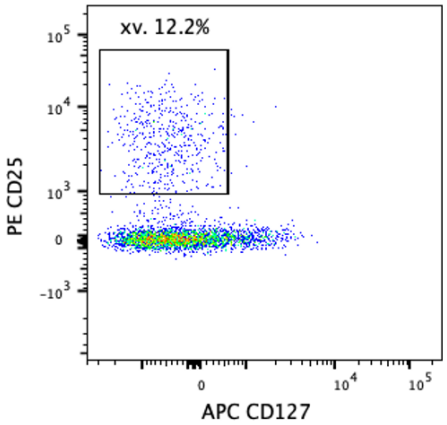

For v, CD16^{-} CD56^{bright} population; vi, CD16^{dim} CD56^{bright}; vii, CD16^{+} CD56^{+}; xi, CD4^{-} CD8a^{+}; xiv, CD4^{+} CD8a^{-}

For PBMCs,

xvi. Plot PE/DAZZLE^{TM} 594 (CD69) vs. SSC-A, record the MFI value in corresponding excel sheet.

Plot PE (CD25) vs. SSC-A, record the MFI value in corresponding excel sheet.

Plot APC (CD127) vs. SSC-A, record the MFI value in corresponding excel sheet.

For HECs,

xvi. Plot PE/DAZZLE^{TM} (CD69) vs. SSC-A, gate on CD69+ population, apply same gates for all subsets.

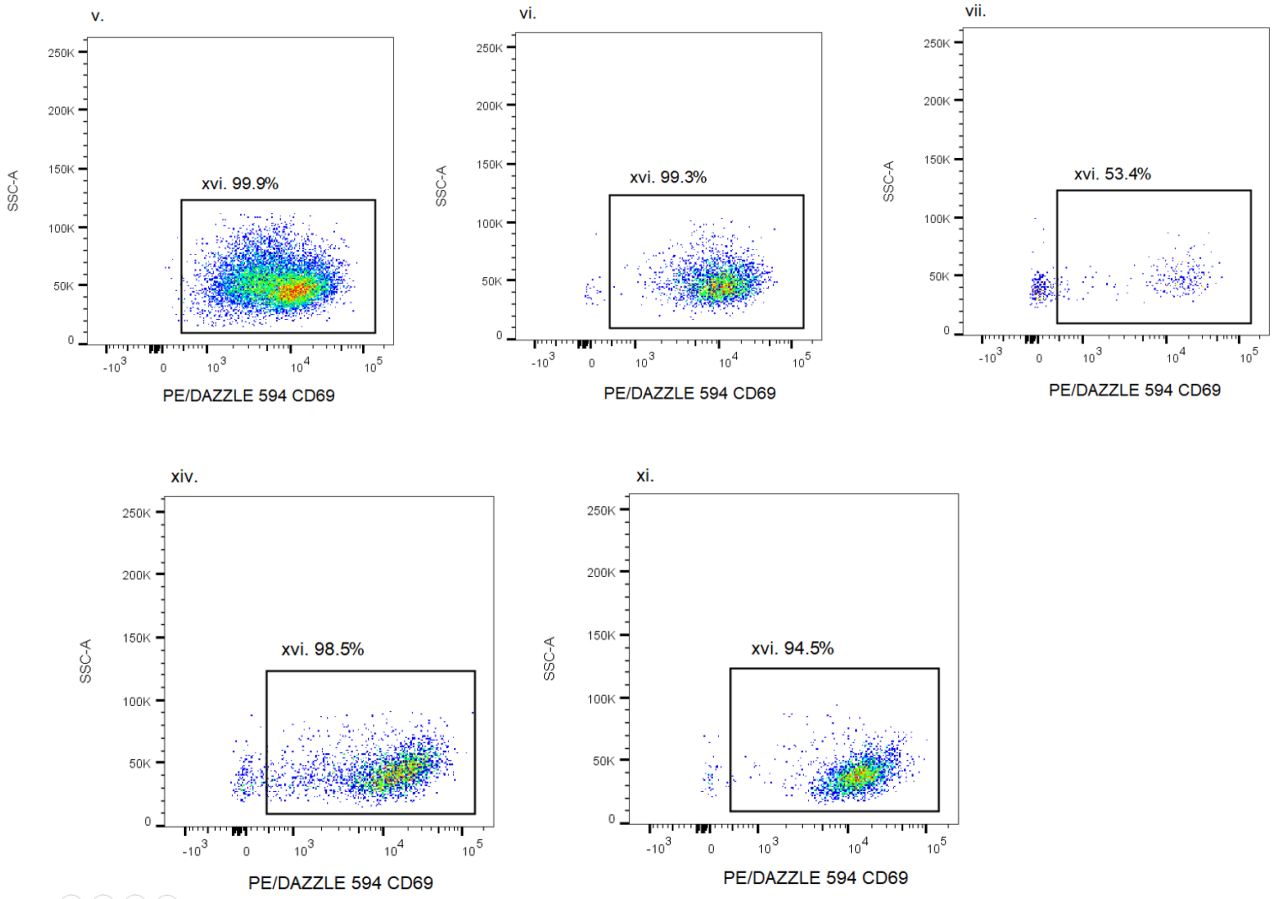

Plot PE (CD25) vs. SSC-A, record the MFI value in corresponding excel sheet.

Plot APC (CD127) vs. SSC-A, record the MFI value in corresponding excel sheet.

G. Comparison between PBMCs and HECs in flow analysis (Table G1, Table G2)

Gating plot	PBMCs	HECs
FSC-A vs. SSC-A	Immune cells usually locate in the middle	Immune cells are surrounded by stromal cells population
BV510^{TM} (Zombie Aqua^{TM}) vs. SSC-A	2-3 populations can be visualized: debris, dead cells, target cells, *etc.*	3-4 populations can be visualized: live stromal cells, live immune cells, dead cells, debris, *etc.*
BV650^{TM} (CD45) vs. SSC-A	Main proportion is BV650^{TM} CD45^{+}	Only a small proportion of cells is BV650^{TM} CD45^{+}, there are two BV650^{TM} CD45^{+} population
APC/Fire^{TM} 750 (CD3) vs. BV421^{TM} (CD56)	Can identify different cell subset based on their BV421^{TM} CD56 intensity	only BV421^{TM} CD56^{+} can be identified not BV421^{TM} CD56^{bright}
BV785^{TM} (CD16) vs. BV421^{TM} (CD56)	Most cells are BV785^{TM} CD16^{+}, while others being BV421^{TM} CD56^{bright} with different level of BV785^{TM} CD16 expression	Majority of cells are BV785^{TM} CD16$^{-/dim}$
FITC (CD4) vs. BV711^{TM} (CD8a)	Majority of cells are FITC CD4^{+}	Majority of cells are BV711^{TM} CD8^{+}
PE/DAZZLE^{TM} 594 (CD69) vs. SSC-A	No obvious positive population	Positive population is easily identified in all cell types

Table G1. Main differences of flow profile between PBMCs and HECs.

Cell Type	PBMCs (%)	HECs (%)
CD45^{+} Zombie Aqua^{TM-} (of total events)	60.4 (±8)	2.7 (±1)
v, vi, CD16$^{-/dim}$ CD56^{bright}	1.96 (±2)	-
vii, CD16^{+} CD56^{+}	10.6 (±5)	41.7 (+25; -9)
iv, CD3^{+}	75 (±7)	44.8 (+9; -19)
xiv, CD4^{+} CD8a^{-}	57.85 (±14)	17.2 (±8)
xi, CD4^{-} CD8a^{+}	13.7 (±8)	18.8 (±12)
x, CD19^{+}	5.57 (±5)	1.0 (±2)
xv, CD127^{dim} CD25^{bright}	3.35 (±2)	2.2 (±1)

Table G2. Comparison of major cell percentage (of CD45^{+} Zombie Aqua^{TM-}) in PBMCs and HECs, mean value, n ≥ 5.

Recipes

Note: Ensure sterility. Work in a Class II microbiological safety cabinet and ensure full aseptic technique.

1. PBS/2% FCS
   49 ml Phosphate-buffered saline, PBS (SIGMA, catalogue number: D8537)
   1 ml Fetal bovine serum (Sera Laboratories International Ltd, catalogue number: EU-000-F)
2. DNase I aliquot
   Dissolve DNase I powder in 0.15 M NaCl (5 mg/ml)
   Prepare 10 mg/ml 10 µl stock aliquots
3. Collagenase D aliquot
   Dissolve Collagenase D powder in PBS/ 10%FCS
   Prepare 20 mg/ml 100 µl stock aliquots
4. Digestion media
   500 ml Dulbecco's Modified Eagle's Medium/Nutrient Mixture F-12 Ham
   50 ml Fetal bovine serum (Sera Laboratories International Ltd, catalogue number: EU-000-F)
5. Zombie Aqua™ aliquot
   Pre-warm Zombie Aqua™ kit to room temperature
   Add 100 µl of DMSO to one vial of Zombie Aqua ™ dye and mix until fully dissolved
   Prepare 1 µl stock aliquots
6. Freezing Medium
   40 ml Fetal bovine serum (Sera Laboratories International Ltd, catalogue number: EU-000-F)
   4 ml Dimethyl sulfoxide (Sigma)

Appendix C

Endometrial T cell RNA isolation, quantification and QC

Gating strategy of endometrial T cell sorting

Endometrial biopsies were collected during the mid-luteal phase of the menstrual cycle and digested by Collagenase D. Different subsets of T cells ($CD25^{bright}$ $CD127^{dim/-}$ Treg cells, $CD4^+$ non-Treg T cells, $CD8^+$ T cells) were obtained by cell sorting using an AriaIII (BD) from endometrial biopsy digests. In total, 2306 ± 1919 (mean ± SD) $CD25^{bright}$ $CD127^{dim/-}$ Treg cells, 31422 ± 31710 (mean ± SD) $CD4^+$ non-Treg T cells, and 29058 ± 23021 (mean ± SD) $CD8^+$ T cells were collected.

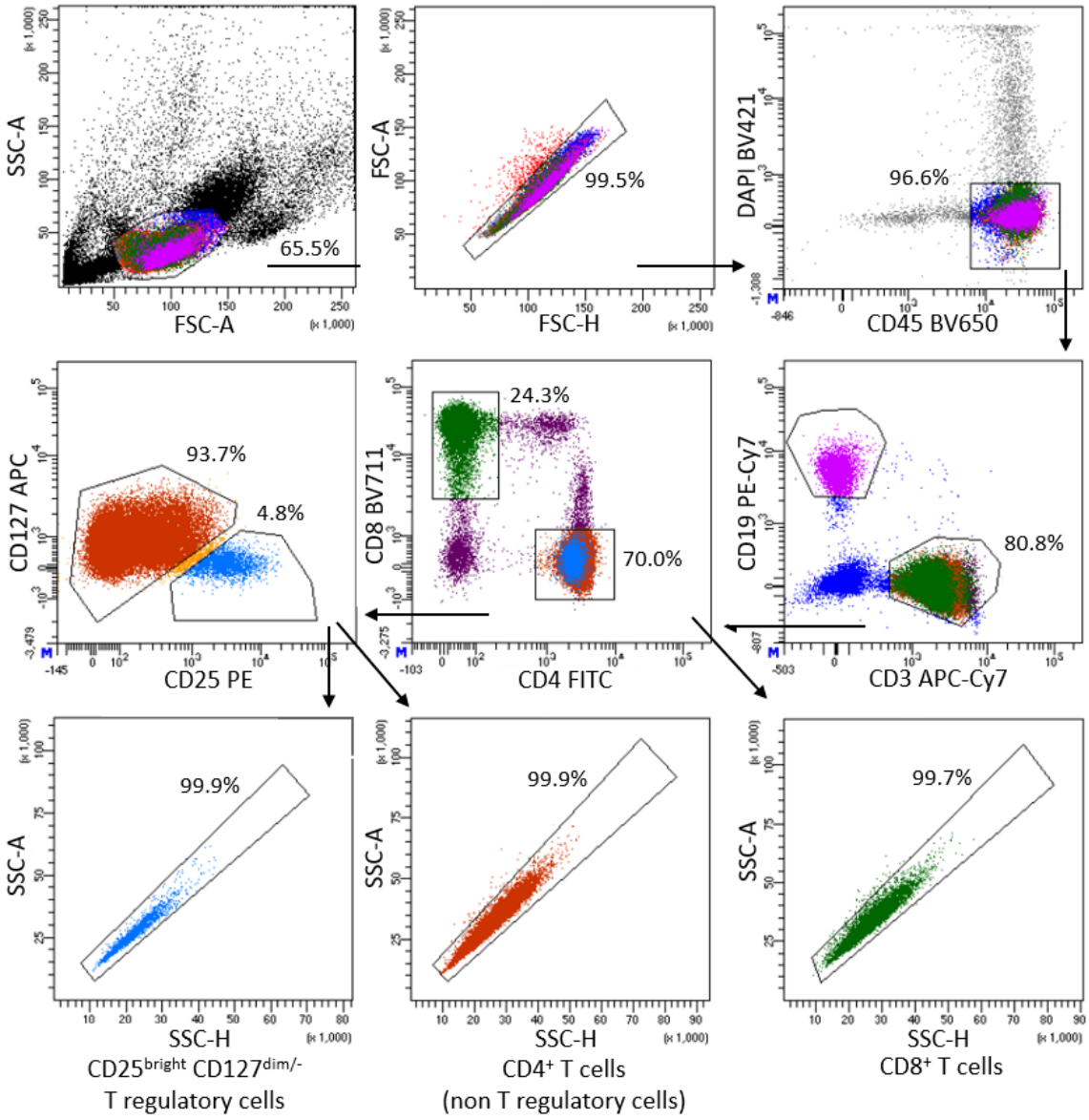

Endometrial Treg cells RNA quality assessment

$CD25^{bright}$ $CD127^{dim/-}$ Treg cells were obtained from endometrial biopsy digests (n=26) by cell sorting and RNA was isolated using QIAGEN RNeasy Mini Kit. RNA quantity and quality were then accessed on Agilent 4200 TapeStation System, High Sensitivity RNA ScreenTape. Total RNA quality assessment based on 18S (1869nt) and 28S rRNA (5070nt). On the left side, marker lane shows electronic RNA ladder. RINe values are displayed below each lane. RNA concentration for all $CD25^{bright}$ $CD127^{dim/-}$ Treg cells were 59.2 $\pm$ 35.5 pg/μl (mean $\pm$ SD).

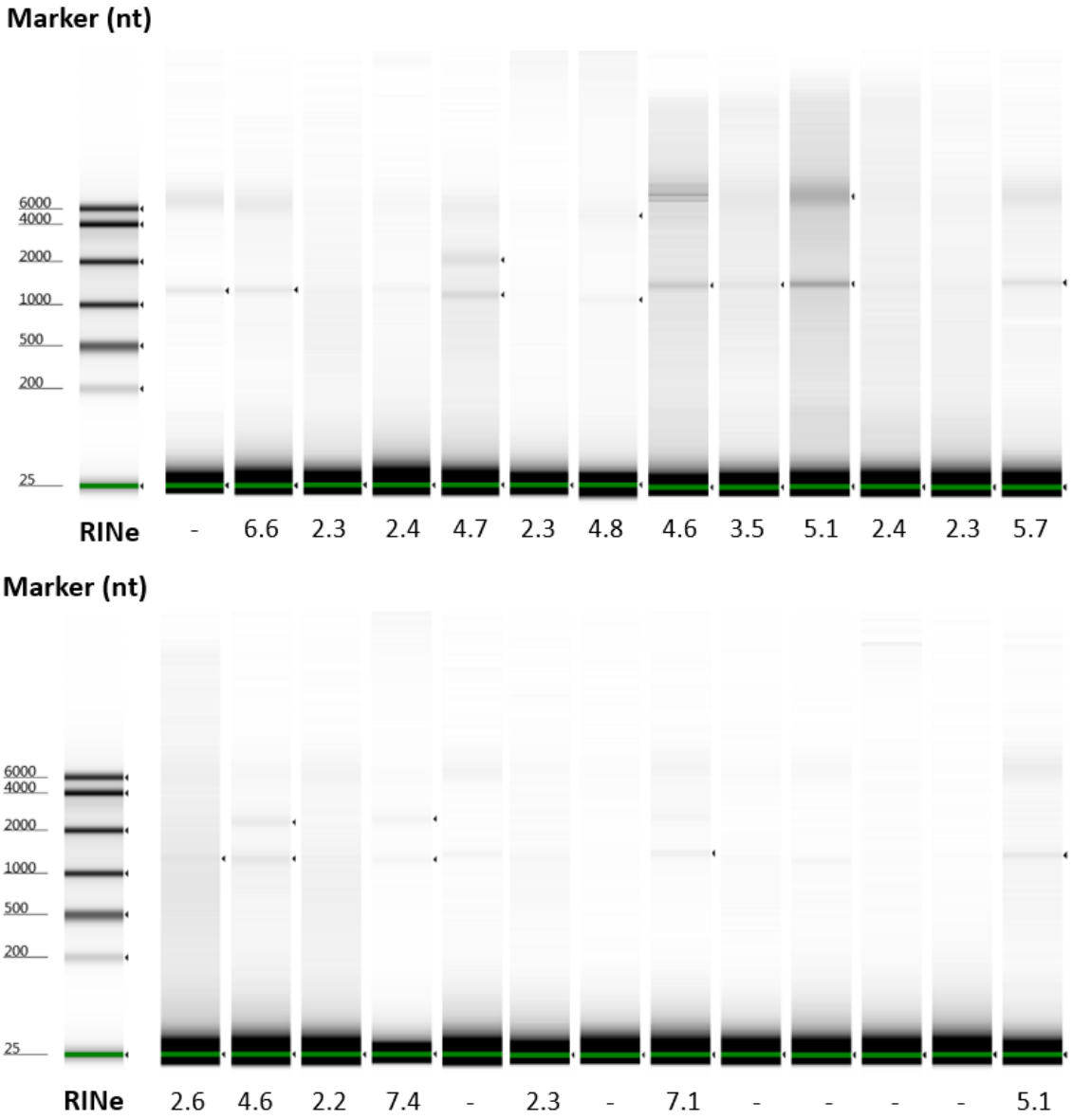

Endometrial CD4$^+$ non-Treg T cells RNA quality assessment

CD4$^+$ non-Treg T cells were obtained from endometrial biopsy digests (n=26) by cell sorting and RNA was isolated using QIAGEN RNeasy Mini Kit. RNA quantity and quality were then accessed on Agilent 4200 TapeStation System, High Sensitivity RNA ScreenTape. Total RNA quality assessment based on 18S (1869nt) and 28S rRNA (5070nt). On the left side, marker lane shows electronic RNA ladder. RINe values are displayed below each lane. RNA concentration for all CD4$^+$ non-Treg T cells were 508.1 $\pm$ 727.2 pg/μl (mean $\pm$ SD).

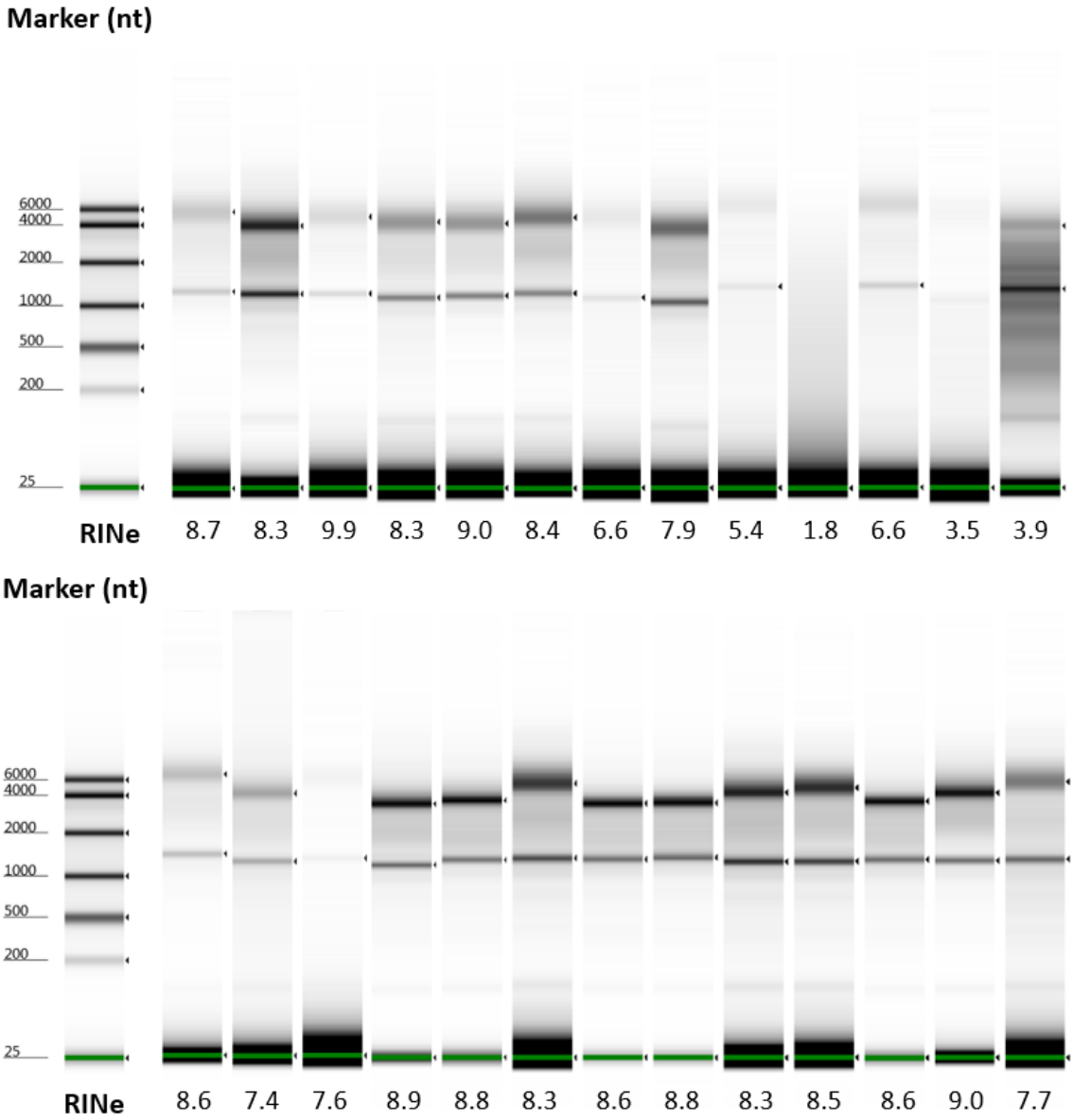

Endometrial CD8$^+$ T cells RNA quality assessment

CD8$^+$ T cells were obtained from endometrial biopsy digests (n=26) by cell sorting and RNA was isolated using QIAGEN RNeasy Mini Kit. RNA quantity and quality were then accessed on Agilent 4200 TapeStation System, High Sensitivity RNA ScreenTape. Total RNA quality assessment based on 18S (1869nt) and 28S rRNA (5070nt). On the left side, marker lane shows electronic RNA ladder. RINe values are displayed below each lane. RNA concentration for all CD8$^+$ T cells were 495.6 $\pm$ 731.7 pg/μl (mean $\pm$ SD).

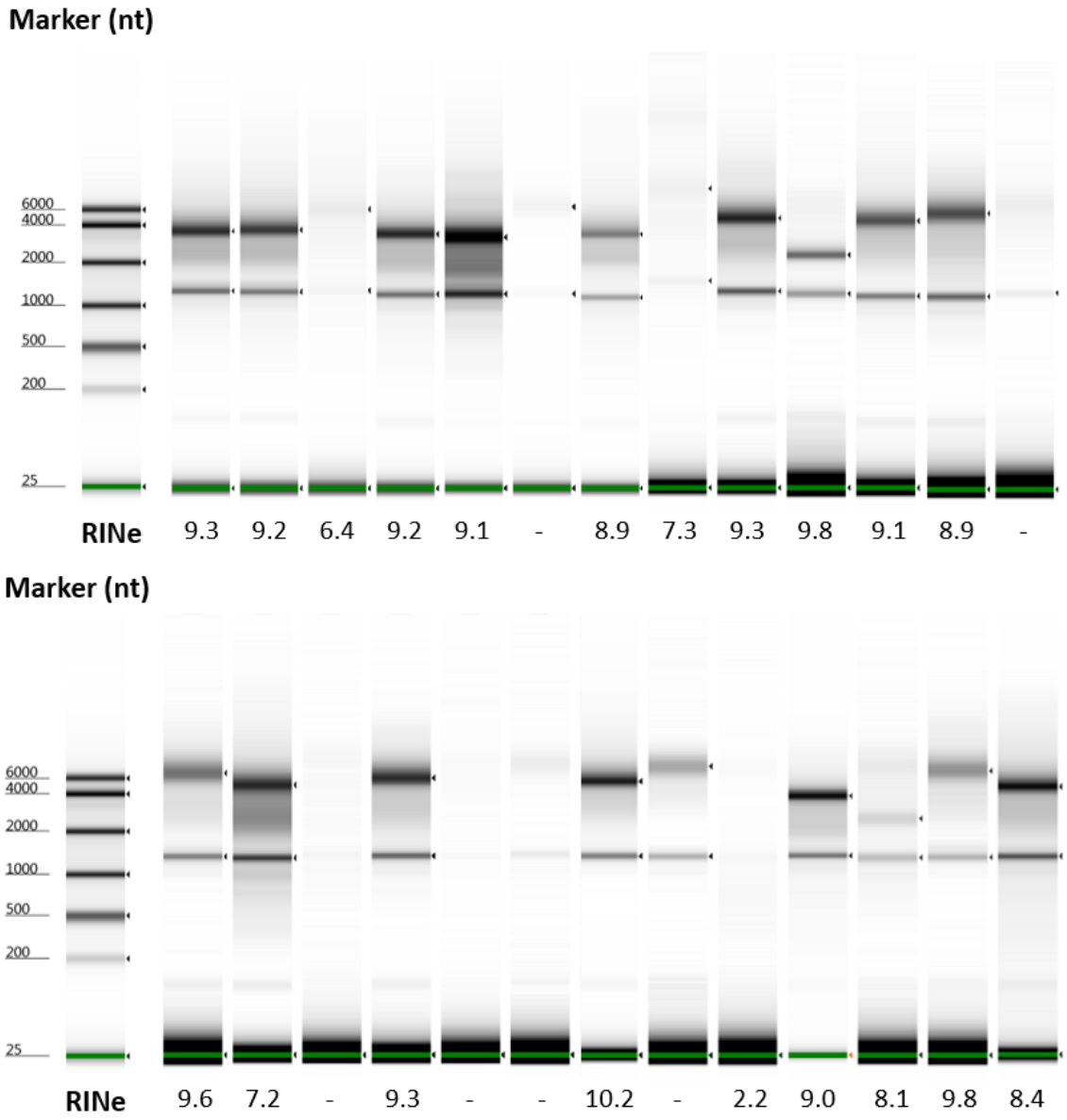

Endometrial T cells RNA sequencing QC results

Representative figures of endometrial T cell RNA sequencing QC results (n=26 for $CD25^{bright}$ $CD127^{dim/-}$ Treg cells, $CD4^{+}$ T cells and $CD8^{+}$ T cells). (a-c) Quality control of raw data. The base position is on the x-axis and the single base percentage is on the y-axis. The left part of the distribution is for reads1 and the right part is for reads2. (a) Distribution of sequencing error rate along reads, (b) distribution of A/T/G/C base along reads, (c) distribution of sequencing quality along reads, shown in quality score.

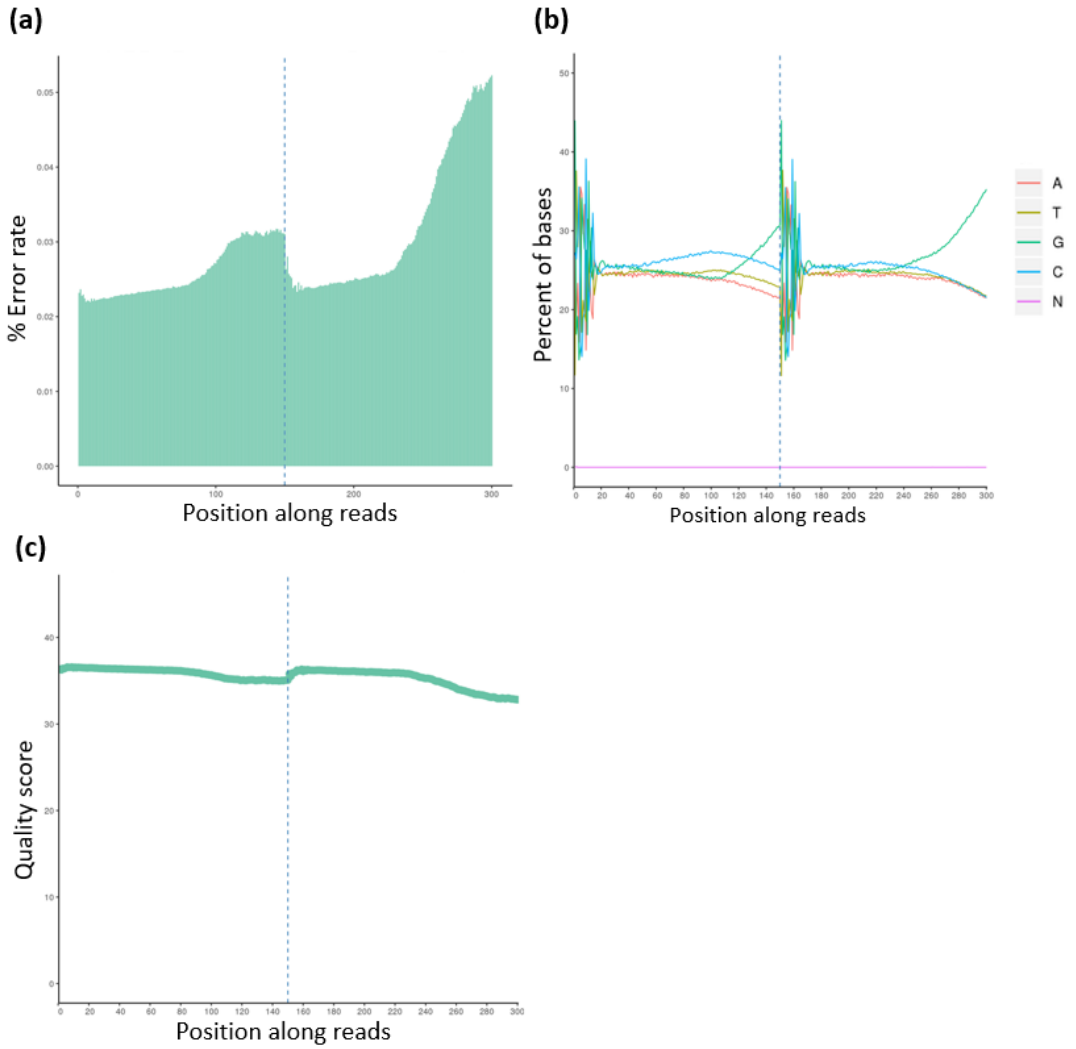

The following tables present the summary of RNA sequencing QC results for all endometrial T cell samples, including $CD25^{bright}$ $CD127^{dim/-}$ Treg cells, $CD4^+$ non-Treg T cells and $CD8^+$ T cells. Raw reads number, raw bases number: (total raw reads) x (sequence length), calculated in billion (G), error rate: base error rate, quality score Q20 and Q30: (Base count of Phred value $>$ 20 or 30) / (Total base count) and GC content: (G & C base count) / (Total base count) are detailed for each sample.

Sample	Raw reads No.	Raw bases No.	Error rate (%)	Q20 (%)	Q30 (%)	GC content (%)
Treg.1	27929713	8.4G	0.03	95.81	91.22	51.20
Treg.2	33145104	9.9G	0.03	95.81	91.27	51.48
Treg.3	42933390	12.9G	0.03	96.13	92.03	48.50
Treg.4	18407328	5.5G	0.03	96.29	91.97	51.58
Treg.5	31875377	9.6G	0.03	95.99	91.45	50.32
Treg.6	68465714	20.5G	0.04	93.84	89.33	51.40
Treg.7	35856443	10.8G	0.03	95.61	90.28	50.08
Treg.8	34374203	10.3G	0.03	96.58	92.28	51.98
Treg.9	35397544	10.6G	0.03	96.52	91.94	51.70
Treg.10	32962322	9.9G	0.03	96.82	92.75	52.07
Treg.11	32685111	9.8G	0.03	96.86	92.37	51.20
Treg.12	31938217	9.6G	0.03	96.88	92.57	51.95
Treg.13	36786910	11.0G	0.03	96.89	92.31	51.25
Treg.14	43920271	13.2G	0.04	94.16	89.09	52.52
Treg.15	36380859	10.9G	0.03	96.38	92.06	51.53
Treg.16	28392261	8.5G	0.03	95.75	90.99	51.97
Treg.17	167802	0.1G	0.04	94.31	87.93	51.23
Treg.18	20499641	6.1G	0.03	96.93	92.55	51.86
Treg.19	28334432	8.5G	0.03	96.56	92.17	52.97
Treg.20	27413047	8.2G	0.03	96.22	91.56	51.95
Treg.21	31875796	9.6G	0.03	96.49	91.95	51.08
Treg.22	27555237	8.3G	0.03	95.76	90.68	50.65
Treg.23	29637292	8.9G	0.03	96.63	92.15	51.41
Treg.24	27121337	8.1G	0.03	96.17	91.66	52.73
Treg.25	532628	0.2G	0.03	95.91	90.75	50.49
Treg.26	30852621	9.3G	0.03	96.79	92.60	51.12

Sample	Raw reads No.	Raw bases No.	Error rate (%)	Q20 (%)	Q30 (%)	GC content (%)
CD4.1	35588451	10.7G	0.03	96.22	91.91	52.36
CD4.2	30742641	9.2G	0.03	96.84	92.57	51.67
CD4.3	26095458	7.8G	0.03	97.25	93.25	52.30
CD4.4	26609721	8.0G	0.03	96.78	92.39	51.70
CD4.5	31051180	9.3G	0.03	96.50	92.16	52.05
CD4.6	39424906	11.8G	0.03	96.54	92.22	51.84
CD4.7	39700937	11.9G	0.03	96.42	92.02	51.70
CD4.8	34895146	10.5G	0.03	96.97	92.81	51.74
CD4.9	28957758	8.7G	0.03	96.27	91.77	52.44
CD4.10	27871934	8.4G	0.03	96.58	92.09	51.19
CD4.11	31058978	9.3G	0.03	97.25	93.21	51.99
CD4.12	28186734	8.5G	0.03	96.70	92.28	52.21
CD4.13	21755572	6.5G	0.03	96.53	91.91	50.88
CD4.14	21150588	6.3G	0.03	96.81	92.25	51.47
CD4.15	29062003	8.7G	0.03	96.77	92.33	51.16
CD4.16	32167717	9.7G	0.03	96.16	91.65	52.40
CD4.17	29840330	9.0G	0.03	96.56	92.29	52.18
CD4.18	28045481	8.4G	0.03	95.59	90.98	54.80
CD4.19	27991544	8.4G	0.03	97.06	92.86	52.34
CD4.20	24711341	7.4G	0.03	96.53	92.11	54.23
CD4.21	31608098	9.5G	0.03	96.91	92.56	51.09
CD4.22	30719509	9.2G	0.03	96.28	91.64	51.47
CD4.23	32053058	9.6G	0.03	97.04	92.81	51.47
CD4.24	33600729	10.1G	0.03	96.02	90.77	53.59
CD4.25	30150902	9.0G	0.03	96.95	92.77	52.39
CD4.26	29751530	8.9G	0.03	97.06	92.84	52.22

Sample	Raw reads No.	Raw bases No.	Error rate (%)	Q20 (%)	Q30 (%)	GC content (%)
CD8.1	27827491	8.3G	0.03	97.09	92.91	51.98
CD8.2	22379364	6.7G	0.03	96.91	92.58	51.28
CD8.3	25669184	7.7G	0.03	96.73	92.44	51.06
CD8.4	25622099	7.7G	0.03	96.49	91.90	53.23
CD8.5	30901479	9.3G	0.03	96.25	91.53	51.74
CD8.6	28131170	8.4G	0.03	96.10	91.38	52.61
CD8.7	234786549	70.4G	0.03	96.87	92.42	51.96
CD8.8	26675396	8.0G	0.03	96.87	92.43	51.16
CD8.9	22345522	6.7G	0.03	96.66	92.09	51.81
CD8.10	32495444	9.7G	0.03	96.03	91.34	51.66
CD8.11	34070972	10.2G	0.03	96.41	91.84	51.70
CD8.12	30493722	9.1G	0.03	95.98	91.15	51.80
CD8.13	25926678	7.8G	0.03	96.85	92.28	51.36
CD8.14	31620795	9.5G	0.03	96.42	91.67	51.99
CD8.15	32265897	9.7G	0.03	96.61	92.26	51.91
CD8.16	35036332	10.5G	0.03	96.81	92.69	51.09
CD8.17	27803583	8.3G	0.03	96.44	92.03	51.25
CD8.18	32968141	9.9G	0.03	96.78	92.41	51.72
CD8.19	29570704	8.9G	0.03	96.35	91.59	51.72
CD8.20	33184196	10.0G	0.03	97.00	92.78	52.14
CD8.21	34120973	10.2G	0.03	95.05	90.04	52.27
CD8.22	30123704	9.0G	0.03	96.40	91.67	51.48
CD8.23	26815047	8.0G	0.03	96.70	92.29	50.92
CD8.24	29670264	8.9G	0.03	96.47	92.02	51.52
CD8.25	27534559	8.3G	0.03	95.97	91.31	51.48
CD8.26	35372994	10.6G	0.03	96.48	92.03	51.53

Appendix D

Negative controls for endometrial B cell flow cytometric analysis

FMO control for CD69 and CD62L, in B cell residency and activation flow panel

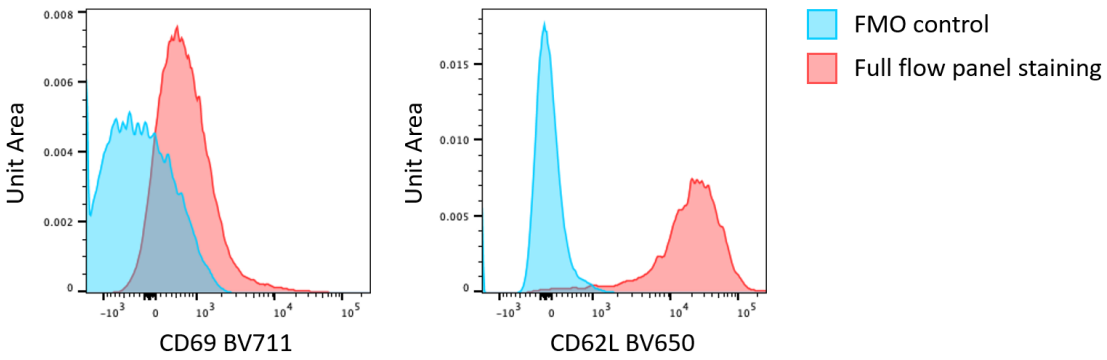

FMO control for CD74, CD83 and HLA-DR, in B cell residency and activation flow panel

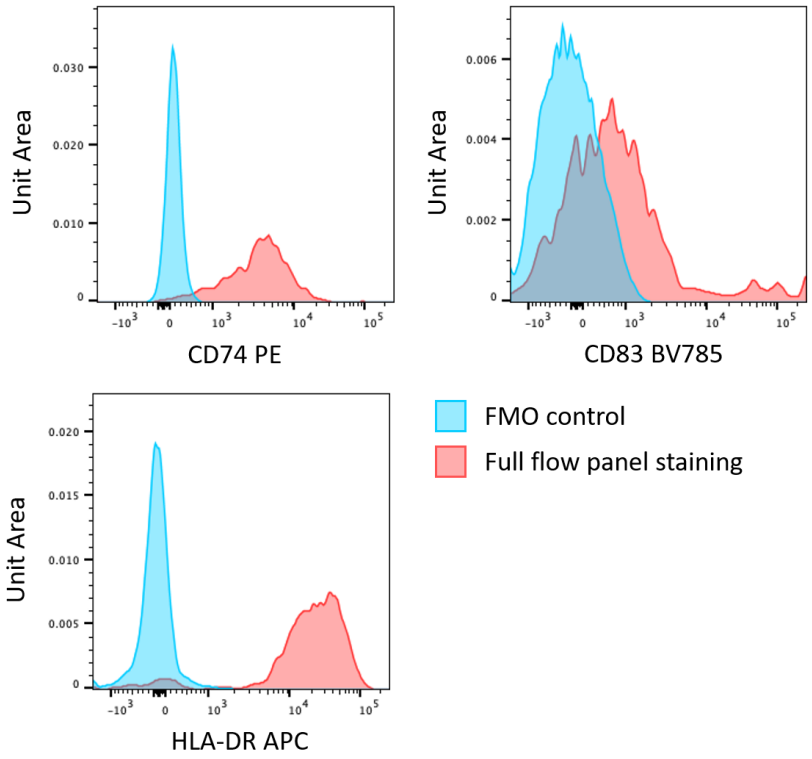

FMO control for FAS, IgD and BCL6, in Tfh and GC B cell flow panel

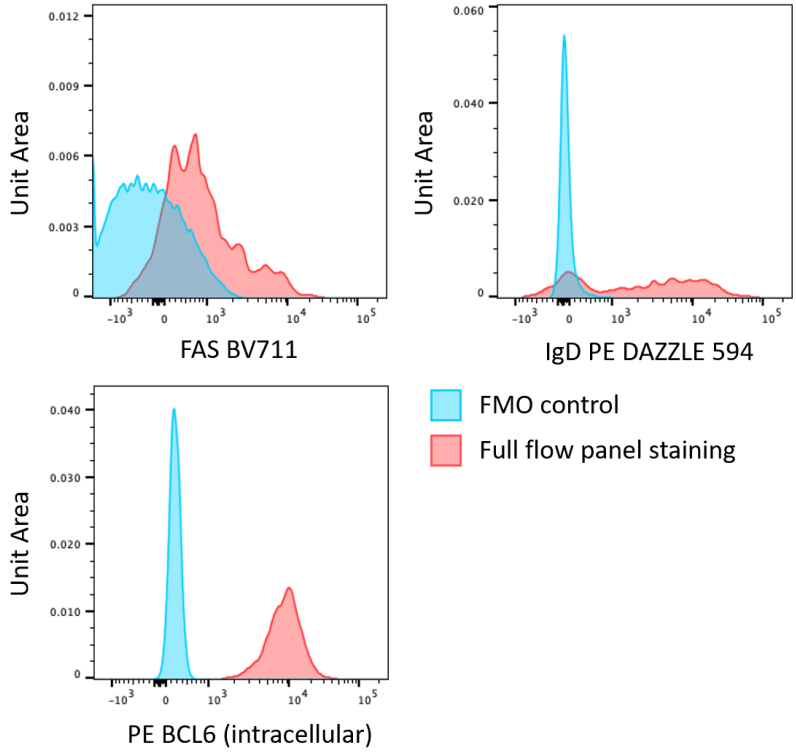

FMO control for PD1, ICOS and CXCR5, in Tfh and GC B cell flow panel

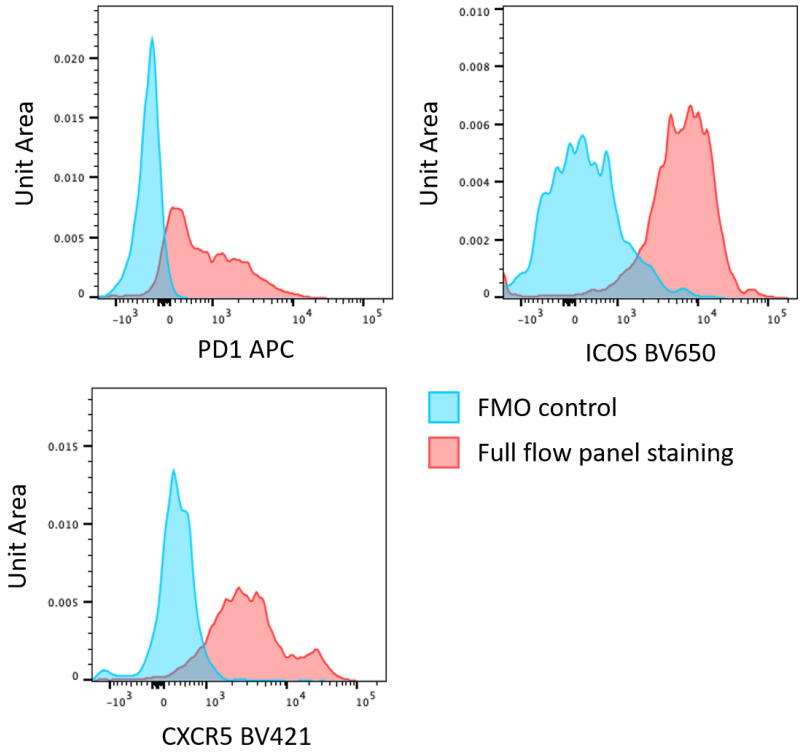

References

Abdolmohammadi, V. S., Ghaebi, M., Ahmadi, M., Nouri, M., Danaei, S., Aghebati-Maleki, L., Mousavi Ardehaie, R., Yousefi, B., Hakimi, P., Hojjat-Farsangi, M. et al.: 2019, Altered T-cell subpopulations in recurrent pregnancy loss patients with cellular immune abnormalities, *Journal of cellular physiology* **234**(4), 4924–4933.

Adachi, Y., Onodera, T., Yamada, Y., Daio, R., Tsuiji, M., Inoue, T., Kobayashi, K., Kurosaki, T., Ato, M. and Takahashi, Y.: 2015, Distinct germinal center selection at local sites shapes memory B cell response to viral escape, *Journal of Experimental Medicine* **212**(10), 1709–1723.

Agematsu, K., Hokibara, S., Nagumo, H. and Komiyama, A.: 2000, CD27: a memory B-cell marker, *Immunology today* **21**(5), 204–206.

Ahmad, F., Hong, H. S., Jäckel, M., Jablonka, A., Lu, I.-N., Bhatnagar, N., Eberhard, J. M., Bollmann, B. A., Ballmaier, M., Zielinska-Skowronek, M. et al.: 2014, High frequencies of polyfunctional CD8+ NK cells in chronic HIV-1 infection are associated with slower disease progression, *Journal of virology* **88**(21), 12397–12408.

Akkaya, M., Kwak, K. and Pierce, S. K.: 2020, B cell memory: building two walls of protection against pathogens, *Nature Reviews Immunology* **20**(4), 229–238.

Alhalabi, M., Samawi, S., Taha, A., Kafri, N., Modi, S., Khatib, A., Sharif, J. and Othman, A.: 2011, Prednisolone improves implantation in ICSI patients with high peripheral CD69+ NK Cells, *Human Reproduction*, Vol. 26, Oxford Univ Press, pp. I219–I219.

Allen, H. C. and Sharma, P.: 2020, Histology, Plasma Cells, *StatPearls*, StatPearls Publishing.

Allie, S. R., Bradley, J. E., Mudunuru, U., Schultz, M. D., Graf, B. A., Lund, F. E. and Randall, T. D.: 2019, The establishment of resident memory B cells in the lung requires local antigen encounter, *Nature immunology* **20**(1), 97–108.

Almquist, L. D., Likes, C. E., Stone, B., Brown, K. R., Savaris, R., Forstein, D. A., Miller, P. B. and Lessey, B. A.: 2017, Endometrial BCL6 testing for the prediction of in vitro fertilization outcomes: a cohort study, *Fertility and sterility* **108**(6), 1063–1069.

Altmäe, S., Koel, M., Võsa, U., Adler, P., Suhorutšenko, M., Laisk-Podar, T., Kukushkina, V., Saare, M., Velthut-Meikas, A., Krjutškov, K. et al.: 2017, Meta-signature of human endometrial receptivity: a meta-analysis and validation study of transcriptomic biomarkers, *Scientific reports* **7**(1), 1–15.

Altmäe, S., Martinez-Conejero, J., Salumets, A., Simon, C., Horcajadas, J. and Stavreus-Evers, A.: 2009, Endometrial gene expression analysis at the time of embryo implantation in women with unexplained infertility, *MHR: Basic science of reproductive medicine* **16**(3), 178–187.

Aluvihare, V. R., Kallikourdis, M. and Betz, A. G.: 2004, Regulatory T cells mediate maternal tolerance to the fetus, *Nature immunology* **5**(3), 266–271.

Amu, S. and Brisslert, M.: 2011, Phenotype and function of CD25-expressing B lymphocytes isolated from human umbilical cord blood, *Clinical and Developmental Immunology* **2011**.

Anders, S., Pyl, P. T. and Huber, W.: 2015, HTSeq—a Python framework to work with high-throughput sequencing data, *Bioinformatics* **31**(2), 166–169.

Andrews, W., Buttram Jr, V., Weed, J., Hammond, C. and Thomas, H.: 1985, Revised American fertility society classification of endometriosis: 1985, *Fertility and sterility* **43**(3), 351–352.

Antsiferova, Y. S., Sotnikova, N. Y., Posiseeva, L. V. and Shor, A. L.: 2005, Changes in the T-helper cytokine profile and in lymphocyte activation at the systemic and local levels in women with endometriosis, *Fertility and sterility* **84**(6), 1705–1711.

Ashburner, M., Ball, C. A., Blake, J. A., Botstein, D., Butler, H., Cherry, J. M., Davis, A. P., Dolinski, K., Dwight, S. S., Eppig, J. T. et al.: 2000, Gene ontology: tool for the unification of biology, *Nature genetics* **25**(1), 25–29.

Autengruber, A., Gereke, M., Hansen, G., Hennig, C. and Bruder, D.: 2012, Impact of enzymatic tissue disintegration on the level of surface molecule expression and immune cell function, *European Journal of Microbiology and Immunology* **2**(2), 112–120.

Bakhtiyar, K., Beiranvand, R., Ardalan, A., Changaee, F., Almasian, M., Badrizadeh, A., Bastami, F. and Ebrahimzadeh, F.: 2019, An investigation of the effects of infertility on women's quality of life: a case-control study, *BMC women's health* **19**(1), 1–9.

Balagué, O. and Martínez, A.: 2015, What is a plasmablast? A commentary to:"Plasmablastic lymphoma versus diffuse large B-cell lymphoma with plasmablastic differentiation: proposal for a novel diagnostic scoring system" by Sonja Catharina Boy et al., J. Hematopathol 2015, *Journal of Hematopathology* **8**(2), 51–52.

Basso, K. and Dalla-Favera, R.: 2010, BCL6: master regulator of the germinal center reaction and key oncogene in B cell lymphomagenesis, *Advances in immunology* **105**, 193–210.

Baumjohann, D., Okada, T. and Ansel, K. M.: 2011, Cutting edge: distinct waves of BCL6 expression during T follicular helper cell development, *The Journal of Immunology* **187**(5), 2089–2092.

Beer, A. E., Kwak, J. and Ruiz, J. E.: 1996, Immunophenotypic profiles of peripheral blood lymphocytes in women with recurrent pregnancy losses and in infertile women with multiple failed in vitro fertilization cycles., *American journal of reproductive immunology (New York, NY: 1989)* **35**(4), 376–382.

Benner, M., Feyaerts, D., García, C. C., Inci, N., López, S. C., Fasse, E., Shadmanfar, W., van der Heijden, O. W., Gorris, M. A., Joosten, I. et al.: 2020, Clusters of tolerogenic B cells feature in the dynamic immunological landscape of the pregnant uterus, *Cell Reports* **32**(13), 108204.

Béziat, V., Descours, B., Parizot, C., Debré, P. and Vieillard, V.: 2010, NK cell terminal differentiation: correlated stepwise decrease of NKG2A and acquisition of KIRs, *PloS one* **5**(8), e11966.

Bohlmann, M. K., Luedders, D. W., Strowitzki, T. and von Wolff, M.: 2010, Specific secretory phase endometrial leukocytes of women with two and more consecutive idiopathic abortions are not significantly different from healthy controls, *Archives of gynecology and obstetrics* **281**(6), 983–990.

Bohner, P., Chevalier, M. F., Cesson, V., Rodrigues-Dias, S.-C., Dartiguenave, F., Burruni, R., Tawadros, T., Valerio, M., Lucca, I., Nardelli-Haefliger, D. et al.: 2019, Double positive CD4+ CD8+ T cells are enriched in urological cancers and favor T helper-2 polarization, *Frontiers in immunology* **10**, 622.

Bouillon, M., El Fakhry, Y., Girouard, J., Khalil, H., Thibodeau, J. and Mourad, W.: 2003, Lipid raft-dependent and-independent signaling through HLA-DR molecules, *Journal of Biological Chemistry* **278**(9), 7099–7107.

Boyson, J. E., Rybalov, B., Koopman, L. A., Exley, M., Balk, S. P., Racke, F. K., Schatz, F., Masch, R., Wilson, S. B. and Strominger, J. L.: 2002, CD1d and invariant NKT cells at the human maternal–fetal interface, *Proceedings of the National Academy of Sciences* **99**(21), 13741–13746.

Brandtzaeg, P.: 2007, Induction of secretory immunity and memory at mucosal surfaces, *Vaccine* **25**(30), 5467–5484.

Bulmer, J. N. and Lash, G. E.: 2019, Uterine natural killer cells: Time for a re-appraisal?, *F1000Research* **8**.

Burgener, A., Tjernlund, A., Kaldensjo, T., Abou, M., McCorrister, S., Westmacott, G. R., Mogk, K., Ambrose, E., Broliden, K. and Ball, B.: 2013, A systems biology examination of the human female genital tract shows compartmentalization of immune factor expression, *Journal of virology* **87**(9), 5141–5150.

Busse, M., Campe, K.-N. J., Nowak, D., Schumacher, A., Plenagl, S., Langwisch, S., Tiegs, G., Reinhold, A. and Zenclussen, A. C.: 2019, IL-10 producing B cells rescue mouse fetuses from inflammation-driven fetal death and are able to modulate T cell immune responses, *Scientific reports* **9**(1), 1–10.

Campbell, J. P., Guy, K., Cosgrove, C., Florida-James, G. D. and Simpson, R. J.: 2008, Total lymphocyte CD8 expression is not a reliable marker of cytotoxic T-cell populations in human peripheral blood following an acute bout of high-intensity exercise, *Brain, behavior, and immunity* **22**(3), 375–380.

Care, A. S., Diener, K. R., Jasper, M. J., Brown, H. M., Ingman, W. V., Robertson, S. A. et al.: 2013, Macrophages regulate corpus luteum development during embryo implantation in mice, *The Journal of clinical investigation* **123**(8), 3472–3487.

Carlino, C., Stabile, H., Morrone, S., Bulla, R., Soriani, A., Agostinis, C., Bossi, F., Mocci, C., Sarazani, F., Tedesco, F. et al.: 2008, Recruitment of circulating NK cells through decidual tissues: a possible mechanism controlling NK cell accumulation in the uterus during early pregnancy, *Blood, The Journal of the American Society of Hematology* **111**(6), 3108–3115.

Carson, D. D., Lagow, E., Thathiah, A., Al-Shami, R., Farach-Carson, M. C., Vernon, M., Yuan, L., Fritz, M. A. and Lessey, B.: 2002, Changes in gene expression during the early to mid-luteal (receptive phase) transition in human endometrium detected by high-density microarray screening, *Molecular human reproduction* **8**(9), 871–879.

Chalouni, C., Banchereau, J., Vogt, A. B., Pascual, V. and Davoust, J.: 2003, Human germinal center B cells differ from naive and memory B cells by their aggregated MHC class II-rich compartments lacking HLA-DO, *International immunology* **15**(4), 457–466.

Chang, C.: 2012, Neonatal autoimmune diseases: a critical review, *Journal of autoimmunity* **38**(2-3), J223–J238.

Chantakru, S., Miller, C., Roach, L. E., Kuziel, W. A., Maeda, N., Wang, W.-C., Evans, S. S. and Croy, B. A.: 2002, Contributions from self-renewal and trafficking to the uterine NK cell population of early pregnancy, *The Journal of Immunology* **168**(1), 22–28.

Chapman, J. C., Chapman, F. M. and Michael, S. D.: 2015, The production of alpha/beta and gamma/delta double negative (DN) T-cells and their role in the maintenance of pregnancy, *Reproductive Biology and Endocrinology* **13**(1), 1–14.

Chazara, O., Xiong, S. and Moffett, A.: 2011, Maternal KIR and fetal HLA-C: a fine balance, *Journal of leukocyte biology* **90**(4), 703–716.

Chen, C.-K., Huang, S.-C., Chen, C.-L., Yen, M.-R., Hsu, H.-C. and Ho, H.-N.: 1995, Increased expressions of CD69 and HLA-DR but not of CD25 or CD71 on endometrial T lymphocytes of nonpregnant women, *Human immunology* **42**(3), 227–232.

Chernyshov, V. P., Sudoma, I. O., Dons' koi, B. V., Kostyuchyk, A. A. and Masliy, Y. V.: 2010, Elevated NK cell cytotoxicity, CD158a expression in NK cells and activated T lymphocytes in peripheral blood of women with IVF failures, *American Journal of Reproductive Immunology* **64**(1), 58–67.

Chung, J. B., Silverman, M. and Monroe, J. G.: 2003, Transitional B cells: step by step towards immune competence, *Trends in immunology* **24**(6), 342–348.

Cibrián, D. and Sánchez-Madrid, F.: 2017, CD69: from activation marker to metabolic gatekeeper, *European journal of immunology* **47**(6), 946–953.

Cicinelli, E., Bettocchi, S., de Ziegler, D., Loizzi, V., Cormio, G., Marinaccio, M., Trojano, G., Crupano, F. M., Francescato, R., Vitagliano, A. et al.: 2019, Chronic endometritis, a common disease hidden behind endometrial polyps in premenopausal women: first evidence from a case-control study, *Journal of minimally invasive gynecology* **26**(7), 1346–1350.

Cimadomo, D., Craciunas, L., Vermeulen, N., Vomstein, K. and Toth, B.: 2021, Definition, diagnostic and therapeutic options in recurrent implantation failure: an international survey of clinicians and embryologists, *Human Reproduction* **36**(2), 305–317.

Clavarino, G., Delouche, N., Vettier, C., Laurin, D., Pernollet, M., Raskovalova, T., Cesbron, J.-Y., Dumestre-Pérard, C. and Jacob, M.-C.: 2016, Novel strategy for phenotypic characterization of human B lymphocytes from precursors to effector cells by flow cytometry, *PloS one* **11**(9), e0162209.

Collins, M. K., Tay, C.-S., Erlebacher, A. et al.: 2009, Dendritic cell entrapment within the pregnant uterus inhibits immune surveillance of the maternal/fetal interface in mice, *The Journal of clinical investigation* **119**(7), 2062–2073.

Colucci, F.: 2017, The role of kir and hla interactions in pregnancy complications, *Immunogenetics* **69**(8), 557–565.

Conesa, A., Madrigal, P., Tarazona, S., Gomez-Cabrero, D., Cervera, A., McPherson, A., Szcześniak, M. W., Gaffney, D. J., Elo, L. L., Zhang, X. et al.: 2016, A survey of best practices for RNA-seq data analysis, *Genome biology* **17**(1), 13.

Consortium, G. O.: 2019, The gene ontology resource: 20 years and still GOing strong, *Nucleic acids research* **47**(D1), D330–D338.

Cooper, M. A., Fehniger, T. A. and Caligiuri, M. A.: 2001, The biology of human natural killer-cell subsets, *Trends in immunology* **22**(11), 633–640.

Coulam, C. B. and Roussev, R. G.: 2003, Increasing circulating T-cell activation markers are linked to subsequent implantation failure after transfer of in vitro fertilized embryos, *American Journal of Reproductive Immunology* **50**(4), 340–345.

Craven, C., Morgan, T. and Ward, K.: 1998, Decidual spiral artery remodelling begins before cellular interaction with cytotrophoblasts, *Placenta* **19**(4), 241–252.

Crick, F.: 1970, Central dogma of molecular biology, *Nature* **227**(5258), 561–563.

Crotty, S.: 2011, Follicular helper CD4 T cells (Tfh), *Annual review of immunology* **29**, 621–663.

Crotty, S.: 2014, T follicular helper cell differentiation, function, and roles in disease, *Immunity* **41**(4), 529–542.

Curry, M. P., Golden-Mason, L., Doherty, D. G., Deignan, T., Norris, S., Duffy, M., Nolan, N., Hall, W., Hegarty, J. E. and O'Farrelly, C.: 2003, Expansion of innate

CD5pos B cells expressing high levels of CD81 in hepatitis C virus infected liver, *Journal of hepatology* **38**(5), 642–650.

Danaii, S., Ghorbani, F., Ahmadi, M., Abbaszadeh, H., Koushaeian, L., Soltani-Zangbar, M. S., Mehdizadeh, A., Hojjat-Farsangi, M., Kafil, H. S., Aghebati-Maleki, L. et al.: 2020, IL-10-producing B cells play important role in the pathogenesis of recurrent pregnancy loss, *International Immunopharmacology* **87**, 106806.

Daridon, C., Pers, J.-O., Devauchelle, V., Martins-Carvalho, C., Hutin, P., Pennec, Y.-L., Saraux, A. and Youinou, P.: 2006, Identification of transitional type II B cells in the salivary glands of patients with Sjögren's syndrome, *Arthritis & Rheumatism: Official Journal of the American College of Rheumatology* **54**(7), 2280–2288.

De Maria, A., Malnati, M., Moretta, A., Pende, D., Bottino, C., Casorati, G., Cottafava, F., Melioli, G., Mingari, M. C., Migone, N. et al.: 1987, CD3+ 4- 8- WT31-(T cell receptor γ+) cells and other unusual phenotypes are frequently detected among spontaneously interleukin 2-responsive T lymphocytes present in the joint fluid in juvenile rheumatoid arthritis. A clonal analysis, *European journal of immunology* **17**(12), 1815–1819.

Diao, L., Cai, S., Huang, C., Li, L., Yu, S., Wang, L., Liu, S., Li, Y. and Zeng, Y.: 2020, New endometrial immune cell-based score (EI-score) for the prediction of implantation success for patients undergoing IVF/ICSI, *Placenta* **99**, 180–188.

Díaz-Hernández, I., Alecsandru, D., García-Velasco, J. A. and Domínguez, F.: 2021, Uterine natural killer cells: from foe to friend in reproduction, *Human Reproduction Update* **27**(4), 720–746.

Dieu-Nosjean, M. C., Goc, J., Giraldo, N. A., Sautès-Fridman, C. and Fridman, W. H.: 2014, Tertiary lymphoid structures in cancer and beyond, *Trends in immunology* **35**(11), 571–580.

Ding, T., Yan, F., Cao, S. and Ren, X.: 2015, Regulatory B cell: New member of immunosuppressive cell club, *Human immunology* **76**(9), 615–621.

Disep, B., Innes, B., Cochrane, H., Tijani, S. and Bulmer, J.: 2004, Immunohistochemical characterization of endometrial leucocytes in endometritis, *Histopathology* **45**(6), 625–632.

Donoghue, J., Paiva, P., Teh, W., Cann, L., Nowell, C., Rees, H., Bittinger, S., Obers, V., Bulmer, J., Stern, C. et al.: 2019, Endometrial uNK cell counts do not predict

successful implantation in an IVF population, *Human Reproduction* **34**(12), 2456–2466.

Donoso, P., Staessen, C., Fauser, B. and Devroey, P.: 2007, Current value of preimplantation genetic aneuploidy screening in IVF, *Human Reproduction Update* **13**(1), 15–25.

Dunn, C. L., Kelly, R. W. and Critchley, H. O.: 2003, Decidualization of the human endometrial stromal cell: an enigmatic transformation, *Reproductive biomedicine online* **7**(2), 151–161.

Egwuagu, C. E. and Yu, C. R.: 2015, Interleukin 35- Producing B Cells (i35-Breg): A New Mediator of Regulatory B-Cell Functions in CNS Autoimmune Diseases, *Critical Reviews™ in Immunology* **35**(1).

El-Azzamy, H., Dambaeva, S. V., Katukurundage, D., Salazar Garcia, M. D., Skariah, A., Hussein, Y., Germain, A., Fernandez, E., Gilman-Sachs, A., Beaman, K. D. et al.: 2018, Dysregulated uterine natural killer cells and vascular remodeling in women with recurrent pregnancy losses, *American Journal of Reproductive Immunology* **80**(4), e13024.

ESHRE: 2018, ESHRE guideline: recurrent pregnancy loss, *Human reproduction open* **2018**(2), hoy004.

Esteve-Solé, A., Luo, Y., Vlagea, A., Deyà-Martínez, Á., Yagüe, J., Plaza-Martín, A. M., Juan, M. and Alsina, L.: 2018, B regulatory cells: players in pregnancy and early life, *International journal of molecular sciences* **19**(7), 2099.

Falini, B., Fizzotti, M., Pucciarini, A., Bigerna, B., Marafioti, T., Gambacorta, M., Pacini, R., Alunni, C., Natali-Tanci, L., Ugolini, B. et al.: 2000, A monoclonal antibody (MUM1p) detects expression of the MUM1/IRF4 protein in a subset of germinal center B cells, plasma cells, and activated T cells, *Blood, The Journal of the American Society of Hematology* **95**(6), 2084–2092.

Farstad, I., Carlsen, H., Morton, H. and Brandtzaeg, P.: 2000, Immunoglobulin A cell distribution in the human small intestine: phenotypic and functional characteristics, *Immunology* **101**(3), 354–363.

Fehniger, T. A., Shah, M. H., Turner, M. J., VanDeusen, J. B., Whitman, S. P., Cooper, M. A., Suzuki, K., Wechser, M., Goodsaid, F. and Caligiuri, M. A.: 1999, Differential cytokine and chemokine gene expression by human NK cells following activation with IL-18 or IL-15 in combination with IL-12: implications for the innate immune response, *The Journal of Immunology* **162**(8), 4511–4520.

Fernandez-Shaw, S., Clarke, M., Hicks, B., Naish, C., Barlow, D. and Starkey, P.: 1995, Immunology: Bone marrow-derived cell populations in uterine and ectopic endometrium, *Human Reproduction* **10**(9), 2285–2289.

Feyaerts, D., Benner, M., van Cranenbroek, B., van der Heijden, O. W., Joosten, I. and van der Molen, R. G.: 2017, Human uterine lymphocytes acquire a more experienced and tolerogenic phenotype during pregnancy, *Scientific reports* **7**(1), 1–10.

Fillatreau, S., Sweenie, C. H., McGeachy, M. J., Gray, D. and Anderton, S. M.: 2002, B cells regulate autoimmunity by provision of IL-10, *Nature immunology* **3**(10), 944–950.

Florek, M., Schneidawind, D., Baker, J., Pierini, A., Leveson-Gower, D. B., Pan, Y., Negrin, R. S. and Meyer, E. H.: 2014, Loss of CD62L expression in CD4+ FoxP3+ regulatory T cells following freeze-and-thaw prevents protection against GVHD in murine models, *Blood* **124**(21), 2427.

Floudas, A., Amu, S. and Fallon, P. G.: 2016, New insights into IL-10 dependent and IL-10 independent mechanisms of regulatory B cell immune suppression, *Journal of clinical immunology* **36**(1), 25–33.

Flynn, L., Byrne, B., Carton, J., O'Farrelly, C., Kelehan, P. and O'Herlihy, C.: 2000, Menstrual cycle dependent fluctuations in NK and T-lymphocyte subsets from non-pregnant human endometrium, *American journal of reproductive immunology* **43**(4), 209–217.

Fontenot, J. D., Gavin, M. A. and Rudensky, A. Y.: 2003, Foxp3 programs the development and function of CD4+ CD25+ regulatory T cells, *Nature immunology* **4**(4), 330–336.

Ford, H. B. and Schust, D. J.: 2009, Recurrent pregnancy loss: etiology, diagnosis, and therapy, *Reviews in obstetrics and gynecology* **2**(2), 76.

Fox, C. W., Savaris, R. F., Jeong, J.-W., Kim, T. H., Miller, P. B., Likes, C. E., Schammel, D. P., Young, S. L. and Lessey, B. A.: 2020, Unexplained recurrent pregnancy loss and unexplained infertility: twins in disguise, *Human Reproduction Open* **2020**(1), hoz021.

Fu, B., Zhou, Y., Ni, X., Tong, X., Xu, X., Dong, Z., Sun, R., Tian, Z. and Wei, H.: 2017, Natural killer cells promote fetal development through the secretion of growth-promoting factors, *Immunity* **47**(6), 1100–1113.

Fukuda, T., Yoshida, T., Okada, S., Hatano, M., Miki, T., Ishibashi, K., Okabe, S., Koseki, H., Hirosawa, S., Taniguchi, M. et al.: 1997, Disruption of the Bcl6 gene results in an impaired germinal center formation, *The Journal of experimental medicine* **186**(3), 439–448.

Fukui, A., Funamizu, A., Fukuhara, R. and Shibahara, H.: 2017, Expression of natural cytotoxicity receptors and cytokine production on endometrial natural killer cells in women with recurrent pregnancy loss or implantation failure, and the expression of natural cytotoxicity receptors on peripheral blood natural killer cells in pregnant women with a history of recurrent pregnancy loss, *Journal of Obstetrics and Gynaecology Research* **43**(11), 1678–1686.

Fukui, A., Funamizu, A., Yokota, M., Yamada, K., Nakamua, R., Fukuhara, R., Kimura, H. and Mizunuma, H.: 2011, Uterine and circulating natural killer cells and their roles in women with recurrent pregnancy loss, implantation failure and preeclampsia, *Journal of reproductive immunology* **90**(1), 105–110.

Gagné, D., Rivard, M., Pagé, M., Shazand, K., Hugo, P. and Gosselin, D.: 2003, Blood leukocyte subsets are modulated in patients with endometriosis, *Fertility and sterility* **80**(1), 43–53.

Gamliel, M., Goldman-Wohl, D., Isaacson, B., Gur, C., Stein, N., Yamin, R., Berger, M., Grunewald, M., Keshet, E., Rais, Y. et al.: 2018, Trained memory of human uterine NK cells enhances their function in subsequent pregnancies, *Immunity* **48**(5), 951–962.

Gellersen, B., Brosens, I. A. and Brosens, J. J.: 2007, Decidualization of the human endometrium: mechanisms, functions, and clinical perspectives, *Seminars in reproductive medicine*, Vol. 25, © Thieme Medical Publishers, pp. 445–453.

Gellersen, B. and Brosens, J. J.: 2014, Cyclic decidualization of the human endometrium in reproductive health and failure, *Endocrine reviews* **35**(6), 851–905.

Ghafourian, M., Karami, N., Khodadadi, A. and Nikbakhat, R.: 2014, Increase of CD69, CD161 and CD94 on NK cells in women with recurrent spontaneous abortion and in vitro fertilization failure, *Iranian Journal of Immunology* **11**(2), 84–96.

Gil-Yarom, N., Radomir, L., Sever, L., Kramer, M. P., Lewinsky, H., Bornstein, C., Blecher-Gonen, R., Barnett-Itzhaki, Z., Mirkin, V., Friedlander, G. et al.: 2017, CD74 is a novel transcription regulator, *Proceedings of the National Academy of Sciences* **114**(3), 562–567.

Giles, J. R., Kashgarian, M., Koni, P. A. and Shlomchik, M. J.: 2015, B cell–specific MHC class II deletion reveals multiple nonredundant roles for B cell antigen presentation in murine lupus, *The Journal of Immunology* **195**(6), 2571–2579.

Gnoth, C., Godehardt, E., Frank-Herrmann, P., Friol, K., Tigges, J. and Freundl, G.: 2005, Definition and prevalence of subfertility and infertility, *Human reproduction* **20**(5), 1144–1147.

Goll, R., Husebekk, A., Isaksen, V., Kauric, G., Hansen, T. and Florholmen, J.: 2005, Increased Frequency of Antral CD4+ T and CD19+ B Cells in Patients with Helicobacter pylori-Related Peptic Ulcer Disease, *Scandinavian journal of immunology* **61**(1), 92–97.

Group, P. et al.: 2009, Reprint–preferred reporting items for systematic reviews and meta-analyses: the PRISMA statement, *Phys Ther* **89**, 873–880.

Guo, C., Cai, P., Jin, L., Sha, Q., Yu, Q., Zhang, W., Jiang, C., Liu, Q., Zong, D., Li, K. et al.: 2021, Single-cell profiling of the human decidual immune microenvironment in patients with recurrent pregnancy loss, *Cell discovery* **7**(1), 1–15.

Guo, W., Castaigne, J. G., Mooney, N., Charron, D. and Al-Daccak, R.: 2003, Signaling through HLA-DR induces PKCβ-dependent B cell death outside rafts, *European journal of immunology* **33**(4), 928–938.

Gupta, S., Jiang, M. and Pernis, A. B.: 1999, IFN-α activates Stat6 and leads to the formation of Stat2: Stat6 complexes in B cells, *The Journal of Immunology* **163**(7), 3834–3841.

Guzeloglu-Kayisli, O., Kayisli, U. A. and Taylor, H. S.: 2009, The role of growth factors and cytokines during implantation: endocrine and paracrine interactions, *Seminars in reproductive medicine*, Vol. 27, NIH Public Access, p. 62.

Guzman-Genuino, R. M. and Diener, K. R.: 2017, Regulatory B cells in pregnancy: lessons from autoimmunity, graft tolerance, and cancer, *Frontiers in immunology* **8**, 172.

Guzman-Genuino, R. M., Eldi, P., Garcia-Valtanen, P., Hayball, J. D. and Diener, K. R.: 2019, Uterine B cells exhibit regulatory properties during the peri-implantation stage of murine pregnancy, *Frontiers in immunology* **10**, 2899.

Hamamah, S. and Haouzi, D.: 2013, Methods for assessing endometrium receptivity of a patient.

Hao, Z., Duncan, G. S., Seagal, J., Su, Y.-W., Hong, C., Haight, J., Chen, N.-J., Elia, A., Wakeham, A., Li, W. Y. et al.: 2008, Fas receptor expression in germinal-center B cells is essential for T and B lymphocyte homeostasis, *Immunity* **29**(4), 615–627.

Haouzi, D., Mahmoud, K., Fourar, M., Bendhaou, K., Dechaud, H., De Vos, J., Reme, T., Dewailly, D. and Hamamah, S.: 2009, Identification of new biomarkers of human endometrial receptivity in the natural cycle, *Human reproduction* **24**(1), 198–205.

Harrity, C., Bereir, M. M., Walsh, D. J. and Marron, K. D.: 2019, Moving from peripheral blood to local uterine immunophenotype analysis in patients with poor reproductive history: pilot study of a novel technique, *Irish Journal of Medical Science (1971-)* **188**(3), 893–901.

Hasan, M. M., Thompson-Snipes, L., Klintmalm, G., Demetris, A. J., O'Leary, J., Oh, S. and Joo, H.: 2019, CD24hiCD38hi and CD24hiCD27+ Human Regulatory B Cells Display Common and Distinct Functional Characteristics, *The Journal of Immunology* **203**(8), 2110–2120.

Herman, A. B. and Autieri, M. V.: 2017, Inflammation-regulated mRNA stability and the progression of vascular inflammatory diseases, *Clinical Science* **131**(22), 2687–2699.

Hershberg, U. and Luning Prak, E. T.: 2015, The analysis of clonal expansions in normal and autoimmune B cell repertoires, *Philosophical Transactions of the Royal Society B: Biological Sciences* **370**(1676), 20140239.

HFEA: 2020, Fertility treatment 2018: trends and figures, human fertilisation and embryology authority.
URL: *https://www.hfea.gov.uk/about-us/publications/research-and-data/fertility-treatment-2018-trends-and-figures/*

Hiby, S. E., Apps, R., Sharkey, A. M., Farrell, L. E., Gardner, L., Mulder, A., Claas, F. H., Walker, J. J., Redman, C. C., Morgan, L. et al.: 2010, Maternal activating KIRs protect against human reproductive failure mediated by fetal HLA-C2, *The Journal of clinical investigation* **120**(11), 4102–4110.

Hoffmann, R., Seidl, T., Neeb, M., Rolink, A. and Melchers, F.: 2002, Changes in gene expression profiles in developing B cells of murine bone marrow, *Genome research* **12**(1), 98–111.

Huang, B., Faucette, A. N., Pawlitz, M. D., Pei, B., Goyert, J. W., Zhou, J. Z., El-Hage, N. G., Deng, J., Lin, J., Yao, F. et al.: 2017, Interleukin-33-induced expression of

PIBF1 by decidual B cells protects against preterm labor, *Nature medicine* **23**(1), 128–135.

Huang, D. W., Sherman, B. T. and Lempicki, R. A.: 2009, Bioinformatics enrichment tools: paths toward the comprehensive functional analysis of large gene lists, *Nucleic acids research* **37**(1), 1–13.

Huang, W., Liu, B., He, Y., Xie, Y., Liang, T., Bi, Y., Yuan, L., Qin, A., Wang, Y. and Yang, Y.: 2020, Variation of diagnostic criteria in women with chronic endometritis and its effect on reproductive outcomes: A systematic review and meta-analysis, *Journal of Reproductive Immunology* **140**, 103146.

Hueber, A.-O. and Koncz, G.: 2012, The Fas/CD95 receptor regulates the death of autoreactive B cells and the selection of antigen-specific B cells, *Frontiers in immunology* **3**, 207.

Hyde, K. J. and Schust, D. J.: 2015, Genetic considerations in recurrent pregnancy loss, *Cold Spring Harbor perspectives in medicine* **5**(3), a023119.

Hystad, M., Myklebust, J. H., Bø, T., Sivertsen, E., Rian, E., Forfang, L., Munthe, E., Rosenwald, A., Chiorazzi, M., Jonassen, I. et al.: 2009, Characterization of early stages of human B cell development by gene expression profiling, *The Journal of Immunology* **182**(9), 5882–5882.

Inki, P.: 1997, Expression of syndecan-1 in female reproductive tract tissues and cultured keratinocytes., *Molecular human reproduction* **3**(4), 299–305.

Jacobs, R., Hintzen, G., Kemper, A., Beul, K., Kempf, S., Behrens, G., Sykora, K.-W. and Schmidt, R. E.: 2001, CD56bright cells differ in their KIR repertoire and cytotoxic features from CD56dim NK cells, *European journal of immunology* **31**(10), 3121–3126.

Jansen, C. H., Kastelein, A. W., Kleinrouweler, C. E., Van Leeuwen, E., De Jong, K. H., Pajkrt, E. and Van Noorden, C. J.: 2020, Development of placental abnormalities in location and anatomy, *Acta obstetricia et gynecologica Scandinavica* **99**(8), 983–993.

Jensen, F., Muzzio, D., Soldati, R., Fest, S. and Zenclussen, A. C.: 2013, Regulatory B10 cells restore pregnancy tolerance in a mouse model, *Biology of reproduction* **89**(4), 90–1.

Jiang, T. T., Chaturvedi, V., Ertelt, J. M., Kinder, J. M., Clark, D. R., Valent, A. M., Xin, L. and Way, S. S.: 2014, Regulatory t cells: new keys for further unlocking the

enigma of fetal tolerance and pregnancy complications, *The Journal of Immunology* **192**(11), 4949–4956.

Johnson, S. E., Capra, J. D. and LeBien, T. W.: 2007, CD127 expression confers enhanced survival on human B-lineage cells; implications for the role of IL-7 signaling in human B lymphopoiesis., *Blood* **110**(11), 1329.

Kakita-Kobayashi, M., Murata, H., Nishigaki, A., Hashimoto, Y., Komiya, S., Tsubokura, H., Kido, T., Kida, N., Tsuzuki-Nakao, T., Matsuo, Y. et al.: 2020, Thyroid hormone facilitates in vitro decidualization of human endometrial stromal cells via thyroid hormone receptors, *Endocrinology* **161**(6), bqaa049.

Kaminski, D. A., Wei, C., Qian, Y., Rosenberg, A. F. and Sanz, I.: 2012, Advances in human B cell phenotypic profiling, *Frontiers in immunology* **3**, 302.

Kanehisa, M. and Goto, S.: 2000, KEGG: kyoto encyclopedia of genes and genomes, *Nucleic acids research* **28**(1), 27–30.

Katikaneni, D. S. and Jin, L.: 2019, B cell MHC class II signaling: A story of life and death, *Human immunology* **80**(1), 37–43.

Keller, C. C., Eikmans, M., van der Hoorn, M.-L. P. and Lashley, L. E.: 2020, Recurrent miscarriages and the association with regulatory T cells; A systematic review, *Journal of reproductive immunology* **139**, 103105.

Khizroeva, J., Nalli, C., Bitsadze, V., Lojacono, A., Zatti, S., Andreoli, L., Tincani, A., Shoenfeld, Y. and Makatsariya, A.: 2019, Infertility in women with systemic autoimmune diseases, *Best Practice & Research Clinical Endocrinology & Metabolism* **33**(6), 101369.

Kim, D., Pertea, G., Trapnell, C., Pimentel, H., Kelley, R. and Salzberg, S. L.: 2013, TopHat2: accurate alignment of transcriptomes in the presence of insertions, deletions and gene fusions, *Genome biology* **14**(4), R36.

Kind, S., Merenkow, C., Büscheck, F., Möller, K., Dum, D., Chirico, V., Luebke, A. M., Höflmayer, D., Hinsch, A., Jacobsen, F. et al.: 2019, Prevalence of syndecan-1 (CD138) expression in different kinds of human tumors and normal tissues, *Disease Markers* **2019**.

King, A., Burrows, T., Verma, S., Hiby, S. and Loke, Y.: 1998, Human uterine lymphocytes, *Human reproduction update* **4**(5), 480–485.

King, C.: 2011, A fine romance: T follicular helper cells and B cells, *Immunity* **34**(6), 827–829.

Kitaya, K., Tada, Y., Hayashi, T., Taguchi, S., Funabiki, M. and Nakamura, Y.: 2014, Comprehensive endometrial immunoglobulin subclass analysis in infertile women suffering from repeated implantation failure with or without chronic endometritis, *American Journal of Reproductive Immunology* **72**(4), 386–391.

Kitaya, K. and Yasuo, T.: 2010a, Aberrant expression of selectin E, CXCL1, and CXCL13 in chronic endometritis, *Modern Pathology* **23**(8), 1136–1146.

Kitaya, K. and Yasuo, T.: 2010b, Leukocyte density and composition in human cycling endometrium with uterine fibroids, *Human immunology* **71**(2), 158–163.

Klentzeris, L., Bulmer, J., Warren, M., Morrison, L., Li, T. and Cooke, I.: 1994, Lymphoid tissue in the endometrium of women with unexplained infertility: morphometric and immunohistochemical aspects, *Human Reproduction* **9**(4), 646–652.

Klentzeris, L. D., Bulmer, J., Liu, D. and Morrison, L.: 1995, Endometrial leukocyte subpopulations in women with endometriosis, *European Journal of Obstetrics & Gynecology and Reproductive Biology* **63**(1), 41–47.

Klentzeris, L. D., Bulmer, J. N., Warren, A., Morrison, L., Li, T.-C. and Cooke, I. D.: 1992, Endometrial lymphoid tissue in the timed endometrial biopsy: morphometric and immunohistochemical aspects, *American journal of obstetrics and gynecology* **167**(3), 667–674.

Koboziev, I., Karlsson, F. and Grisham, M. B.: 2010, Gut-associated lymphoid tissue, T cell trafficking, and chronic intestinal inflammation, *Annals of the New York Academy of Sciences* **1207**(Suppl 1), E86.

Kolar, G. R., Mehta, D., Pelayo, R. and Capra, J. D.: 2007, A novel human B cell subpopulation representing the initial germinal center population to express AID, *blood* **109**(6), 2545–2552.

Koot, Y. E., Van Hooff, S. R., Boomsma, C. M., Van Leenen, D., Koerkamp, M. J. G., Goddijn, M., Eijkemans, M. J., Fauser, B. C., Holstege, F. C. and Macklon, N. S.: 2016, An endometrial gene expression signature accurately predicts recurrent implantation failure after IVF, *Scientific Reports* **6**, 19411.

Kort, J. D., McCoy, R. C., Demko, Z. and Lathi, R. B.: 2018, Are blastocyst aneuploidy rates different between fertile and infertile populations?, *Journal of assisted reproduction and genetics* **35**(3), 403–408.

Koushaeian, L., Ghorbani, F., Ahmadi, M., Eghbal-Fard, S., Zamani, M., Danaii, S., Yousefi, B., Jadidi-Niaragh, F., Hamdi, K. and Yousefi, M.: 2019, The role of IL-10-producing B cells in repeated implantation failure patients with cellular immune abnormalities, *Immunology letters* **214**, 16–22.

Krzyzak, L., Seitz, C., Urbat, A., Hutzler, S., Ostalecki, C., Gläsner, J., Hiergeist, A., Gessner, A., Winkler, T. H., Steinkasserer, A. et al.: 2016, CD83 modulates B cell activation and germinal center responses, *The Journal of Immunology* **196**(9), 3581–3594.

Kuon, R.-J., Strowitzki, T., Sohn, C., Daniel, V. and Toth, B.: 2015, Immune profiling in patients with recurrent miscarriage, *Journal of reproductive immunology* **108**, 136–141.

Kwak-Kim, J., Agcaoili, M. S. L., Aleta, L., Liao, A., Ota, K., Dambaeva, S., Beaman, K., Kim, J. W. and Gilman-Sachs, A.: 2013, Management of women with recurrent pregnancy losses and antiphospholipid antibody syndrome, *American Journal of Reproductive Immunology* **69**(6), 596–607.

Lachapelle, M.-H., Miron, P., Hemmings, R. and Roy, D. C.: 1996, Endometrial T, B, and NK cells in patients with recurrent spontaneous abortion. Altered profile and pregnancy outcome., *The Journal of Immunology* **156**(10), 4027–4034.

Laresgoiti-Servitje, E., Gómez-López, N. and Olson, D. M.: 2010, An immunological insight into the origins of pre-eclampsia, *Human reproduction update* **16**(5), 510–524.

LeBien, T. W. and Tedder, T. F.: 2008, B lymphocytes: how they develop and function, *Blood* **112**(5), 1570–1580.

Lédée, N., Petitbarat, M., Prat-Ellenberg, L., Dray, G., Cassuto, G., Chevrier, L., Kazhalawi, A., Vezmar, K. and Chaouat, G.: 2020, The uterine immune profile: A method for individualizing the management of women who have failed to implant an embryo after IVF/ICSI, *Journal of Reproductive Immunology* p. 103207.

Lee, J. Y., Lee, M. and Lee, S. K.: 2011, Role of endometrial immune cells in implantation, *Clinical and experimental reproductive medicine* **38**(3), 119.

Lee, S. K., Kim, J. Y., Lee, M., Gilman-Sachs, A. and Kwak-Kim, J.: 2012, T h17 and Regulatory T cells in Women with Recurrent Pregnancy Loss, *American Journal of Reproductive Immunology* **67**(4), 311–318.

Leng, Y., Romero, R., Xu, Y., Galaz, J., Slutsky, R., Arenas-Hernandez, M., Garcia-Flores, V., Motomura, K., Hassan, S. S., Reboldi, A. et al.: 2019, Are B cells altered in the decidua of women with preterm or term labor?, *American Journal of Reproductive Immunology* **81**(5), e13102.

Lentz, V. M. and Manser, T.: 2001, Cutting edge: germinal centers can be induced in the absence of T cells, *The Journal of Immunology* **167**(1), 15–20.

Li, H. and Pauza, C. D.: 2015, CD25+ Bcl6low T follicular helper cells provide help to maturing B cells in germinal centers of human tonsil, *European journal of immunology* **45**(1), 298–308.

Li, Q.: 2014, Transforming growth factor β signaling in uterine development and function, *Journal of animal science and biotechnology* **5**(1), 1–9.

Li, Z., Ju, X., Silveira, P. A., Abadir, E., Hsu, W.-H., Hart, D. N. and Clark, G. J.: 2019, CD83: Activation marker for antigen presenting cells and its therapeutic potential, *Frontiers in immunology* **10**, 1312.

Lieberman, L. A., Zeng, W., Singh, C., Wang, W., Otipoby, K. L., Loh, C., Plavina, T., Gorelik, L., Ransohoff, R. M. and Cahir-McFarland, E.: 2016, CD62L is not a reliable biomarker for predicting PML risk in natalizumab-treated R-MS patients, *Neurology* **86**(4), 375–381.

Lima, J., Martins, C., Leandro, M. J., Nunes, G., Sousa, M.-J., Branco, J. C. and Borrego, L.-M.: 2016, Characterization of B cells in healthy pregnant women from late pregnancy to post-partum: a prospective observational study, *BMC pregnancy and childbirth* **16**(1), 1–13.

Lin, W., Zhang, P., Chen, H., Chen, Y., Yang, H., Zheng, W., Zhang, X., Zhang, F., Zhang, W. and Lipsky, P. E.: 2017, Circulating plasmablasts/plasma cells: a potential biomarker for IgG4-related disease, *Arthritis research & therapy* **19**(1), 1–14.

Lin, X., Wang, X., Xiao, F., Ma, K., Liu, L., Wang, X., Xu, D., Wang, F., Shi, X., Liu, D. et al.: 2019, IL-10-producing regulatory B cells restrain the T follicular helper cell response in primary Sjögren's syndrome, *Cellular & Molecular Immunology* **16**(12), 921–931.

Liu, W., Putnam, A. L., Xu-Yu, Z., Szot, G. L., Lee, M. R., Zhu, S., Gottlieb, P. A., Kapranov, P., Gingeras, T. R., de St. Groth, B. F. et al.: 2006, CD127 expression inversely correlates with FoxP3 and suppressive function of human CD4+ T reg cells, *The Journal of experimental medicine* **203**(7), 1701–1711.

Liu, Y., Chen, X., Huang, J., Wang, C.-C., Yu, M.-Y., Laird, S. and Li, T.-C.: 2018, Comparison of the prevalence of chronic endometritis as determined by means of different diagnostic methods in women with and without reproductive failure, *Fertility and sterility* **109**(5), 832–839.

Lodish, H., Berk, A., Zipursky, S. L., Matsudaira, P., Baltimore, D. and Darnell, J.: 2000, The three roles of RNA in protein synthesis, *Molecular Cell Biology. 4th edition*, WH Freeman.

Love, M. I., Huber, W. and Anders, S.: 2014, Moderated estimation of fold change and dispersion for RNA-seq data with DESeq2, *Genome biology* **15**(12), 550.

Lu, S. J., Fathiah Muzaffar Shah, F., Saberi Mohamad, M., Moorthy, K., Deris, S., Zakaria, Z. and Napis, S.: 2015, A review on bioinformatics enrichment analysis tools towards functional analysis of high throughput gene set data, *Current Proteomics* **12**(1), 14–27.

Lucas, E. S., Vrljicak, P., Muter, J., Diniz-da Costa, M. M., Brighton, P. J., Kong, C.-S., Lipecki, J., Fishwick, K. J., Odendaal, J., Ewington, L. J. et al.: 2020, Recurrent pregnancy loss is associated with a pro-senescent decidual response during the peri-implantation window, *Communications biology* **3**(1), 1–14.

L'Heveder, A., Jones, B. P., Naja, R., Serhal, P. and Ben Nagi, J.: 2020, Pre-implantation genetic testing for aneuploidy: the past, present and future, *The Obstetrician & Gynaecologist* **22**(4), 293–304.

Mackay, L. K. and Kallies, A.: 2017, Transcriptional regulation of tissue-resident lymphocytes, *Trends in immunology* **38**(2), 94–103.

Male, V., Hughes, T., McClory, S., Colucci, F., Caligiuri, M. A. and Moffett, A.: 2010, Immature NK cells, capable of producing IL-22, are present in human uterine mucosa, *The Journal of Immunology* **185**(7), 3913–3918.

Manaster, I. and Mandelboim, O.: 2008, The unique properties of human NK cells in the uterine mucosa, *Placenta* **29**, 60–66.

Manaster, I., Mizrahi, S., Goldman-Wohl, D., Sela, H. Y., Stern-Ginossar, N., Lankry, D., Gruda, R., Hurwitz, A., Bdolah, Y., Haimov-Kochman, R. et al.: 2008, Endometrial NK cells are special immature cells that await pregnancy, *The Journal of Immunology* **181**(3), 1869–1876.

Marron, K. and Harrity, C.: 2019, Endometrial lymphocyte concentrations in adverse reproductive outcome populations, *Journal of assisted reproduction and genetics* **36**(5), 837–846.

Marron, K., Walsh, D. and Harrity, C.: 2019, Detailed endometrial immune assessment of both normal and adverse reproductive outcome populations, *Journal of assisted reproduction and genetics* **36**(2), 199–210.

Matteo, M. G., Greco, P., Rosenberg, P., Mestice, A., Baldini, D., Falagario, T., Martino, V., Santodirocco, M., Massenzio, F., Castellana, L. et al.: 2007, Normal percentage of CD56 bright natural killer cells in young patients with a history of repeated unexplained implantation failure after in vitro fertilization cycles, *Fertility and sterility* **88**(4), 990–993.

Mauri, C.: 2010, CD19 CD24 hi CD38 hi B Cells Exhibit Regulatory Capacity in Healthy Individuals but Are Functionally Impaired in Systemic Lupus Erythematosus Patients, *Immunity* **32**, 129–140.

Mauri, C. and Menon, M.: 2015, The expanding family of regulatory B cells, *International immunology* **27**(10), 479–486.

Mauri, C., Menon, M. et al.: 2017, Human regulatory B cells in health and disease: therapeutic potential, *The Journal of clinical investigation* **127**(3), 772–779.

McGhee, J. R. and Fujihashi, K.: 2012, Inside the mucosal immune system, *PLoS Biol* **10**(9), e1001397.

Messaoudi, S., Kasmi, I. E., Bourdiec, A., Crespo, K., Bissonnette, L., Le Saint, C., Bissonnette, F. and Kadoch, I.-J.: 2019, 15 years of transcriptomic analysis on endometrial receptivity: what have we learnt?, *Fertility Research and Practice* **5**(1), 9.

Mettler, L., Jürgensen, A., Volkov, N., Kulakov, V. and Parwaresch, M.: 1997, Immuno Histochemical Profile of Endometrium in Patients With Genital Endometriosis, *Diagnostic and Therapeutic Endoscopy* **3**(3), 127–145.

Michimata, T., Ogasawara, M. S., Tsuda, H., Suzumori, K., Aoki, K., Sakai, M., Fujimura, M., Nagata, K., Nakamura, M. and Saito, S.: 2002, Distributions of endometrial NK cells, B cells, T cells, and Th2/Tc2 cells fail to predict pregnancy outcome following recurrent abortion, *American Journal of Reproductive Immunology* **47**(4), 196–202.

Mirkin, S., Arslan, M., Churikov, D., Corica, A., Diaz, J., Williams, S., Bocca, S. and Oehninger, S.: 2005, In search of candidate genes critically expressed in the human endometrium during the window of implantation, *Human reproduction* **20**(8), 2104–2117.

Modesti, P. A., Reboldi, G., Cappuccio, F. P., Agyemang, C., Remuzzi, G., Rapi, S., Perruolo, E., Parati, G. and on CV Risk in Low Resource Settings, E. W. G.: 2016, Panethnic differences in blood pressure in Europe: a systematic review and meta-analysis, *PloS one* **11**(1), e0147601.

Moffett, A., Chazara, O., Colucci, F. and Johnson, M. H.: 2016, Variation of maternal KIR and fetal HLA-C genes in reproductive failure: too early for clinical intervention, *Reproductive biomedicine online* **33**(6), 763–769.

Moffett, A. and Loke, C.: 2006, Immunology of placentation in eutherian mammals, *Nature Reviews Immunology* **6**(8), 584–594.

Moffett, A. and Shreeve, N.: 2015, First do no harm: uterine natural killer (NK) cells in assisted reproduction, *Human reproduction* **30**(7), 1519–1525.

Montaldo, E., Vacca, P., Chiossone, L., Croxatto, D., Loiacono, F., Martini, S., Ferrero, S., Walzer, T., Moretta, L. and Mingari, M. C.: 2016, Unique Eomes+ NK cell subsets are present in uterus and decidua during early pregnancy, *Frontiers in immunology* **6**, 646.

Mooney, N., Grillot-Courvalin, C., Hivroz, C., Ju, L. and Charron, D.: 1990, Early biochemical events after MHC class II-mediated signaling on human B lymphocytes., *The Journal of Immunology* **145**(7), 2070–2076.

Mor, G., Aldo, P. and Alvero, A. B.: 2017, The unique immunological and microbial aspects of pregnancy, *Nature Reviews Immunology* **17**(8), 469–482.

Moreno, I. and Simon, C.: 2019, An endometrial pathology in the inflammation cloud that can be accessed with a microbial app, *Fertility and sterility* **111**(4), 679–680.

Morris, H., Edwards, J., Tiltman, A. and Emms, M.: 1985, Endometrial lymphoid tissue: an immunohistological study., *Journal of clinical pathology* **38**(6), 644–652.

Morrison, V. L., Barr, T. A., Brown, S. and Gray, D.: 2010, TLR-mediated loss of CD62L focuses B cell traffic to the spleen during Salmonella typhimurium infection, *The Journal of Immunology* **185**(5), 2737–2746.

Moser, B.: 2015, CXCR5, the defining marker for follicular B helper T (TFH) cells, *Frontiers in immunology* **6**, 296.

Murphy, S. P., Tayade, C., Ashkar, A. A., Hatta, K., Zhang, J. and Croy, B. A.: 2009, Interferon gamma in successful pregnancies, *Biology of reproduction* **80**(5), 848–859.

Muzzio, D., Zenclussen, A. C. and Jensen, F.: 2013, The role of B cells in pregnancy: the good and the bad, *American Journal of Reproductive Immunology* **69**(4), 408–412.

Nagler, A., Lanier, L., Cwirla, S. and Phillips, J.: 1989, Comparative studies of human FcRIII-positive and negative natural killer cells., *The Journal of Immunology* **143**(10), 3183–3191.

Nancy, P. and Erlebacher, A.: 2014, T cell behavior at the maternal-fetal interface, *The International journal of developmental biology* **58**, 189.

Nera, K.-P., Kyläniemi, M. and Lassila, O.: 2015, Regulation of B cell to plasma cell transition within the follicular B cell response, *Scandinavian journal of immunology* **82**(3), 225–234.

Nielsen, H. S.: 2011, Secondary recurrent miscarriage and HY immunity, *Human reproduction update* **17**(4), 558–574.

Niessl, J. and Kaufmann, D. E.: 2018, Harnessing T follicular helper cell responses for HIV vaccine development, *Viruses* **10**(6), 336.

Ning, F., Liu, H. and Lash, G. E.: 2016, The role of decidual macrophages during normal and pathological pregnancy, *American journal of reproductive immunology* **75**(3), 298–309.

Norris, S., Collins, C., Doherty, D. G., Smith, F., McEntee, G., Traynor, O., Nolan, N., Hegarty, J. and O'Farrelly, C.: 1998, Resident human hepatitis lymphocytes are phenotypically different from circulating lymphocytes, *Journal of hepatology* **28**(1), 84–90.

O'Donnell, E., Shen, M., Becker, C., Lindgren, C., Zondervan, K., Southcombe, J., Granne, I. and Melo, P.: 2020, The role of human endometrial B cells in health and benign female reproductive pathologies: a systematic review. PROSPERO 2020 CRD42020152915.
URL: *https://www.crd.york.ac.uk/prospero/display_record.php?RecordID=152915*

Oleinika, K., Mauri, C. and Salama, A. D.: 2019, Effector and regulatory B cells in immune-mediated kidney disease, *Nature Reviews Nephrology* **15**(1), 11–26.

Olooto, W. E., Amballi, A. A., Banjo, T. A. et al.: 2012, A review of Female Infertility; important etiological factors and management, *J Microbiol Biotech Res* **2**(3), 379–385.

Otasek, D., Morris, J. H., Bouças, J., Pico, A. R. and Demchak, B.: 2019, Cytoscape automation: empowering workflow-based network analysis, *Genome biology* **20**(1), 1–15.

O'Connell, F. P., Pinkus, J. L. and Pinkus, G. S.: 2004, CD138 (syndecan-1), a plasma cell marker: immunohistochemical profile in hematopoietic and nonhematopoietic neoplasms, *American journal of clinical pathology* **121**(2), 254–263.

Panthee, D. R., Shi, R. and Lewis, R. S.: 2018, Filter paper-based spin column method for cost-efficient DNA or RNA purification., *PLoS ONE* **13**(12).

Parks, R. N., Kim, C. J., Al-Safi, Z. A., Armstrong, A. A., Zore, T. and Moatamed, N. A.: 2019, Multiple Myeloma 1 Transcription Factor Is Superior to CD138 as a Marker of Plasma Cells in Endometrium, *International Journal of Surgical Pathology* **27**(4), 372–379.

Pattanapanyasat, K., Khowawisetsut, L., Chuansumrit, A., Chokephaibulkit, K., Tangnararatchakit, K., Apiwattanakul, N., Techasaensiri, C., Thitilertdecha, P., Sae-Ung, T. and Onlamoon, N.: 2018, B cell subset alteration and the expression of tissue homing molecules in dengue infected patients, *Journal of biomedical science* **25**(1), 1–11.

Perez-Andres, M., Paiva, B., Nieto, W. G., Caraux, A., Schmitz, A., Almeida, J., Vogt Jr, R., Marti, G., Rawstron, A., Van Zelm, M. et al.: 2010, Human peripheral blood B-cell compartments: a crossroad in B-cell traffic, *Cytometry Part B: Clinical Cytometry* **78**(S1), S47–S60.

Picelli, S., Faridani, O. R., Björklund, Å. K., Winberg, G., Sagasser, S. and Sandberg, R.: 2014, Full-length RNA-seq from single cells using Smart-seq2, *Nature protocols* **9**(1), 171–181.

Pillarisetty, L. S. and Gupta, N.: 2020, Recurrent Pregnancy Loss, *StatPearls* .

Pipi, E., Nayar, S., Gardner, D. H., Colafrancesco, S., Smith, C. and Barone, F.: 2018, Tertiary lymphoid structures: autoimmunity goes local, *Frontiers in Immunology* **9**, 1952.

Poli, A., Michel, T., Thérésine, M., Andrès, E., Hentges, F. and Zimmer, J.: 2009, CD56bright natural killer (NK) cells: an important NK cell subset, *Immunology* **126**(4), 458–465.

Quenby, S., Bates, M., Doig, T., Brewster, J., Lewis-Jones, D., Johnson, P. and Vince, G.: 1999, Pre-implantation endometrial leukocytes in women with recurrent miscarriage, *Human reproduction* **14**(9), 2386–2391.

Racanelli, V., Sansonno, D., Piccoli, C., D'Amore, F. P., Tucci, F. A. and Dammacco, F.: 2001, Molecular characterization of B cell clonal expansions in the liver of chronically hepatitis C virus-infected patients, *The Journal of Immunology* **167**(1), 21–29.

Rahimzadeh, M., Norouzian, M., Arabpour, F. and Naderi, N.: 2016, Regulatory t-cells and preeclampsia: an overview of literature, *Expert review of clinical immunology* **12**(2), 209–227.

Rai, R., Clifford, K., Cohen, H. and Regan, L.: 1995, High prospective fetal loss rate in untreated pregnancies of women with recurrent miscarriage and antiphospholipid antibodies, *Human reproduction* **10**(12), 3301–3304.

Rawlings, D. J., Metzler, G., Wray-Dutra, M. and Jackson, S. W.: 2017, Altered B cell signalling in autoimmunity, *Nature reviews Immunology* **17**(7), 421.

RCOG: 2011, The investigation and treatment of couples with recurrent first-trimester and second-trimester miscarriage, *RCOG Green-top Guideline* .

Riccio, L., Baracat, E., Chapron, C., Batteux, F. and Abrão, M.: 2017, The role of the B lymphocytes in endometriosis: A systematic review, *Journal of Reproductive Immunology* **123**, 29–34.

Riesewijk, A., Martín, J., van Os, R., Horcajadas, J. A., Polman, J., Pellicer, A., Mosselman, S. and Simón, C.: 2003, Gene expression profiling of human endometrial receptivity on days LH+ 2 versus LH+ 7 by microarray technology, *MHR: Basic science of reproductive medicine* **9**(5), 253–264.

Rinehart, J.: 2007, Recurrent implantation failure: definition, *Journal of Assisted Reproduction and Genetics* **24**(7), 284–287.

Robertson, S. A. and Moldenhauer, L. M.: 2014, Immunological determinants of implantation success, *International Journal of Developmental Biology* **58**(2-3-4), 205–217.

Robinson, M. W., Harmon, C. and O'Farrelly, C.: 2016, Liver immunology and its role in inflammation and homeostasis, *Cellular & molecular immunology* **13**(3), 267–276.

Rolle, L., Memarzadeh Tehran, M., Morell-García, A., Raeva, Y., Schumacher, A., Hartig, R., Costa, S.-D., Jensen, F. and Zenclussen, A. C.: 2013, Cutting edge: IL-10-

producing regulatory B cells in early human pregnancy, *American Journal of Reproductive Immunology* **70**(6), 448–453.

Rosser, E. C. and Mauri, C.: 2015, Regulatory B cells: origin, phenotype, and function, *Immunity* **42**(4), 607–612.

Ruddle, N. H. and Akirav, E. M.: 2009, Secondary lymphoid organs: responding to genetic and environmental cues in ontogeny and the immune response, *The Journal of Immunology* **183**(4), 2205–2212.

Sabouri, Z., Perotti, S., Spierings, E., Humburg, P., Yabas, M., Bergmann, H., Horikawa, K., Roots, C., Lambe, S., Young, C. et al.: 2016, IgD attenuates the IgM-induced anergy response in transitional and mature B cells, *Nature communications* **7**(1), 1–11.

Sacks, G.: 2015, Enough! Stop the arguments and get on with the science of natural killer cell testing, *Human reproduction* **30**(7), 1526–1531.

Saini, V., Arora, S., Yadav, A. and Bhattacharjee, J.: 2011, Cytokines in recurrent pregnancy loss, *Clinica chimica acta* **412**(9-10), 702–708.

Saito, S., Nakashima, A., Shima, T. and Ito, M.: 2010, Th1/Th2/Th17 and regulatory T-cell paradigm in pregnancy, *American journal of reproductive immunology* **63**(6), 601–610.

Salamonsen, L. A. and Lathbury, L. J.: 2000, Endometrial leukocytes and menstruation, *Human reproduction update* **6**(1), 16–27.

Sancho, D., Gómez, M. and Sánchez-Madrid, F.: 2005, CD69 is an immunoregulatory molecule induced following activation, *Trends in immunology* **26**(3), 136–140.

Santos, D. S., Thaís, I., Andressa, L., Corrêa, D. C. H., Sell, A. M., Lonardoni, M. V. C., Demarchi, I. G., Neto, D. L., Quirino, A. and Teixeira, J. J. V.: 2017, Antiphospholipid syndrome and recurrent miscarriage: A systematic review and meta-analysis, *Journal of reproductive immunology* **123**, 78–87.

Sathaliyawala, T., Kubota, M., Yudanin, N., Turner, D., Camp, P., Thome, J. J., Bickham, K. L., Lerner, H., Goldstein, M., Sykes, M. et al.: 2013, Distribution and compartmentalization of human circulating and tissue-resident memory T cell subsets, *Immunity* **38**(1), 187–197.

Schioppa, T., Moore, R., Thompson, R. G., Rosser, E. C., Kulbe, H., Nedospasov, S., Mauri, C., Coussens, L. M. and Balkwill, F. R.: 2011, B regulatory cells and the

tumor-promoting actions of TNF-α during squamous carcinogenesis, *Proceedings of the National Academy of Sciences* **108**(26), 10662–10667.

Schumacher, A., Sharkey, D. J., Robertson, S. A. and Zenclussen, A. C.: 2018, Immune cells at the fetomaternal interface: how the microenvironment modulates immune cells to foster fetal development, *The Journal of Immunology* **201**(2), 325–334.

Schweet, R. and Heintz, R.: 1966, Protein synthesis, *Annual review of biochemistry* **35**(1), 723–758.

Seshadri, S. and Sunkara, S. K.: 2014, Natural killer cells in female infertility and recurrent miscarriage: a systematic review and meta-analysis, *Human reproduction update* **20**(3), 429–438.

Sharma, S.: 2014, Natural killer cells and regulatory T cells in early pregnancy loss, *The International journal of developmental biology* **58**, 219.

Shekhar, S. and Yang, X.: 2012, The darker side of follicular helper T cells: from autoimmunity to immunodeficiency, *Cellular & molecular immunology* **9**(5), 380–385.

Shen, Z., Rodriguez-Garcia, M., Patel, M. and Wira, C.: 2021, Direct and Indirect endocrine-mediated suppression of human endometrial CD8+ T cell cytotoxicity, *Scientific Reports* **11**(1), 1–14.

Shigesi, N., Kvaskoff, M., Kirtley, S., Feng, Q., Fang, H., Knight, J. C., Missmer, S. A., Rahmioglu, N., Zondervan, K. T. and Becker, C. M.: 2019, The association between endometriosis and autoimmune diseases: a systematic review and meta-analysis, *Human reproduction update* **25**(4), 486–503.

Shima, T., Sasaki, Y., Itoh, M., Nakashima, A., Ishii, N., Sugamura, K. and Saito, S.: 2010, Regulatory T cells are necessary for implantation and maintenance of early pregnancy but not late pregnancy in allogeneic mice, *Journal of reproductive immunology* **85**(2), 121–129.

Siegel, R. M., Chan, F. K.-M., Chun, H. J. and Lenardo, M. J.: 2000, The multifaceted role of Fas signaling in immune cell homeostasis and autoimmunity, *Nature immunology* **1**(6), 469–474.

Silverthorn, D. U.: 2015, *Human physiology, Chapter 11 Reproduction and Fetal Developmen*, Jones & Bartlett Publishers.

Sims, G. P., Ettinger, R., Shirota, Y., Yarboro, C. H., Illei, G. G. and Lipsky, P. E.: 2005, Identification and characterization of circulating human transitional B cells, *Blood* **105**(11), 4390–4398.

Skulska, K., Wegrzyn, A. S., Chelmonska-Soyta, A. and Chodaczek, G.: 2019, Impact of tissue enzymatic digestion on analysis of immune cells in mouse reproductive mucosa with a focus on γ δ T cells, *Journal of immunological methods* **474**, 112665.

Smith, S. D., Dunk, C. E., Aplin, J. D., Harris, L. K. and Jones, R. L.: 2009, Evidence for immune cell involvement in decidual spiral arteriole remodeling in early human pregnancy, *The American journal of pathology* **174**(5), 1959–1971.

Somigliana, E., Vigano, P., Busnelli, A., Paffoni, A., Vegetti, W. and Vercellini, P.: 2018, Repeated implantation failure at the crossroad between statistics, clinics and over-diagnosis, *Reproductive biomedicine online* **36**(1), 32–38.

Sommer, S. S. and Cohen, J. E.: 1980, The size distributions of proteins, mRNA, and nuclear RNA, *Journal of Molecular Evolution* **15**(1), 37–57.

Song, D., Li, T.-C., Zhang, Y., Feng, X., Xia, E., Huang, X. and Xiao, Y.: 2019, Correlation between hysteroscopy findings and chronic endometritis, *Fertility and sterility* **111**(4), 772–779.

Southcombe, J., Mounce, G., McGee, K., Elghajiji, A., Brosens, J., Quenby, S., Child, T. and Granne, I.: 2017, An altered endometrial CD8 tissue resident memory T cell population in recurrent miscarriage, *Scientific reports* **7**(1), 1–8.

Southcombe, J., Redman, C. and Sargent, I.: 2010, Peripheral blood invariant natural killer T cells throughout pregnancy and in preeclamptic women, *Journal of reproductive immunology* **87**(1-2), 52–59.

Sovalat, H., Ojeda, M., Arkam, Y., Lewandowsky, H., Chabouté, V. and Hénon, P.: 2000, Effect of cryopreservation on adhesion molecule expression in peripheral blood derived CD34+ cells, *Experimental Hematology* **28**(7), 66.

Stebegg, M., Kumar, S. D., Silva-Cayetano, A., Fonseca, V. R., Linterman, M. A. and Graca, L.: 2018, Regulation of the germinal center response, *Frontiers in immunology* **9**, 2469.

Stephenson, M. and Kutteh, W.: 2007, Evaluation and management of recurrent early pregnancy loss, *Clinical obstetrics and gynecology* **50**(1), 132–145.

Subramanian, A., Tamayo, P., Mootha, V. K., Mukherjee, S., Ebert, B. L., Gillette, M. A., Paulovich, A., Pomeroy, S. L., Golub, T. R., Lander, E. S. et al.: 2005, Gene set enrichment analysis: a knowledge-based approach for interpreting genome-wide expression profiles, *Proceedings of the National Academy of Sciences* **102**(43), 15545–15550.

Tagliani, E. and Erlebacher, A.: 2011, Dendritic cell function at the maternal–fetal interface, *Expert review of clinical immunology* **7**(5), 593–602.

Talbi, S., Hamilton, A., Vo, K., Tulac, S., Overgaard, M. T., Dosiou, C., Le Shay, N., Nezhat, C., Kempson, R., Lessey, B. et al.: 2006, Molecular phenotyping of human endometrium distinguishes menstrual cycle phases and underlying biological processes in normo-ovulatory women, *Endocrinology* **147**(3), 1097–1121.

Taylor, E. B. and Sasser, J. M.: 2017, Natural killer cells and t lymphocytes in pregnancy and pre-eclampsia, *Clinical Science* **131**(24), 2911–2917.

Tellier, J. and Nutt, S. L.: 2017, Standing out from the crowd: How to identify plasma cells, *European Journal of Immunology* **47**(8), 1276–1279.

Thiruchelvam, U., Wingfield, M. and O'Farrelly, C.: 2016, Increased uNK progenitor cells in women with endometriosis and infertility are associated with low levels of endometrial stem cell factor, *American Journal of Reproductive Immunology* **75**(4), 493–502.

Thornhill, A. R., Dedie-Smulders, C., Geraedts, J. P., Harper, J., Harton, G., Lavery, S., Moutou, C., Robinson, M., Schmutzler, A., Scriven, P. et al.: 2005, ESHRE PGD Consortium 'Best practice guidelines for clinical preimplantation genetic diagnosis (PGD) and preimplantation genetic screening (PGS)', *Human Reproduction* **20**(1), 35–48.

Thum, M.-Y., Bhaskaran, S., Abdalla, H. I., Ford, B., Sumar, N. and Bansal, A.: 2008, Prednisolone suppresses NK cell cytotoxicity in vitro in women with a history of infertility and elevated NK cell cytotoxicity, *American Journal of Reproductive Immunology* **59**(3), 259–265.

Ticconi, C., Pietropolli, A., Di Simone, N., Piccione, E. and Fazleabas, A.: 2019, Endometrial immune dysfunction in recurrent pregnancy loss, *International Journal of Molecular Sciences* **20**(21), 5332.

Tilburgs, T., Claas, F. and Scherjon, S.: 2010, Elsevier Trophoblast Research Award Lecture: Unique properties of decidual T cells and their role in immune regulation during human pregnancy, *Placenta* **31**, S82–S86.

Toth, M., Patton, D. L., Esquenazi, B., Shevchuk, M., Thaler, H. and Divon, M.: 2007, Association between Chlamydia trachomatis and abnormal uterine bleeding, *American Journal of Reproductive Immunology* **57**(5), 361–366.

Vacca, P., Vitale, C., Montaldo, E., Conte, R., Cantoni, C., Fulcheri, E., Darretta, V., Moretta, L. and Mingari, M. C.: 2011, CD34+ hematopoietic precursors are present in human decidua and differentiate into natural killer cells upon interaction with stromal cells, *Proceedings of the National Academy of Sciences* **108**(6), 2402–2407.

Vajdy, M.: 2006, Generation and maintenance of mucosal memory B cell responses?, *Current medicinal chemistry* **13**(25), 3023–3037.

Vallés, C. S., Almansa, J. A. H., Gimeno, P. D. and Martínez, A. P.: 2018, Gene expression profile as an endometrial receptivity marker. US Patent 10,081,840.

Vallvé-Juanico, J., Houshdaran, S. and Giudice, L. C.: 2019, The endometrial immune environment of women with endometriosis, *Human reproduction update* **25**(5), 565–592.

Van De Pavert, S. A. and Mebius, R. E.: 2010, New insights into the development of lymphoid tissues, *Nature Reviews Immunology* **10**(9), 664–674.

Van Gassen, S., Callebaut, B., Van Helden, M. J., Lambrecht, B. N., Demeester, P., Dhaene, T. and Saeys, Y.: 2015, FlowSOM: Using self-organizing maps for visualization and interpretation of cytometry data, *Cytometry Part A* **87**(7), 636–645.

Vander Borght, M. and Wyns, C.: 2018, Fertility and infertility: Definition and epidemiology, *Clinical biochemistry* **62**, 2–10.

Velculescu, V. E., Zhang, L., Vogelstein, B. and Kinzler, K. W.: 1995, Serial analysis of gene expression, *Science* **270**(5235), 484–487.

Vento-Tormo, R., Efremova, M., Botting, R. A., Turco, M. Y., Vento-Tormo, M., Meyer, K. B., Park, J.-E., Stephenson, E., Polański, K., Goncalves, A. et al.: 2018, Single-cell reconstruction of the early maternal–fetal interface in humans, *Nature* **563**(7731), 347–353.

Vernel-Pauillac, F. and Merien, F.: 2006, Proinflammatory and immunomodulatory cytokine mRNA time course profiles in hamsters infected with a virulent variant of Leptospira interrogans, *Infection and immunity* **74**(7), 4172–4179.

Victora, G. D., Dominguez-Sola, D., Holmes, A. B., Deroubaix, S., Dalla-Favera, R. and Nussenzweig, M. C.: 2012, Identification of human germinal center light and dark zone cells and their relationship to human B-cell lymphomas, *Blood* **120**(11), 2240–2248.

Vinuesa, C. G., Linterman, M. A., Goodnow, C. C. and Randall, K. L.: 2010, T cells and follicular dendritic cells in germinal center B-cell formation and selection, *Immunological reviews* **237**(1), 72–89.

Vomstein, K., Voss, P., Molnar, K., Ainsworth, A., Daniel, V., Strowitzki, T., Toth, B. and Kuon, R.-J.: 2020, Two of a kind? Immunological and clinical risk factors differ between recurrent implantation failure and recurrent miscarriage, *Journal of Reproductive Immunology* **141**, 103166.

Vossenkämper, A., Lutalo, P. and Spencer, J.: 2012, Translational Mini-Review Series on B cell subsets in disease. Transitional B cells in systemic lupus erythematosus and Sjögren's syndrome: clinical implications and effects of B cell-targeted therapies, *Clinical & Experimental Immunology* **167**(1), 7–14.

Wallace, A. E., Fraser, R. and Cartwright, J. E.: 2012, Extravillous trophoblast and decidual natural killer cells: a remodelling partnership, *Human reproduction update* **18**(4), 458–471.

Wang, W., Vilella, F., Alama, P., Moreno, I., Mignardi, M., Isakova, A., Pan, W., Simon, C. and Quake, S. R.: 2020, Single-cell transcriptomic atlas of the human endometrium during the menstrual cycle, *Nature Medicine* pp. 1–10.

Wang, X., He, Y., Zhang, Q., Ren, X. and Zhang, Z.: 2021, Direct comparative analyses of 10x genomics chromium and smart-seq2, *Genomics, Proteomics & Bioinformatics* **S1672-0229**(21), 00048–6.

Wang, Z., Gerstein, M. and Snyder, M.: 2009, RNA-Seq: a revolutionary tool for transcriptomics, *Nature reviews genetics* **10**(1), 57–63.

Waschbisch, A., Sammet, L., Schröder, S., Lee, D.-H., Barrantes-Freer, A., Stadelmann, C. and Linker, R.: 2014, Analysis of CD4+ CD8+ double-positive T cells in blood, cerebrospinal fluid and multiple sclerosis lesions, *Clinical & Experimental Immunology* **177**(2), 404–411.

Weisel, N. M., Weisel, F. J., Farber, D. L., Borghesi, L. A., Shen, Y., Ma, W., Luning Prak, E. T. and Shlomchik, M. J.: 2020, Comprehensive analyses of B-cell compartments across the human body reveal novel subsets and a gut-resident memory phe-

notype, *Blood, The Journal of the American Society of Hematology* **136**(24), 2774–2785.

Wells, G., Shea, B., O'connell, D., Peterson, J., Welch, V., Losos, M. and Tugwell, P.: 2020, The Newcastle-Ottawa Scale (NOS) for assessing the quality of nonrandomised studies in meta-analyses.
URL: *http://www.ohri.ca/programs/clinical_epidemiology/oxford.asp*

White, H. D., Prabhala, R. H., Humphrey, S. L., Crassi, K. M., Richardson, J. M. and Wira, C. R.: 2000, A method for the dispersal and characterization of leukocytes from the human female reproductive tract, *American journal of reproductive immunology* **44**(2), 96–103.

WHO: 2009, Mental health aspects of women's reproductive health: a global review of the literature.

WHO: 2020, WHO infertility fact sheet.
URL: *https://www.who.int/health-topics/infertility#tab=tab_1*

Winger, E. E. and Reed, J. L.: 2011, Low circulating CD4+ CD25+ Foxp3+ T regulatory cell levels predict miscarriage risk in newly pregnant women with a history of failure, *American Journal of Reproductive Immunology* **66**(4), 320–328.

Wira, C. R., Fahey, J. V., Rodriguez-Garcia, M., Shen, Z. and Patel, M. V.: 2014, Regulation of mucosal immunity in the female reproductive tract: the role of sex hormones in immune protection against sexually transmitted pathogens, *American journal of reproductive immunology* **72**(2), 236–258.

Wira, C. R., Rodriguez-Garcia, M. and Patel, M. V.: 2015, The role of sex hormones in immune protection of the female reproductive tract, *Nature Reviews Immunology* **15**(4), 217–230.

Wortel, C. and Heidt, S.: 2017, Regulatory B cells: phenotype, function and role in transplantation, *Transplant immunology* **41**, 1–9.

Yao, Y., Xu, X.-H. and Jin, L.: 2019, Macrophage polarization in physiological and pathological pregnancy, *Frontiers in immunology* **10**, 792.

Yeaman, G., Collins, J., Fanger, M. and Wira, C.: 2001, CD8+ T cells in human uterine endometrial lymphoid aggregates: evidence for accumulation of cells by trafficking, *Immunology* **102**(4), 434–440.

Yeaman, G. R., Guyre, P. M., Fanger, M. W., Collins, J. E., White, H. D., Rathbun, W., Orndorff, K. A., Gonzalez, J., Stern, J. E. and Wira, C. R.: 1997, Unique CD8+ T cell-rich lymphoid aggregates in human uterine endometrium, *Journal of leukocyte biology* **61**(4), 427–435.

Young, M. D., Wakefield, M. J., Smyth, G. K. and Oshlack, A.: 2010, Gene ontology analysis for RNA-seq: accounting for selection bias, *Genome biology* **11**(2), R14.

Youssef, A., Vermeulen, N., Lashley, E. L. O., Goddijn, M. and van der Hoorn, M. L. P.: 2019, Comparison and appraisal of (inter) national recurrent pregnancy loss guidelines, *Reproductive biomedicine online* **39**(3), 497–503.

Yu, G., Wang, L.-G., Han, Y. and He, Q.-Y.: 2012, clusterProfiler: an R package for comparing biological themes among gene clusters, *Omics: a journal of integrative biology* **16**(5), 284–287.

Zargar, M., Ghafourian, M., Nikbakht, R., Hosseini, V. M. and Choghakabodi, P. M.: 2020, Evaluating chronic endometritis in women with recurrent implantation failure and recurrent pregnancy loss by hysteroscopy and immunohistochemistry, *Journal of Minimally Invasive Gynecology* **27**(1), 116–121.

Zenclussen, A. C., Gerlof, K., Zenclussen, M. L., Sollwedel, A., Bertoja, A. Z., Ritter, T., Kotsch, K., Leber, J. and Volk, H.-D.: 2005, Abnormal T-cell reactivity against paternal antigens in spontaneous abortion: adoptive transfer of pregnancy-induced CD4+ CD25+ T regulatory cells prevents fetal rejection in a murine abortion model, *The American journal of pathology* **166**(3), 811–822.

Zeng, W., Liu, X., Liu, Z., Zheng, Y., Yu, T., Fu, S., Li, X., Zhang, J., Zhang, S., Ma, X. et al.: 2018, Deep surveying of the transcriptional and alternative splicing signatures for decidual CD8+ T cells at the first trimester of human healthy pregnancy, *Frontiers in immunology* **9**, 937.

Zhao, J., Zhang, S., Liu, Y., He, X., Qu, M., Xu, G., Wang, H., Huang, M., Pan, J., Liu, Z. et al.: 2020, Single-cell RNA sequencing reveals the heterogeneity of liver-resident immune cells in human, *Cell discovery* **6**(1), 1–19.

Zhou, J. Z., Way, S. S. and Chen, K.: 2018, Immunology of the uterine and vaginal mucosae, *Trends in immunology* **39**(4), 302–314.

Ziegler, K. B., Muzzio, D. O., Matzner, F., Bommer, I., Ventimiglia, M., Malinowsky, K., Ehrhardt, J., Zygmunt, M. and Jensen, F.: 2018, Human pregnancy is accompa-

nied by modifications in B cell development and immunoglobulin profile, *Journal of reproductive immunology* **129**, 40–47.

Ziegler, S. F., Ramsdell, F., Hjerrild, K. A., Armitage, R. J., Grabstein, K. H., Hennen, K. B., Farrah, T., Fanslow, W. C., Shevach, E. M. and Alderson, M. R.: 1993, Molecular characterization of the early activation antigen CD69: a type II membrane glycoprotein related to a family of natural killer cell activation antigens, *European journal of immunology* **23**(7), 1643–1648.

Zondervan, K., Becker, C. and Missmer, S.: 2020, Endometriosis, *N Engl J Med* **382**, 1244–56.